Systemic ectomycorrhizal defense induction in poplar

Dissertation

For the award of the degree

"Doctor rerum naturalium"

of the University of Göttingen

Within the doctoral program

"IRTG2172: PRoTECT: Plant Responses To Eliminate Critical Threats"

of the Georg-August-University School of Science (GAUSS)

submitted by

Steven Dreischhoff

from Castrop-Rauxel, Germany

Göttingen, 2023

I. Members of the Examination Board

Thesis Advisory Committee

Prof. Dr. Andrea Polle, Department of Forest Botany and Tree Physiology, Büsgen-Institute, University of Göttingen, Germany

Prof. Dr. Guus Bakkeren, Department of Botany, University of British Columbia, Vancouver, Canada, and Summerland Research and Development Centre, Agriculture and Agri-Food Canada

Prof. Dr. Volker Lipka, Department of Plant Cell Biology, Albrecht-von-Haller-Institute for Plant Sciences, University of Göttingen, Germany

1st Referee:

Prof. Dr. Andrea Polle, Department of Forest Botany and Tree Physiology, Büsgen-Institute, University of Göttingen, Germany

2nd Referee:

Prof. Dr. Guus Bakkeren, Department of Botany, University of British Columbia, Vancouver, Canada, and Summerland Research and Development Centre, Agriculture and Agri-Food Canada

Further members of the Examination Board:

Prof. Dr. Gerhard Braus, Department of Molecular Microbiology and Genetics, Institute of Microbiology and Genetics, University of Göttingen, Germany

Prof. Dr. Ivo Feußner, Department of Plant Biochemistry, Albrecht-von-Haller-Institute for Plant Sciences, University of Göttingen, Germany

Prof. Dr. Kai Heimel, Department of Microbial Cell Biology, Institute of Microbiology and Genetics, University of Göttingen, Germany

Prof. Dr. Marcel Wiermer, Department of Biochemistry of Plant-Microbe Interactions, Institute of Biology, Free University of Berlin, Germany

Date of oral examination: 29.03.2023

II. Table of contents

III. List of figures

IV. List of tables

V. List of abbreviations

Abbreviation	Definition
ABA	abscisic acid
ACC	aminocyclopropane-1-carboxylic acid
AMF	arbuscular mycorrhizal fungi
Ara.id	gene identifiers for *Arabidopsis*
At	*Arabidopsis thaliana*
BTH	acibenzolar-S-methyl
ddH_2O	double distilled water
DEG	differentially expressed gene
EMF	ectomycorrhizal fungi
ETI	effector-triggered immunity
FAE	formalin/glacial acetic acid/ethanol
FC	fold change
GO	gene ontology
INRA	institut national de la recherche agronomique
ISR	induced systemic resistance
JA	jasmonic acid
JA-Ile	jasmonic acid-isoleucine
KEGG	Kyoto Encyclopedia of Genes and Genomes
KO	knockout
KTI	Kunitz trypsin inhibitor
Lb	*Laccaria bicolor*
*Lb*HK	*Laccaria bicolor* heat killed
*Lb*Su	*Laccaria bicolor* culture supernatant
LCO	lipochitooligosaccharides
MAMP	microbe-associated molecular pattern
MAP	mitogen-activated protein
MeJA	methyl jasmonic acid
MLP	major latex protein
M-MMNS	modified-Melin-Norkrans-Sucrose medium

MPK	MAP kinase
Na	*Nicotiana attenuata*
Os	*Oryza sativa*
PAR	photosynthetic active radiation
Pc	*Populus* × *canescens*
PDA	potato dextrose agar
Potri.id	gene identifiers for poplar
Pt	*Populus trichocarpa*
PTI	pattern-triggered immunity
qRT-PCR	quantitative real-time PCR
RIN	RNA Integrity Number
RNAseq	RNA sequencing
rpm	rounds per minute
SA	salicylic acid
SAR	systemic acquired resistance
SDS	sodium dodecyl sulfate
VOC	volatile organic compound
WT	wildtype

1. Summary

Ectomycorrhizal fungi (EMF) are important soil symbiotes in boreal and temperate forests. They form beneficial interactions (ectomycorrhizae) with the roots of tree species. Ectomycorrhizae facilitate plant nutrient supply and, in return, receive carbohydrates from the host. EMF also modulate plant stress resistance, for example, by negative effects on the fitness of leaf-feeding insects. In non-host interactions, the negative impact of EMF on herbivores is mediated by chitin signaling via the CHITIN ELICITOR RECEPTOR KINASE 1 (CERK1). It is unknown whether this pathway is also involved in defense activation in EMF host plants. To gain new insights into the mechanisms of ectomycorrhizal-induced systemic resistance, leaf responses to the interaction of the symbiotic fungus *Laccaria bicolor* with its host species poplar (*Populus* x *canescens*) were investigated. Specifically, this thesis aimed to characterize early effects on the poplar leaf transcriptome while *L. bicolor* was colonizing the roots and to investigate the possible involvement of chitin and CERK1 in mediating the systemic defense responses. In addition, a bioassay for *Botrytis cinerea*-induced damage was developed and applied to test if *L. bicolor* affected the defenses of poplar against a necrotizing foliar pathogen.

The initial transcriptional changes in poplar leaves after *L. bicolor* root inoculation were examined in an axenic setup and used to identify potential marker genes for systemic effects. Changes in the leaf transcriptome were not found after one or two days but occurred only four days after *L. bicolor* treatment. This result suggests that the presence of *L. bicolor* without direct interaction was not sufficient, but that initial root colonization was required for systemic changes. After seven days, genes involved in defense metabolism, including biosynthetic genes for phenolic compounds and flavonoids, had increased transcript abundances. Defense signaling components with increased transcript abundances included genes involved in the regulation and biosynthesis of jasmonate signaling and negative and positive regulators of ethylene signaling. *KUNITZ TRYPSIN INHIBITOR* (*KTI*) and *MAJOR LATEX PROTEIN LIKE 423* (*MLP423*) were identified to have robustly increased transcript abundances after different ectomycorrhizal treatments and were selected as marker genes for further experiments. In addition, *KTI* was responsive toward methyl jasmonate treatment. This observation underpins the results of the transcriptome analysis that jasmonic acid signaling may play a role in ectomycorrhizal systemic defense induction.

Using poplar *cerk1* KO mutants, the role of CERK1 in systemic ectomycorrhizal defense induction was investigated. *KTI* and *MLP423* served as marker genes for defense activation. The transcript abundances of *KTI* and *MLP423* increased less after *L. bicolor* treatment in *cerk1* KO lines than in wildtype poplars, suggesting that CERK1 is involved in ectomycorrhizal defense induction. However, the induction of *KTI* and *MLP423* was not entirely abolished in the *cerk1* KO lines, indicating that additional factors are likely implicated in the EMF-induced systemic induction of the defense marker genes. Since chitin did not induce the defense marker genes, a direct link between CERK1-mediated defense activation and EMF-induced systemic defense is unlikely. However, a global transcriptome analysis is required to find out if other defenses than the two selected marker genes were responding to chitin. Mycorrhizal colonization of the *cerk1* mutants was reduced, suggesting that CERK1 might participate in the establishment of ectomycorrhizae, similarly as known for arbuscular mycorrhizae. If this can be further corroborated, then the reduced activation transcript levels of *KTI* or *MLP423* in leaves of *cerk1* mutants might be due to delayed mycorrhization and, thus, indicate only an indirect involvement of CERK1 in the systemic defense changes. This idea requires further analyses.

Reliable bioassays to study the interaction of foliar pathogens and poplar are scarce. Therefore, a test system to quantify *B. cinerea* infections on poplar leaves was developed. Initial experiments with this new bioassay showed a positive relationship between mycorrhizal root colonization and the degree of *B. cinerea* infection. This result suggests that resistance by *L. bicolor* may not be broadly induced against various biological threats and opens the question of how jasmonate-dependent processes are modulated in ectomycorrhizal-induced systemic defense.

In summary, this thesis suggests that initial root colonization by EMF may be required to induce systemic defense changes in the leaf transcriptome. The systemic signaling events include jasmonate-dependent and ethylene-responsive components. The responses of defense marker genes *KTI* and *MLP423* suggest a contribution of CERK1, but the effect might be indirect through a potential involvement of CERK1 in symbiosis establishment. Based on the analyses of the marker genes, chitin is unlikely to play a role in the systemic induction process. The results further point toward ectomycorrhizal-mediated trade-off between herbivorous leaf insects and necrotrophic pathogens and thus may direct future research.

2. Introduction

2.1. Mycorrhiza form symbiotic interactions with numerous plants

Plants share their space with numerous microorganisms. These microbes form relationships that can be beneficial for the plant (mutualistic) or harmful for the plant (pathogenic; Bonfante and Anca, 2009; Vandenkoornhuyse et al., 2015). Besides many bacteria, for example, rhizobacteria important for nitrogen fixation in legume plants (Lugtenberg and Kamilova, 2009), also fungi associate with plants in beneficial ways (Almario et al., 2022; Ghorbanpour et al., 2018). Some beneficial fungi live endophytically inside the plant and, for example, can boost plant defenses (Yan et al., 2019). Others colonize the plants (especially the roots) from the outside, forming structures outside of the plant but also invading the plant (Smith and Read, 2008).

One important group of fungi which colonizes the roots are mycorrhizal fungi. During the colonization, a new organ is formed, the mycorrhiza (from Greek μύκης mýkēs, "fungus," and ῥίζα rhiza, "root"). The most studied feature of this interaction is the bidirectional exchange of nutrients (Smith and Read, 2008). The fungi supply essential but often rare nutrients like phosphorus or nitrogen from the soil to the plant, and in return, they get photosynthesis-derived carbohydrates (Nehls and Plassard, 2018; van der Heijden et al., 2015). The beneficial interaction of mycorrhizal fungi and plants enhances the overall performance of the plants, for instance, through increasing plant growth or water uptake (Smith and Read, 2008). The improved performance of plants associated with mycorrhizal fungi is likely to have facilitated the evolution of land plants (Wang et al., 2010). Approximately 340,000 land plant species (≈ 85 % of all land plant species) can be colonized by mycorrhizal fungi (≈ 50,000 species; Brundrett and Tedersoo, 2018; Genre et al., 2020; van der Heijden et al., 2015). Among the species which mycorrhizal fungi cannot colonize is the model plant *Arabidopsis thaliana* (hereafter *Arabidopsis*; Fernández et al., 2019).

Mycorrhizal fungi generate extraradical hyphae as the main structures for nutrient uptake from soil. The mycorrhizal fungi are distinguished on the basis of the hosts they can colonize, and by the structures they form in association with roots. There are four major mycorrhizal types. The two less-studied types are orchid mycorrhiza, which interact with orchids, and ericoid mycorrhiza, which associate with members of the Ericaceae and some liverworts and woody species (Kohout, 2017; van der Heijden et al., 2015). The most widespread and oldest

form of mycorrhizal fungi are arbuscular mycorrhizal fungi (AMF; Bonfante and Anca, 2009; Martin et al., 2018). AMF colonize most herbs, grasses, trees, hornworts, and liverworts (van der Heijden et al., 2015). These three mycorrhizal types share that the hyphae penetrate the root cells to establish an intracellular symbiosis. They are also called endomycorrhizal fungi (Bonfante and Anca, 2009).

The fourth type of mycorrhiza is formed by ectomycorrhizal fungi (EMF, Figure 1). EMF are soil symbiotes in forests of the boreal and temperate zone, where they associate with the roots of most shrub and tree species (Brundrett, 2009). EMF are no homogenous group because they evolved independently multiple times from saprotrophic clades (Genre et al., 2020; Martin et al., 2016). They share that they cover the root tip with a hyphal mantle (Figure 1b+d) and grow between the root epidermis cells and outer layers of cortical cells, forming the Hartig net (Figure 1f). EMF do not invade the cell lumen and never cross the Casparian strip (Bonfante and Anca, 2009). One of the most studied members in the group of ectomycorrhizal fungi is *Laccaria bicolor* (used in this study). It belongs to the Basidiomycota and the family of Hydnangiaceae. *L. bicolor* is distributed across temperate and boreal forests of North America and Northern Europe (Mueller and Gardes, 1991). *L. bicolor* is used as a model species to study the molecular processes during the symbiosis development of EMF and their hosts. The genome of *L. bicolor* was the first EMF genome sequenced (Martin et al., 2008). The host range of *L. bicolor* is broad, including members of the genera *Pinus* (Hazard et al., 2017), *Pseudotsuga,* and *Populus* (Plett et al., 2014).

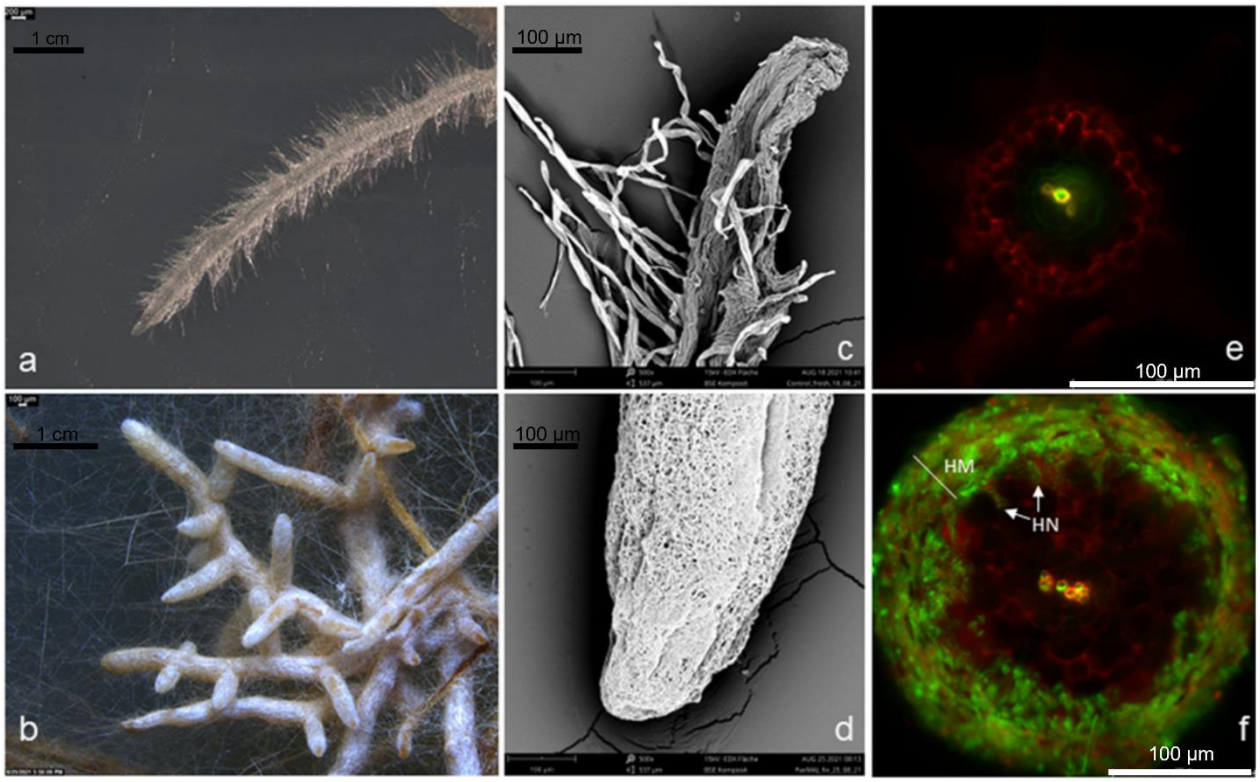

Figure 1 Morphological and anatomical characteristics of non-mycorrhizal (a, c, e) and poplar root tips colonized by ectomycorrhizal fungus (b, d, f)

(a, b) Poplar roots tips were observed under a compound microscope (a: nonmycorrhizal root tip, b: ectomycorrhizal root tips) and a scanning electron microscope (c: non-mycorrhizal root tip, d: ectomycorrhizal root tips). In (a, c), root hairs emerging from non-mycorrhizal roots are visible, and in (b, d), colonized root tips with very fine hyphae (b) and the net-like mantle formed around the root tip by the fungus are observable (d). Cross sections of non-mycorrhizal (e) and ectomycorrhizal (f) poplar root tips stained with propidium iodide to view plant cell walls (red) and with wheat germ agglutinin, Alexa Fluor 488 conjugate to view fungal hyphae (green). HM: hyphal mantle, HN: Hartig net. (a, b) scale bar = 1 cm, (c, d, e, f) scale bar = 100 µm. The fungus in the pictures is *Paxillus involutus,* but the structures represent all ectomycorrhizal fungi. Reproduced from Rosenkranz et al. (2022) with permission of the corresponding author.

2.2. *Populus* is an ecologically and scientifically important tree genus

Poplars (*Populus* spec., Saliaceae) occur in boreal and temperate forests, subtropical and arid regions, and lowland riverbanks (Rennenberg et al., 2010; Stettler, 1996). They are a tree species with numerous ecological and economic functions worldwide (Polle and Douglas, 2010). One member that has been used frequently is *Populus* × *canescens* (grey poplar). It is a natural hybrid of *P. alba* and *P. tremula*. In its native habitat in Eurasian floodplain forests, it is often found together with *P. alba*, *Salix alba,* and *S. fragilis* (Stimm and Weisgerber, 2014). *P.* × *canescens* is cultivated for industrial biomass production or wood industry (Eimil-Fraga et al., 2019; Stimm and Weisgerber, 2014). In addition, it is used for reforestation and in parks, gardens, and along roads for ornamental purposes (Stimm and Weisgerber, 2014). Even though the first tree genome was the genome of a female *Populus trichocarpa* tree from the Nisqually River in Washington in the United States (Tuskan et al., 2006), the *P.* × *canescens* INRA 717-1B4 clone (used in this study) was the first tree species used for genetic engineering (Leple et al., 1992). The genome of *P.* × *canescens* INRA 717-1B4 was published in 2016 by Mader and colleagues. The INRA 717-1B4 clone is a cross of a female *Populus tremula* and a male *Populus alba* from a breeding program (Lemoine, 1973). The hybrid clone was used in more than 300 publications (January 2023, Google Scholar), including molecular studies about nutrition (Hunter et al., 2022; Kasper et al., 2022), stress physiology (Gordon et al., 2022; Ullah et al., 2022), ectomycorrhizal fungi (Cope et al., 2021; Kang et al., 2020) and combinations of the latter two factors (Kaling et al., 2018; Sivaprakasam Padmanaban et al., 2022). The interaction of mycorrhizal fungi and poplar was investigated in about 50 studies using the INRA 717-1B4 clone (January 2023, Google Scholar).

2.3. Plants can recognize pathogens to induce defenses

Plants are threatened by changing environmental conditions because of climate change. The resulting consequences are severe abiotic stress or geographic spread of pathogens (Chaudhry and Sidhu, 2022; Elad and Pertot, 2014; Polle et al., 2019). Pathogens like rust fungi (e.g., *Melampsora larici-populina*) or necrotizing fungi (e.g., *Botrytis cinerea*) and herbivorous insects (e.g., *Chrysomela populi*) are critical threats to poplar (Büsgen, 1918; Urban, 2006; Wan et al., 2015).

Plants have an immune system to defend themselves against biological threats either via constitutive defenses or inducible defenses (Jones and Dangl, 2006). Constitutive defenses are, for instance, barriers that prevent the pathogens from entering the plant (rigid cell walls or cuticular waxes) and the accumulation of metabolites (phytoanticipins) that are toxic to pathogens, for example, caffeine or tannins (Miedes et al., 2014; Reina-Pinto and Yephremov, 2009; Tiku, 2020). Besides constitutive defenses, there are, in principle, two ways of inducible defenses: molecular pattern- and effector-triggered defenses against primary pathogen attack in local tissues and inducible defenses in distant, systemic tissues (Sun and Zhang, 2021). Plants can recognize pathogens by sensing microbe-associated molecular patterns (MAMPs) via pattern recognition receptors on the cell surface (Zipfel, 2009). Examples of MAMPs are flg22 (22 amino acids of bacterial flagellin; Felix et al., 1999) and chitin (a fungal cell wall component; Felix et al., 1993). FLAGELLIN-SENSITIVE 2 (FLS2) was identified as the receptor for flg22 (Gómez-Gómez et al., 2001), and CHITIN ELICITOR RECEPTOR KINASE 1 (CERK1) is the primary receptor for chitin (Miya et al., 2007). The receptors form complexes with co-receptors to activate downstream processes (Zipfel, 2014).

Pathogens secrete so-called effectors into the plant to interfere with their recognition and suppress the resulting defense events (Barsoum et al., 2019). On the other side, plant cells contain intercellular nucleotide-binding/leucine-rich-repeat receptors to sense the effectors and subsequently mount defenses (Cui et al., 2015). The so-called pattern-triggered immunity (PTI) and effector-triggered immunity (ETI) are not two separate mechanisms but are closely intertwined and potentiate each other (Ngou et al., 2021; Yuan et al., 2021). It was long believed that effector-triggered immunity evolved on top of pattern-triggered immunity due to an evolutionary “arms race” between pathogens and plants where pathogens develop new effectors and plants evolve new receptors for these new effectors (Jones and Dangl, 2006).

However, the recent evidence of the direct interplay between PTI and ETI challenges this theory and may suggest the co-evolution of both recognition mechanisms (Pruitt et al., 2021). PTI and ETI result in similar signaling events and means of local defense against pathogens. These include, among others, a hypersensitive response (induced cell death to prevent the spreading of the pathogen; Balint-Kurti, 2019), cell wall fortification (e.g., callose deposition on entry sides; Wang et al., 2021), and the accumulation of secondary metabolism (phytoalexins, e.g., flavonoids in poplar) or biocidal proteins (Ullah et al., 2022; Zhu-Salzman and Zeng, 2015). Subsequent to local defense triggered by PTI and ETI, defenses in distant, systemic tissues can be induced. Besides pathogens, beneficial microbes can also induce systemic defenses (Sun and Zhang, 2021).

2.4. Microbes induce systemic defenses

2.4.1. Salicylic acid and jasmonic acid are drivers of systemic defense

Understanding the major signaling pathways involved in plant defense is essential to comprehend systemic inducible defenses. In a simplified view, two phytohormones drive defense signaling: salicylic acid (SA) and jasmonic acid (JA). SA is produced either via the isochorismate or phenylalanine pathway. Both pathways have different shares of total SA production in different species (Lefevere et al., 2020). Although the SA biosynthesis in poplar is not fully understood, the isochorismate synthase pathway seems not to be a major driver of SA accumulation because the expression pattern of genes involved in the isochorismate synthase pathway does not correlate with SA contents (Xiao et al., 2021). JA is a lipid-derived phytohormone produced via α-linolenic acid metabolism (Wasternack and Feussner, 2018). SA and JA phytohormones induce resistance against different classes of attackers. While SA generally mediates defenses against (hemi)-biotrophic pathogens, JA mediates the response against necrotizing pathogens, wounding, and insects (N. Li et al., 2019). SA and JA can work antagonistically (Hou and Tsuda, 2022; Figure 2). When JA signaling is upregulated, SA signaling is suppressed. This results in a trade-off for the resistance against biotrophic pathogens when the defense against necrotizing pathogens is upregulated and vice versa (Pieterse et al., 2012).

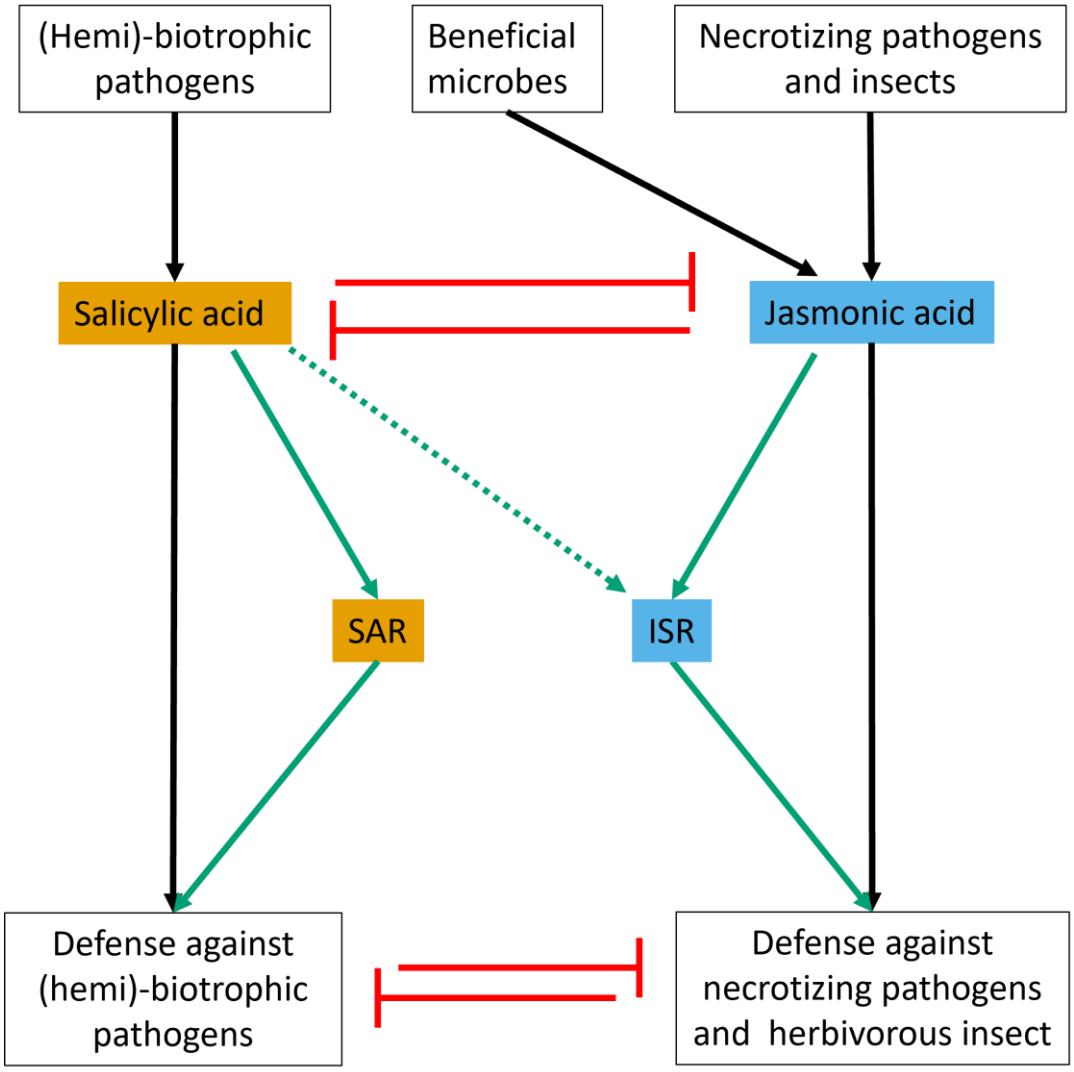

Figure 2 Simplified defense signaling regulated by salicylic acid and jasmonic acid
(Hemi)-biotrophic pathogens induce salicylic acid-dependent signaling pathways and defense against (hemi)-biotrophic pathogens. Necrotizing pathogens and herbivorous insects induce jasmonic acid-dependent signaling pathways and defense against necrotizing pathogens and herbivorous insects. (Hemi)-biotrophic pathogens induce salicylic acid-dependent systemic acquired resistance (SAR). Beneficial microbes induce jasmonic acid-dependent induced systemic resistance (ISR). Black arrows indicate positive effects, and red inhibition lines represent negative effects. The dashed line indicates situational involvement of salicylic acid in ISR. Green arrow indicates systemic effects.

2.4.2. Systemic acquired resistance and defense against biotrophic pathogens is mediated by salicylic acid

Systemic defense mediated by SA is called “systemic acquired resistance” (SAR; Spoel and Dong, 2012). Systemic refers to uninfected, distant tissues of the plant. SAR is usually induced after a primary attack of a biotrophic pathogen and confers broad-spectrum resistance in systemic tissues against secondary infections (Conrath et al., 2015). SAR is associated with local and systemic SA accumulation (Vlot et al., 2009; Figure 2). In addition to SA, many other

secondary metabolites have been proposed to play a role in SAR signaling. Methyl salicylic acid can be transported via the phloem to distant tissues, where it is hydrolyzed into bioactive SA (Park et al., 2007). Furthermore, methyl salicylic acid can act as a volatile signal for defense induction or attrackt predators of herbivores (Rowen et al., 2017). The non-proteinogenic amino acid pipecolic acid and its bio-active derivative *N*-hydroxypipecolic acid were found to be essential for SAR (Y.-C. Chen et al., 2018; Hartmann et al., 2018). Similar to SA, pipecolic acid has various derivates with potential involvement in defense against biotrophic pathogens (Mohnike et al., 2023, 2021). In addition, there are also synthetic molecules (e.g., the SA structural analog acibenzolar-S-methyl [BTH]) that induce responses in plants similar to SA (Vallad and Goodman, 2004). However, most proposed signal molecules have not been clearly assigned to be a SAR mobile signal (Sun and Zhang, 2021).

In systemic tissues, the mobile signals induce the expression of pathogenesis-related (PR) proteins, especially PR1 (PATHOGENESIS-RELATED 1) and the antagonistic key regulators NPR1 and NPR3/4 (NONEXPRESSER OF PR GENES; Ding et al., 2018). SA can bind to NPR1 and NPR3/4, which leads to the activation of NPR1 and inhibition of NPR3/4 (Liu et al., 2020). In addition, the mobile signals activate MAP (MITOGENACTIVATED PROTEIN KINASE) kinase cascades (Conrath et al., 2015). The induced defense is, in the end, either achieved through direct activation of defense measures (described before) or through priming. Priming describes the state of a plant where it does not activate direct defenses but exhibits a faster and stronger defense response upon a later challenge, for instance, through increased sensitivity to phytohormones or the accumulation of enzymes ready to be activated posttranslationally (Conrath et al., 2006; De Kesel et al., 2021; Jung et al., 2009; Mauch-Mani et al., 2017).

2.4.3. Jasmonic acid mediates induced systemic resistance and defense against necrotizing pathogens and herbivorous insects

Compared to SA, JA activates a different kind of systemic defense (Ruan et al., 2019; Figure 2). On the one hand, JA induces systemic defenses during herbivorous insect feeding to limit damage in subsequent attacks. This is referred to as herbivore-induced resistance (Frost et al., 2008). In this process, JA is also proposed to be the mobile signal (Sun et al., 2011). On the other hand, JA is involved in “induced systemic resistance” (ISR). Contrary to SAR, ISR is induced by beneficial soil microbes (Pieterse et al., 2014a). ISR activates defenses against

necrotizing pathogens and insects (Pieterse et al., 2014a). However, there is evidence of negative effects on the defense against insects in plants associated with ISR-inducing microbes because they improve the nutritional status of their hosts, making the plant more attractive to insect herbivores (Pineda et al., 2013). Similar to SAR, ISR can induce direct defenses, for example, callose deposition (Van der Ent et al., 2009) or accumulation of phytoalexins (Hossain et al., 2008; Mathys et al., 2012). In addition, it can prime the plant for a more robust response to a subsequent attack (Mauch-Mani et al., 2017; Pieterse et al., 2014a). JA has many derivatives with different functions. These are collectively referred to as JAs. Important to mention are methyl jasmonic acid (MeJA) and jasmonoyl-isoleucine (JA-Ile). MeJA can act as a transportable intracellular transducer of defense responses but can also pass cell membranes and act as a volatile to activate defenses independent of transport within the plant (Farmer and Ryan, 1990; Ruan et al., 2019; Yu et al., 2018). JA-Ile is the bioactive form of JA for inducing JA-dependent defenses (Ruan et al., 2019). The *in planta* transport of mobile ISR signal(s) is still unclear. Even though JA, MeJA, and JA-Ile can be transported cell-to-cell and via the vascular bundle to distant tissues of the plant, they are also newly synthesized along the transport route and in systemic tissues (Heil and Ton, 2008; Larrieu and Vernoux, 2016; Thorpe et al., 2007).

On the molecular level, an essential component of JA-dependent defenses is COI1 (CORONATINE INSENSITIVE 1; Feys et al., 1994). COI1 was long thought to be the JA receptor until studies suggested that COI1 is a component of an E3 ubiquitin ligase, which is referred to as SCF^{COI1} (Xie et al., 1998). JA-Ile mediates the binding of SCF^{COI1} to JAZ proteins, making SCF^{COI1} and JAZ proteins co-receptors of JA signaling (Sheard et al., 2010). JAZs are repressors of JA signaling. Binding of SCF^{COI1} to JAZ results in the ubiquitination of JAZ and subsequent degradation via the 26s proteasome. Degradation of JAZ releases transcription factors and activates downstream genes (Chini et al., 2007; Thines et al., 2007; Yan et al., 2007). Two additional phytohormones modulate JA signaling: ethylene and abscisic acid (ABA). ISR and the general defense against necrotizing pathogens are modulated by ethylene via the ERF1 (ETHYLENE RESPONSE FACTOR 1) pathway, and the defense against insects is modulated by ABA via the MYC pathway. The two modulating phytohormones and their signaling pathways work antagonistically (Pieterse et al., 2012; Figure 3). Furthermore, in some interactions with beneficial microbes that induce ISR also, SA and SA-dependent components (e.g., PR proteins) are involved (Figure 2).

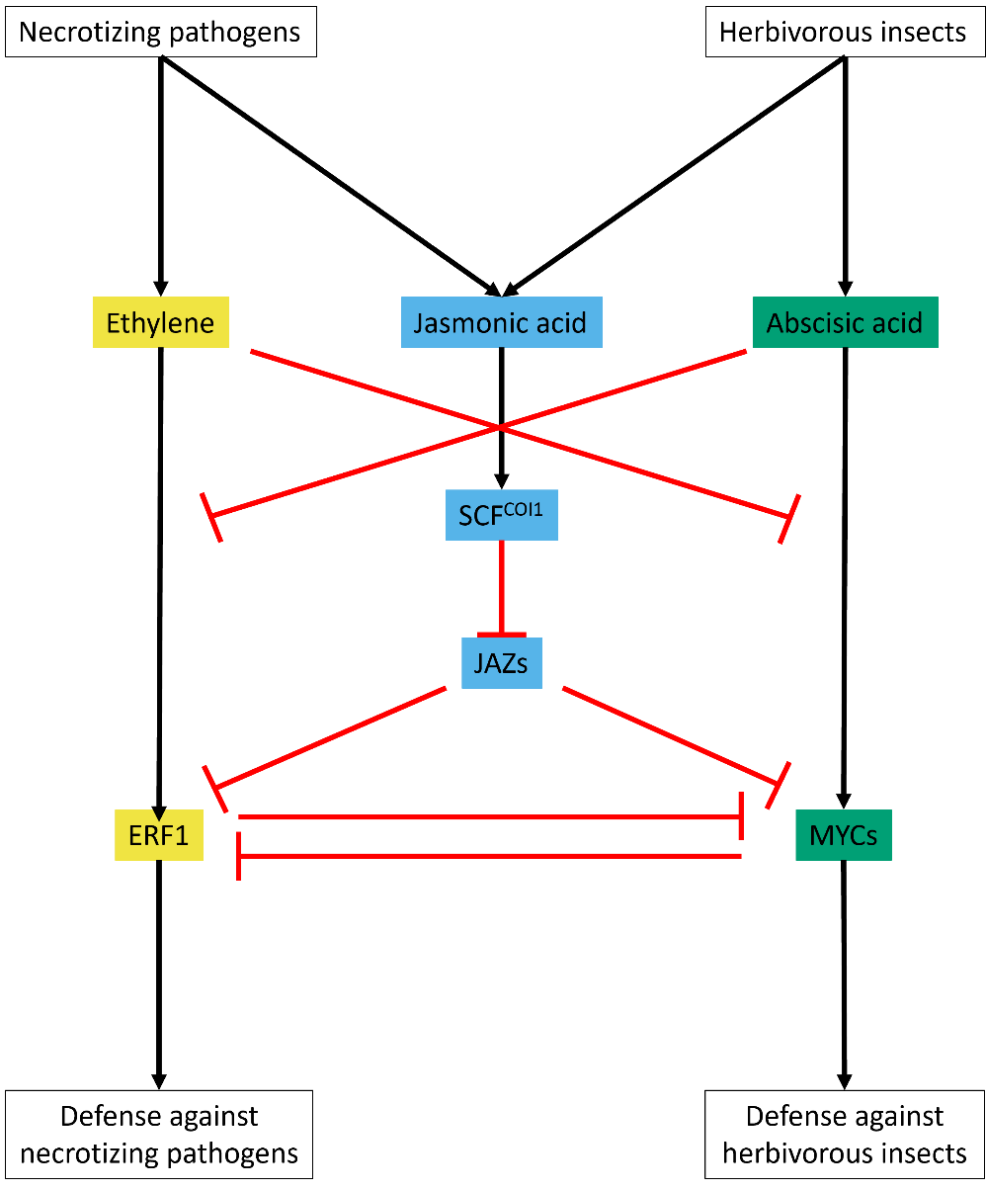

Figure 3 Simplified scheme of the modulation of the jasmonic acid signaling pathway by ethylene and abscisic acid

Necrotrophic pathogens induce JA- and ET-dependent signaling pathways; herbivorous insects induce JA- and ABA-dependent signaling pathways. The ET- and ABA-regulated branches of the JA pathway are mutually antagonistic. Arrows indicate positive effects, and red inhibition lines represent negative effects. SCF: SKP1, CULLIN AND F-BOX PROTEINS, COI1: CORONATINE INSENSITIVE 1, JAZ: JASMONATE ZIM-DOMAIN, ERF1: ETHYLENE RESPONSE FACTOR 1, MYC: MYC-related protein. Figure based on Pieterse et al., 2012.

2.5. Ectomycorrhizal fungi change defense responses in their hosts

2.5.1. Mycorrhizal fungi induce systemic resistance in their hosts

ISR by mycorrhizal fungi is often referred to as mycorrhiza-induced resistance and was mostly studied for AMF and their hosts (Cameron et al., 2013). AMF can induce resistance in below- and above-ground parts of the plant against phytopathogenic nematodes (de Sá and Campos, 2020; Liu et al., 2012), bacteria (Kamble and Agre, 2014; Miransari, 2011), fungi (Gallou et al., 2011; Steinkellner et al., 2012), and insects (Jiang et al., 2021; Shafiei et al., 2022). The molecular processes behind arbuscular mycorrhiza-induced resistance have been studied intensively (Kadam et al., 2020). Mycorrhiza-induced resistance by EMF is less studied, but various effects of EMF colonization on the performance of insects have been described (Dreischhoff et al., 2020; Schädler and Ballhorn, 2017). Even though the mechanisms for inducing and maintaining the defense by EMF are not well understood, there is evidence for local and systemic defense-related processes influenced during EMF symbiosis.

2.5.2. EMF affect local defense in roots

EMF and their hosts exchange a vast array of molecules during the establishment of the symbiosis, including flavonoids, auxin, and small RNAs (Felten et al., 2009; Garcia et al., 2015; Wong-Bajracharya et al., 2022). In addition, a massive number of small secreted proteins are induced during EMF colonization (de Freitas Pereira et al., 2018; Doré et al., 2015; Vincent et al., 2012). The small secreted protein *Lb*MiSSP7 from *L. bicolor* is an example of their effects on host defense. It interacts locally in *P.* × *canescens* roots with JAZ6 and stabilizes this protein (Plett et al., 2014). Thus, by stabilizing *P.* × *canescens* JAZ6, the JA signaling pathways are locally suppressed (Figure 4). In addition, MiSSP7 increases the transcript abundance of auxin-responsive genes in root tissues (Figure 4). Auxin signaling shares commonalities with JA signaling, which are essential for defense induction (Kazan and Manners, 2009). Furthermore, *L. bicolor* reduces the sensitivity of poplar roots to exogenous jasmonic acid and suppresses the activation of genes likely involved in cell wall remodeling and defense (Basso et al., 2020).

Chitin-related components can induce local responses. Lipochitooligosaccharides and chitin oligomers are components of the complex Myc factors. Rhizobacteria and AMF use Myc factors to communicate with their hosts (Maillet et al., 2020; Sun et al., 2015). *L. bicolor* also produces lipochitooligosaccharides which activate the common symbiosis pathway, including calcium-spiking (Cope et al., 2021, 2019). Calcium spiking also plays a role in defense

responses (Yuan et al., 2017). These local responses are often only transient and may be suppressed in later stages of colonization (Bouffaud et al., 2020; Le Quéré et al., 2005; Tarkka et al., 2013).

Further evidence that chitin might play a role in ectomycorrhizal defense induction was gained when *Arabidopsis* roots were treated with *L. bicolor*. Heat-killed *L. bicolor* and chitin treatment on *Arabidopsis* roots reduced *Trichoplusia ni* weight gain, similar to living *L. bicolor* (Vishwanathan et al., 2020). *At*CERK1 was necessary for *L. bicolor*-mediated effects on the weight gain of the caterpillars feeding on *Arabidopsis* (Vishwanathan et al., 2020). It is known that during EMF colonization, chitinases, enzymes that hydrolyze glycosidic bonds of chitin, are induced (Albrecht et al., 1994a, 1994b, 1994c; Sauter and Hager, 1989). Thus, it is conceivable that chitin can activate defense responses in the EMF-host interaction. Studies on the role of *Os*CERK1 in the interaction of AMF and rice showed that it plays a double role in defense and AMF symbiosis establishment (Huang et al., 2020; X. Zhang et al., 2015). Whether CERK1 plays a role in EMF symbiosis development or EMF-induced systemic changes in host plants like poplar is unknown. Investigating the roles of CERK1 and chitin in EMF-host interactions is necessary to transfer knowledge gained from the non-host interaction to the host interaction. Finding the initial signal receptor, which subsequently activates defenses in systemic tissues, can help to find the molecular signaling processes behind the defense induction.

2.5.3. The systemic signal in systemic ectomycorrhizal defense is unknown

In order to establish systemic resistance in above-ground tissues, an inter-organ signal is required. It might be that the local defense responses induce a mobile signal which subsequently travels to above-ground tissues, through the xylem, phloem, or as a volatile. Xylem and phloem sap contain not only water and nutrients but also many compounds (Notaguchi and Okamoto, 2015; Shabala et al., 2015), such as phytohormones (Kasper et al., 2022; Park et al., 2007; Schachtman and Goodger, 2008; Thorpe et al., 2007), proteins (Ligat et al., 2011; Z. Zhang et al., 2015), peptides (Okamoto et al., 2013; Pearce et al., 1991), and (small) RNAs (Begheldo et al., 2015; Thieme et al., 2015). In AMF and rhizobia symbiosis, specific small peptides transported via the xylem are required to establish symbiosis (Le Marquer et al., 2019; Okamoto et al., 2013). A multi-omics study found metabolites such as flavonol rhamnetin, which has antimicrobial properties (Papp, 2005), and proteins such as SAR

long-distance signal DEFECTIVE IN INDUCED RESISTANCE1 (Shah and Zeier, 2013) enriched in the xylem sap of ectomycorrhizal poplar compared to non-inoculated poplar but could not identify the mobile signal required for systemic effects (Kasper, 2020).

The signal might not be transported in the plant but may be volatile. It is known that EMF emit volatile organic compounds (VOCs). VOCs are undirected signals released into the air and serve the communication between plants and fungi (Schulz-Bohm et al., 2017; Werner et al., 2016). For example, β-caryophyllene is released, which in leaves mounts plant defenses against bacterial pathogens (Hammerbacher et al., 2019). VOCs emitted by EMF influence genes that are also induced during defense responses, for example, JAZ proteins (responsive to wounding and JA) or WRKY40 transcription factor, which is responsive to chitin and MeJA (Dreischhoff et al., 2020).

Finding the initial receptor which leads to systemic defense induced by EMF might help to reveal the systemic signal.

2.5.4. Components of JA- and SA-dependent systemic defenses mediate ectomycorrhizal-induced defense

The AMF-induced defense relies on SA and JA signaling components. AMF induce priming in their hosts (Pozo and Azcón-Aguilar, 2007), marked, for instance, by increased transcript abundance of the SAR components *PR1* and *NPR1* (Cameron et al., 2013). Furthermore, AMF increase the transcript abundance of genes involved in JA-signaling, for example, MYB transcription factors, *COI1*, and the JA synthesis enzymes *ALLENE OXIDE CYCLASE* and *ALLENE OXIDE SYNTHASE* (Jung et al., 2012; Pozo and Azcón-Aguilar, 2007).

A literature survey suggests that EMF induce components of SA- and JA-dependent defenses in leaves (Dreischhoff et al., 2020). JA-mediated signaling pathway transcripts were enriched in leaves of poplar colonized by *L. bicolor* (Figure 4; Kaling et al., 2018) and in the non-host interaction of *L. bicolor* and *Arabidopsis, coi1* mutants could not mount defenses against caterpillars after *L. bicolor* treatment (Vishwanathan et al., 2020). So far, increased levels of JAs after EMF treatment were not detected (Luo et al., 2011; Vishwanathan et al., 2020).

SA signaling was enhanced through increased transcript abundance of NPR1, which is required for SA perception (Liu et al., 2020) in the leaves of EMF-colonized poplars compared to non-inoculated plants (Kaling et al., 2018). From the non-host interaction of *Arabidopsis* and

L. bicolor, there is evidence that NPR1 and negative SA signal regulators NPR3/4 (Ding et al., 2018) participate in the effect which reduces the larval weight gain (Vishwanathan et al., 2020). Treatment of *Arabidopsis* roots with *L. bicolor* and chitin caused phosphorylation of MAP kinases 3, 4, and 6, which are important for SAR (Figure 4; Beckers et al., 2009; Vishwanathan et al., 2020). Poplar colonized by the ectomycorrhizal fungi *Hebeloma mesophaeum* had increased SA levels similar to the SA levels after rust infection (Pfabel et al., 2012).

As demonstrated, there is no clear picture of the signaling pathways involved in ectomycorrhizal-induced defense in leaves. JA- and SA-dependent signaling are involved, but the specific components inducing systemic resistance are still elusive. Studying the initial systemic events induced by EMF can shed light on the processes occurring in the induction of the systemic defense. Furthermore, investigation of the performance of different pathogens (e.g., necrotizing *Botrytis cinerea*) can give insights into the defense pathways induced by EMF.

2.5.5. EMF increases substances that can confer resistance in leaves

Many molecules that potentially confer systemic resistance accumulate in the leaves of ectomycorrhizal plants. EMF trigger changes in the leaf metabolome (Figure 4; Adolfsson et al., 2017; Cameron et al., 2013; Kaling et al., 2018; Kebert et al., 2022; Pfabel et al., 2012; Sillo et al., 2022). Phenolic or nitrogenous compounds and terpenes are important components that increase plant resistance (Wink, 2018). Phenolic compounds are often more abundant in mycorrhizal plants than in non-mycorrhizal plants (Baum et al., 2009; Gange and West, 1994; Pfabel et al., 2012; Schweiger et al., 2014). However, they are ineffective against adapted herbivores (Boeckler et al., 2014; Lindroth and St. Clair, 2013). Transcriptional down-regulation of enzymes required for producing carbon-based secondary compounds (e.g., tannins or flavonoids) in EMF-colonized poplar and upregulation of aldoxime production suggests that EMF can trigger a metabolic shift from carbon-based to N-based defense (Kaling et al., 2018). Nitrile-derived compounds are very effective against herbivorous insects (Irmisch et al., 2014, 2013). EMF change the VOCs composition of their hosts (Kaling et al., 2018; Sivaprakasam Padmanaban et al., 2022). VOCs like terpenes and terpenoids can either directly act on the fitness of the herbivores or attract predators of these insects (Loreto and Schnitzler, 2010; Pieterse et al., 2014a). The production of these VOCs in plants is downstream of JA signaling pathways (Ament et al., 2004; van Schie et al., 2007).

In addition to metabolites, EMF induce defense proteins (Figure 4). In leaves, the transcript and activity of chitinases increase after EMF colonization (Albrecht et al., 1994c; Kaling et al., 2018). In EMF colonized poplars and common hazel, the transcript abundance of a specific class of protease inhibitors, the Kunitz trypsin inhibitors (KTI), was increased (Kaling et al., 2018; Sillo et al., 2022). Protease inhibitors are an important class of biocidal proteins against herbivorous insects (Divekar et al., 2022). Protases are central enzymes in the digestive system of insects. Inhibition of gut proteases leads to a significant decrease in the fitness of these insects (Zhu-Salzman and Zeng, 2015). In addition, protease inhibitors have antimicrobial activity (Jashni et al., 2015). The enhanced expression of protease inhibitors has also been described for AMF-colonized plants (Schoenherr et al., 2019; Song et al., 2013).

All these metabolites and proteins can confer enhanced resistance toward insects by reducing insect fitness. An example of decreased fitness is that significantly fewer nymphs are produced by the birch aphid *Calaphis flava* on ectomycorrhizal birch (Nerg et al., 2008) or the poplar leaf beetle *Chrysomela populi* had reduced oviposition on ectomycorrhizal poplars (Kaling et al., 2018). However, the effects of EMF colonization on plant defenses are not always positive. EMF colonization can have no impact on insect fitness (Manninen et al., 1998) or have a negative effect (Thompson, 2022). This suggests that the effects EMF have on their hosts are very diverse.

In contrast to the defense induction by EMF against insects, the effect of EMF colonization on biotrophic and necrotizing pathogens is much less investigated. EMF inoculation alleviated the negative physiological changes of powdery mildew (biotrophic pathogen) infection in oak (Kebert et al., 2022). EMF-inoculation increased the resistance of Norway spruce against necrotizing *Heterobasidion* root rot but decreased defense against foliar necrotizing pathogens (Velmala et al., 2018). Until now, the direct link between the accumulation of defense metabolites and proteins induced by EMF and the impaired performance of insects is missing. Disentangling the signaling pathways induced by EMF can help to explain the diverse effects.

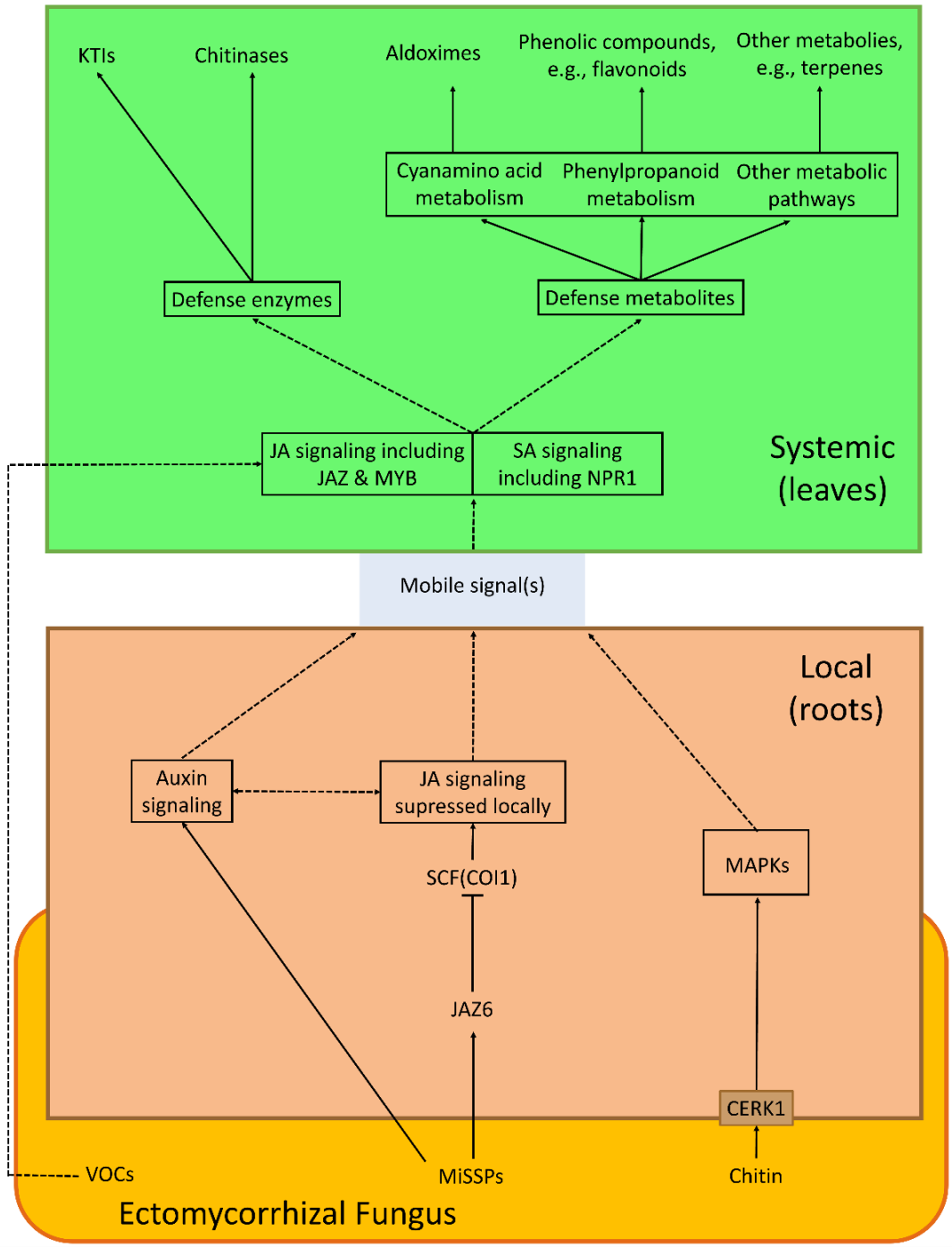

Figure 4 EMF-induced signaling cascade(s)

The figure summarizes signaling components induced by an ectomycorrhizal fungus (orange) in the root (brown) and leaves (green). Arrows represent interactions/connections (full lines: direct evidence, dashed lines: speculative). VOCs—Volatile organic compounds; JAZ6—JASMONATE-ZIM-DOMAIN PROTEIN 6; CERK1—CHITIN ELICITOR RECEPTOR KINASE 1; SCF(COI1) CORONATINE INSENSITIVE 1—Skp, Cullin, F-box containing complex; MAPKs—Mitogen-activated protein kinases; JA—Jasmonic acid; MYB—MYB DOMAIN PROTEIN; SA —Salicylic acid; NPR1 —NONEXPRESSER OF PR GENES 1; KTIs—Kunitz trypsin inhibitors. Figure modified from Dreischhoff et al., 2020.

2.6. Research questions

The overarching goal of this thesis was to enhance our understanding of systemic effects that occur in poplar leaves in response to mycorrhizal colonization with *L. bicolor*. Towards this aim, the initial transcriptional changes in systemic leaves were determined, a possible role of CERK1 in mediating the long-distance signal was tested, and the consequences of EMF for poplar susceptibility to a necrotizing pathogen were studied.

Specifically, the following questions were addressed:

- How does the systemic defense transcriptome change in leaves after initial *L. bicolor* contact and in the early phase of colonization on *Populus* × *canescens* roots? (4.1)

In poplar colonized with mature mycorrhizas, the leaf defense transcriptome is activated (Kaling et al., 2018). However, the time course in which these responses are stimulated is unknown. Here, an axenic system composed of *P.* × *canescens* and *L. bicolor* was used to avoid interference with other organisms. The transcriptional changes provided insights into the upregulation of defense signaling and defense metabolism. I selected and tested genes with increased transcript abundance as potential marker genes for systemic ectomycorrhizal defense induction.

- Are PcCERK1 and chitin key components for ectomycorrhizal-induced systemic defense responses in poplar? (0)

Since previous studies assigned a role to CERK1 and chitin in mediating *L. bicolor*-induced systemic resistance in the non-host *Arabidopsis*, it was obvious to investigate if *L. bicolor* also employed this pathway for systemic defense induction in the host plant poplar. For this purpose, poplar *cerk1* KO mutants, which became recently available (Muhr, 2022), were used. The stability of the transformants was confirmed, and their performance under axenic and greenhouse conditions was studied. Furthermore, the effects of root chitin application on systemic tissues were analyzed.

- Does *L. bicolor* induce systemic resistance against a necrotizing pathogen*?* (4.3 & 4.4)

To find out if transcriptional changes observed in systemic tissues have biological consequences, I strived to study pathogens on poplar leaves. A hurdle toward this goal was that no reliable bioassay for poplar pathogens was available. Therefore, the first task was to

select a suitable pathogen, and the second was to establish a bioassay before the impact of *L. bicolor* could be tested. Here, I focused on *Botrytis cinerea*, which is an opportunistic necrotizing pathogen that can infect more than 1,400 plant species, including poplar (Roca-Couso et al., 2021). It has been used for decades to study the effects of necrotizing fungi on plants, but a state-of-the-art bioassay for the interaction with poplar is missing (Bi et al., 2023). A *B. cinerea* strain was isolated from poplar leaves, and I established a quantitative method to determine B. cinerea growth (Dreischhoff et al., under revision). I studied the growth of *B. cinerea* in *P.* × *canescens* leaves using mycorrhizal and non-mycorrhizal plants.

3. Material and methods

3.1. Plant propagation

Populus × *canescens*, clone INRA 717 1B4 (INRA, Nancy, France), and the transgenic *Populus* × *canescens* lines *cerk1* KO 19 and *cerk1* KO 20, which are two independent *cerk1-like1* (Potri.002G226600) and *cerk1-like2* (Potri.014G156400) double knock-out lines generated by Muhr (2022; provided by Prof. Dr. Lipka and PD Dr. Teichmann, Department of Plant Cell Biology, University of Göttingen; Supplemental Table 1) were maintained using similar protocols as described by Müller et al. (2013b). The plants were propagated *in vitro* by micro cuttings and grown on half-strength Murashige and Skoog medium (Supplemental Table 2; (Murashige and Skoog, 1962) in 540 mL glass jars (J. Weck, Wehr-Öflingen, Germany) and sealed with Leucopore tape (Duchefa Biochemie, Haarlem, Netherlands). The plants were kept at 23 °C to 24 °C and 60 to 85 µE m^{-2} s^{-1} photosynthetically active radiation (PAR; L18W/840, Osram, Munich, Germany). After four weeks, rooted plantlets were used for further processing. Plants were propagated every four weeks for maintenance and multiplication.

3.2. *Laccaria bicolor* propagation and cultivation

Laccaria bicolor, diploid strain S238N (Di Battista et al., 1996) was propagated by transferring nine 5 mm x 5 mm agar plugs with vegetative mycelium upside down to a 12 cm x 12 cm plate (Greiner, Kremsmünster, Austria) filled with 50 mL modified-Melin-Norkrans-Sucrose medium with 10 g sucrose (Supplemental Table 3; M-MMNS; Kulmann, 2005). The fungus was cultivated at 23 °C in darkness and propagated every four weeks for maintenance.

One hundred milliliter M-MMN (Supplemental Table 3, agar omitted) were inoculated with 20 agar plugs with vegetative mycelium in 500 mL glass flasks to cultivate *L. bicolor* in liquid medium. The liquid cultures were incubated at 23 °C and 100 rpm on a rotary shaker in darkness for three weeks.

3.3. Co-cultivation of *L. bicolor* and *poplar* (sandwich culture)

Sandwich cultures were adapted from Müller et al. (2013b). Cellophane membrane strips (5.5 cm x 11.5 cm, Deti, Meckesheim, Germany) were boiled twice for one hour in ddH_2O and washed after each cooking step with ddH_2O. Thereafter, the strips were autoclaved in ddH_2O twice at 121 °C and 2.2 bar for 20 minutes (HST 6x6x6, Zirbus technology, Bad Grund, Germany). The membrane strips were placed on M-MMNS medium with 10 g sucrose and subsequently inoculated with *L. bicolor* by transferring eight 5 mm x 5 mm agar plugs with

vegetative mycelium onto the cellophane at equal distances to each other. The plates were sealed with parafilm (Bemis Company, Neenah, USA). Cellophane membranes were treated in the same manner but without plug inoculation and used as controls. The *L. bicolor*-inoculated or control cellophane membranes were incubated for four weeks at 23 °C and constant darkness.

Plates (12 cm x 12 cm; Greiner) were filled with 90 mL M-MMNS with 2 g saccharose for the sandwich culture. After solidification, the medium was cut in half, and one half was transferred to a new plate. The half-filled medium was subsequently covered with a fresh (cooked and autoclaved) cellophane membrane strip prepared as described above (5.5 cm x 11.5 cm, Deti). The roots of a four-week-old poplar plantlet from *in vitro* culture were placed on the cellophane membrane, and the shoot faced into the empty part of the Petri dish (Figure 5A). Afterward, mycelium-covered cellophane membranes, from which the initial inoculation plugs had been removed, were placed upside down onto the roots and gently pressed to ensure contact between the mycelium and the roots (Figure 5). A non-inoculated cellophane membrane was used for controls. The plates were sealed with parafilm (Bemis Company) for the RNA sequencing experiment (3.10, 4.1) and the first two replicates of the *cerk1* KO sterile gene transcript abundance experiment (3.13, 4.2.5) and with Leucopore tape (Duchefa Biochemie) for all other experiments. The bottom (root) part of the plate was enwrapped in aluminum foil (Carl Roth, Darmstadt, Germany). Plant and fungus were co-cultivated for one day to three weeks at 22 °C at day, 20 °C night temperature, 60 % air humidity, 100 µE m^{-2} s^{-1} PAR 16 h/8 h day/night regime in a cultivation chamber (AR-75L, Percival Scientific, Perry, USA). The light source was Alto 32 Watt (Philips, Amsterdam, Netherlands) and LG4507.4 (Megaman, Langenselbold, Germany). Individual plates were randomized regularly.

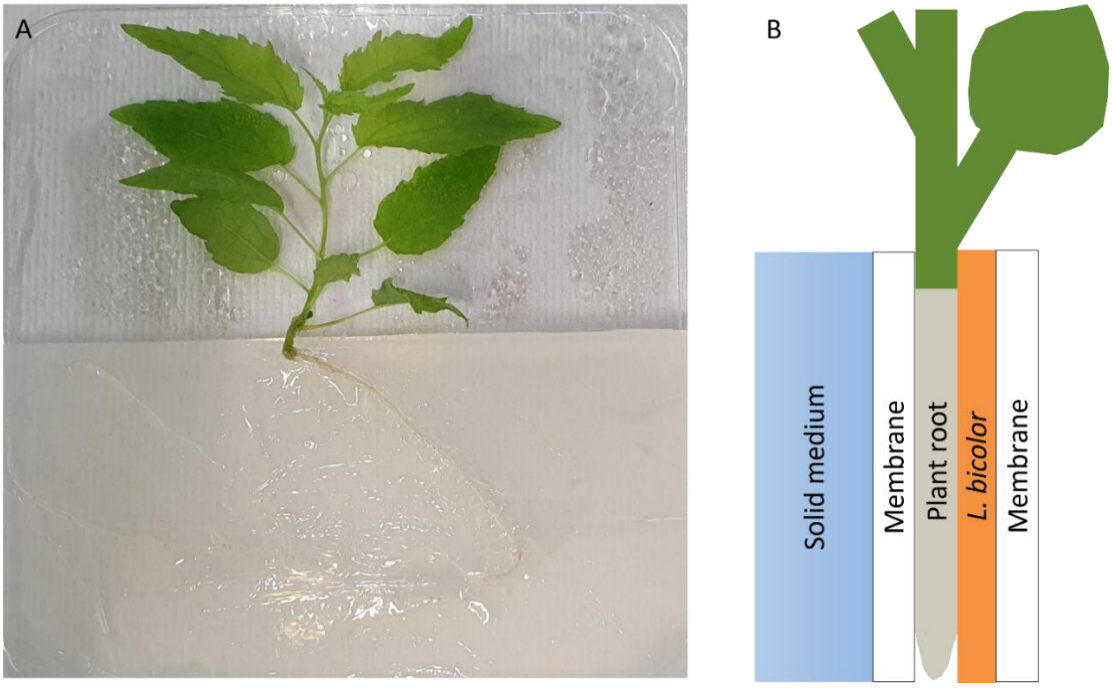

Figure 5 Scheme of the *P.* × *canescens* and *L. bicolor* co-cultivation (sandwich culture)
The sandwich set-up was placed in a Petri dish (A). The scheme shows the stacking order of the components to create the sandwich system in a Petri dish (B).

3.4. Plant cultivation in the greenhouse

Four-weeks-old, rooted *P.* × *canescens* plantlets from *in vitro* culture were potted in 3 L pots (Lamprecht-Verpackungen, Göttingen, Germany) containing soil (Fruhstorfer Erde "Type N," Hawita Gruppe, Vechta, Germany) when used for greenhouse experiments without *L. bicolor*. The plants were covered with a plastic beaker. After one week, the beaker was gradually lifted and removed two weeks after potting. The plants were watered daily with tap water and cultivated under ambient greenhouse conditions, as specified below.

Sandwich cultures described above (3.3) were prepared to generate mycorrhizal and non-mycorrhizal plants for experiments with *L. bicolor*. After three weeks, mycorrhizal and non-mycorrhizal plants were potted in a sand-soil mixture in 3 L pots (Lamprecht-Verpackungen) and covered with a plastic beaker. The beaker was gradually removed, as described above. Sand with 0.71 mm to 1.21 mm particle size and sand with 0.4 mm to 0.8 mm particle size (Dorfner, Hirschau, Germany) was mixed 1:1 (v/v), washed and twice autoclaved (HST 6x6x6, Zirbus technology). The sand mixture was blended with twice autoclaved soil (Fruhstorfer Erde "Nullerde," Hawita Gruppe) in a ratio of 8:2 (v/v). The sand-soil mixture was inoculated three weeks before potting with either 500 mL (five flasks) culture homogenized three-week-old liquid culture of *L. bicolor* for 30 L sand-soil mixture or 500 mL fresh M-MMNS medium for 30 L sand-soil mixture for control. Plants were watered daily with nutrient solutions with a low

nitrogen supply (Supplemental Table 4; Langenfeld-Heyser et al., 2007; Matzner et al., 1982). All greenhouse-grown poplar were kept under the following conditions: The temperature variations followed roughly outdoor conditions except that heating was switched on when the temperature fell below 21 °C, and aeration started when the air temperature exceeded 23 °C. Thereby, the air temperature ranged from 13 °C to 41 °C. The plants received ambient light conditions with additional illumination of 150 µE m^{-2} s^{-1} PAR (163 15L34, Adolf Schuch, Worms, Germany) with a 16/8 h day/night rhythm. Individual plants were randomized regularly.

3.5. Growth measuring and biomass determination of poplar

Growth measurements started one week after the beaker had been removed from the poplars (*P.* × *canescens*) in the greenhouse. Plant stem height was measured with a folding ruler, and stem diameter (at the level of the pot's rim) was measured with an electronic caliper (Toolland, Velleman, Gavere, Belgium). Leaves were counted, considering only fully developed leaves with a length of the leaf blade longer than 2.5 cm. Measurements were conducted weekly, and the final measurements were performed on the day of harvest. Stems and Leaves, including petioles, were weighed to determine whole-plant fresh weight before freezing in liquid nitrogen. In addition, roots were washed to remove sand and soil, padded dry with paper tissues, and weighed before freezing in liquid nitrogen.

3.6. Spectrometric measurements of leaf chlorophyll and specialized metabolites

The indices for chlorophyll, flavone, anthocyanin, and nitrogen balance of the fourth fully developed leaf were measured weekly with a DUALEX optical sensor (Metos, Weiz, Austria) at the wavelengths of 375 nm, 500 nm, 650 nm, 710 nm, and 800 nm. The sensor's signals were transformed into index units, according to Cerovic et al. (2012).

3.7. Gas exchange measurements

Gas exchange was measured weekly. A portable photosynthesis system (LI-6800, LI-COR Biosciences, Bad Homburg, Germany) was used. The clamp of the instrument was attached to the fourth fully developed top leaf. Measurements of photosynthesis rate, stomatal conductance, transpiration rate, and intercellular CO_2 were conducted under saturating light conditions provided by the photosynthesis system (PAR of 800 µE m^{-2} s^{-1}) at ambient CO_2 concentrations of 397 ± 1 ppm and a mean leaf temperature of 30.2 ± 1 °C. Each leaf was

acclimated to the measuring conditions for 60 seconds and then measured three times in intervals of 60 seconds.

3.8. Determination of mycorrhizal colonization

Three root segments were collected from the fine roots of each plant. The root segments were stored in 10 % glycerol at -20 °C until processing. Root tips were observed under a stereomicroscope (DFC 420, Leica Camera AG, Wetzlar, Germany) and inspected for vitality of root tips. Only a minimal number of root tips were found not vital. Therefore, dead root tips were not considered. Approximately two hundred root tips per sample were inspected and categorized as mycorrhizal (swollen brownish tip) or non-mycorrhizal (white tip; Figure 6). The mycorrhization rate was calculated according to the equation:

$$mycorrhization\ rate\ (\%) = \frac{n\ mycorrhized\ root\ tips}{n\ total\ vital\ root\ tips} \times 100$$

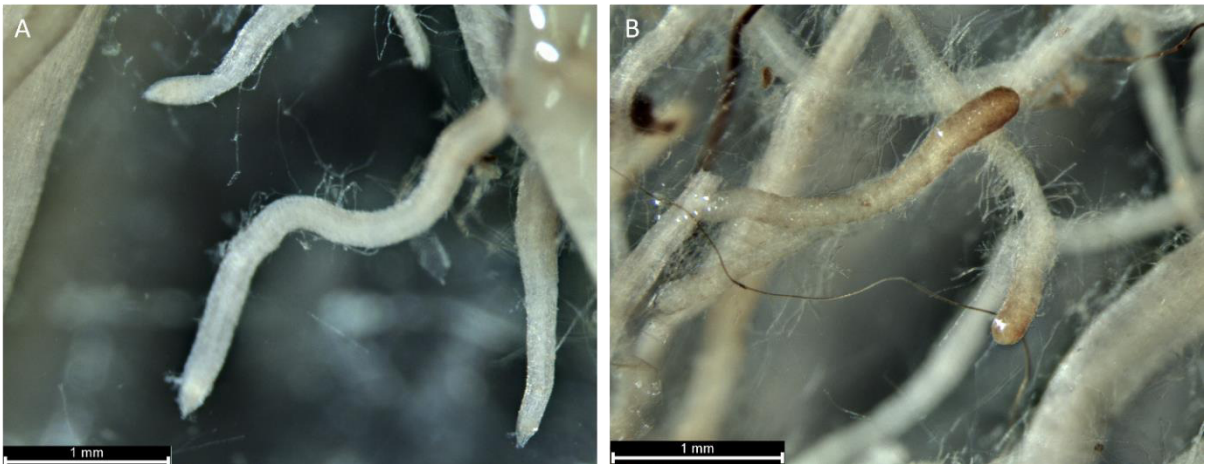

Figure 6 Pictures of non-mycorrhizal (A) and mycorrhizal (B) root tips
Roots from greenhouse-grown poplars (*P.* × *canescens*) tips were stored in 10 % glycerol at -20 °C and subsequently observed in water under a stereomicroscope. Non-mycorrhizal root tips are white and pointy (A), and mycorrhizal root tips are round, swollen, and brownish (B). Scale bar = 1 mm.

3.9. Sectioning and histological staining of root tips

Root tips were harvested (from further sandwich culture experiments 3.13) after seven days and stored in FAE (37 % formalin/glacial acetic acid/70 % ethanol; 5:5:90 (v/v)) until further processing. The samples were transferred individually to 2 cm x 2 cm wells of a sixteen-well plate (Greiner). The wells were then filled with liquid 5 % agarose (Duchefa Biochemie), closed

with a lid, and solidified at 4 °C overnight. During initial solidification, the samples were pushed down several times with forceps to prevent floating.

The agarose blocks containing the root samples were removed from the well plate, orientated for cross-sectioning, and trimmed with a razor blade (Wilkinson Sword, Solingen, Germany). The vibratome VT1200 (Leica Microsystems, Wetzlar, Germany) was used to produce cross sections of 30-50 µm thickness with a cutting speed of 1 mm sec^{-1} and an amplitude of 0.5 mm. For this purpose, the vibratome was equipped with a double-edge bendable razor blade (Wilkinson Sword). The cross-sections were then submerged in a solution containing 10 µg mL^{-1} wheat germ agglutinin, Alexa Fluor 488 conjugate (Thermo Fisher Scientific, Waltham, USA), and 10 µg mL^{-1} propidium iodide (Thermo Fisher Scientific) in phosphate-buffered saline buffer (NaCl 137 mmol L^{-1}, KCl 2.7 mmol L^{-1}, Na_2HPO_4 10 mmol L^{-1}, KH_2PO_4 1.8 mmol L^{-1}) for 15 min. After staining, the cross-sections were washed once with phosphate-buffered saline buffer and then transferred to specimen slides. They were mounted with ROTIMount FluorCare (Carl Roth), a medium for fluorescence microscopy. The sections were viewed at 200x and 400x magnification with a Zeiss Axio Observer Z1 microscope (Carl Zeiss, Oberkochen, Germany), using filters with the wavelengths for excitation at 493 nm and emission at 520 nm for wheat germ agglutinin, Alexa Fluor 488 conjugate and with excitation at 538 nm and emission at 617 nm for propidium iodide. Photos were taken with an AxioCam MRc camera (Carl Zeiss).

3.10. mRNA sequencing experiment

Four days before the assembly of the sandwich cultures (3.3), rooted plantlets were transferred from the culture room into the cultivation chamber (AR-75L, Percival Scientific) to 22 °C at day, 20 °C night temperature, 60 % air humidity, and 100 µE m^{-2} s^{-1} PAR with 16 h/8 h day/night regime. At the starting point (t0), the sandwich cultures were assembled (as described under 9.3.3), and the leaves were immediately harvested. In addition, leaves were harvested directly from the *in vitro* culture. The third, fourth, and fifth fully developed leaves were pooled, frozen in liquid nitrogen, and stored at -80 °C until further processing. Further plates were assembled to conduct a time-course experiment with the sandwich cultures. The plates were placed upright in the cultivation chamber (AR-75L, Percival Scientific). After one, two, four, and seven days, plants were harvested, and leaves were sampled as described

above. The leaves were harvested three hours after the start of the light cycle. Three independent experiments were conducted, each with n = 6 plants per treatment.

3.11. Phytohormone treatment under greenhouse conditions

P.× *canescens* were cultivated in soil (Fruhstorfer Erde "Type N," Hawita Gruppe) in the greenhouse as described above but irrigated daily with Long Ashton solution (Supplemental Table 5). After ten weeks, plants were placed in different greenhouse cells per treatment. Methyl jasmonate (200 µM; MeJA; Sigma-Aldrich, Taufkirchen, Germany) and aminocyclopropane-1-carboxylic acid (100 µM; ACC; Sigma-Aldrich) were dissolved in ddH_2O supplemented with 0.01 % Tween-20 (Sigma-Aldrich). For these treatments, 0.01 % Tween-20 in ddH_2O served as control. Acibenzolar-S-methyl (1 mM; BTH; Sigma-Aldrich) was dissolved in 10 % methanol (Sigma-Aldrich) supplemented with 0.01 % Tween-20. The corresponding control treatment was 10 % methanol with 0.01 % Tween-20. The plants for individual phytohormone treatments were placed in separate greenhouse cells to prevent cross-contamination of phytohormones. An 80 L autoclave bag (Sarstedt, Nümbrecht, Germany) was cut open at both sides, and one plant was inserted into one bag to apply the phytohormones. The plants were sprayed from all sides with the respective phytohormone until runoff (approximately 25 mL per plant) using a 250 mL spray bottle suitable for overhead spraying (Carl Roth). Then, the bags were closed, and the plants were incubated for four hours. The bags were removed, and the plants were incubated for another four hours (eight hours of treatment in total) under greenhouse conditions (3.4) before harvesting the first fully developed leaf. A second batch of plants was used to harvest the first fully developed leaf after 20 hours (i.e., 24 hours of treatment in total). The leaves were immediately frozen in liquid nitrogen and stored at -80 °C until further processing.

3.12. MeJA treatment in sterile conditions

P. × *canescens* plantlets were cultivated, and sandwich systems (with and without *L. bicolor*) were assembled as described above (3.3). After ten days, plates were opened, and half a cotton pad (approximately 2 cm x 2 cm; B. Braun, Melsungen, Germany) was placed inside the plate (not touching anything but the plate) and attached to the plate with tape. Afterward, 1 mL of either 200 µM methyl jasmonate in ddH_2O or ddH_2O was pipetted onto the cotton pad. Plates were sealed with Leucopore tape (Duchefa Biochemie). MeJA-treated and control plants were kept in separate cultivation chambers (AR-75L, Percival Scientific) under the above

conditions (3.3) to prevent volatile MeJA from affecting control plants. The third, fourth, and fifth fully developed leaves were harvested, pooled, frozen in liquid nitrogen, and stored at -80 °C until further processing.

3.13. Further sandwich culture experiments with *L. bicolor*

P.× *canescens* plantlets and *L. bicolor* sandwich cultures were assembled and cultivated as described under 3.3. After seven and 14 days, the third, fourth, and fifth fully developed leaves were pooled, frozen in liquid nitrogen, and stored at -80 °C until further processing. The leaves were harvested three hours after the start of the light cycle. Two independent experiments were conducted with WT and *cerk1* KO 19, and three independent experiments for WT, *cerk1* KO 19, and *cerk1* KO 20, each with n = 6 plants per treatment.

3.14. Chitin agar treatment

The chitin stock was prepared as follows: Ten milligrams of chitin per milliliter ddH_2O were ground with mortar and pestle for several minutes to create a homogenous slurry (10 mg mL^{-1} stock). M-MMNS medium was prepared as described above (3.2), and 100 µg mL^{-1}, 300 µg mL^{-1}, or 1000 µg mL^{-1} chitin (from shrimp shell, BioReagent grade, Lot#SLBN7584V, C9752-5G, Sigma-Aldrich) from a 10 mg mL^{-1} stock was added before autoclaving the medium.

Ninety milliliters of the chitin-supplemented agar were poured into 12 cm x 12 cm Petri dishes (Greiner). The autoclaved medium was allowed to cool to achieve a minimum solidification time in the plates to prevent chitin from sinking. Before pouring, the medium was shaken to distribute the chitin homogenous in the medium. After solidification, the medium was cut in half, and one half was transferred to a new plate. The plates were assembled similarly as before (3.3). The roots of a four-week-old *P.* × *canescens* plantlet from *in vitro* culture were placed directly onto the chitin agar. A cellophane membrane strip (boiled and autoclaved twice as described above) was used to fix the root onto the agar to ensure contact of the roots and chitin medium. M-MMNS agar without chitin was used to assemble control plates with poplars. The plates were sealed with Leucopore tape (Duchefa Biochemie). The bottom (root) part of the plate was covered with tin foil. After assembly, the plates were placed upright in the cultivation chamber (AR-75L, Percival Scientific). Plants were treated for eight hours up to one week at 22 °C at day, 20 °C at night, 60 % air humidity, 100 µE m^{-2} s^{-1} PAR 16 h/8 h day/night regime. The light source was Alto 32 Watt (Philips, Amsterdam, Netherlands) and LG4507.4 (Megaman, Langenselbold, Germany).

3.15. Soil injection treatments

L. bicolor liquid culture was prepared as described above (3.2). After three weeks, the culture from 20 flasks was harvested by sieving the mycelium balls through a metal sieve (mesh size 1.5 mm) and collecting the liquid culture media. The mycelium was washed three times in sterile ddH_2O. Thereafter, the mycelium was transferred to approximately 20 mL of sterile 10 mM $CaCl_2$ solution. The culture was homogenized (Ultra-Turrax, IKA-Werke GmbH & CO. KG, Staufen, Germany) for 30 seconds at 8000 rpm. The optical density at 600 nm of three technical replicates was measured in a photometer (Biophotometer 6131, Eppendorf, Hamburg, Germany). The mean was calculated, and optical densities were adjusted to 0.1 for living *L. bicolor* treatments (*Lb*). A suspension with an optical density of 2 was heat-treated for 25 minutes in a water bath at 80 °C for dead (heat-killed) *L. bicolor* treatment (*LbHK*). The liquid culture medium was centrifuged for 5 minutes at 2000 rpm to remove debris. The supernatant was collected, and 1 M $CaCl_2$ was added to reach a final concentration of 10 mM $CaCl_2$ (*LbSu*). Chitin (from shrimp shell, BioReagent grade, Lot#SLBN7584V, C9752-5G, Sigma-Aldrich) was ground with mortar and pistil in ddH_2O to create a slurry with 10 mg chitin mL^{-1}. The slurry was mixed with 10 mM sterile $CaCl_2$ to reach a final chitin concentration of 500 µg mL^{-1}. An autoclaved 10 mM $CaCl_2$ solution served as a control. Fresh M-MMNS plates were inoculated with the living, heat-killed, or supernatant of *L. bicolor* cultures to check for the growth of the fungus. After seven days, the homogenized *L. bicolor* suspension showed fungal growth, while no growth was visible for the other two treatments.

Ten-week-old *P.* × *canescens* potted in a 3 L soil-sand mixture (described above 3.4) were used for the experiments. The *Lb, Lb*HK, *Lb*Su, chitin, and control solutions (20 mL) were injected into the soil at five points (5-7 cm deep) around the stem using a 60 mL syringe (B. Braun) equipped with a 10 cm needle (Carl Roth) with a diameter of 2 mm. The plants were treated again after five days and harvested eleven days after the first treatment. The 3rd fully developed leaf was harvested and used for qRT-PCR analysis.

3.16. *Botrytis cinerea* infection experiments

The *B. cinerea* CBS 261.71 strain was used for this study (see 4.3). Cultivation, infection assay, and damage quantification as necrotic leaf area and fungal DNA were determined, as described in chapter 4.3.

Ten-week-old *P.* × *canescens* plants were cultivated in a soil-sand mixture in the greenhouse (3.4) and treated with the same preparations described above (3.15). After ten days, the treatments were repeated in the same manner. Eleven days after the second treatment (three weeks treatment in total), the 3rd fully developed leaf was inoculated with *B. cinerea*.

Sandwich cultures were prepared as described above, and plants were incubated with and without mycorrhiza for ten days. Subsequently, the third leaf was inoculated with *B. cinerea*. The leaf area of the infected leaves was measured using ImageJ (Schindelin et al., 2012).

3.17. Insect feeding assay

Helicoverpa armigera eggs were obtained from Prof. Dr. Michael Rostás (Agricultural Entomology, Department for Crop Sciences, University of Göttingen). The eggs were allowed to hatch, and larvae were reared in a plastic container with an artificial diet (Gergs and Baden, 2021) at 25 °C and 60 % air humidity in a cultivation chamber (AR-75L, Percival Scientific, Perry, USA) with 16 hours of light per day. The third instar was reached after seven days. At this point, 20 larvae were weighed on an analytical balance (Sartorius, Göttingen, Germany) to determine the mean start weight. Leaf disks (⌀ 27 mm) from 10-week-old greenhouse-grown and outdoor-grown poplar were punched out and placed in 8 cm glass Petri dishes (Carl Roth) with wet filter paper (Macherey-Nagel, Düren, Germany). One larva was placed on the leaf disk, and the plates were sealed with Leucopore tape (Duchefa Biochemie). The plates were returned into the cultivation chamber and kept in the same conditions under which the larvae were reared. After two days, the weight of each larva was determined on an analytical balance (Sartorius), and the weight difference to the mean starting weight was calculated. Greenhouse-grown poplars for this experiment were cultivated in soil as described above (3.4). Outdoor-grown poplars were grown in soil for four weeks in greenhouse conditions (3.4) and transferred outdoors for the next six weeks. The poplars were regularly watered with tap water.

3.18. RNA extraction

Frozen leaves were homogenized to a fine powder (Ball mill MM200 equipped with two 3 mm and one 4 mm steel ball, Retsch, Haan, Germany) for 90 seconds at 30 Hz while cooling with liquid nitrogen. RNA was extracted using the innuPrep Plant RNA kit (Analytik Jena, Jena, Germany) following the manufacturer's instructions with the only modification that the drying step was elongated to five minutes to ensure that no ethanol was on the column. The

concentration and purity of each sample (measured as absorbance ratios at 260/280 nm and 260/230 nm) were checked with a NanoDrop One spectrophotometer (Thermo Fisher Scientific). Afterward, the RNA of three biological samples per treatment and time point were pooled and adjusted to an RNA concentration of 100 ng μL^{-1}, resulting in one sample per independent experimental run (described under 3.9). The pooled samples from three experiments were used for the RNAseq experiment (described in 3.19).

RNA was extracted as described above and used directly without pooling for cDNA synthesis when used for qRT-PCR reactions (described in 3.21).

3.19. RNA sequencing

Quality control of the RNA, sequencing library preparation, and mRNA sequencing was carried out by NGS-Integrative Genomics (University Medicine Göttingen, Göttingen, Germany). The quality and integrity of RNA were assessed with the Fragment Analyzer (Advanced Analytical Technologies, Heidelberg, Germany). All samples had an RNA Integrity Number (RIN) of over 7.5 (Supplemental Table 6). Thirty samples were used (five time points, two treatments, and three experiments) for mRNA sequencing. Each sample represented a pool of three plants. Before sequencing, the samples were processed with the TruSeq RNA Library Preparation Kit v2, Set A (Illumina, San Diego, USA). Afterward, single-end sequencing was performed on a HiSeq4000 (Illumina) with 50 base pair reads and 21 - 42 Mio reads per sample. The exact reads per raw and processed sample are in Supplemental Table 6.

3.20. Bioinformatic analysis

The computational data processing and differential transcription analysis were carried out by Dr. Johannes Ballauff (Department of Forest Botany and Tree Physiology, University of Göttingen, Germany)

After removing specific Illumina sequencing adapters, individual read cutting by quality score and quality filtering was performed using fastp v.0.21.0 (S. Chen et al., 2018) with default cutting and filtering options enabled. Sequence with an average quality score < Q20 in a sliding window of size four base pairs were cut from individual reads. Additionally, all reads with more than 40 % low-quality bases (< Q15) or more than five N bases were removed prior to future analysis. Quality-filtered reads were aligned to the annotated *Populus trichocarpa* reference genome *Populus trichocarpa* v3.1 (Tuskan et al., 2006) using hisat2 v.2.1.0 (Kim et al., 2015) with default settings. Subsequently, alignment-based gene annotation and the creation of the

Porti.id gene count table per sample was performed using featureCount v.2.0.0 (Liao et al., 2014). Only sequences with exactly one alignment to the reference genome were used as the basis for the count table. Additional information on Eukaryotic Orthologs, Gene Ontology (GO), and best *Arabidopsis thaliana* BLASTP (blast+ v2.2.26, (Camacho et al., 2009) hits against the TAIR10 proteome (Berardini et al., 2015) were retrieved from the information file provided with the *P. trichocarpa* reference genome v3.1. Counts were normalized to account for differences in sequencing depth between samples. Sample normalization factors were estimated using R v. 4.1.0 (R Core Team, 2022) package DESeq2 v.1.32.0 (Love et al., 2014). Differential transcription analysis, as implemented in the DESeq2 package, was carried out for all genes between the contrasts control and *L. bicolor* treatment within each time point. Differentially expressed gene (DEG) refers to significant differences in transcript abundance. The p-values attained by Wald Test were corrected for multiple testing using the Benjamini and Hochberg method for controlling the false discovery rate (Benjamini and Hochberg, 1995). The exact reads after each processing step for each sample are in Supplemental Table 6, and the data is available at ArrayExpress (https://www.ebi.ac.uk/biostudies/arrayexpress) under the accession E-MTAB-12654.

After computational processing, the list with the Log2(fold change [FC]) and P values were filtered for Log2FC > 1 or LogFC < -1 and P value < 0.05. Metascape was used for GO (gene ontology) term analysis for “biological processes” with default settings (Zhou et al., 2019) using the gene ids of *Arabidopsis* homolog. In addition, a Kyoto Encyclopedia of Genes and Genomes (KEGG) analysis was performed with default settings (Kanehisa and Goto, 2000) using the gene ids of *Arabidopsis* homolog genes. The list of *Arabidopsis* genes with the GO terms "induced systemic resistance" (ISR) and "systemic acquired resistance" (SAR) was downloaded from www.arabidopsis.org (version date November 1st, 2022).

For all bioinformatic analyses, the gene ids of *Arabidopsis* homologous genes were used because most processes are better characterized in *Arabidopsis* than in poplar, and homologous genes are likely to have similar functions (Lyons and Freeling, 2008). In the particular case of poplar, one *Arabidopsis* gene can be homologous to multiple poplar genes because the poplar genome underwent genome duplications (Tuskan et al., 2006). In addition, many bioinformatics tools used here are unavailable for poplar genes.

3.21. cDNA synthesis and qRT-PCR

After RNA extraction (3.18), cDNA was synthesized from 1000 ng RNA using the RevertAid First Strand cDNA Synthesis Kit with oligo dT primers (Thermo Fischer Scientific). The cDNA was diluted 1:10 with ddH_2O to create a stock cDNA solution. The stock cDNA solution was diluted 1:3 to get a working solution. Afterward, qRT-PCR was performed. The qRT-PCR reaction mixture contained 10 µL innuMIX qPCR DSGreen Standard master mix (Analytik Jena), 5 µL cDNA working solution, 4 µL ddH_2O, and 1 µL primer mix of forward and reverse primer (10 µM). The reactions were carried out with a qTower3G (Analytik Jena) and the following conditions: initial denaturation at 95 °C for 2 min, 40 cycles of 1) denaturation at 95 °C for 20 s, 2) annealing at 58 °C for 20 s and 3) elongation at 72 °C for 20 s. The qRT-PCR ended with a melting curve, starting from 60 °C to 95 °C in 15 s with an increase of 0.5 °C per s. Three technical replicates were analyzed per sample. Ct-values were determined with the qPCRsoft-Software v4 (Analytik Jena). The relative normalized transcript abundance was calculated according to Pfaffl et al. (2001). Target-specific primers were designed using PerlPrimer (Marshall, 2004) and synthesized by Microsynth (Microsynth, Wolfurt, Austria). As reference genes, A_Ref (Potri.015G001600) and C_Ref (Potri.012G141400) were used (Strijkstra, 2021). All primers used in this study are in Supplemental Table 7.

3.22. Reactive oxygen species burst measurement

Four-week-old *in vitro*-grown *P.* × *canescens* were used for this experiment. Eighth leaf disks (4 mm diameter) from three plants (3+3+2) were punched out. Leaf disks were floated in 100 µL ddH_2O in a pure-grade white 96-well plate (Brand, Wertheim, Germany). The next day, after approximately 16 hours, the water was exchanged for a mixture of 100 µM luminol L-012 (Wako Chemicals, Neuss, Germany) and 10 µg mL^{-1} horseradish peroxidase (Sigma-Aldrich). Chitin (final concentration 100 µg mL^{-1}; from shrimp shell, BioReagent grade, Lot#SLBN7584V, C9752-5G), flg22 (final concentration 100 nM; Thermo Fisher Scientific), or ddH_2O (control) was added, and total luminescence was detected every minute using an Infinite M200 plate reader (Tecan Group, Männedorf, Switzerland) for 1 hour with an integration time of 350 ms. Four-week-old soil-grown *Arabidopsis thaliana* (Col-0) plants were treated similarly and used as a control.

3.23. Mitogen-activated protein kinase assay

Four-week-old *in vitro*-grown *P.* × *canescens* were used for this experiment. Three leaves of three plants (in total, nine) were harvested individually and incubated overnight in ddH_2O to allow recovery from the wounding stress of the detaching. The following day after approximately 16 hours, the leaves were vacuum infiltrated for ten minutes with either 10 µg mL^{-1} chitin (from shrimp shell, BioReagent grade, Lot#SLBN7584V, C9752-5G, Sigma-Aldrich, Taufkirchen, Germany), 100 nM flg22 (Thermo Fisher Scientific) or ddH_2O. Ten minutes after the infiltration, the leaves were taken out of the infiltration solution and padded dry gently with paper tissues. Afterward, three leaves (one leaf per plant) were pooled and frozen in liquid nitrogen. Leaf proteins were extracted, and the MAP kinase assay was conducted according to Petutschnig et al. (2010). Phosphorylated MAP kinases 3 and 6 were detected using phospho-p44/42 (Cell Signaling Technology, Danvers, USA) as the primary antibody. Four-week-old *Arabidopsis thaliana* (Col-0) plants were used as a control and treated in the same manner.

3.24. Statistical analysis

Usually, three to six biological replicates were harvested and analyzed for each condition in all experiments. The figure and table legends mention the exact number of biological and technical replicates.

The normal distribution of the data sets was tested by visual inspection of residuals in RStudio (RStudio Team, 2020) to compare means. If data were not normally distributed, they were log-transformed to achieve normal distribution. If data in percent included 0 or 100, they were transformed according to Smithson & Verkuilen (2006). ANOVA and Tukey's test were conducted with R (R Core Team, 2022) and RStudio (RStudio Team, 2020), using linear generalized mixed models or beta regression (Cribari-Neto and Zeileis, 2010) in the R packages "multcomp" (Hothorn et al., 2008), "car" (Fox and Weisberg, 2019) and "lme4" (Bates et al., 2015). Where more than one experiment was analyzed, random effects of different experiments were considered. Differences between treatments were considered significant when the values of ANOVA and Tukey's test were $P < 0.05$. Correlations were tested using R's built-in cor.test() function, and linear regression was conducted in Graphpad Prism 9 (GraphPad Software, 2022; license holder: Steven Dreischhoff) with default settings. All data was visualized using Graphpad Prism 9 (GraphPad Software, 2022).

4. Results

4.1. Transcriptional analysis reveals systemic changes related to defense in leaves after *Laccaria bicolor* treatment

4.1.1. The systemic transcription in leaves was changed at the early stages of mycorrhization

The leaf transcriptome was investigated one, two, four, and seven days after inoculation to analyze the systemic changes at early time points of the interaction of *Populus* × *canescens* roots with *Laccaria bicolor*. There were no genes with significant differences in transcript abundances (differentially expressed genes [DEGs]; 2-fold change; $P < 0.05$) for the two earliest time points (one and two days; Figure 7). After four days, 27 genes had increased transcript abundances, and 20 genes had decreased transcript abundances (Figure 7). The biggest change was observed after seven days, where the transcript abundances of 1105 genes increased, and the transcript abundances of 384 genes decreased (Figure 7).

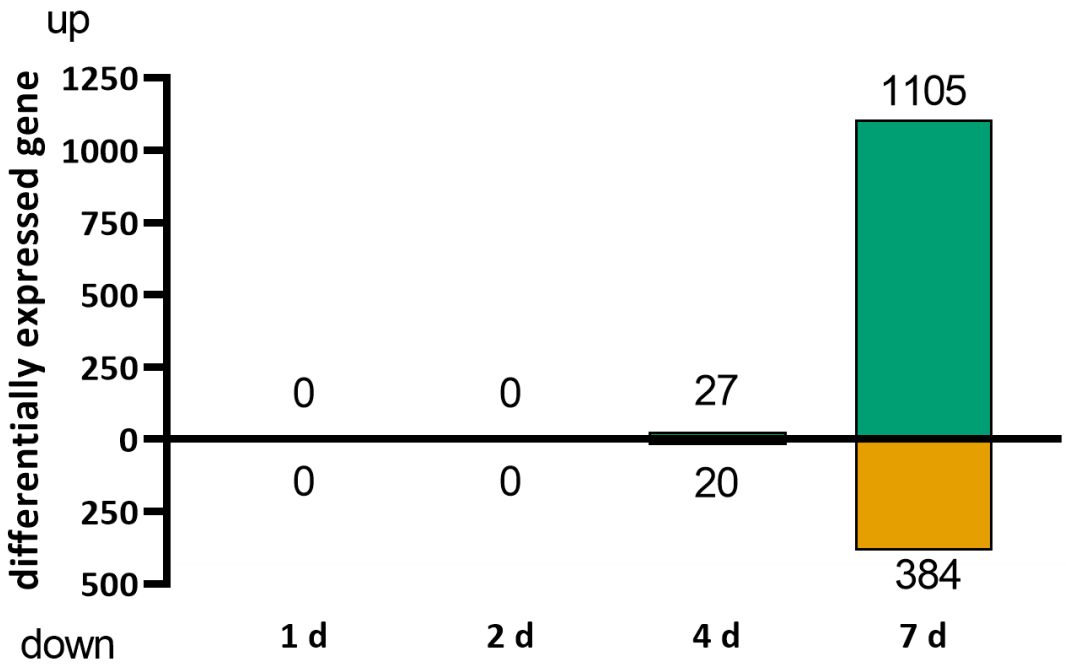

Figure 7 Time course of differentially expressed genes (DEGs) in *P.* × *canescens* leaves after *L. bicolor* treatment of roots

The roots of four-week-old, *in vitro*-grown *P.* × *canescens* were inoculated with *L. bicolor* in a sterile sandwich system (3.3). The pooled RNA of leaves from three plants per independent experiments (n = 3) per time point was used for transcriptional analyses (3.19 & 3.20). DEGs were determined in comparison with controls (non-inoculated plants) harvested at the same time points as the *L. bicolor* inoculated plants. The bar chart shows DEGs with $P < 0.05$ and 2-fold differences in transcript abundances. Upward bars (green) represent the number of genes with increased transcript abundances, and downward bars (orange) represent the number of genes with decreased transcript abundances.

4.1.2. GO term analysis and pathway analysis reveal changes in secondary metabolism

GO term analysis was performed for the category “biological process” to get insights into the affected metabolic and regulatory pathways. Four days after EMF inoculation, the only enriched GO term was "cellular response to hypoxia" in the set of genes with decreased transcript abundances (GO:0071456; Figure 8A). Four GO terms were present in the gene set with increased transcript abundances (Figure 8B). Among these, two GO terms were related to ethylene responses, i.e., "negative regulation of ethylene-activated signaling pathway" and "response to ethylene" (GO:0010105 and GO:0009723; Figure 4b). Among those genes were homologs of *Arabidopsis EIN3-BINDING F BOX PROTEIN 1* (*AtEBF1*) and *CONSTITUTIVE TRIPLE RESPONSE 1* (*AtCTR1*), suggesting that ethylene might contribute to modulating the early systemic effects in leaves when *L. bicolor* root starts to colonize the roots.

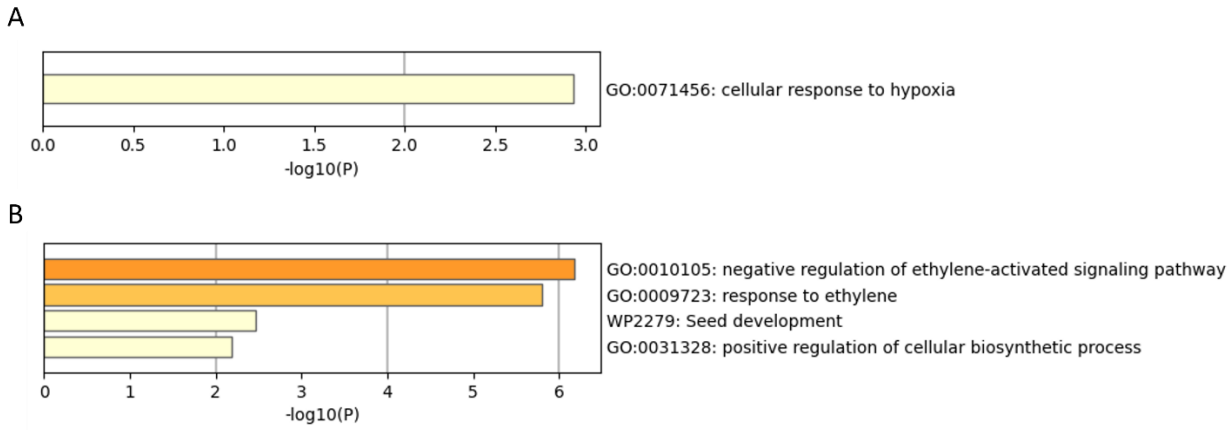

Figure 8 GO term analysis of differentially expressed genes in *P.* × *canescens* leaves after four days of *L. bicolor* treatment of roots

The pooled RNA of leaves from three plants per independent experiments (n = 3) was used for transcriptional analyses (3.19 & 3.20). Leaf DEGs with P < 0.05 and 2-fold differences in transcript abundances (Figure 7) were subjected to GO term analysis with Metascape, as described in 3.20. The enriched GO terms with IDs, names, and significance levels are displayed. The lists are sorted by P value, and stronger colors of bars represent lower P values. (A) shows GO terms for DEGs with decreased transcript abundances, and (B) shows GO terms for DEGs with increased transcript abundances.

After seven days of *L. bicolor* inoculation, the strong transcriptional responses resulted in 17 enriched GO terms in the set of genes with decreased transcript abundances and 44 enriched GO terms for the genes with increased transcript abundances (Figure 9). The most significant GO term for the genes with decreased transcript abundances after seven days was "response to hypoxia" (GO:0001666, Figure 9A), which was also enriched after four days (Figure 8). Furthermore, the GO terms "response to nutrient levels" and "nitrate metabolic process"

were significantly enriched among genes with decreased transcript abundances (GO:0031667 and GO:0042126; Figure 9A), which was unexpected because it is known that EMF improve the nutrient status of their hosts (Nehls and Plassard, 2018). CC-Type Glutaredoxins known to regulate transcription factors (Gutsche et al., 2015) known to be involved in systemic defense were found under the GO Term “negative regulation of transcription by RNA polymerase II” (GO:0000122; Figure 9A).

The two most significantly enriched GO terms for the genes with increased transcript abundances were "secondary metabolite biosynthetic process" (GO:0044550) and "cell wall biogenesis" (GO:0042546; Figure 9B). Related GO terms to "secondary metabolite biosynthetic process" with more specific information about secondary metabolism processes were also found to be enriched, i.e., “chorismate metabolic process” (GO:0046417), “flavonoid biosynthetic process” (GO:0003813), “regulation of flavonol biosynthetic process” (GO:1900384) and “regulation of phenylpropanoid metabolic process” (GO:2000762; Figure 9B). It was notable that the GO terms "monocarboxylic acid catabolic process" (GO:0072329), "response to fatty acid" (GO:0070542), "salicylic acid catabolic process" (GO:0042244), and "jasmonic acid metabolic process" (GO:0009694; Figure 9B) were enriched because the literature suggests that JA signaling plays a role in mycorrhizal induced systemic defense (Dreischhoff et al., 2020). Related to that point, also the GO term “defense response to fungus” (GO:0050832) was enriched (Figure 9B).

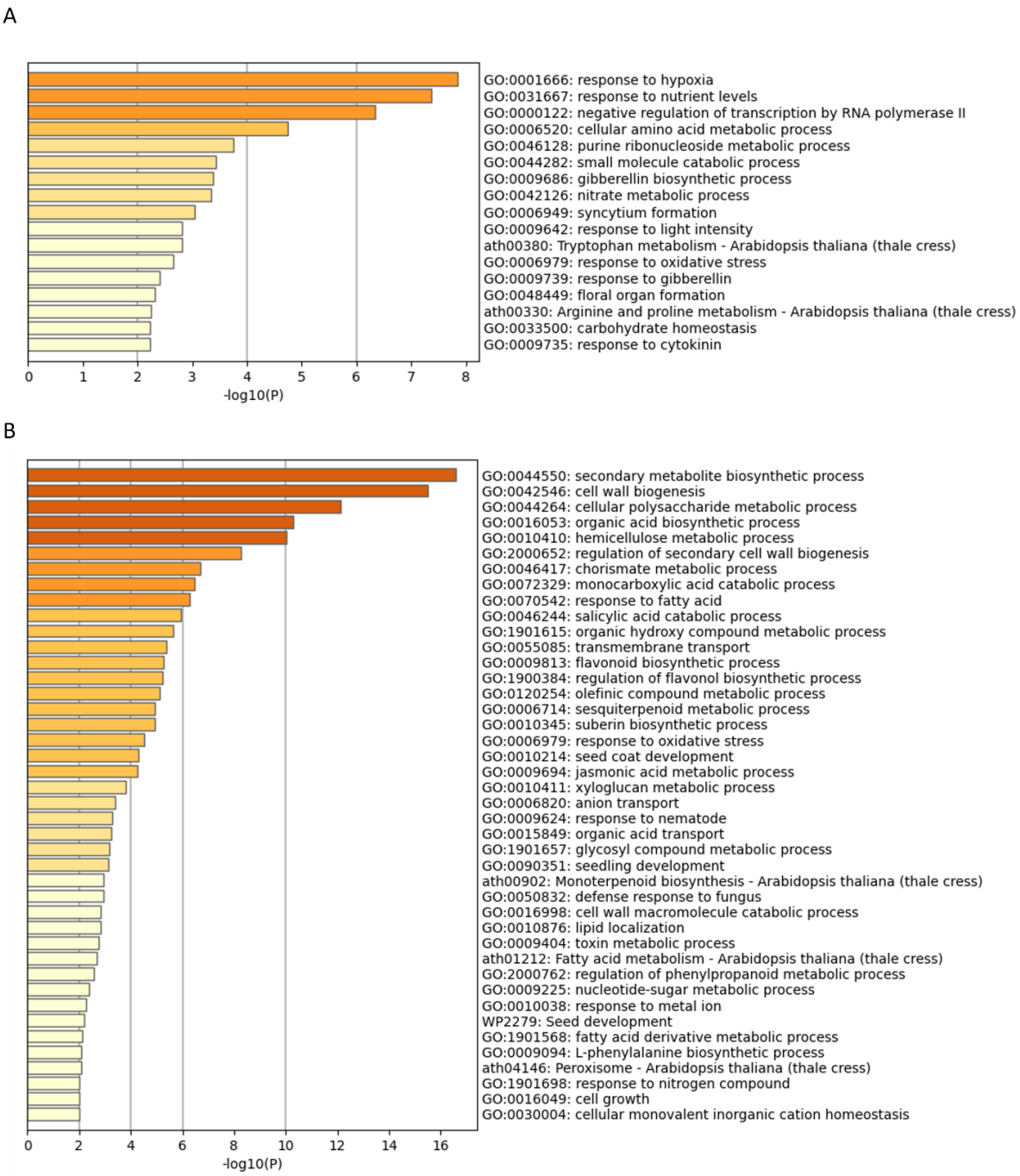

Figure 9 GO term analysis of differentially expressed genes in *P.* × *canescens* leaves after seven days of *L. bicolor* treatment of roots

The pooled RNA of leaves from three plants per independent experiments (n = 3) was used for transcriptional analyses (3.19 & 3.20). Leaf DEGs with P < 0.05 and 2-fold differences in transcript abundances (Figure 7) were subjected to GO term analysis with Metascape, as described in 3.20. The enriched GO terms with IDs, names, and significance levels are displayed. The lists are sorted by P value, and stronger colors of bars represent lower P values. (A) shows GO terms for DEGs with decreased transcript abundances, and (B) shows GO terms for DEGs with increased transcript abundances.

“Secondary metabolite biosynthetic process" was the most significant GO term in the analysis. It is a very broad GO term. Therefore a KEGG analysis (Kanehisa and Goto, 2000) was performed to look deeper into metabolic pathways with increased transcript abundances after seven days. Emphasis was on secondary metabolic processes which produce defense products and their precursors and on phytohormones for defense signaling. Products of the shikimate pathway are important precursors for secondary metabolites, including defense metabolites (Herrmann and Weaver, 1999; Kumar et al., 2020). These defense metabolites were also found in EMF-treated plants (Pfabel et al., 2012). The KEGG analysis revealed that the transcript abundances of almost all synthesis genes leading to phenylalanine in the shikimate pathway were enriched (Figure 10).

Phenylalanine is the starting product of the phenylpropanoid pathway, which in addition to precursors for defense metabolites, also gives rise to products used for cell wall synthesis. Furthermore, the GO term “cell wall biosynthesis” was enriched. Cell walls are the first barrier that pathogens have to overcome. They play an important role in plant defense, and cell wall fortifications are induced by many pathogens (Underwood, 2012). In addition, EMFs are known to induce cell wall modifications in roots during symbiosis (Martin et al., 2016; Sillo et al., 2016). The transcript abundances of genes involved in the monolignol synthesis (within the phenylpropanoid pathway) increased after *L. bicolor* treatment (Figure 11). Monolignols are the precursors for lignin formation in plant cell walls (Wang et al., 2013).

The flavonoid biosynthesis pathway is driven by metabolites generated in the phenylpropanoid pathway. Flavonoids are a class of metabolites with known defense capacity (Treutter, 2006). Pfabel et al. (2012) found elevated levels of flavonoids in EMF colonized poplar after rust infection compared to non-mycorrhizal plants. The enrichment of genes with the GO terms “flavonoid biosynthetic process” and “regulation of flavonol biosynthetic process” was also reflected in the KEGG analysis of the flavonoid biosynthesis pathway (Figure 12). Here, genes across the whole biosynthesis had increased transcript abundances, and no specific metabolic route was definable. Products of flavonoid biosynthesis are precursors for flavone and flavonol biosynthesis. Only four genes in the pathway had increased transcript abundances (Figure 13). The anthocyanin biosynthetic pathway also uses precursors generated in flavonoid biosynthesis. However, no genes had increased transcript abundances (Figure 14).

Among the GO terms related to phytohormones, the α-linolenic acid metabolism, which produces JA, was of special interest. The transcript abundances of genes involved in this pathway were significantly increased, as highlighted by the KEGG analysis (Figure 15).

Even though GO terms related to ethylene signaling or biosynthesis were not enriched after seven days, the KEGG analysis revealed that the transcript abundances of genes within the cysteine and methionine metabolic pathway toward ethylene were increased (Figure 16). All three genes catalyzing the steps from methionine to ethylene (Lin et al., 2009) had increased transcript abundances.

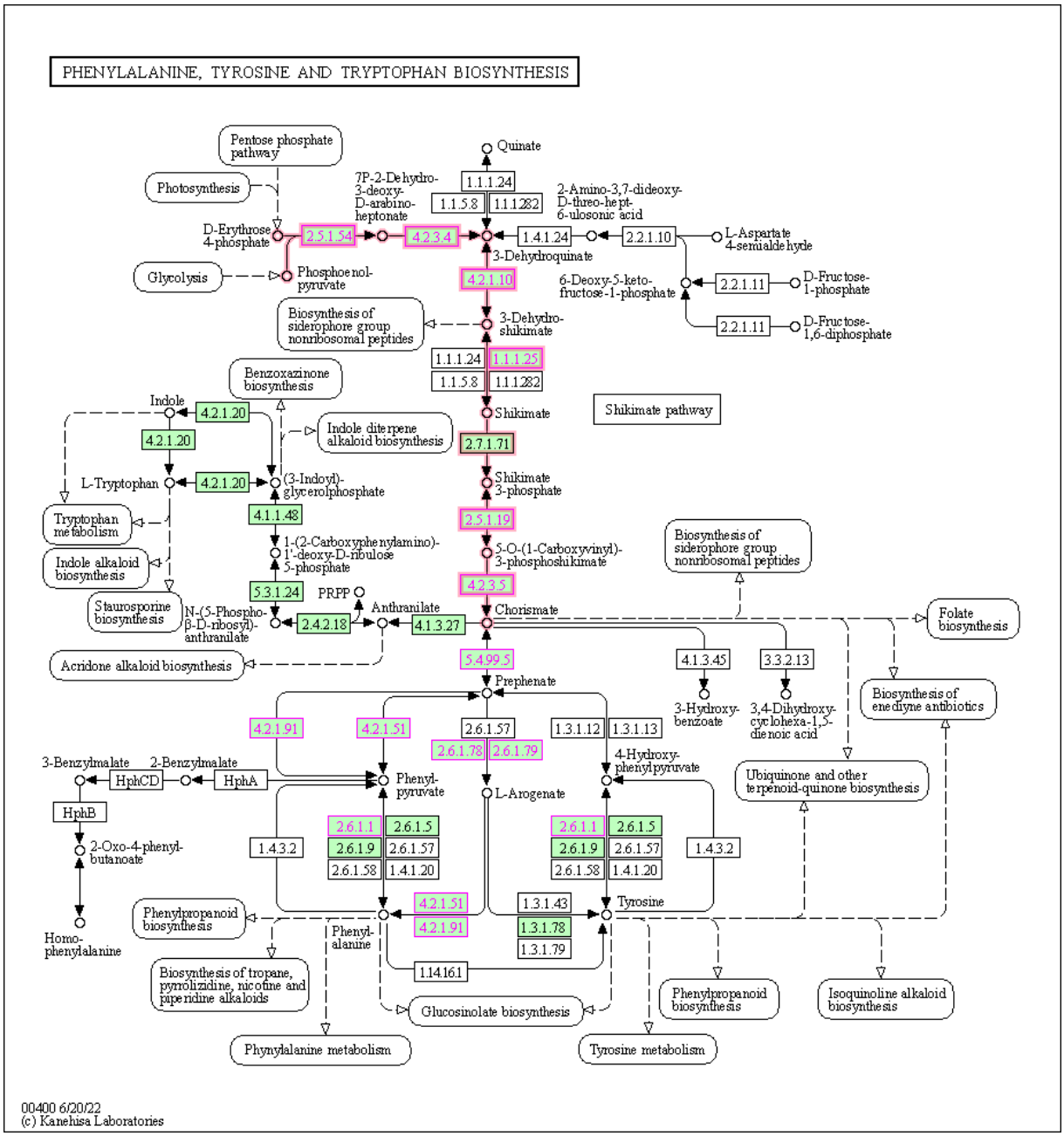

Figure 10 Mapping genes with increased transcript abundances on the phenylalanine, tyrosine, and tryptophan biosynthesis pathway.

The pooled RNA of leaves from three plants per independent experiments (n = 3) was used for transcriptional analyses (3.19 & 3.20). Genes with increased transcript abundances (Figure 7) in leaves of *P.* × *canescens* detected after seven days of *L. bicolor* treatment of roots were mapped on pathways of the KEGG database (3.20). The numbers in the boxes are enzyme commission numbers. Red numbers and boxes display genes with increased transcript abundances in leaves after seven days of *L. bicolor* treatment of roots. Thick red boxes and arrows highlight the shikimate synthesis pathway. Green-filled boxes were hyperlinks to the KEGG database.

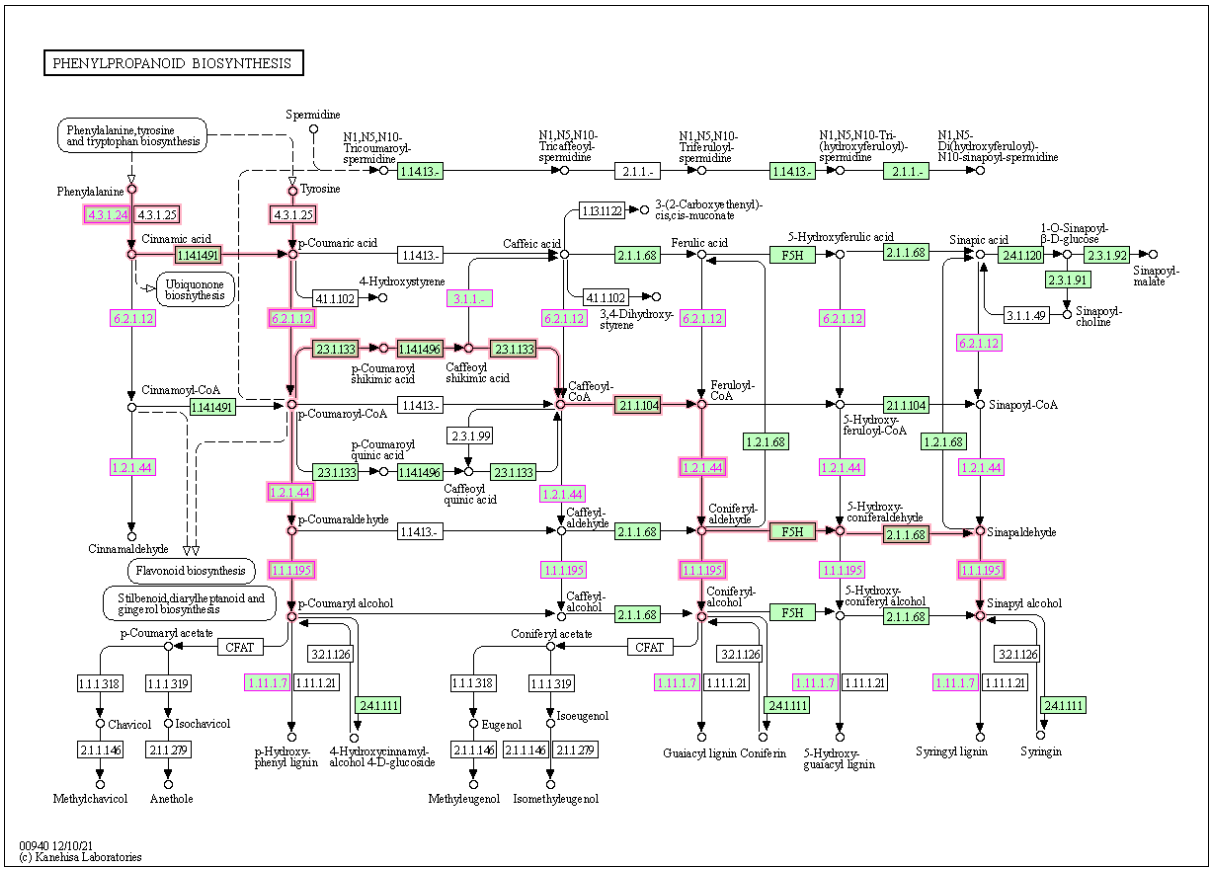

Figure 11 Mapping genes with increased transcript abundances on the phenylpropanoid biosynthesis pathway

The pooled RNA of leaves from three plants per independent experiments (n = 3) was used for transcriptional analyses (3.19 & 3.20). Genes with increased transcript abundances (Figure 7) in leaves of *P.* × *canescens* detected after seven days of *L. bicolor* treatment of roots were mapped on pathways of the KEGG database (3.20). The numbers in the boxes are enzyme commission numbers. Red numbers and boxes display genes with increased transcript abundances in leaves after seven days of *L. bicolor* treatment of roots. Thick red boxes and arrows highlight the monolignol synthesis pathway. Green-filled boxes were hyperlinks to the KEGG database.

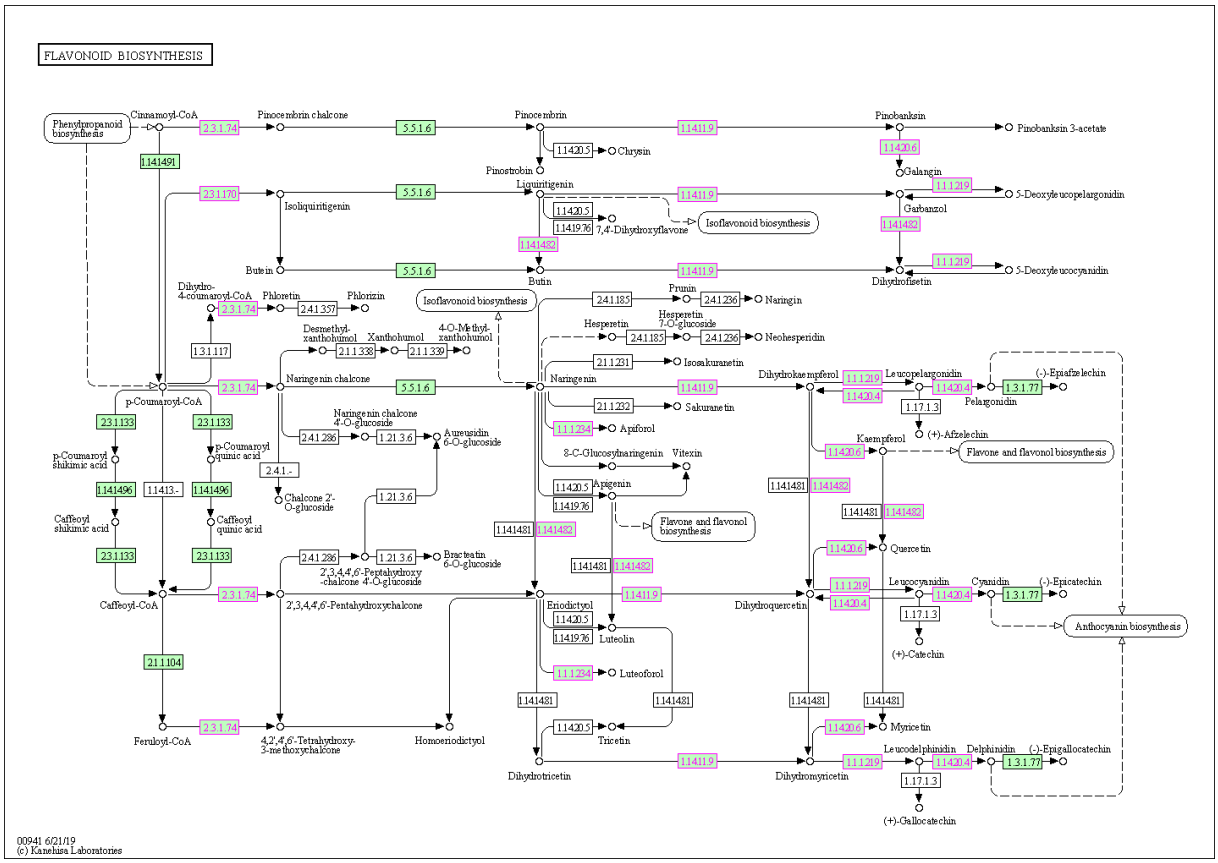

Figure 12 Mapping genes with increased transcript abundances on the flavonoid biosynthesis pathway

The pooled RNA of leaves from three plants per independent experiments (n = 3) was used for transcriptional analyses (3.19 & 3.20). Genes with increased transcript abundances (Figure 7) in leaves of *P.* × *canescens* detected after seven days of *L. bicolor* treatment of roots were mapped on pathways of the KEGG database (3.20). The numbers in the boxes are enzyme commission numbers. Red numbers and boxes display genes with increased transcripts in leaves after seven days of *L. bicolor* treatment of roots. Green-filled boxes were hyperlinks to the KEGG database.

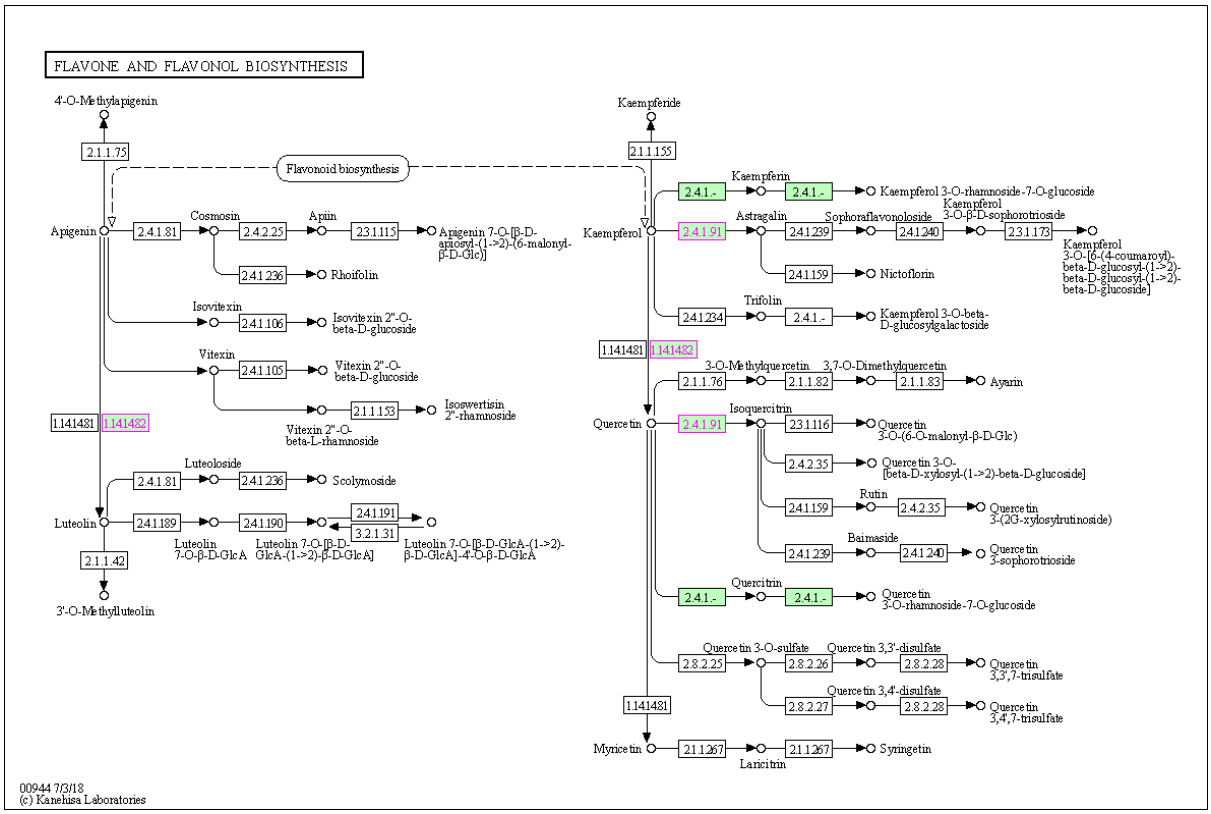

Figure 13 Mapping genes with increased transcript abundances on the flavone and flavonol biosynthesis

The pooled RNA of leaves from three plants per independent experiments (n = 3) was used for transcriptional analyses (3.19 & 3.20). Genes with increased transcript abundances (Figure 7) in leaves of *P.* × *canescens* detected after seven days of *L. bicolor* treatment of roots were mapped on pathways of the KEGG database (3.20). The numbers in the boxes are enzyme commission numbers. Red numbers and boxes display genes with increased transcript abundances in leaves after seven days of *L. bicolor* treatment of roots. Green-filled boxes were hyperlinks to the KEGG database.

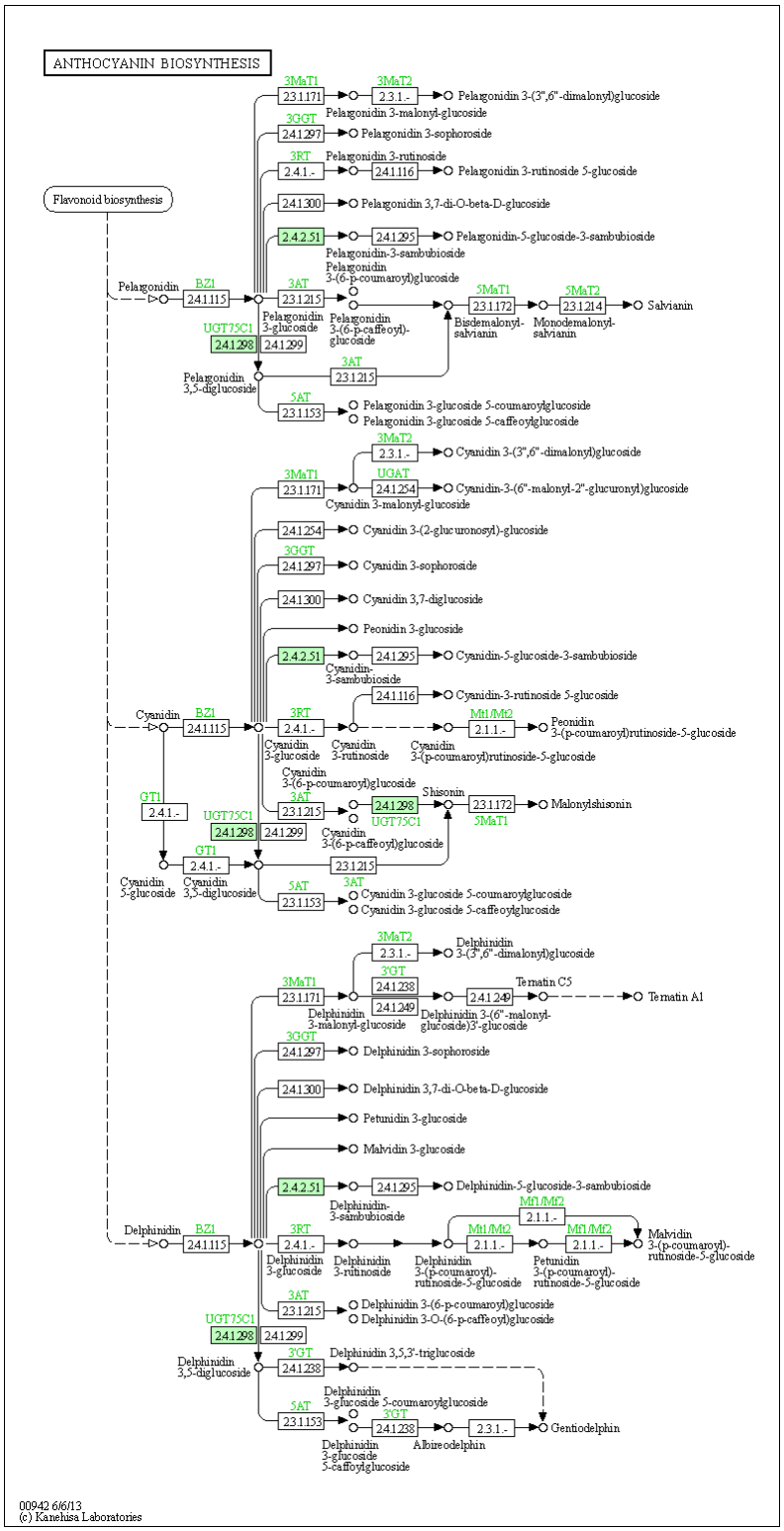

Figure 14 Mapping genes with increased transcript abundances on the anthocyanin

The pooled RNA of leaves from three plants per independent experiments (n = 3) was used for transcriptional analyses (3.19 & 3.20). Genes with increased transcript abundances (Figure 7) in leaves of *P.* × *canescens* detected after seven days of *L. bicolor* treatment of roots were mapped on pathways of the KEGG database (3.20). The numbers in the boxes are enzyme commission numbers. Red numbers and boxes display genes with increased transcript abundances in leaves after seven days of *L. bicolor* treatment of roots. Green-filled boxes were hyperlinks to the KEGG database.

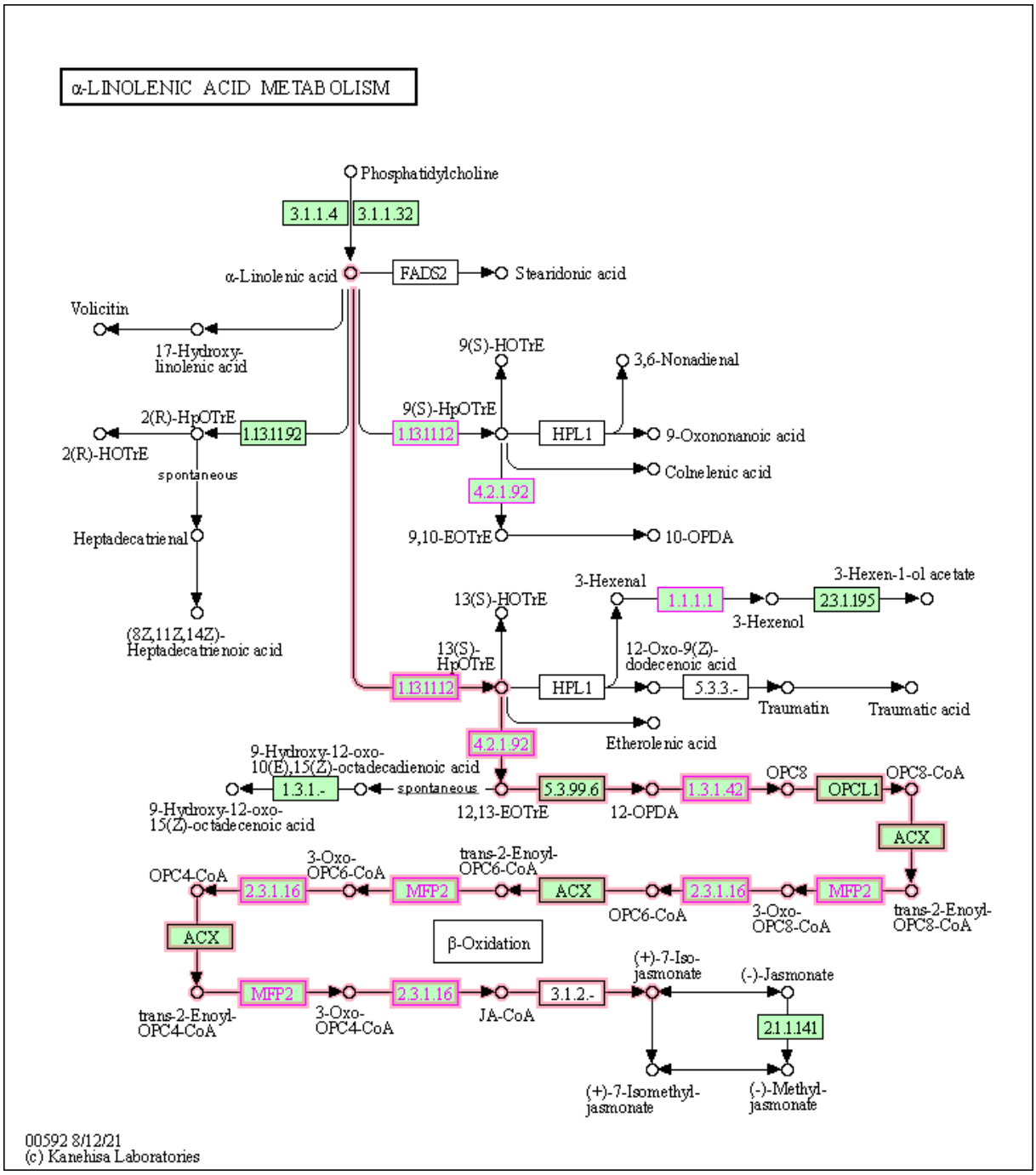

Figure 15 Mapping genes with increased transcript abundances on the α-linolenic acid metabolism

The pooled RNA of leaves from three plants per independent experiments (n = 3) was used for transcriptional analyses (3.19 & 3.20). Genes with increased transcript abundances (Figure 7) in leaves of *P.* × *canescens* detected after seven days of *L. bicolor* treatment of roots were mapped on pathways of the KEGG database (3.20). The numbers in the boxes are enzyme commission numbers. Red numbers and boxes display genes with increased transcript abundances in leaves after seven days of *L. bicolor* treatment of roots. Thick red boxes and arrows highlight the JA synthesis pathway. Green-filled boxes were hyperlinks to the KEGG database.

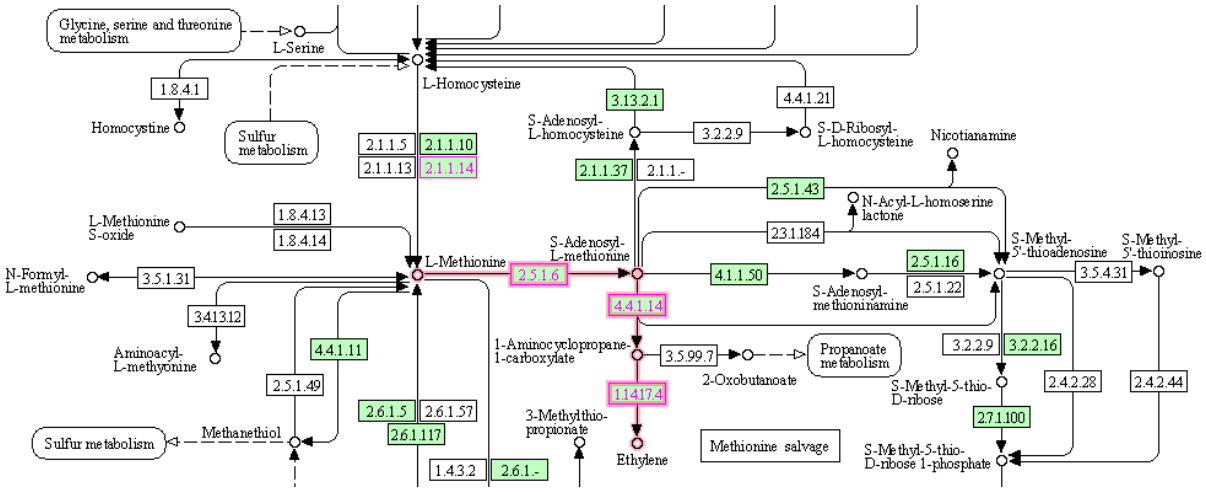

Figure 16 Mapping genes with increased transcript abundances on the ethylene biosynthesis pathway

The pooled RNA of leaves from three plants per independent experiments (n = 3) was used for transcriptional analyses (3.19 & 3.20). Genes with increased transcript abundances (Figure 7) in leaves of *P.* × *canescens* detected after seven days of *L. bicolor* treatment of roots were mapped on pathways of the KEGG database (3.20). Red numbers and boxes display genes with increased transcript abundances in leaves after seven days of *L. bicolor* treatment of roots. Thick red boxes and arrows highlight the ethylene synthesis pathway. Green-filled boxes were hyperlinks to the KEGG database.

4.1.3. Mycorrhization affects genes involved in IRS and SAR in systemic tissue

Two defense processes in which systemic transcription is altered are "induced systemic resistance" (ISR) and "systemic acquired resistance" (SAR). Mycorrhizal defense induction signaling may involve components of both processes (Dreischhoff et al., 2020; Jung et al., 2009, 2012), although SAR (SA) and ISR (JA) can induce antagonistic responses (Hou and Tsuda, 2022). To investigate this further, a gene list of the GO terms for ISR and SAR was compared to all genes with significantly changed (increased and decreased) transcript abundances after seven days (Table 1).

The GO term for ISR has 36 genes. Here, the transcript abundances of nine poplar genes (seven *Arabidopsis* homologs) were increased (Table 1, upper part). The two transcription factors, *WRKY70* and *WRKY11,* had increased transcript abundances. Many WRKY transcription factors, including WRKY70 and WRKY11, are known to be key regulators for systemic defense (Wani et al., 2021). Two *CYP83B1* genes had the second and third highest change in transcript abundances. These genes modulate systemic defenses and are involved in auxin signaling (Truman et al., 2010).

In the SAR GO term are 142 *Arabidopsis* genes, of which 20 genes (33 poplar genes were in the list of genes with changed transcript abundances after seven days of mycorrhization (Table 1, bottom part). Two genes with the highest increase in transcript abundances were homologs of *AtGGL5* (GDSL-motif esterase/acyltransferase/lipase). *AtGGL5* was found to be involved in systemic defense in a screen with *eds5* mutants (Breitenbach et al., 2014). EDS5 is a regulation hub for defense against pathogens (Wiermer et al., 2005). In *Arabidopsis*, PATHOGENESIS-RELATED GENE 1 (PR1) accumulates in an SA-dependent manner in SAR (Durrant and Dong, 2004). Here one *AtPR1* homolog had increased transcript abundance while another had decreased transcript abundance. Another PR gene with decreased transcript abundance was *PR4*, which was found to bind chitin and be involved in defense against necrotizing pathogens (Petutschnig et al., 2010; Trusov et al., 2009; van Loon et al., 2006). Five homologs to *AtCRK14* (encodes a cysteine-rich receptor-like protein kinase) had increased transcript abundances after seven days of *L. bicolor* inoculation. In addition, the transcript abundances of six homologs of the gene encoding for the receptor-like kinase *AtRLK1* were altered. The processes in which receptor-like kinases are involved are diverse, including development, plant-mycorrhiza interaction, and defense. So far, the involvement of receptor-like kinases in the interaction of mycorrhiza and plants has only been described in roots (Gibelin-Viala et al., 2019; Labbé et al., 2019; Shi et al., 2022). NPR1, a key regulator for the antagonism between SA and JA-mediated signaling (Backer et al., 2019), was present in both GO terms, i.e., ISR and SAR.

Table 1 List of genes with altered transcript abundances from the GO terms "induced systemic resistance" and "systemic squired resistance" after seven days in *P.* × *canescens* leaves after *L. bicolor* treatment of roots

The pooled RNA of leaves from three plants per independent experiments (n = 3) was used for transcriptional analyses (3.19 & 3.20). Genes with altered transcript abundances (Figure 3) in leaves of *P.*× *canescens* detected after seven days of *L. bicolor* treatment of roots were compared to the gene lists of the GO terms "induced systemic resistance" (ISR) and "systemic acquired resistance" (SAR). The gene identifiers for poplar (Potri.id), *Arabidopsis* (Ara.id), and the *Arabidopsis* gene symbol are displayed. The colors of the last column indicate levels of increased transcript abundances (blue) and decreased transcript abundances (red), with white indicating no change.

ISR

Potri.id	Ara.id	*Arabidopsis* gene symbol	*Arabidopsis* gene description	Log2FC
Potri.006G072400	AT4G31550	*WRKY11*	*WRKY DNA-BINDING PROTEIN 11*	0.44
Potri.006G109100	AT3G56400	*WRKY70*	*WRKY DNA-BINDING PROTEIN 70*	2.08
Potri.006G148100	AT1G64280	*NPR1*	*NONEXPRESSER OF PR GENES 1*	-0.42
Potri.002G025800	AT4G31500	*CYP83B1*	*CYTOCHROME P450, FAMILY 83, SUBFAMILY B, POLYPEPTIDE 1*	1.18
Potri.002G026100	AT4G31500	*CYP83B1*	*CYTOCHROME P450, FAMILY 83, SUBFAMILY B, POLYPEPTIDE 1*	1.46
Potri.010G178800	AT5G36890	*BGLU42*	*BETA GLUCOSIDASE 42*	0.78
Potri.011G151200	AT1G32960	*SBT3.3*	Subtilase family protein	1.01
Potri.005G253800	AT1G42540	*GLR3.3*	*GLUTAMATE RECEPTOR 3.3*	-0.34
Potri.002G007400	AT1G42540	*GLR3.3*	*GLUTAMATE RECEPTOR 3.3*	0.81

Table 1 continued
SAR

Potri.id	Ara.id	*Arabidopsis* gene symbol	*Arabidopsis* gene description	Log2FC
Potri.018G089500	AT1G29660	*GGL5*	GDSL-motif esterase/acyltransferase/lipase	4.90
Potri.018G088800	AT1G29660	*GGL5*	GDSL-motif esterase/acyltransferase/lipase	1.47
Potri.011G029200	AT4G23220	*CRK14*	*CYSTEINE-RICH RECEPTOR-LIKE PROTEIN KINASE 14*	2.55
Potri.011G029800	AT4G23220	*CRK14*	*CYSTEINE-RICH RECEPTOR-LIKE PROTEIN KINASE 14*	1.89
Potri.011G030100	AT4G23220	*CRK14*	*CYSTEINE-RICH RECEPTOR-LIKE PROTEIN KINASE 14*	1.78
Potri.011G029100	AT4G23220	*CRK14*	*CYSTEINE-RICH RECEPTOR-LIKE PROTEIN KINASE 14*	1.50
Potri.011G030200	AT4G23220	*CRK14*	*CYSTEINE-RICH RECEPTOR-LIKE PROTEIN KINASE 14*	1.25
Potri.T084500	AT5G60900	*RLK1*	*RECEPTOR-LIKE PROTEIN KINASE 1*	1.13
Potri.013G060000	AT5G60900	*RLK1*	*RECEPTOR-LIKE PROTEIN KINASE 1*	1.05
Potri.019G011800	AT5G60900	*RLK1*	*RECEPTOR-LIKE PROTEIN KINASE 1*	0.97
Potri.013G059900	AT5G60900	*RLK1*	*RECEPTOR-LIKE PROTEIN KINASE 1*	0.84
Potri.T084300	AT5G60900	*RLK1*	*RECEPTOR-LIKE PROTEIN KINASE 1*	0.50
Potri.001G014300	AT5G60900	*RLK1*	*RECEPTOR-LIKE PROTEIN KINASE 1*	-0.76
Potri.006G148100	AT1G64280	*NPR1*	*NONEXPRESSER OF PR GENES 1*	-0.42
Potri.012G118500	AT5G45110	*NPR3*	*NONEXPRESSER OF PR GENES 3*	-0.48
Potri.009G082800	AT2G14610	*PR1*	*PATHOGENESIS-RELATED GENE 1*	1.01
Potri.001G288600	AT2G14610	*PR1*	*PATHOGENESIS-RELATED GENE 1*	-1.56
Potri.013G041600	AT3G04720	*PR4*	*PATHOGENESIS-RELATED GENE 4*	-0.86
Potri.002G162500	AT4G01370	*MPK4*	*MAP KINASE 4*	0.54
Potri.008G110500	AT1G26190	*TTM2*	*TRIPHOSPHATE TUNNEL METALLOENZYME 2*	0.53

Table 1 continued

Potri.id	Ara.id	*Arabidopsis* gene symbol	*Arabidopsis* gene description	Log2FC
Potri.005G164700	AT4G08920	*CRY1*	*CRYPTOCHROME 1*	0.22
Potri.005G118400	AT4G36280	*CRH1*	*CRT1 HOMOLOGUE 1*	-0.37
Potri.007G037700	AT2G23620	*MES1*	*METHYL ESTERASE 1*	-1.26
Potri.007G037300	AT2G23620	*MES1*	*METHYL ESTERASE 1*	-1.49
Potri.007G036800	AT2G23560	*MES7*	*METHYL ESTERASE 7*	-0.32
Potri.003G022900	AT5G64570	*XYL4*	*BETA-XYLOSIDASE4*	1.18
Potri.009G013400	AT5G60600	*HDS*	*4-HYDROXY-3-METHYLBUT-2-ENYL DIPHOSPHATE SYNTHASE*	0.23
Potri.010G189700	AT5G05680	*MOS7*	*MODIFIER OF SNC1,7*	-0.27
Potri.006G048500	AT2G41640	*GT61*	Potential heat-priming associated target of ATAF1	-1.15
Potri.016G104300	AT3G53980	/	seed storage 2S albumin superfamily protein	2.49
Potri.008G061800	AT5G05960	/	Involved in adventitious root organogenesis	1.39
Potri.004G199300	AT2G27310	/	F-box family protein	1.31
Potri.005G208200	AT2G27310	/	F-box family protein	-0.50

4.1.4. Transcript abundances of 16 genes are commonly increased across different *L. bicolor* treatments

The genes with increased transcript abundances after seven days of *L. bicolor* treatment found in this study (1-week sterile setup) were compared to genes with increased transcript abundances after twelve weeks of *L. bicolor* treatment in outdoor conditions to find transcripts that are robustly increased in leaves of *P.* × *canescens* (Kaling et al., 2018; Figure 17). In general, the number of genes with increased transcript abundances after mycorrhiza treatment found by Kaling et al. (2018) was much smaller than the number of genes found in this study. Nevertheless, 16 genes with increased transcript abundances overlapped between both studies (Figure 17).

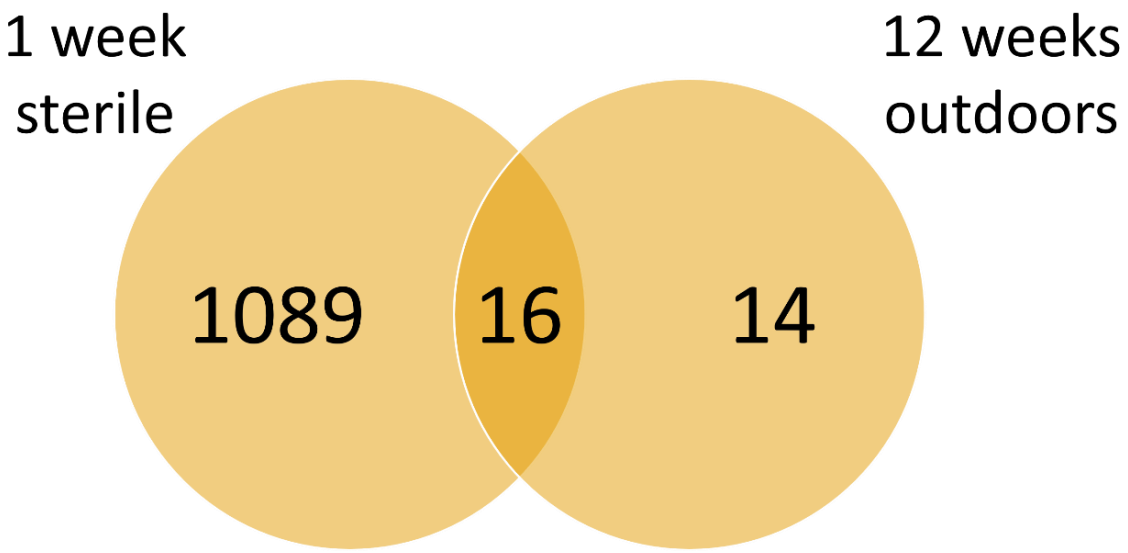

Figure 17 Number of genes with increased transcript abundances in *P.* × *canescens* leaves after one week of sterile and twelve weeks outdoors *L. bicolor* treatment
Genes with increased transcript abundance in leaves of *P.* × *canescens* detected after seven days of sterile (Figure 7) or twelve weeks outdoors (Kaling et al., 2018) *L. bicolor* treatment of roots were compared. Displayed is a Venn diagram of the overlap.

The changes were generally greater after one week of *L. bicolor* treatment in the sterile setup than after twelve weeks of outdoor treatment (Table 2). The gene with the highest increase in transcript abundance was *INDOLE-3-ACETATE BETA-D-GLYCOSYLTRANSFERASE* (Potri.016G052500), which is part of the auxin metabolism (Ostin et al., 1998). Auxin is involved in the modulation of ectomycorrhizal symbiosis in roots (Felten et al., 2009; Vayssières et al., 2015). In addition, the transcript abundances of three *GLUTATHIONE S-*

TRANSFERASE TAU 19, which are involved in stress tolerance (Foyer and Noctor, 2005; Xu et al., 2016), were increased in both datasets (Potri.011G140700, Potri.011G140600, and Potri.011G140400). Two genes from the list were connected directly to defense responses against various factors. It was a *KUNITZ FAMILY TRYPSIN AND PROTEASE INHIBITOR PROTEIN* gene (hereafter KTI; Potri.019G088200) and major latex protein (*MLP*)-*like protein 423* gene (hereafter MLP423; Potri.010G000600). KTIs interfere with the digestion of herbivorous attackers (Major and Constabel, 2008; McManus and Burgess, 1995), and MLPs are responsive to drought and pathogen stress (Chen and Dai, 2010; Song et al., 2020; Yuan et al., 2020).

Table 2 Genes with increased transcript abundances in *P.* × *canescens* leaves after one week *of L. bicolor* treatment in a sterile setup and twelve weeks outdoors *L. bicolor* treatment

Genes with increased transcript abundances in leaves of *P.* × *canescens* detected after seven days of sterile (Figure 3) or twelve weeks outdoors (Kaling et al., 2018) *L. bicolor* treatment of roots were compared. A list of the overlap is shown. The list includes the poplar gene ids (Potri.id) and the homolog *Arabidopsis* gene ids (Ara.id) with functional descriptions. In the two right columns, the transcriptional abundance increase (Log2FC) after 1 week in sterile conditions and 12 weeks outdoors is shown.

Potri.id	Ara.id	*Arabidopsis* gene symbol	*Arabidopsis* gene description	Log2FC 1 week sterile	Log2FC 12 weeks outdoors
Potri.016G052500	AT4G15550	/	*INDOLE-3-ACETATE BETA-D-GLUCOSYLTRANSFERASE*	5.42	1.01
Potri.003G066400	AT5G07990	*CYP75B1*	*CYTOCHROME P450 SUPERFAMILY PROTEIN*	4.89	1.02
Potri.019G118900	AT2G31180	*MYB14*	*MYB DOMAIN PROTEIN 14*	4.38	1.38
Potri.004G082000	AT1G75960	/	*AMP-DEPENDENT SYNTHETASE AND LIGASE FAMILY PROTEIN*	4.21	1.17
Potri.019G024600	AT5G18430	*GGL26*	*GDSL-LIKE LIPASE/ACYLHYDROLASE SUPERFAMILY PROTEIN*	4.17	1.04
Potri.019G088200	AT1G73325	*KTI*	*KUNITZ FAMILY TRYPSIN AND PROTEASE INHIBITOR PROTEIN*	4.10	1.04
Potri.010G000600	AT1G24020	*MLP423*	*MLP-LIKE PROTEIN 423*	3.96	1.02
Potri.009G104600	AT3G48700	*ATCXE13*	*CARBOXYESTERASE 13*	3.96	1.24
Potri.002G120700	AT4G24220	*VEP1*	*NAD(P)-BINDING ROSSMANN-FOLD SUPERFAMILY PROTEIN*	3.63	1.10
Potri.011G140700	AT1G78380	*GST8*	*GLUTATHIONE S-TRANSFERASE TAU 19*	3.62	1.31
Potri.011G140600	AT1G78380	*GST8*	*GLUTATHIONE S-TRANSFERASE TAU 19*	3.35	1.10
Potri.011G140400	AT1G78380	*GST8*	*GLUTATHIONE S-TRANSFERASE TAU 19*	2.99	1.15

Table 2 continued

Potri.id	Ara.id	*Arabidopsis* gene symbol	*Arabidopsis* gene description	Log2FC 1 week sterile	Log2FC 12 weeks outdoors
Potri.005G081000	AT4G02340	/	*ALPHA/BETA-HYDROLASES SUPERFAMILY PROTEIN*	2.62	1.04
Potri.003G205900	AT3G02645	/	Putative transmembrane protein	2.22	1.20
Potri.019G125000	AT4G03210	*XTH9*	*XYLOGLUCAN ENDO-TRANSGLUCOSYLASE/HYDROLASE 9*	1.46	1.08
Potri.006G065500	AT2G10940	/	*BIFUNCTIONAL INHIBITOR/LIPID-TRANSFER PROTEIN/SEED STORAGE 2S ALBUMIN SUPERFAMILY PROTEIN*	1.06	1.08

4.1.5. Phytohormone application changes KTI and marker gene transcript abundances

Since the transcriptomic data in this thesis suggested that the systemic changes after EMF colonization might involve JA, SA, and ethylene, the response of *KTI* to exogenously applied methyl jasmonate (MeJA), 1-aminocyclopropane-1-carboxylic acid (ACC, a precursor of ethylene), and acibenzolar-S-methyl (BTH, an analog of SA) were investigated. The selected phytohormones are known to influence systemic defense (Pieterse et al., 2012), and their effects can typically be traced by measuring the transcript abundances of marker genes such as *ALLENE OXIDE SYNTHASE (AOS), ETHYLENE RESPONSE FACTOR 1* (*ERF1*) and *PR1*.

After eight hours, the transcript levels of *KTI* were 20-fold higher in MeJA-treated plants than in mock-treated controls. ACC and BTH did not significantly change the transcript abundance of *KTI* after eight hours Figure 18A). Twenty-four hours after the MeJA application, the average transcript abundance of *KTI* was about 5-fold higher than the transcript levels in the control. ACC did not lead to a significant change in transcription levels of *KTI*. The treatment with BTH yielded a reduced transcript abundance of *KTI* compared to controls after 24 hours (Figure 18B).

The transcript abundances of marker genes (*AOS, ERF1, PR1*) were measured to assess whether the phytohormones were taken up by the plant and subsequently affected the transcript abundances in the plant.

AOS is a component of the jasmonic acid synthesis pathway, and a feedback loop induces *AOS* after MeJA treatment (Jost et al., 2005; Turner et al., 2002). The transcript abundance was not significantly different 8 hours after MeJA treatment, even though the average of the transcript abundance was slightly higher than the control. ACC treatment did not change the transcript levels of *AOS,* and BTH did not lead to any changes (Figure 18C). After 24 hours, there was no statistically significant difference in *AOS* transcript levels for MeJA- and ACC-treated plants. The transcript abundance of *AOS* after 24 hours of BTH treatment was lower than that in mock-treated plants but not significantly different (Figure 18D).

ERF1 is part of the ethylene signaling (Lorenzo et al., 2003), and the transcript abundance of *ERF1* was increased after one week of *L. bicolor* treatment (Figure 7). The gene showed no altered transcript abundance by MeJA application after eight hours. ACC treatment elevated the transcript level of *ERF1* to about 7-fold, and BTH also induced a significant change after eight hours but to a lower extent than ACC (Figure 18E). After 24 hours, MeJA and ACC

treatment did not significantly increase *ERF1* transcript abundance. BTH, on the other hand, led to a significant rise in ERF1 transcript abundance (Figure 18F).

PR1 is involved in SA-mediated defenses (Durrant and Dong, 2004). Eight hours after MeJA treatment, the transcript abundance of *PR1* was slightly lower than the control but not significantly different. MeJA and ACC did not lead to a significant change in the transcript levels. BTH-treated plants has a statistically significant reduced transcript abundance after eight hours of treatment (Figure 18G). After 24 hours, all transcript levels are not different from each other (Figure 18H)

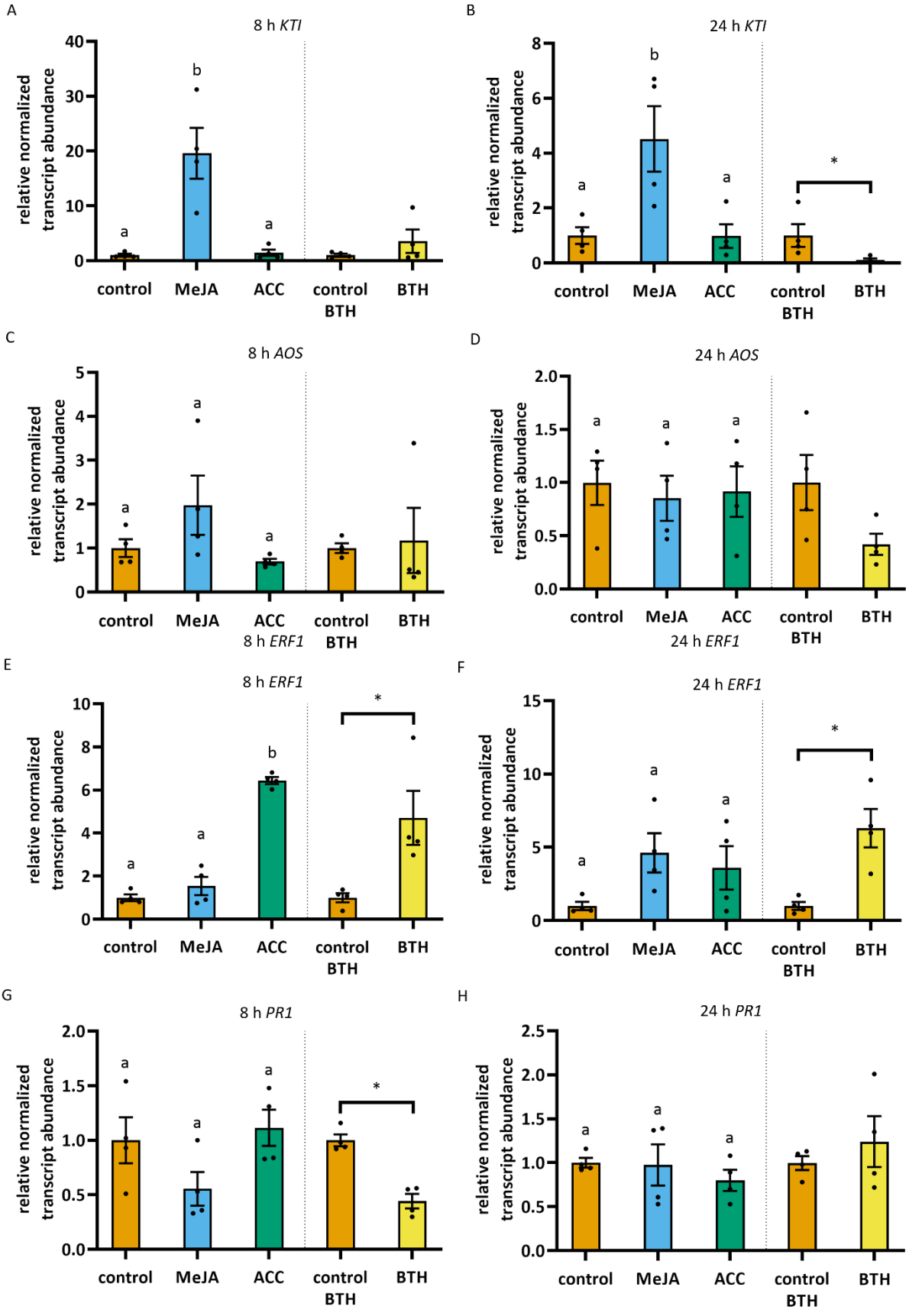
A
8 h KTI
relative normalized transcript abundance
control
MeJA
ACC
control BTH
BTH
B
24 h KTI
C
8 h AOS
D
24 h AOS
8 h ERF1
24 h ERF1
E
8 h ERF1
F
24 h ERF1
G
8 h PR1
H
24 h PR1

Figure 18 Relative normalized transcript abundances of *KTI* and phytohormone marker genes after application of different phytohormones on *P.* × *canescens* leaves
Different sets of *P.* × *canescens* plants were sprayed with either methyl jasmonate (MeJA; blue), 1-aminocyclopropane-1-carboxylic acid (ACC; green), acibenzolar-S-methyl (BTH; yellow) or their respective solvent controls (orange). MeJA and ACC were solved in ddH_2O, and BTH was solved in 10 % methanol. The plants were incubated for eight or 24 hours in separate greenhouse cells. Afterward, the transcript abundances of *KTI* (A+B), *AOS* (C+D), *ERF1* (E+F), and *PR1* (G+H) were measured. Bars show the means of the relative transcript abundance and the standard error. Data were expressed relative to the mean transcript abundance of the respective solvent-treated controls. Each dot represents one biological replicate (n = 4) of one experiment. Different letters above the bars indicate statistically significant differences at $P < 0.05$ calculated by ANOVA and Tukey's post hoc test. Asterisks indicate a statistically significant difference at $P < 0.05$ calculated by ANOVA for BTH and its control.

L. bicolor alters the sensitivity toward JA in roots (Basso et al., 2020). A sterile experimental setup (3.13) was chosen to compare the effect of MeJA treatment with the plant responses to EMF inoculation and to assess whether *L. bicolor* alters the sensitivity toward JA in leaves. Poplars were grown for ten days in the presence or absence of *L. bicolor* and then exposed to MeJA or the solvent (mock-treated controls). The transcript abundance of *KTI* increased in response to both MeJA and *L. bicolor* treatment. The combination of *L. bicolor* and MeJA treatment yielded reduced transcript abundance compared to the single treatments. This difference was not statistically significant compared with the *KTI* transcript levels in control, *L. bicolor*- or MeJA-treated plants (Figure 19). In this experiment, the variation between samples of the single treatments was high.

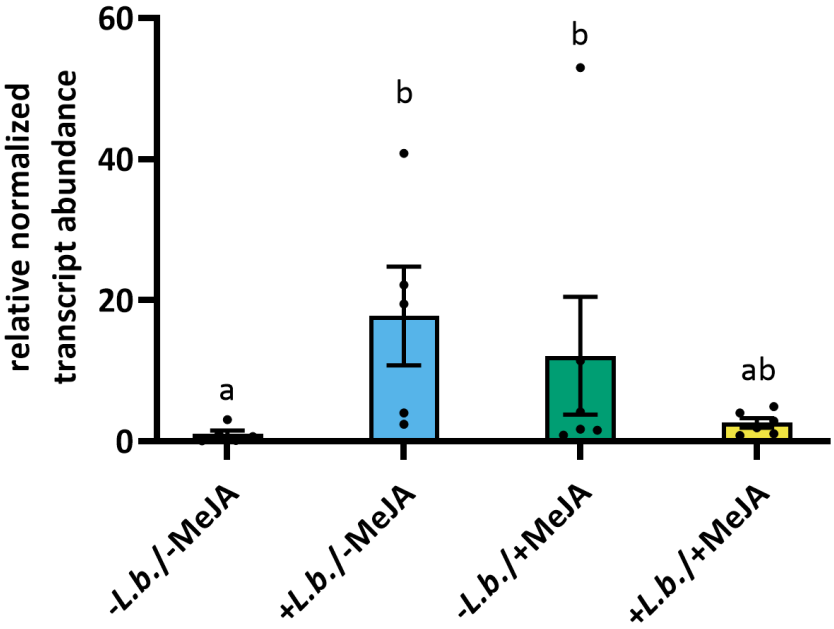

Figure 19 Relative normalized transcript abundance of *KTI* in *P.* × *canescens* leaves after application of *L. bicolor*, MeJA, or the combination of both

L. bicolor-inoculated (*L.b.*) or non-inoculated *P.* × *canescens* were treated for eight hours with methyl jasmonate (MeJA) or the solvent. The transcript abundance of *KTI* was measured. Bars show the means of the relative transcript abundance and the standard error. Each dot represents one biological replicate (n = 5) of one experiment. Different letters above the bars indicate statistically significant differences at $P < 0.05$ calculated by ANOVA and Tukey's post hoc test.

4.2. Role of CERK1 in systemic defense

4.2.1. *cerk1* KO poplars are insensitive to chitin

The involvement of chitin and CERK1 (the primary chitin receptor, Miya et al., 2007) in *L. bicolor*-mediated defense induction was shown in *Arabidopsis* (Vishwanathan et al., 2020). Here, two independent *cerk1-like1 (Potri.002G226600) and cerk1-like2 (Potri.014G156400)* double KO poplar lines in the *P.* × *canescens* background were used to test whether CERK1 is involved in *L. bicolor*-mediated defense induction in poplar.

First, the *cerk1* KO lines 19 and 20 were confirmed to be non-responsive to chitin. The *cerk1* KO lines 19 and 20 did not show a response toward chitin in the reactive oxygen species (ROS; 3.22) burst assay (Figure 20). In the mitogen-activated protein kinase assay (MAP kinase; 3.23), weak signals were detected on the western blot after chitin treatment of the *cerk1* KO lines (Figure 21). These signals were much weaker than in WT plants treated with chitin and comparable to control-treated plants. The weak signal could be due to stress, e.g., wounding caused during the harvest. MAP kinases 3 and 6 respond to many stresses, including wounding (Tena et al., 2001). ROS burst and MAP kinase phosphorylation are early signs of MAMP-induced effects in plants (Boller and Felix, 2009). The flg22 (a bacterial MAMP, Felix et al., 1999) response was used as a control and was still intact in *cerk1* KO plants similar to WT plants (Figure 20 & Figure 21). These results confirm the data of Muhr (2022), who generated the transgenic *cerk1* lines in her thesis. *Arabidopsis* WT plants were treated in the same manner and served as a control for the experimental setup because both assays were adapted from *Arabidopsis* assays. Chitin and flg22 led to ROS burst and MAP kinase phosphorylation in *Arabidopsis* leaves, as described in the literature (Petutschnig et al., 2010).

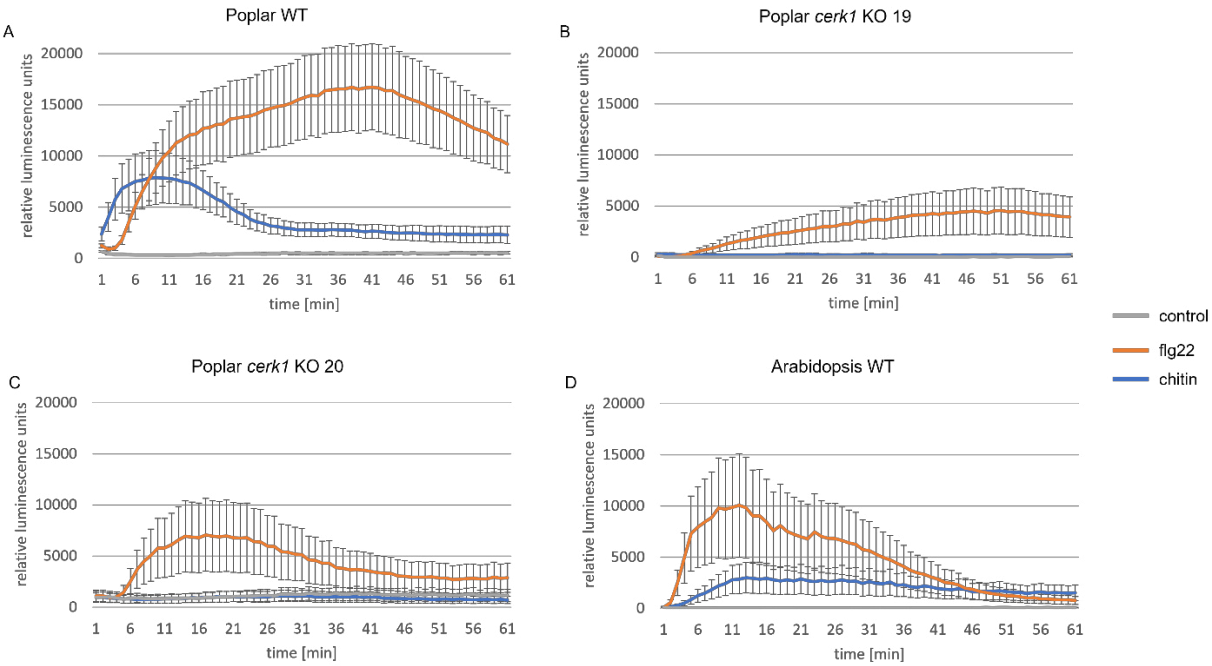

Figure 20 ROS burst assay of leaves of WT *P.* × *canescens* (A), *cerk1* KO 19 (B), *cerk1* KO 20 (C), and *Arabidopsis* (D) after chitin and flg22 treatment

Leave disks per line of WT *P.* × *canescens*, *cerk1* KO 19, and *cerk1* KO 20, as well as wildtype *Arabidopsis thaliana* (Col-0), were treated with H_2O, flg22, or chitin, and the relative fluorescence induced by reactive oxygen species was measured (3.22). The graphs show relative fluorescence units in a time course of 60 minutes. The grey line represents control (H_2O)-treated leaf disks, the orange line represents flg22-treated leaf disks, and the blue line represents chitin-treated leaf disks. Each data point is the average of eight technical replicates from three plants in one experiment. Error bars indicate the standard deviation of the replicates.

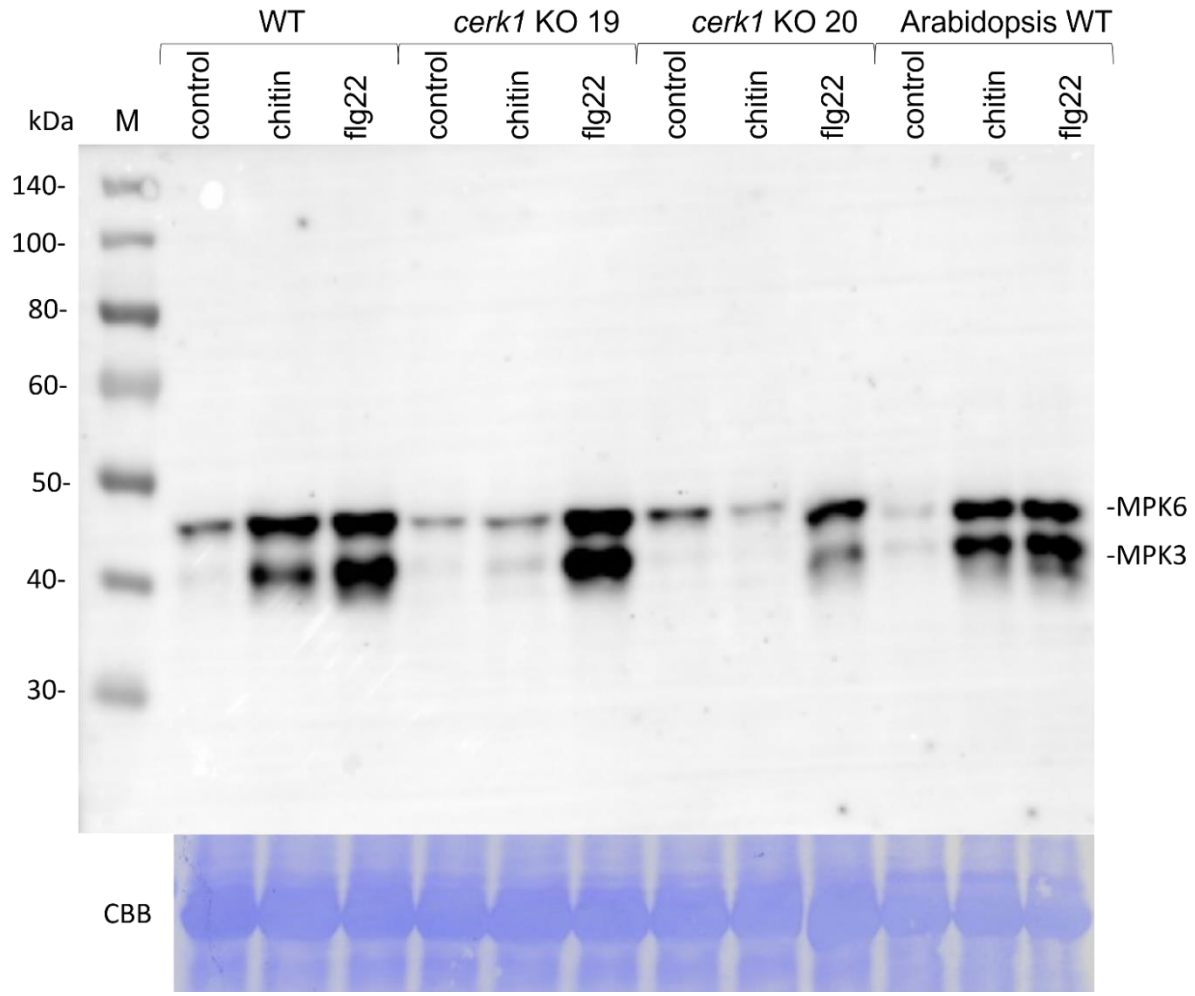

Figure 21 Western blot for the phosphorylation of MAP kinases in leaves of WT *P.* × *canescens*, *cerk1* KO 19, *cerk1* KO 20, and *Arabidopsis* after chitin and flg22 treatment
Three leaves of three plants per line WT *P.* × *canescens*, *cerk1* KO 19, and *cerk1* KO 20, as well as wildtype *Arabidopsis thaliana* (Col-0), were treated with H_2O, flg22, or chitin. Subsequently, phosphorylated MAP kinases (MPK) 3 and 6 were detected using primary antibody phospho-p44/42 (3.23). A picture of the western blot membrane is shown with the protein size marker (M) and the corresponding size on the left. As loading control, the membrane was stained with Coomassie Brilliant Blue (CBB).

4.2.2. *cerk1* KO poplars are physiologically similar to WT poplars when grown without *L. bicolor*

The performance of the *cerk1* KO lines 19 and 20 were characterized in comparison to WT poplars. The plants were grown in a mixture of soil and sand and irrigated with nutrient solutions with a low nitrogen supply (3.4). WT plants showed a slightly higher growth rate than the *cerk1* KO lines (Figure 22A), whereas *cerk1* KO line 19 produced more stem and leaf biomass than the WT or line 20 (Figure 22D+F). There were no statistically significant differences in the diameter increase of the stem, the number of leaves produced during one week, or the final fresh weight of the roots (Figure 22B, C, E). Over the time of the experiment,

WT and *cerk1* KO 19 plants had an almost identical mean height. The *cerk1* KO 20 plants were smaller, but only for one time point (27th May) there was a statistically significant difference. Toward the harvest, the mean heights became more similar (Figure 23).

Since the previous analyses (4.1.2) suggested an impact of *L. bicolor* mycorrhization on secondary metabolism and different stresses (e.g., insect attack) can induce secondary metabolite production (Philippe and Bohlmann, 2007), relative chlorophyll, flavone, anthocyanin, and nitrogen abundances were measured with an optical sensor. There were no differences in the indices of these components in a sand-soil mixture (Figure 24). During growth, red spots on leaves developed on *cerk1* KO plants, whereas no spots developed on WT plants (representative picture of the phenotype Figure 25).

Transpiration and photosynthesis are often used as parameters to assess plant stress levels (Liew et al., 2008). The stomatal conductance, photosynthesis rate, transpiration rate, and intercellular CO_2 (3.7) were not different between genotypes (Figure 21) but were low compared to published data for *P.* x *canescens* (Kasper et al., 2022; Sharmin et al., 2021; Shi et al., 2015).

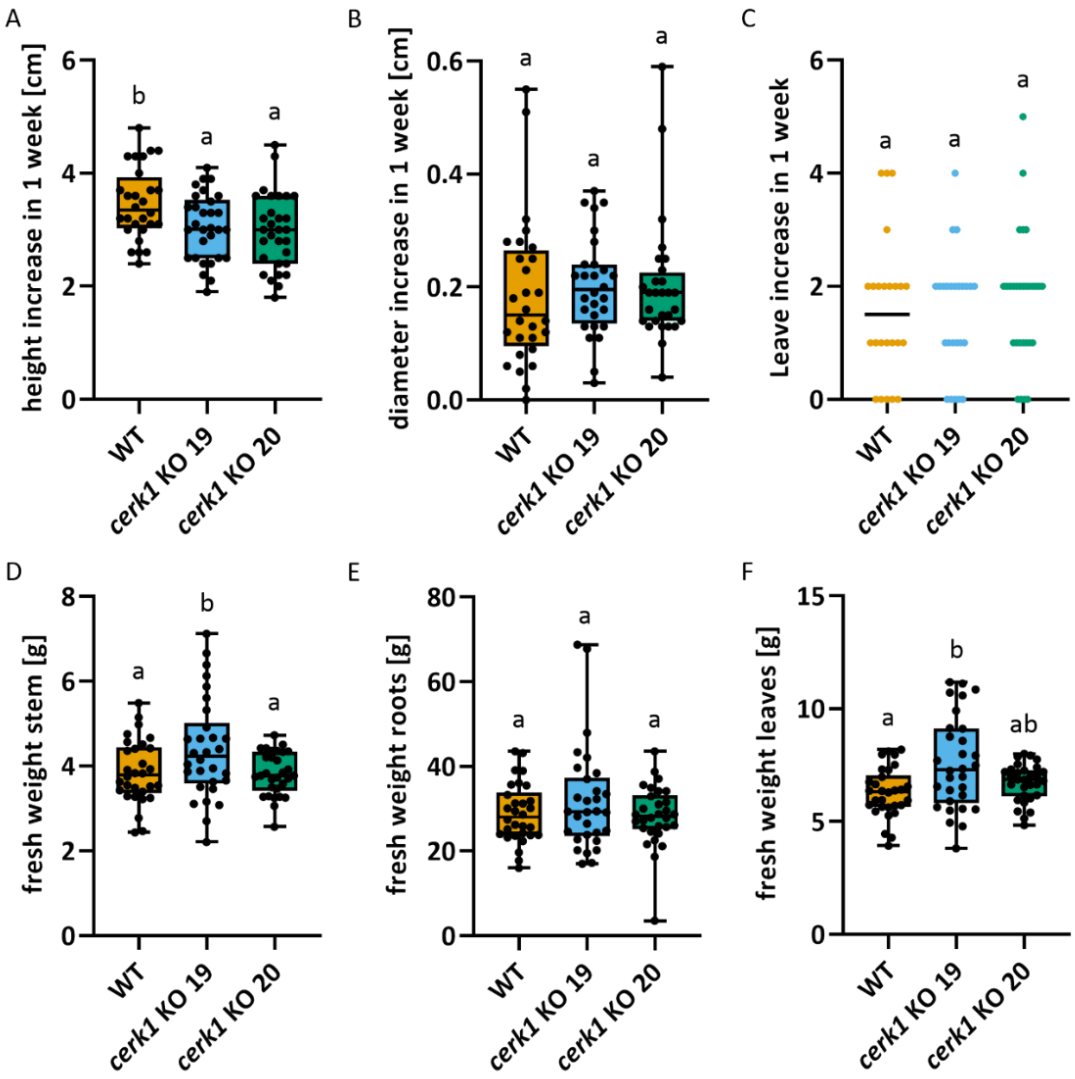

Figure 22 Height increase (A), stem diameter increase (B), leave increase (B), and fresh weights of the stem (D), roots (E), and leaves (F) of *P.* × *canescens* WT and *cerk1* KO lines
P. × *canescens* WT (orange), *cerk1* KO 19 (blue), and *cerk1* KO 20 (green) were grown for ten weeks in the greenhouse and irrigated daily nutrient solutions with a low nitrogen supply. The height, stem diameter, and leaf number were measured weekly, and the increase in one week was calculated. At the harvest, the fresh weights of the stem, the roots, and the leaves were determined (3.5). The figures show min-max boxplots with the whiskers spanning across the range of the data points of one experiment except for (C), which displays data points and the mean. (A-C) WT n = 28, *cerk1* KO 19 n= 25, *cerk1* KO 20 n = 29; (D-E) n = 30. Different letters above the boxplots indicate statistically significant differences at $P < 0.05$, calculated by ANOVA and Tukey's post hoc test.

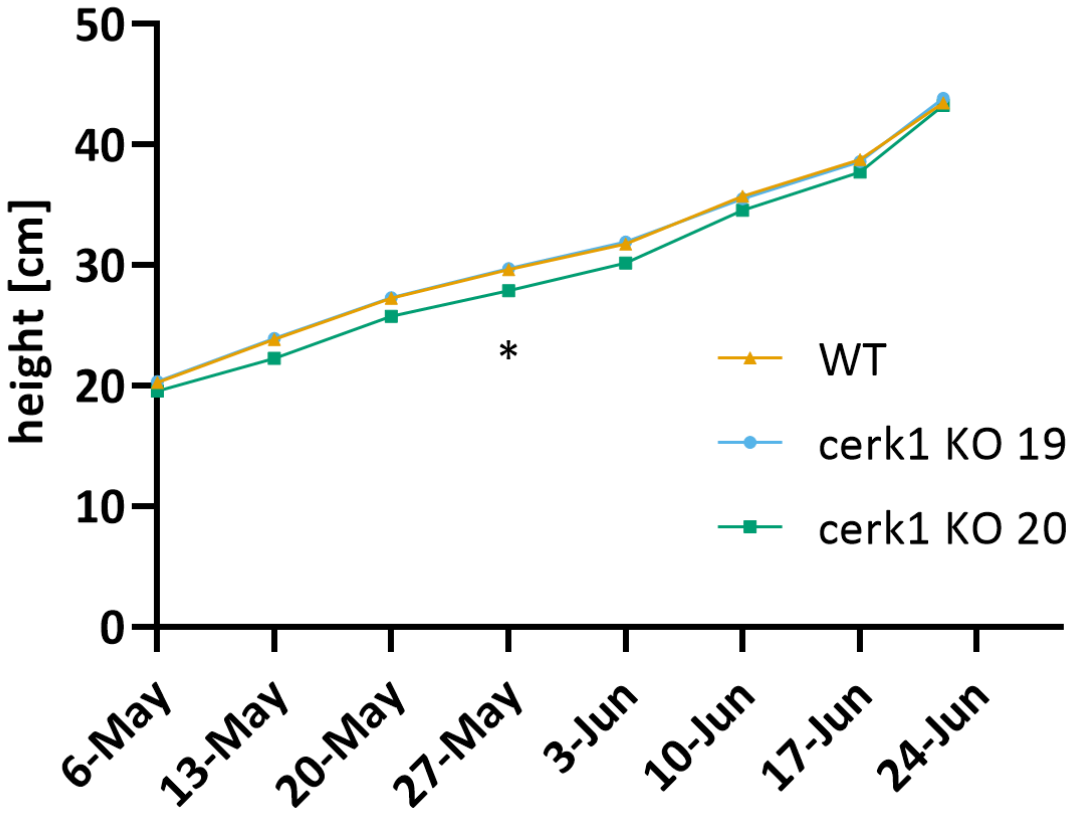

Figure 23 Height of WT, *cerk1* KO 19, and *cerk1* KO 20 plants over seven weeks
P. × *canescens* WT (orange), *cerk1* KO 19 (blue), and *cerk1* KO 20 (green) were grown for in total ten weeks in the greenhouse and irrigated daily nutrient solutions with a low nitrogen supply. The height was measured weekly, starting three weeks after potting. The figure shows the mean height (WT n = 41-30, *cerk1* KO 19 n= 42-30, *cerk1* KO 20 n = 42-30) at different dates of one experiment. Asterisks indicate statistically significant differences at $P < 0.05$, calculated by ANOVA.

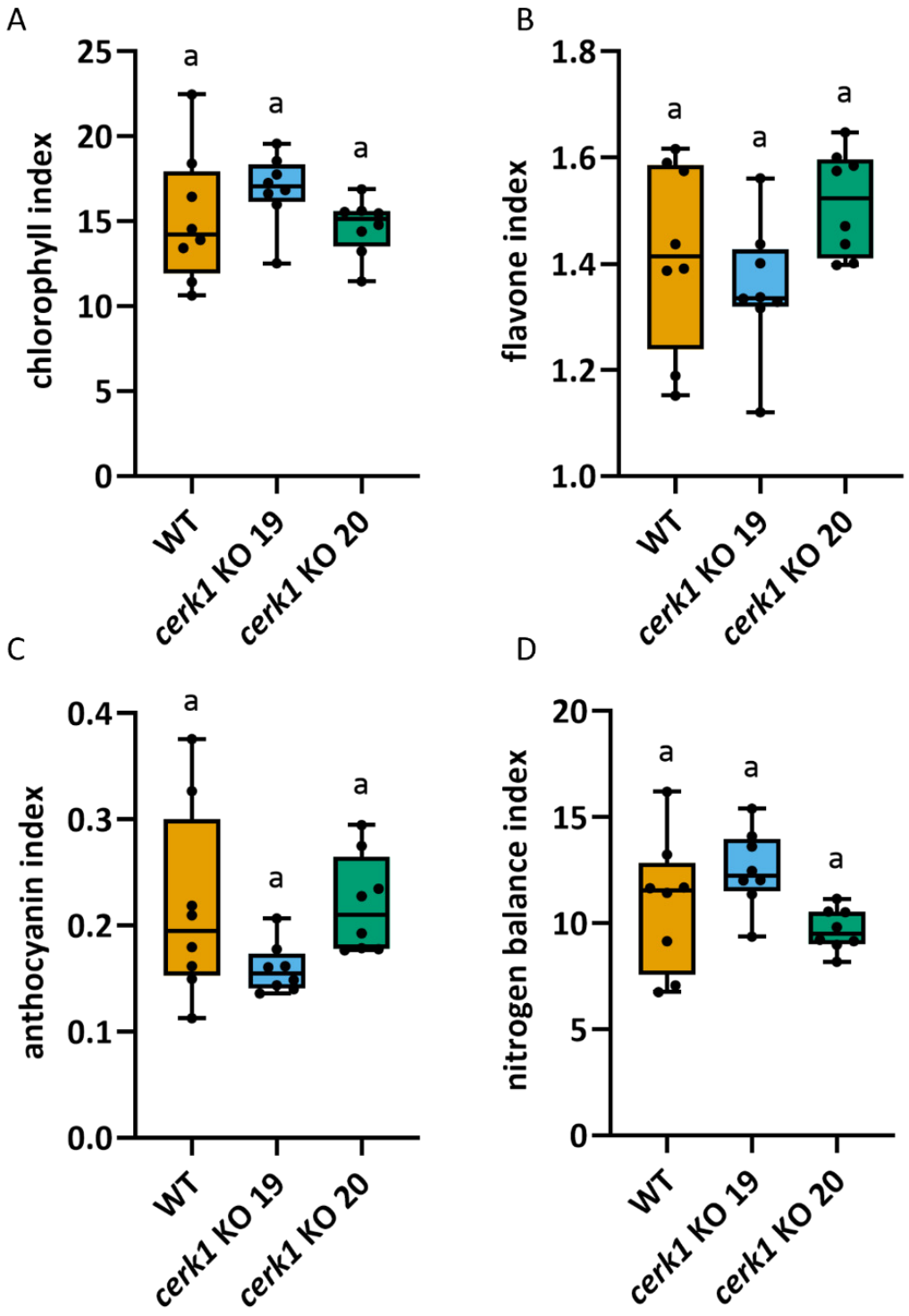

Figure 24 Chlorophyll (A), flavone (B), anthocyanin (C), and nitrogen balance (D) indices in WT and *cerk1* KO leaves

WT *P.* × *canescens* (orange), *cerk1* KO 19 (blue), and *cerk1* KO 20 (green) were grown in the greenhouse and irrigated daily nutrient solutions with low nitrogen supply. The chlorophyll, flavone, anthocyanin, and nitrogen balance index of the fourth fully developed leaf were measured with a DUALEX optical sensor (3.6). The figures show min-max box plots with the whiskers spanning the range of the data points and with each point representing a biological replicate (n = 8) of one experiment. Different letters above the boxplots indicate statistically significant differences at $P < 0.05$, calculated by ANOVA and Tukey's post hoc test.

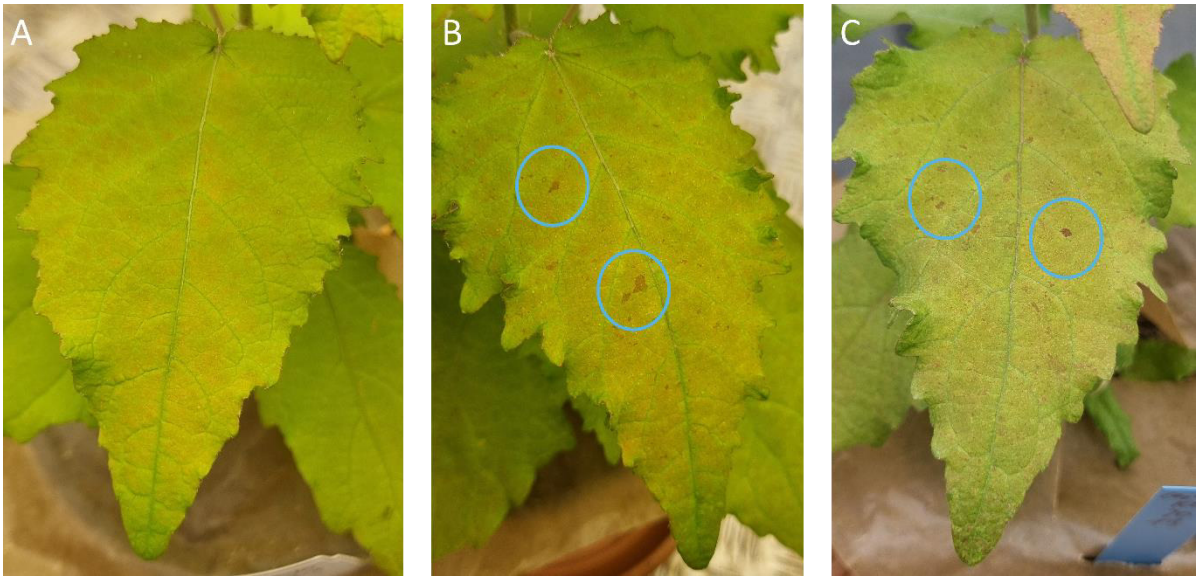

Figure 25 Leaves of WT poplars and *cerk1* KO

WT *P.* × *canescens* (A), *cerk1* KO 19 (B), and *cerk1* KO 20 (C) were grown under greenhouse conditions. Representative pictures of leaves of eight-week-old plants. Blue circles mark representative red spots.

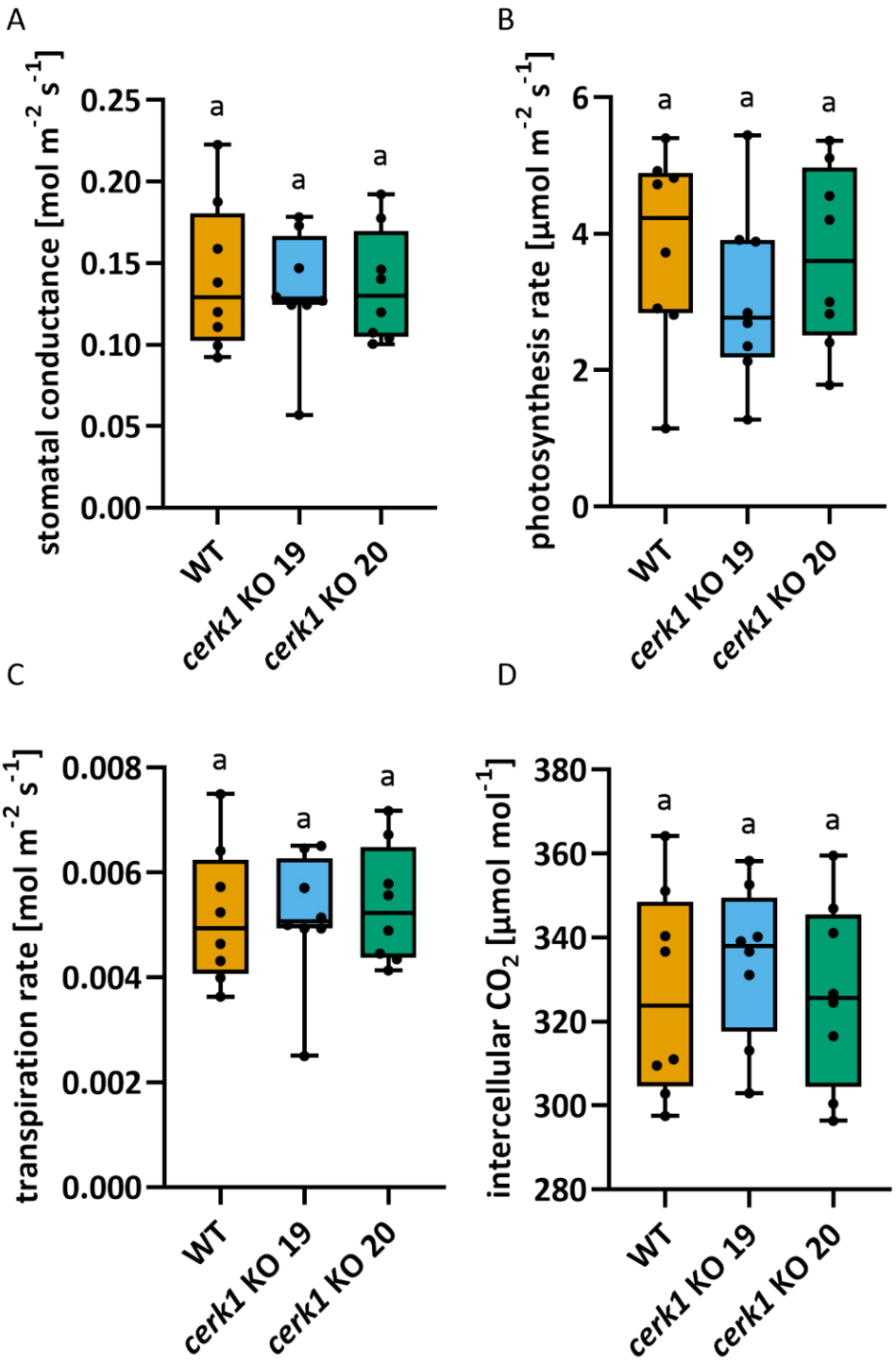

Figure 26 Stomatal conductance (A), photosynthesis rate (B), transpiration rate (C), and intercellular CO_2 (D) of WT and *cerk1* KO poplars

P. × *canescens* WT (orange), *cerk1* KO 19 (blue), and *cerk1* KO 20 (green) were grown in the greenhouse and irrigated daily nutrient solutions with low nitrogen supply. The stomatal conductance, photosynthesis rate, transpiration rate, and intercellular CO_2 of the fourth fully developed leaf were measured (3.7). The leaf temperature was 30.2 ± 1 °C, and the ambient CO_2 concentration was 397 ± 1 ppm. The figures show min-max box plots with the whiskers spanning the range of the data points and with each point representing a biological replicate (n = 8) of one experiment. Different letters above the boxplots indicate statistically significant differences at $P < 0.05$, calculated by ANOVA and Tukey's post hoc test.

4.2.3. *cerk1* KO poplars are physiologically similar to WT poplars when grown with *L. bicolor*

When plants were treated with *L. bicolor cerk1* KO 19 plants had a lower but not statistically significant different mycorrhization rate than WT *L. bicolor*-pretreated plants (Figure 27).

There were no statistically significant differences in height or stem diameter increase between mycorrhiza-treated and nontreated WT and *cerk1* KO 19 plants. Also, the increase in leaf number was not different. Furthermore, the Leaf, stem, and root fresh weights were the same at the harvest time (Figure 29).

When treated with *L. bicolor*, the *cerk1* KO 19 plants had a higher chlorophyll index and nitrogen balance index (Figure 30). The same red spots as described above (Figure 25) developed on *cerk1* KO 19 plants.

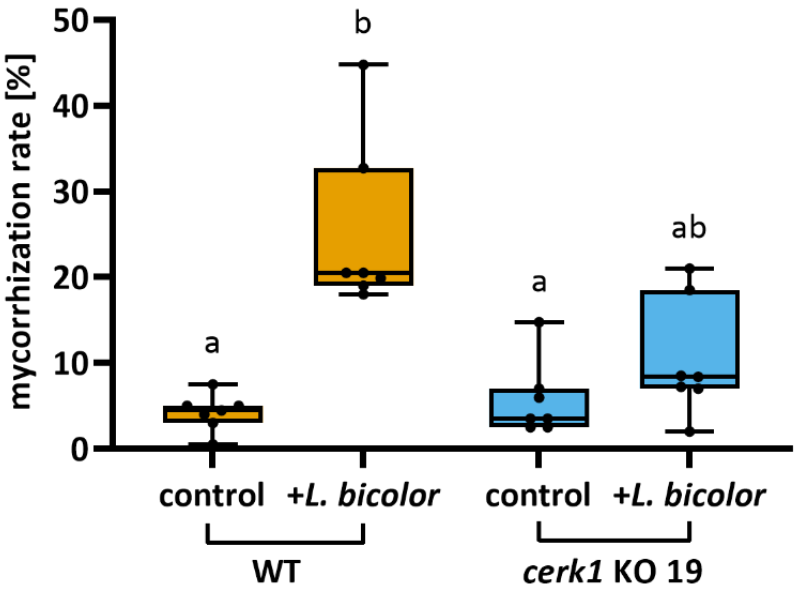

Figure 27 Mycorrhization rate of WT and *cerk1* KO 19 plants
WT *P.* × *canescens* and *cerk1* KO 19 plants with or without *L. bicolor* were grown in the greenhouse and irrigated daily nutrient solutions with low nitrogen supply. After ten weeks, the mycorrhization rate in percent was determined (3.8). Displayed are min max box plots with the whiskers spanning the range of the data points and each point representing a biological replicate (n = 6) of one experiment. Different letters above the boxplots indicate statistically significant differences at $P < 0.05$, calculated by ANOVA and Tukey's post hoc test.

Cross-sections of visually mycorrhizal root tips and control root tips were prepared after seven days of *L. bicolor* treatment in the sterile sandwich system (3.3). The sections were stained with propidium iodide (red, plant cell wall) and wheat germ agglutinin, Alexa Fluor 488 conjugate (green, fungus; 3.9). The cross-sections of non-mycorrhizal root tips of both cerk1

KO lines looked similar to cross-sections of WT root tips (Figure 28, left). Cross-sections of visually mycorrhizal root tips showed that the fungus formed a mantle and grew into the root between cortex cells (Figure 28, right). The extensions of the root and fungal mantle, which are usually round, are root material or fungal mycelium which was compressed because of the sandwich setup (see Figure 5).

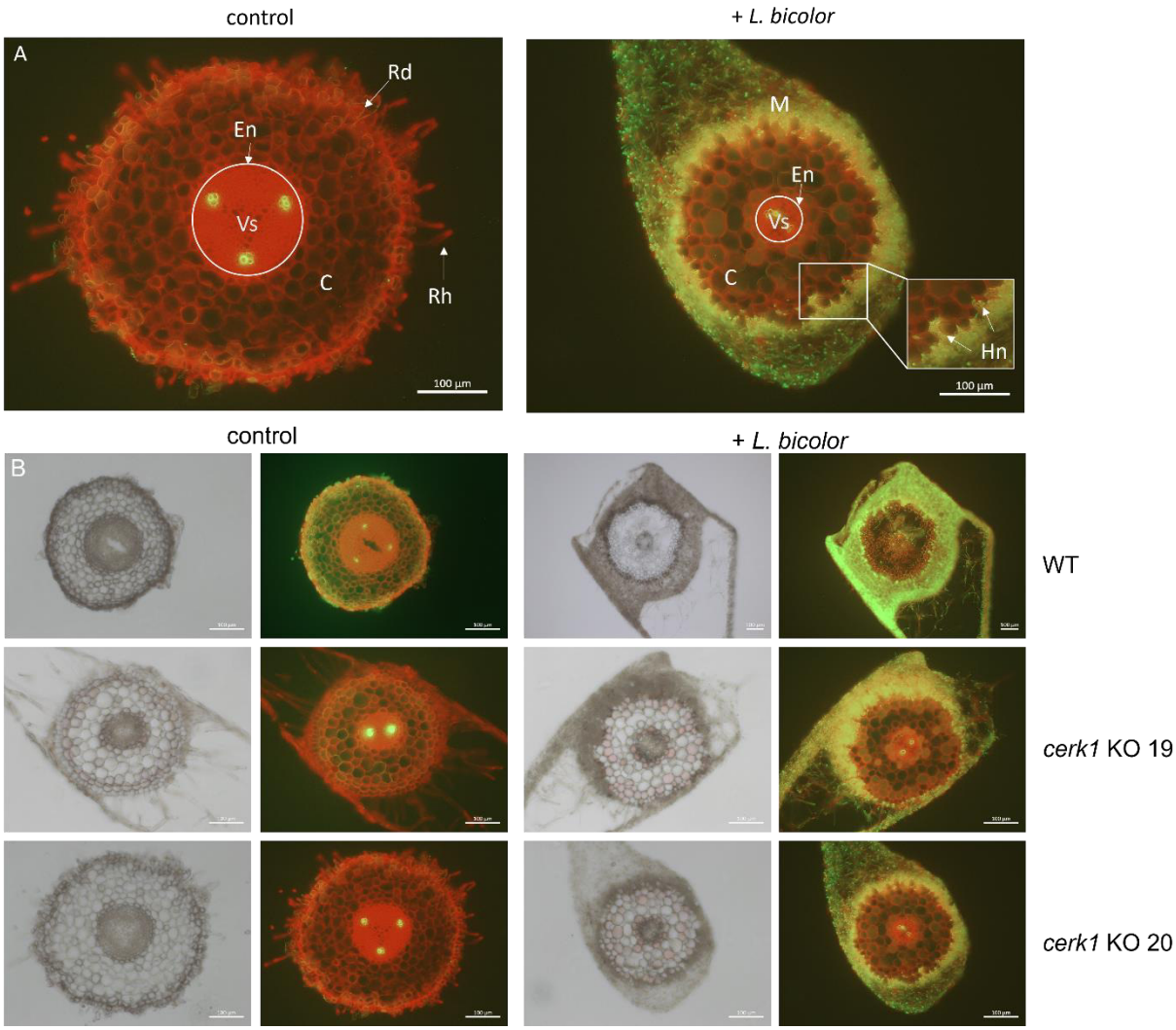

Figure 28 Cross-sections of *L. bicolor*-inoculated and control WT, *cerk1* KO 19, and *cerk1* KO 20 root tips

Seven days after inoculation with *L. bicolor* or control treatment in a sterile sandwich system, *P.* × *canescens* WT, *cerk1* KO 19, and *cerk1* KO 20 cross-sections of root tips were produced. Subsequently, sections were stained with wheat germ agglutinin, Alexa Fluor 488 conjugate (green, fungus), and propidium Iodide (red, plant cell wall; 3.9). The brightness of the pictures was enhanced by 20 %. Scale bar = 100 µm. (A) Enlarged pictures with labels: C: cortex cells, En: endodermis, Hn: developing Hartig net, M: fungal mantle, Rd: rhizodermis, Rh: root hair, Vs: vascular system (inside circle). (B) Bright-field (grey) and fluorescence pictures (green/red) of WT and *cerk1* KO line cross-sections.

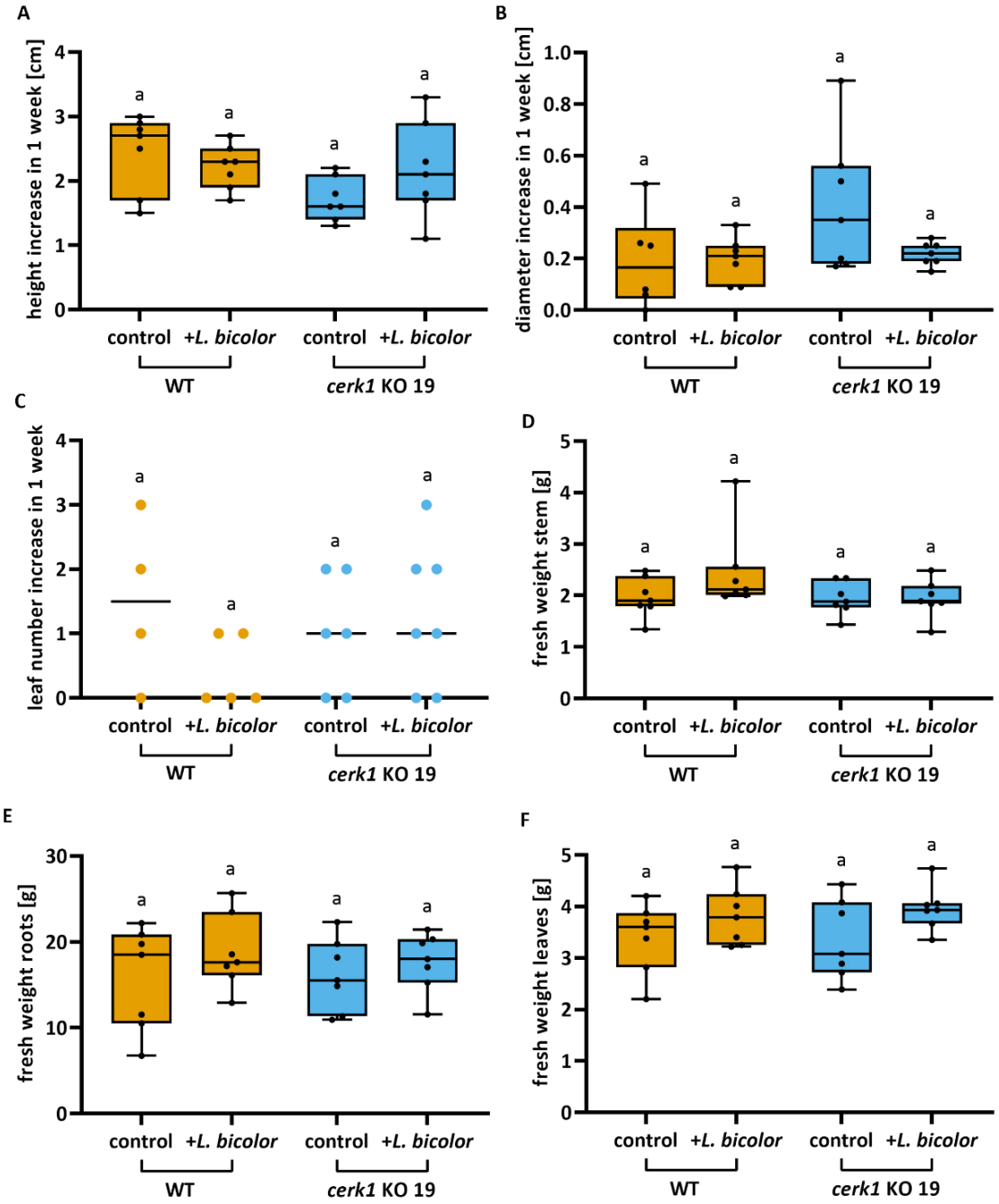

Figure 29 Height increase (A), stem diameter increase (B), leave number increase (B), and fresh weights of the stem (D), roots (E), and leaves (F) of mycorrhizal WT and *cerk1* KO 19
P. × *canescens* WT (orange) and *cerk1* KO 19 (blue) plants with or without *L. bicolor* were grown for ten weeks in the greenhouse and irrigated daily nutrient solutions with low nitrogen supply. The height, stem diameter, and leaf number were measured weekly, and the increase in one week was calculated. At the harvest, the fresh weights of the stem, the roots, and the leaves were determined (3.5). The figures show min-max boxplots with the whiskers spanning across the range of the data points except for (C), which displays data points and the mean (n = 6) of one experiment. Different letters above the boxplots indicate statistically significant differences at $P < 0.05$, calculated by ANOVA and Tukey's post hoc test.

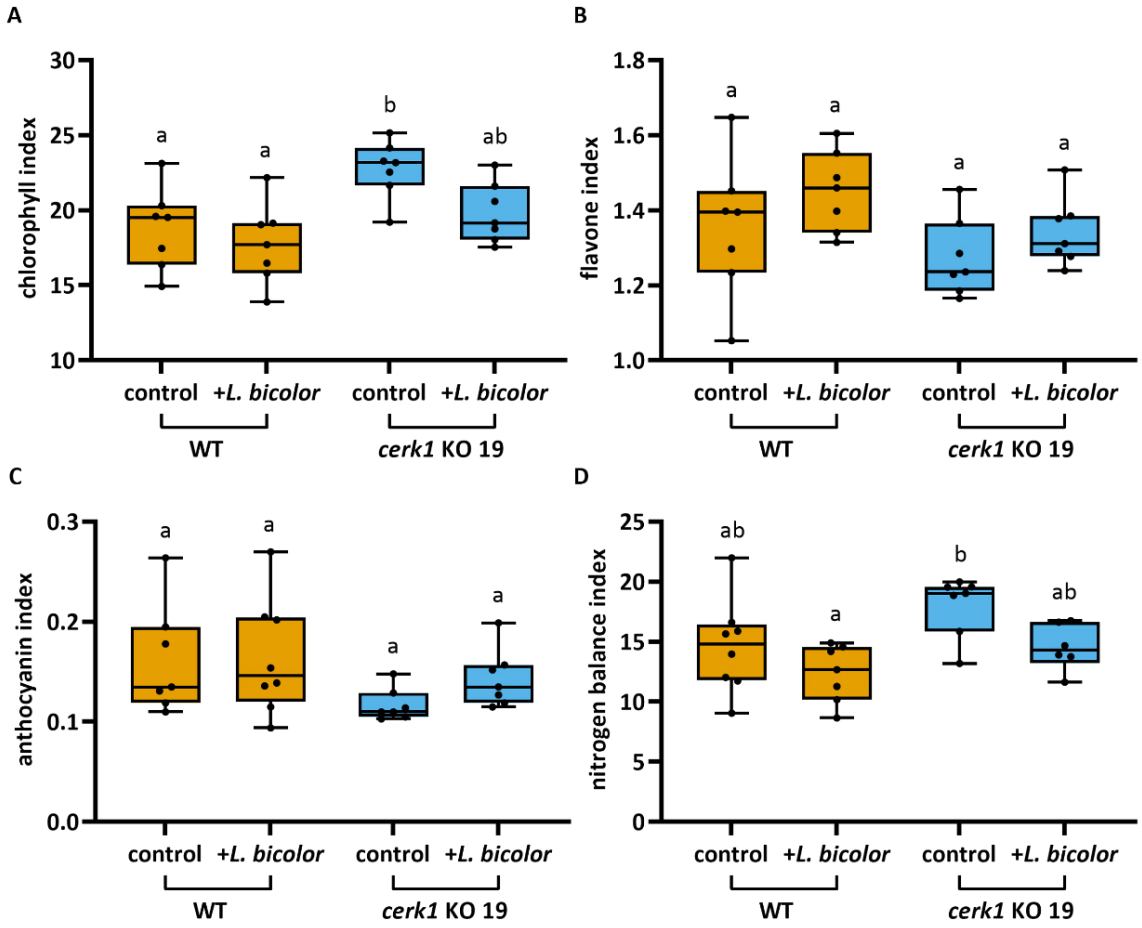

Figure 30 Chlorophyll (A), flavone (B), anthocyanin (C), and nitrogen balance (D) indices in leaves of the WT and *cerk1* KO poplars pretreated with *L. bicolor*

P. × *canescens* WT and *cerk1* KO 19 plants with or without *L. bicolor* were grown for ten weeks in the greenhouse and irrigated daily with nutrient solutions with a low nitrogen supply. After ten weeks, the chlorophyll, flavone, anthocyanin, and nitrogen balance indices of the fourth fully developed leaf were measured with a DUALEX optical sensor (3.6). The figures show min-max boxplots with the whiskers spanning across the range of the data points. Each point represents one biological replicate (n = 8) of one experiment. Different letters above the boxplots indicate statistically significant differences at $P < 0.05$, calculated by ANOVA and Tukey's post hoc test.

4.2.4. *Helicoverpa armigera* weight gain was unaltered on *cerk1* KO plants

Since it was expected that *cerk1* KO lines were compromised in defense signaling, insect feeding on both *cerk1* KO lines and WT poplar plants grown in the greenhouse and under outdoor conditions was tested. The plants were grown without *L. bicolor* treatment to analyze whether the plants were affected in their defense capacity without mycorrhiza-induced defense. *Helicoverpa armigera* larvae in the third instar were allowed to feed for two days on leaf disks from the fourth leaf of ten-week-old plants (3.17). The weight differences were similar regardless of genotype or growth condition (Figure 31).

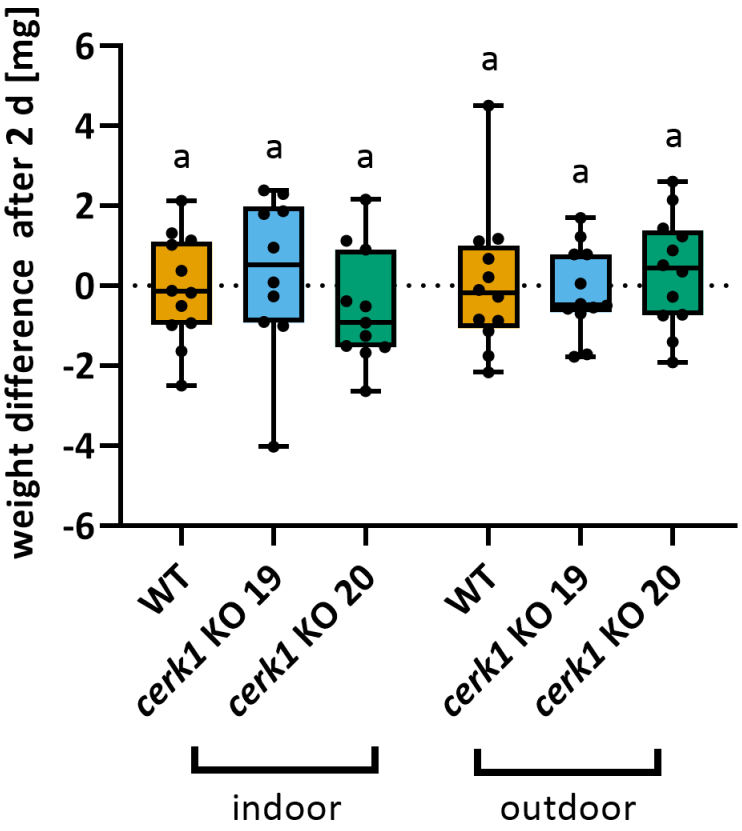

Figure 31 *Helicoverpa armigera* larvae weight differences after feeding on WT and *cerk1* KO leaf disks

P. × *canescens* WT, *cerk1* KO 19, and *cerk1* KO 20 were grown in a greenhouse (3.4). After four weeks, half of the plants were transferred outdoors, and after another six weeks, leaf disks from greenhouse-grown and outdoor-grown plants were used for a feeding assay with *Helicoverpa armigera*. After two days, all larvae were weighed (3.17). The figure shows min max box plots with the whiskers spanning the range of the data points and each point representing a biological replicate (n = 12) of one experiment. Different letters above the boxplots indicate statistically significant differences at $P < 0.05$, calculated by ANOVA and Tukey's post hoc test.

4.2.5. *cerk1* KO leads to altered *KTI* and *MLP423* gene induction after *L. bicolor* treatment

Vishwanathan et al. (2020) showed that CERK1 is necessary for *L. bicolor*-induced systemic defense in *Arabidopsis*. The *cerk1* KO plants were used to examine whether CERK1 is involved in *L. bicolor*-induced systemic defense induction in poplar. As a readout for the systemic defense response, the transcriptional responses of *KUNITZ FAMILY TRYPSIN AND PROTEASE INHIBITOR PROTEIN* (*KTI*) and *MAJOR LATEX PROTEIN (MLP)-LIKE PROTEIN 423* (*MLP423*) was used. *KTI* and *MLP423* were chosen since they showed increased transcript abundances after *L. bicolor* treatment under sterile (3.3) and outdoor conditions (Kaling et al., 2018) and are

directly connected to defense responses (Chen and Dai, 2010; Major and Constabel, 2008; Song et al., 2020). Here the sterile setup (3.13) was used to test the responses of *KTI* and *MLP423* in the WT and *cerk1* KO lines in response to *L. bicolor*. The induction of these genes varied between experiments and had an overall high variance. However, transcriptional levels of both genes increased in WT leaves after seven days of treatment with *L. bicolor* of the roots. *KTI* levels were induced about 5-fold (Figure 32A, orange bars), and *MLP423* levels were induced about 3-fold (Figure 32B, orange bars). After seven days of treatment, non-inoculated control plants of *cerk1* KO 19 and *cerk1* KO 20 showed a similar level of transcript abundance of *KTI* as WT control plants (Figure 32A). Mycorrhizal *cerk1* KO 19 plants showed a reduction of *KTI* levels, which were statistically not different from control and *L. bicolor*-treated WT plants. In *cerk1* KO 20, there was no difference in *KTI* transcript abundance in control and *L. bicolor*-treated plants (Figure 32A). *MLP423* transcript abundances are significantly increased three-fold in *cerk1* KO 19 plants. In *cerk1* KO 20, the transcript abundance was the same as in the WT control, and there was no difference between the treatments (Figure 32B).

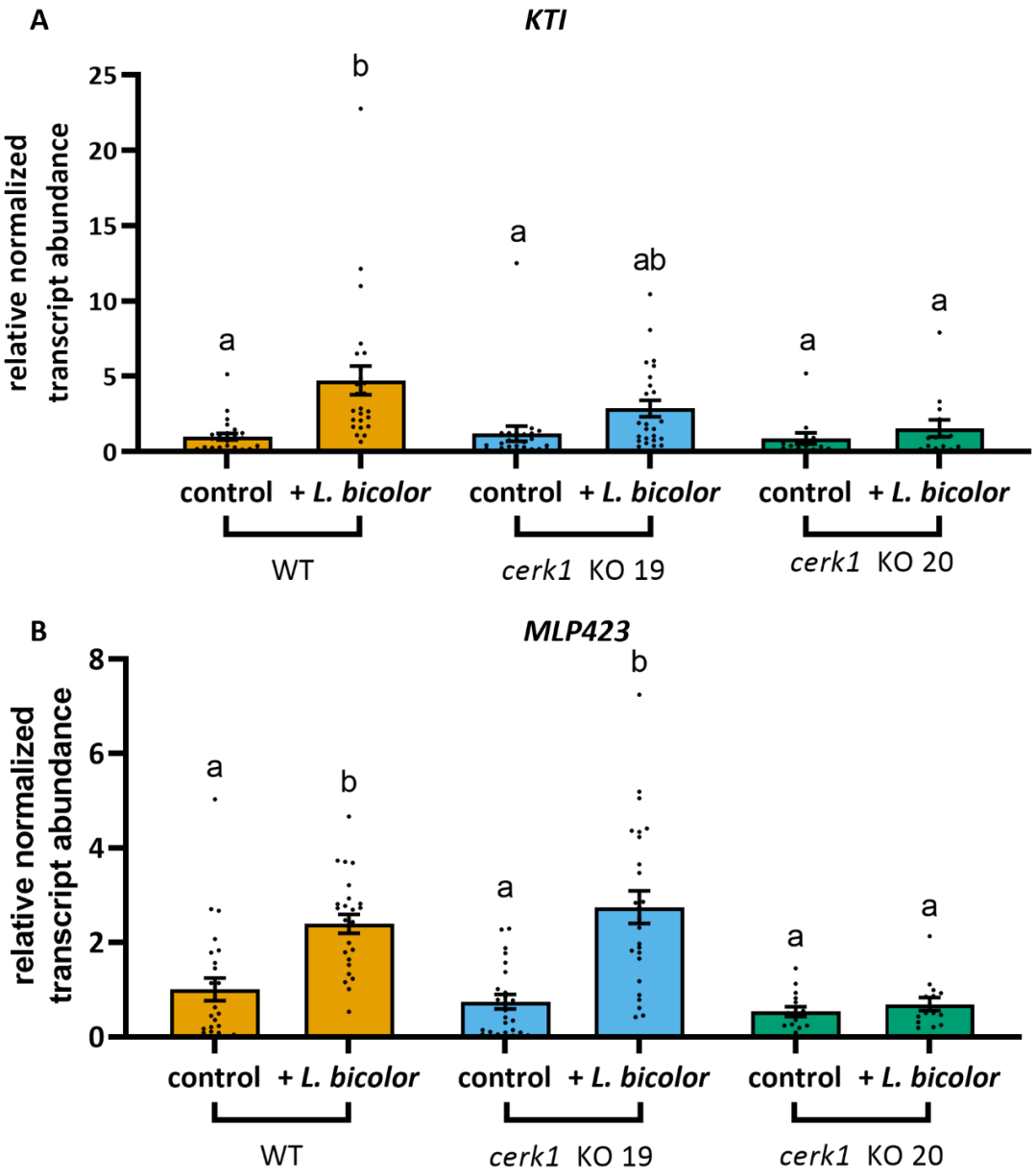

Figure 32 Relative transcript abundances of (A) *KTI* and (B) *MLP423* in leaves after *L. bicolor* root inoculation for seven days in WT, *cerk1* KO 19, and *cerk1* KO 20

P. × *canescens* WT (orange), *cerk1* KO 19 (blue), and *cerk1* KO 20 (green) were treated with *L. bicolor* for seven days in a sterile sandwich system (3.3). Afterward, the transcript abundances of *KTI* (Potri.019G088200) and *MLP423* (Potri.010G000600) were measured (3.21). The data were normalized to the respective WT control. The bars show the mean of the relative transcript abundance and the standard error. Each dot represents one biological replicate. WT n = 25, *cerk1* KO 19 n = 25 in five independent experiments, and *cerk1* KO 20 n = 14 in three independent experiments. Different letters above the bars indicate statistically significant differences at $P < 0.05$ calculated by ANOVA and Tukey's post hoc test, considering the independent experiments as a random factor.

After 14 days of *L. bicolor* treatment, WT plants showed elevated levels of *KTI* transcript abundance in leaves when treated with *L. bicolor* of roots, whereas there was no difference between control and *L. bicolor*-treated *cerk1* KO 19 plants (Figure 33A). The *MLP423* transcript abundance was elevated in WT and *cerk1* KO 19 plants, but there was no statistically significant difference (Figure 33B).

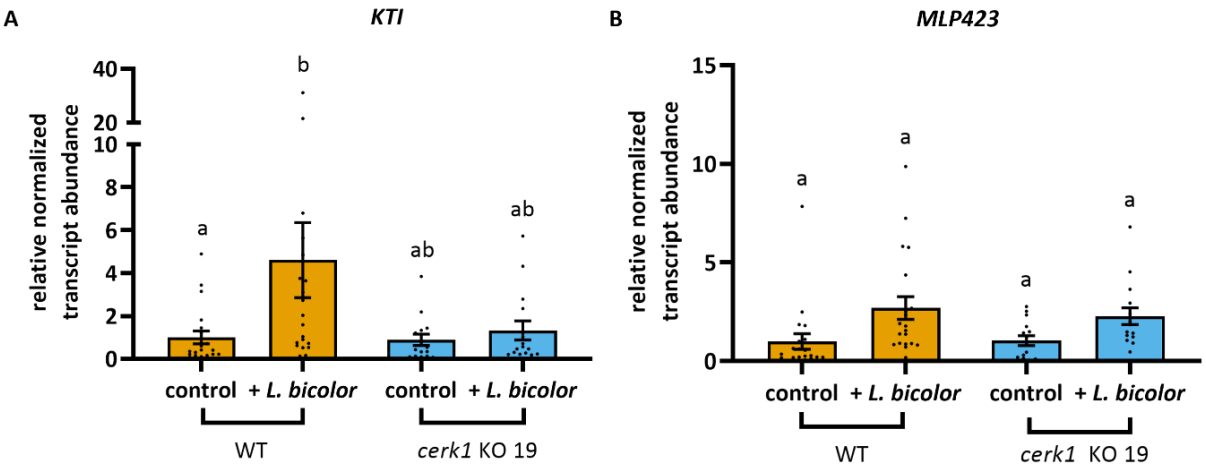

Figure 33 Relative transcript abundances of (A) *KTI* and (B) *MLP423* in leaves after *L. bicolor* root inoculation for 14 days in WT and *cerk1* KO 19
P. × *canescens* WT (orange), and *cerk1* KO 19 (blue) were treated with *L. bicolor* for 14 days in a sterile sandwich system (3.3). Afterward, the transcript abundances of *KTI* (Potri.019G088200) and *MLP423* (Potri.010G000600) were measured (3.21). The data were normalized to the respective WT control. The bars show the mean of the relative transcript abundance and the standard error. Each dot represents one biological replicate (n = 15) in three independent experiments. Different letters above the bars indicate statistically significant differences at $P < 0.05$ calculated by ANOVA and Tukey's post hoc test, considering the independent experiments as a random factor.

4.2.6. Chitin does not change *KTI* and *MLP423* transcript abundances in systemic leaves

Vishwanathan et al. (2020) found that not only living *L. bicolor* elicits a systemic defense response in *Arabidopsis* plants but also heat-killed *L. bicolor* and even chitin could elicit the same systemic response.

WT poplar grown in the greenhouse were treated two times within eleven days with living *L. bicolor*, heat-killed *L. bicolor*, the supernatant of the *L. bicolor* liquid culture, chitin, or only buffer as described in 3.15. The mycorrhization rate was not significantly different between treatments (Figure 34). Some plant roots were mycorrhizal, typical for experiments with non-inoculated greenhouse-grown plants because of the non-sterile environment. Mycorrhization could have has an impact on the outcome of the experiment. The transcript abundance of *KTI*

was not significantly different between the treatments (Figure 35A). The heat-killed *L. bicolor* treatment resulted in a trend toward higher *MLP423* transcript abundance (Figure 35B). The plants with higher mycorrhization rates were not those with higher transcript abundances (Figure 36).

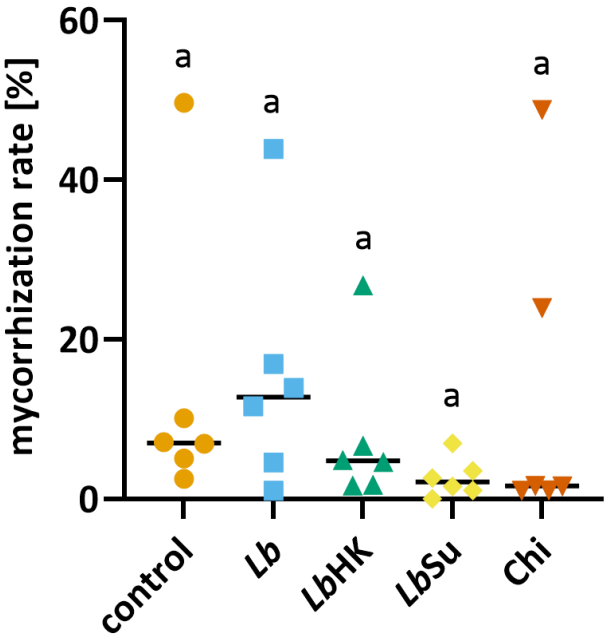

Figure 34 Mycorrhization rate of WT treated with different *L. bicolor* preparations
Greenhouse-grown WT *P.* × *canescens* were treated two times over eleven days with buffer (control; orange), *L. bicolor* (*Lb*; blue), heat-killed *L. bicolor* (*Lb*HK; green), the supernatant of *L. bicolor* liquid culture (*Lb*Su; yellow) or 500 µg mL^{-1} chitin (red) for eleven days (3.15). After the treatment, the mycorrhization rate in percent was determined (3.8). The Graph shows data points (biological replicates, n = 6) and the mean of one experiment. Different letters above the data points indicate statistically significant differences at $P < 0.05$ calculated by ANOVA and Tukey's post hoc test.

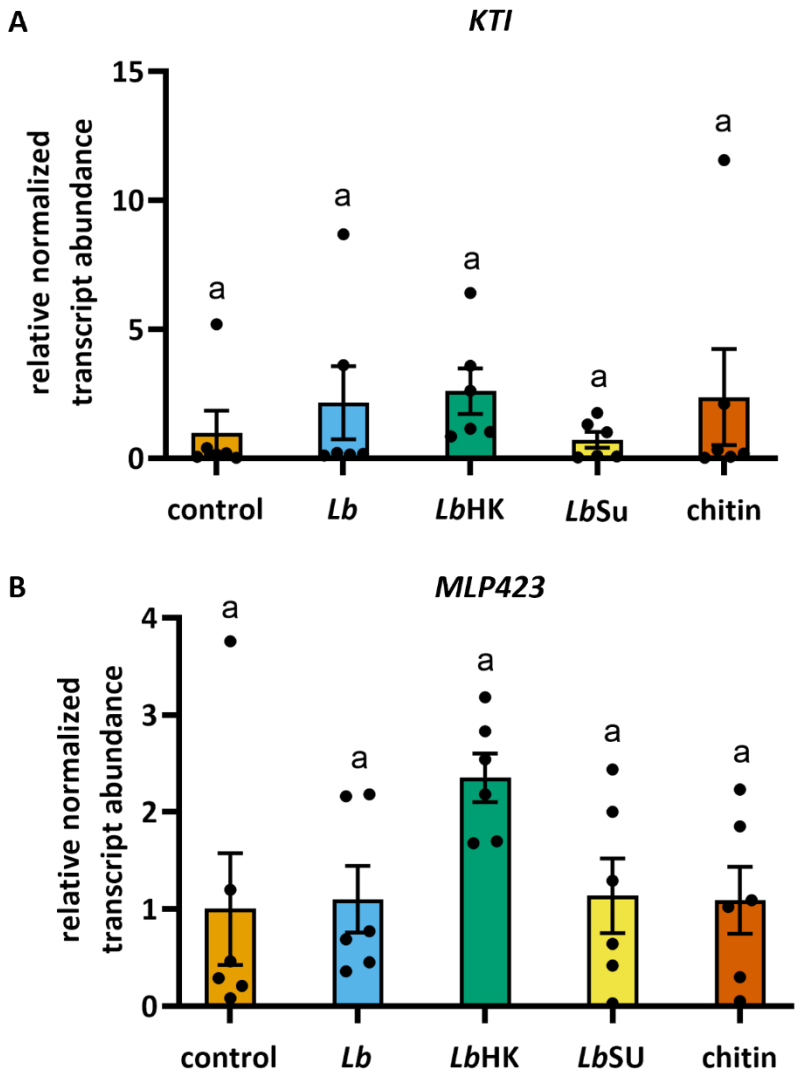

Figure 35 Relative transcript abundances of (A) *KTI* and (A) *MLP423* in leaves after eleven days of root treatment with different *L. bicolor* preparations

Greenhouse-grown WT *P.* × *canescens* were treated two times over eleven days with buffer (control; orange), *L. bicolor* (*Lb*; blue), heat-killed *L. bicolor* (*Lb*HK; green), the supernatant of *L. bicolor* liquid culture (*Lb*Su; yellow) or 500 µg mL^{-1} chitin (red) for eleven days (3.15). After the treatment, the transcript abundances for *KTI* (Potri.019G088200) and *MLP423* (Potri.010G000600) were measured (3.21). The bars show the mean of the relative normalized transcript abundance and the standard error. Each dot represents one biological replicate (n = 6) of one experiment. Different letters above the bars indicate statistically significant differences at $P < 0.05$ calculated by ANOVA and Tukey's post hoc test.

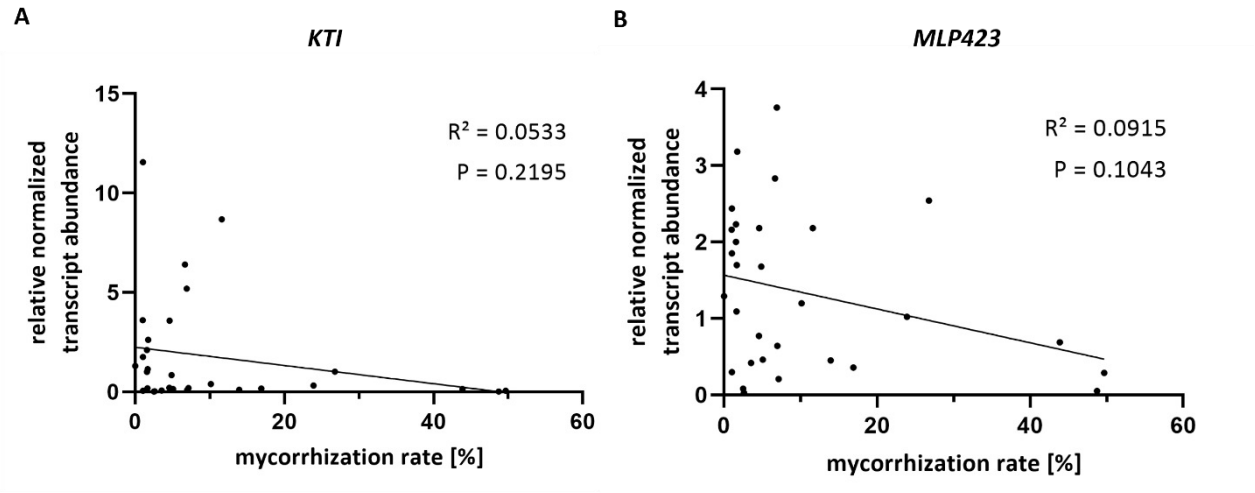

Figure 36 Correlation of mycorrhization rate and *KTI* (A) and *MLP423* (B) relative transcript abundances
The mycorrhization rate (Figure 34) was correlated to the relative transcript abundances of *KTI* and *MLP423* (Figure 35). Linear regression was performed to test for the dependency of the parameters.

The experimental chitin treatment was repeated under sterile conditions to avoid disturbance which might have been introduced by the uncontrolled EMF colonization of the greenhouse plants. WT poplars were incubated on M-MMNS agar supplemented with 100 µg mL^{-1} chitin in a similar sandwich setup as before (3.14) and used to determine the transcriptional levels of *KTI* and *MLP423* during a time course of seven days (Figure 37). The average transcript level of *KTI* was higher but not significantly after eight hours of chitin treatment (Figure 37A). The transcript abundance was, on average lower after chitin application for the other time points. There were no significant differences between treatments. There were also no statistically significant differences between time points. The relative transcript abundances of *MLP423* in leaves were unaffected by the chitin treatment of the roots (Figure 37B).

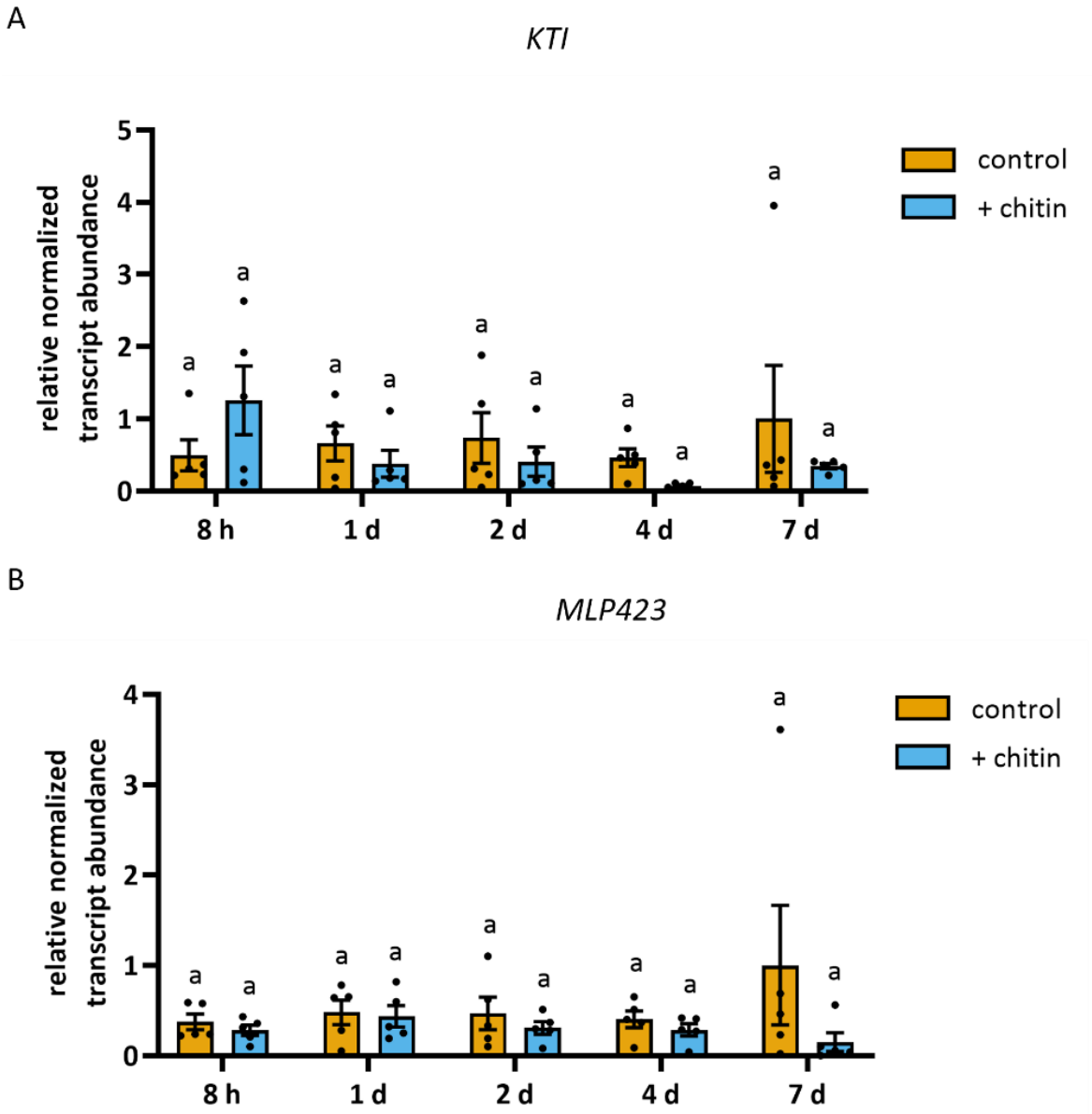

Figure 37 Time course of relative transcript abundances of (A) *KTI* and (B) *MLP423* after root chitin treatment in WT leaves

P. × *canescens* WT were incubated on M-MMNS agar supplemented with 100 µg mL^{-1} chitin in a sterile sandwich system (3.14). The transcript abundances of *KTI* (Potri.019G088200) and *MLP423* (Potri.010G000600) were measured (3.21). The bars show the mean of the relative normalized transcript abundance in bar charts with the standard error. Each dot represents one biological replicate (n = 4) of one experiment. The data were normalized to 7 days control for comparability with previous experiments. Different letters above the bars indicate statistically significant differences at $P < 0.05$ calculated by ANOVA and Tukey's post hoc test considering the time point as a random factor.

Furthermore, the influence of increasing chitin amounts on the transcript levels of *KTI* was tested. The relative transcriptional levels of *KTI* were unaffected by rising amounts of chitin

after one day and seven days of chitin exposure (Figure 38A+B). Since the defense against insects requires JA-dependent signaling (Pieterse et al., 2012) and JA signaling components were found to be induced by *L. bicolor* before (Kaling et al., 2018), the transcript level of the JA synthesis pathways gene *AOS* was also checked. The transcript abundance was not different between treatments or time points (Figure 38B). Because the experiments with chitin did not lead to *KTI* induction, additional studies with the *cerk1* KO lines were not pursued.

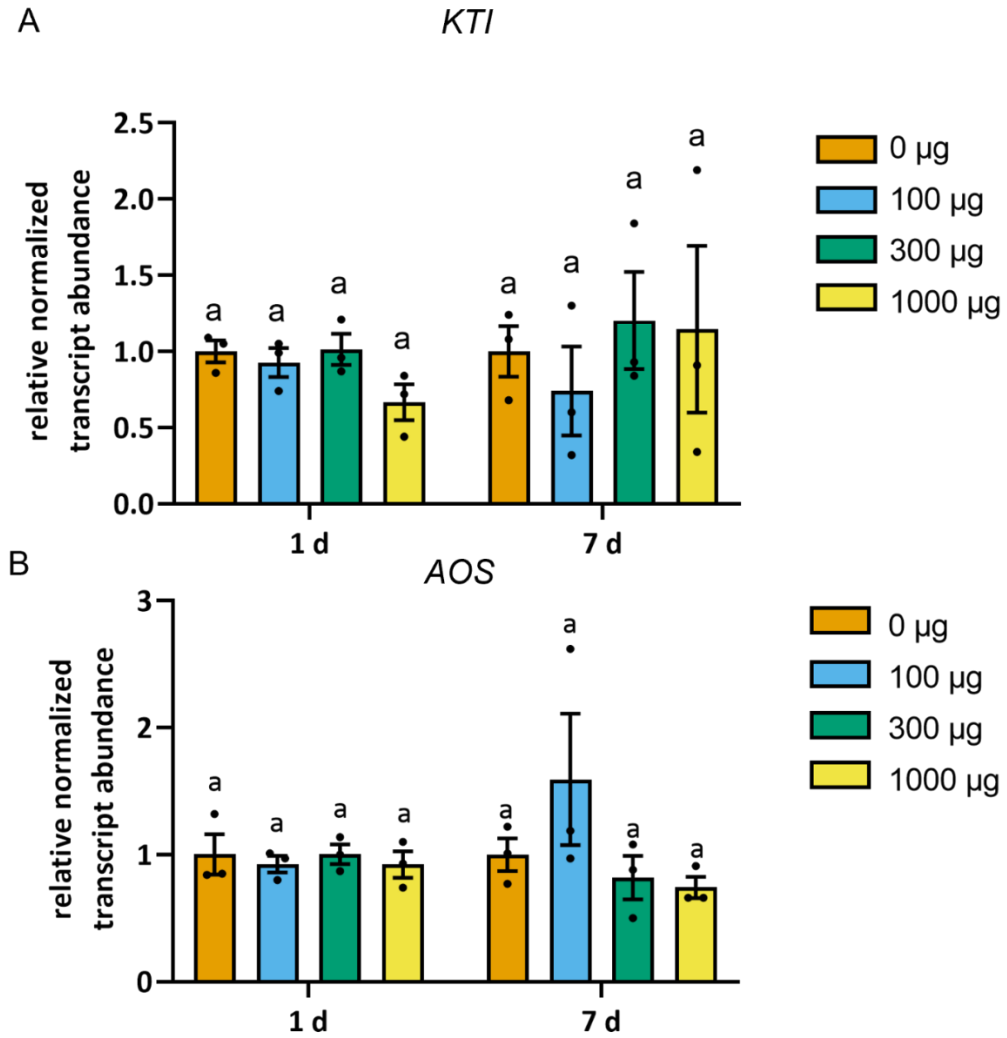

Figure 38 Relative transcript abundances of (A) KTI and (B) AOS in leaves after root treatment with different amounts of chitin in WT leaves

P. × *canescens* WT were incubated on M-MMNS agar supplemented with 0 µg mL^{-1} (orange), 100 µg mL^{-1} (blue), 300 µg mL^{-1} (green), and 1000 µg mL^{-1} (yellow) chitin in a sterile sandwich system (3.14). After one day and seven days, the transcript abundances of *KTI* (Potri.019G088200) and *AOS* (Potri.002G130700) were measured (3.21). Bars show the mean of the relative normalized transcript abundance and the standard error. Each dot represents one biological replicate (n = 3) of one experiment. All data were normalized to the respective 0 µg mL^{-1} treatment. Different letters above the bars indicate statistically significant differences at $P < 0.05$ calculated by ANOVA and Tukey's post hoc test for each time point.

4.3. Fast and easy bioassay for the necrotizing fungus *Botrytis cinerea* on poplar leaves

Steven Dreischhoff, Ishani Shankar Das, Felix Häffner, Anna Malvine Wolf, Andrea Polle, Karl Henrik Kasper

Author contributions:

KHK and SD developed the methodology, performed experiments, and wrote the first draft of the manuscript. KHK supervised the project. ISD worked on fungal sporulation and spore infection. FH conducted scanning electron and fluorescence microscopy. AMW isolated and identified the *Botrytis cinerea* strain used in this study. AP acquired funding, supervised SD, ISD, AMW and FH, and revised the manuscript. All authors have read and agreed to the final version of the manuscript.

This article was published in *Plant Methods* on 29th March 2023
https://doi.org/10.1186/s13007-023-01011-3

Plant Methods

METHODOLOGY Open Access

Fast and easy bioassay for the necrotizing fungus *Botrytis cinerea* on poplar leaves

Steven Dreischhoff[1], Ishani Shankar Das[1], Felix Häffner[2], Anna Malvine Wolf[3], Andrea Polle[1] and Karl Henrik Kasper[1*]

Abstract

Background Necrotizing pathogens pose an immense economic and ecological threat to trees and forests, but the molecular analysis of these pathogens is still in its infancy because of lacking model systems. To close this gap, we developed a reliable bioassay for the widespread necrotic pathogen *Botrytis cinerea* on poplars (*Populus* sp.), which are established model organisms to study tree molecular biology.

Results *Botrytis cinerea* was isolated from *Populus* x *canescens* leaves. We developed an infection system using fungal agar plugs, which are easy to handle. The method does not require costly machinery and results in very high infection success and significant fungal proliferation within four days. We successfully tested the fungal plug infection on 18 poplar species from five different sections. Emerging necroses were phenotypically and anatomically examined in *Populus* x *canescens* leaves. We adapted methods for image analyses of necrotic areas. We calibrated *B. cinerea* DNA against Ct-values obtained by quantitative real-time polymerase chain reaction and measured the amounts of fungal DNA in infected leaves. Increases in necrotic area and fungal DNA were strictly correlated within the first four days after inoculation. Methyl jasmonate pretreatment of poplar leaves decreased the spreading of the infection.

Conclusions We provide a simple and rapid protocol to study the effects of a necrotizing pathogen on poplar leaves. The bioassay and fungal DNA quantification for *Botrytis cinerea* set the stage for in-depth molecular studies of immunity and resistance to a generalist necrotic pathogen in trees.

Keywords *Botrytis cinerea*, Poplar, Necrosis, Pathogen, Fungus, Quantification, Jasmonate, *Populus* spec., Infection assay

*Correspondence:
Karl Henrik Kasper
kkasper@gwdg.de
Full list of author information is available at the end of the article

Background

Botrytis cinerea is the anamorph of *Botryotinia fuckeliana* and the causal agent of grey mold disease [1]. It is one of the most widespread pathogens threatening the health of over 1400 species in the plant kingdom [2, 3]. *B. cinerea* infections destroy fruits, field crops, shrubs, and trees [1], causing annual economic losses of up to $100 billion worldwide [4]. The airborne disease can remain symptomless within a plant until favorable conditions for the outbreak of the infection prevail [5].

Often overshadowed by its tremendous impact on crop production, it has been overlooked that *B. cinerea* is also a major problem for many forest tree species [6, 7]. Büsgen [8] described necroses caused by *B. cinerea* on leaves of several broadleaf tree species, such as *Ulmus montana*, *Populus alba*, *Tilia parvifolia,* and *Prunus avium*. Seedlings and saplings of economically important tree species such as *Abies* spp., *Pinus* ssp., *Cupressus* ssp., *Larix* ssp., *Tsuga* ssp., and *Cornus florida* can be damaged or killed by *B. cinerea* [9, 10]. *B. cinerea* does not show distinct habitat specificity and is endemic in boreal and hot and dry environments [11]. These conditions stress many tree species in the northern hemisphere, rendering them more susceptible to pathogen infections with the progression of climate change [12].

Poplar species are model organisms to study tree-pathogen interactions [13] and are widely used for biomass production [14, 15]. Modern protocols are available to research poplar interactions with biotrophic pathogens, such as *Melampsora larici-populina* [16]. Poplars employ salicylic acid-dependent defense pathways to fend off biotrophic fungal diseases, e.g., [16, 17]. Extensive studies in herbaceous plants such as *Arabidopsis thaliana* and arable crops [18, 19] showed that defense against necrotizing pathogens is regulated via jasmonate-dependent signaling pathways. To date, no state-of-the-art protocol is available for research on the interaction between poplar and necrotizing pathogens. Instead, even recent studies rely on the quantification of lesion area as a proxy for infection severity [20], a method prone to errors and uncertainties [21].

Here, we report the isolation of the potentially necrotizing pathogen *B. cinerea* from *Populus* x *canescens.* We present a fast and reliable protocol to infect various poplar species. We optimized fungal DNA extraction and quantification. The protocol uses the fast growth of *B. cinerea* under controlled conditions, its rapid infection cycle under optimal conditions [22], and the availability of highly specific qRT-PCR primers [23]. We demonstrate a correlation between necrotic leaf area and fungal DNA in the leaf. We conducted histological and anatomical analyses of necrotic and healthy leaf structures.

Methods

Origin and cultivation of poplar species

In vitro cultures of *P.* x *canescens* (INRA 717 1B4) and *P. euphratica* (clone B2 obtained from trees grown in the Ein Avdat region, Israel) were micropropagated as described by Müller et al. [24]. After four weeks of growth and rooting, the plantlets were potted in 3 L pots containing complete soil (Fruhstorfer Erde Type N, Hawita Gruppe, Vechta, Germany) and covered individually with transparent plastic beakers. To acclimate the plants to greenhouse conditions, the beakers were gradually lifted in the second week and removed at the beginning of the third week. The plants were cultivated in the greenhouse for five to eight weeks under ambient light with supplemental illumination of 150 µE m^{-2} s^{-1} photosynthetically active radiation with a 16/8 h day/night rhythm. The temperature ranged from 15 °C to 30 °C, and air humidity was between 53 and 82%. The plants were watered regularly with tap water.

Twigs (length: about 30–40 cm) were collected (13.04.2022, after bud break) from different poplar species grown in the Forest Botanical Garden (location: 51° 34'N 9° 57'O; mean annual precipitation sum: 624 mm; mean annual temperature: 9.2 °C). The twigs were placed in the greenhouse with the cut end submerged in tap water and kept for four days under greenhouse conditions as described above.

Isolation and cultivation of *Botrytis cinerea*

Fourteen leaves of 12-week-old greenhouse-cultivated *P.* x *canescens* were cut and surface sterilized with 70% ethanol. The leaves were three times sterilized for five seconds, the maximal length without damaging the poplar leaf surface, as shown in pre-tests. Each leaf was placed on a 2% water agar (20 g micro Agar in ddH_2O, Duchefa Biochemie, Haarlem, The Netherlands) in a Petri dish (12 × 12 cm, Greiner Bio-One International, Kremsmünster, Austria), with the petiole stuck in the agar. The Petri dishes were closed with gas permeable Parafilm® M (Bemis, Neenah, USA) and incubated in a climate cabinet (Percival Scientific, Perry, USA) at 21 °C, 60% relative air humidity, and a 16/8 h day/night rhythm. The development of lesions was inspected daily. Necrotic tissue was cut with a scalpel after 16 days and placed on PDA-S-medium (Potato-Dextrose-Agar [Carl Roth, Karlsruhe, Germany] with streptomycin [50 µg/mL, Duchefa], pH 5.5). The necrotic leaf tissue samples were incubated on PDA-S for three days in a climate cabinet as described above. Outgrowing fungal mycelia were transferred to new PDA-S plates. This step was repeated three times. Each time, the newly formed mycelia were optically differentiated according to Smith et al. [25] by color, the texture of the colony surface, and characteristics of hyphae

and placed on individual plates. Based on these criteria, four optically different fungal morphotypes were differentiated. For optical identification and analysis of growth patterns, the cultures were observed under a binocular stereomicroscope (M205 FA, Leica Camera Deutschland GmbH, Wetzlar, Germany). Squeeze preparations of mycelia were generated according to the CBS Handbook of mycology [26]. Hyphal growth and morphology of conidia were observed with an inverse light microscope (Axio Observer Z1, Carl Zeiss, Oberkochen, Germany). One morphotype showed fast growth, a flat, powdery and white mycelium without aerial hyphae and branched, sporadically septated, formed hyaline hyphae, thus, fulfilling the description of *B. cinerea* [27].

The selected morphotype was used for molecular identification as follows: The genomic DNA was extracted from pinhead-sized mycelium samples with the innuPREP DNA kit (Analytik Jena, Jena, Germany) according to the suppliers' instructions. The extracted genomic DNA was used as the template for a polymerase chain reaction (PCR), using the ITS primer pair ITS1-F *forward* (3 '-CTTGGTCATTTAGAGGAAGTAA-5') and ITS4 *reverse* (5′-TCCTCCGCTTATTGATATGC-3′) [28, 29]. Following the Taq DNA polymerase protocol (Thermo Fisher Scientific, Waltham, USA), 2 µL genomic DNA in 20 µL reaction volume was used for PCR. PCR products and a technical replicate of a PCR product from a previous extraction using the same protocol as with the samples (positive control), and a ddH_2O sample (negative control), were run on a 1.2% agarose gel containing 0.003% ethidium bromide (Carl Roth). After the run, the product lengths of the PCR products were evaluated under UV light (Typhoon FLA 9500, GE Healthcare, Chicago, USA). Signals at a size of approx. 280 base pairs indicated successful PCR. Samples were purified with the innuPREP PCRpure kit (Analytik Jena) according to the manufacturer´s instructions. Twelve µL purified PCR product was mixed with 3 µL of the primer and sent for Sanger sequencing to a company (Microsynth Seqlab, Göttingen, Germany). The resulting forward and reverse sequences were combined with the Gap4 Staden package [30]; https://sourceforge.net/projects/staden/). The resulting ITS sequences were compared with the NCBI (National Center for Biotechnology Information, Rockville Pike, USA) database using the nucleotide BLAST tool (https://blast.ncbi.nlm.nih.gov/Blast.cgi) and identified as *B. cinerea* strain CBS 261.71.

The ITS sequences obtained from two independently sequenced samples, one after isolation, and one before starting the infection experiments, were deposited in the NCBI Genbank under accession numbers ON740896 and ON740897. The *B. cinerea* cultivar isolated in this study from poplar leaves was deposited in the public collection of the German Collection of Microorganisms and Cell Cultures (DSMZ, Braunschweig, Germany) under the collection number: DSM 114,993.

Cultivation of Botrytis cinerea

The identified fungal species *B. cinerea* was cultivated on PDA (Carl Roth) with 2% micro agar (Duchefa). Stock cultures of fungal mycelia were transferred to fresh PDA plates bi-weekly. To collect fungal mycelium, *B. cinerea* was grown for 7 days at 23 °C in darkness. To obtain spores, the fungus was grown in darkness at 28 °C for eight days [31]. For the harvest of spores, 1.5 mL 10% sterile glycerol was pipetted on the culture plate, and the spores were gently scraped with a sterile plate spreader (TH Geyer, Höxter, Germany). Spores in glycerol were stored at − 80 °C.

Liquid cultures of *B. cinerea* were produced by inoculating 100 mL Potato-Dextrose-Broth (Carl Roth) in 500 mL Erlenmeyer flasks with five 6 mm fungal agar plugs punched out with a cork borer from a seven-day-old PDA plate with *B. cinerea* mycelium. The cultures were grown for 7 days on a shaker at 120 rpm at 23 °C in darkness.

Plug infection protocol

PDA plugs with fungus attached were punched with a 6 mm (diameter) cork borer (Carl Roth) from the actively growing edge of a seven-day-old *B. cinerea* culture on PDA (Carl Roth). One plug was transferred with a needle on the adaxial side of an intact leaf attached to a poplar plant (Fig. 1). Generally, we used the 4^{th} fully expanded poplar leaf from the top of the shoot for the experiments. When plants were grown under non-sterile conditions, a brief surface sterilization of the leaf prior to inoculation is recommend. We wiped the upper leaf surface three times for 5 s with a 70% ethanol-soaked paper tissue interference with other potential leaf-colonizing microbes (Additional file 1: Fig. S1). Then, the plug was placed between major veins with the mycelium faced upwards (Fig. 1a). The fungus grew through the agar plug to reach the leaf surface. A PDA plug without fungus from a non-inoculated PDA plate was used for mock infection of control leaves. The growth conditions were the same as mentioned above. After inoculation, the plants were cultivated for up to four days under ambient light with 16 h of supplemental illumination of 150 µE m^{-2} s^{-1} photosynthetically active radiation. The temperature ranged from 15 °C to 30 °C, and air humidity was between 53 and 82%. The plants were watered regularly with tap water. Infected and non-infected leaves were harvested at different days post inoculation (dpi).

To inoculate leaves from the outdoor poplars, fully expanded leaves attached to twigs were chosen.

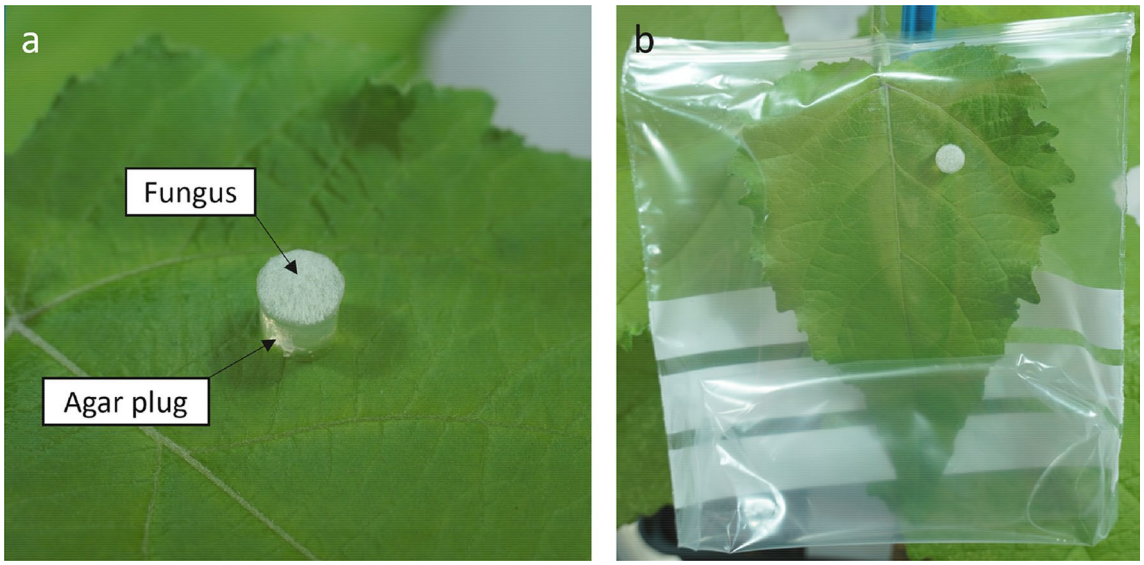

Fig. 1 *Botrytis cinerea* infection-PDA plug on the 4th poplar leaf. From a seven-day-old *B. cinerea* culture on a Potato-Dextrose-Agar (PDA) plate, a *B. cinerea*-inoculated PDA plug was punched out with a 6 mm cork borer. **a** The *B. cinerea*-inoculated PDA plug was transferred to the 4th fully expanded *Populus* x *canescens* leaf and placed in between major veins with a needle. **b** Thereafter, the leaf was sealed with a plastic bag

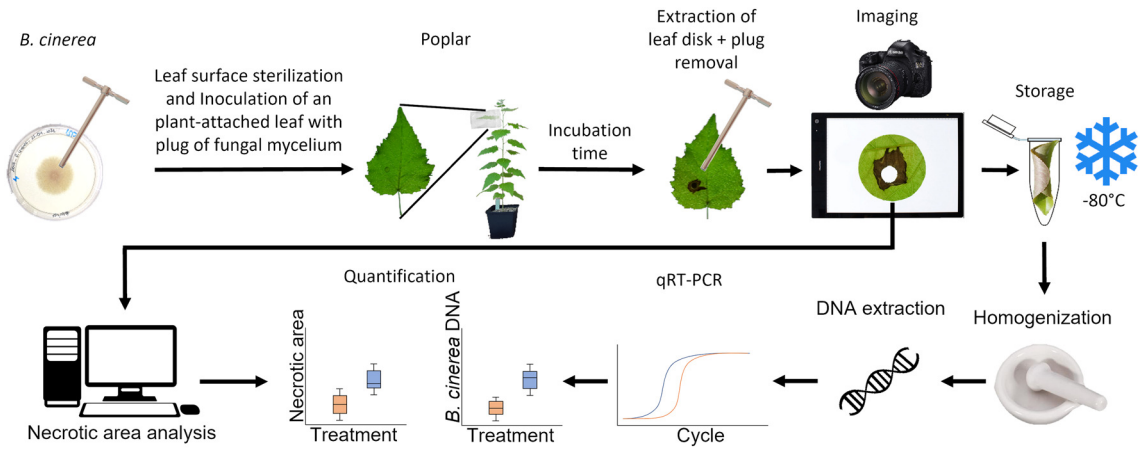

Fig. 2 Flow chart of the poplar-*Botrytis cinerea* pathoassay inoculation, harvest process, and quantification

Inoculated leaves were placed in a low-density polyethylene zipper bag (Carl Roth). The lower end of the bag was pushed slightly inside the bag to create an air space to ensure that the plug did not stick to the bag (Fig. 1b). The plastic above the zipper was cut-off to ensure sufficient humidity and spread of fungal material while being able to place the zipper as near as possible to the stem (Fig. 1b). A flow chart of the infection method and tissue harvest is shown in Fig. 2.

The 4th leaf of *Populus* x *canescens* was sterilized by wiping the upper leaf surface three times for five seconds with a 70% ethanol-soaked paper tissue. Plugs were punched out at the actively growing edge of a 7-day-old *B. cinerea* culture. One plug was placed with the mycelium upwards on the *Populus* x *canescens* leaf. The leaf was sealed in a plastic bag. Leaves were harvested after different incubation times and digital pictures were taken. A leaf disk (diameter: 27 mm) around the centered necrosis was plunged out, and the area of the initial plug position was removed with the 6 mm cork borer before the sample was snap-frozen in liquid nitrogen and stored at − 80 °C. The total DNA was extracted from the leaf disks. Fungal DNA was measured via qRT-PCR. Ct-values were converted into the amount of DNA. The

necrotic area was determined from the photos of the leaf disks using the R package pliman (Olivoto, 2022).

Spore infection protocol

To test the ability of the spores to germinate, harvested spores were allowed to germinate for 24 h in darkness at 23 °C. Twenty microliters of germinated spores on a glass slide were mounted with glycerol and observed with an Axio Observer Z1 microscope (Carl Zeiss). Photos were taken with an AxioCam MRc (Carl Zeiss).

For inoculation, spores were diluted to a concentration of 1×10^6 [31] in tap water, and a volume of 20 µL was pipetted onto the fourth, fifth, and sixth fully developed leaf of a –greenhouse-cultivated *P.* x *canescens* plant. The inoculated leaves were individually enclosed in plastic bags to maintain high air humidity and incubated as described above. The leaves were monitored regularly.

Sampling of leaf disks

Inoculated leaves were cut from the stem with a blade after one to four days of infection. If not stated otherwise, the infection plug was punched out with a 6 mm cork borer and discarded. A leaf disk (27 mm diameter) was punched out around the 6 mm-wide hole. For further analyses, these leaf disks were used. The advantage of this approach is that we could use normalized leaf areas for image processing and fungal DNA quantification. Leaf disks for DNA quantification were frozen in liquid nitrogen and stored at − 80 °C (Fig. 2).

Determination of lesion area by image analysis

All photographs of leaves and leaf disks were taken with a Sony Alpha 6400 camera with a Sony SEL 18-135 mm f3.5–5.6 lens (Sony, Tokyo, Japan) and the following settings: 1/60 s exposure time, aperture F5.6, iso 200, 55 mm zoom, and manual focus. The samples were placed on an LED light table (Shenzhen Huion Animation Technology, Shenzhen, China) with maximum light intensity. A scale bar was included in each photograph, and no additional light source was used to avoid reflections.

The digital pictures of the leaf disks were used to determine the necrotic area. Infected areas were defined manually using a freely available imaging program (GIMP v2.10.32, https://www.gimp.org/, The GIMP Development Team, 2022). We distinguished green, healthy leaf tissue and brownish, pathogen-affected tissue using the foreground color selection tool and colored the necrotic area in bright red. The processed images were stored as png files and opened in ImageJ (Schindelin et al., 2012). The scale on each image was used to define the cm-to-pixel ratio, and then the necrotic area was determined using the "ROI Manager" tool. The total leaf area of interest (TLAI) was defined as the total leaf area of the disk minus area of the punched hole. TLAI and infected area were used to calculate the relative infected area.

R [32] and Rstudio [33] with the pliman package v 1.1.0 [34] were used for the automated analysis of symptomatic areas. For each experiment, corresponding references (i.e., images of healthy tissue, necrosis and background, img_healthy, img_symptoms, and img_background) were recorded and used in GIMP v2.10.32 [35]. Batches of pictures were analyzed using the pattern function of "pliman". The function to fill holes (fill_hull = FALSE) was disabled to achieve correct recognition of the punched hole. Processed pictures were saved (save_image = TRUE) to check for correct processing by inspection of the white lines the R package draws around the recognized necrotic area. After processing, percent values of necrotic and healthy areas were saved in.csv format. The script used here was deposited at Github (https://github.com/) under: https://github.com/StevenDreischoff/Fast-and-easy-infection-assay-for-necrotizing-pathogen-Botrytis-cinerea-on-Poplar

Calibration and Quantification of Fungal DNA by qRT-PCR

Frozen leaf disks (TLAI) were milled twice in a ball mill (MM200, Retsch, Haan, Germany) equipped with two 3 mm and one 4 mm steel balls for 90 s at 30 Hz. Total DNA was extracted from frozen leaf powder using the innuPREP PlantDNA Kit (Analytik Jena) with an extended lysis time of 1 h. Afterward, the DNA concentration and purity were determined in 1 µL of extract in a NanoDrop One (Thermo Fisher Scientific) spectrophotometer. The DNA concentrations of the leaf extracts were adjusted to 5 ng/µL.

We employed the *B. cinerea*-specific primers Bc3F (5'-GCTGTAATTTCAATGTGCAGAATCC-3') and Bc3R (5'-GGAGCAACAATTAATCGCATTTC-3') reported by Suarez et al. [36] and Diguta et al. [23] to quantify fungal DNA in the leaf extracts. The primers target the ribosomal region between the 28S and 18S genes (intergenic spacer). The quantitative real-time PCRs (qRT-PCR) reaction mixture contained 10 µL innuMIX qPCR DSGreen Standard master mix (Analytik Jena), 5 µL DNA (concentration 5 ng/µL, equaling 25 ng total DNA), 4 µL ddH_2O and 1 µL primer mix of forward and reverse primer (10 µM each). The qRT-PCRs reactions were carried out with a qTower3G (Analytik Jena) at the following conditions: initial denaturation at 95 °C for 2 min, 40 cycles of 1 denaturation at 95 °C for 20 s, 2 annealing at 58 °C for 20 s and 3 elongation at 72 °C for 20 s. The qRT-PCR ended with a melting curve, starting from 60 °C to 95 °C in 15 s with an increase of 5 °C per s. Three technical replicates were analyzed per biological sample.

Determination of Ct-values was performed with the qPCRsoft-Software v4 (Analytik Jena).

To calibrate the fungal Ct values, we produced pure *B. cinerea* DNA. For this purpose, mycelium was harvested from a liquid culture after one week of growth. The whole mycelium from one culture was lyophilized (Gamma 2–16 LSCplus, Martin Christ Gefriertrocknungsanlagen GmbH, Osterode am Harz, Germany). A hundred mg of freeze-dried mycelium was rehydrated with 150 µL ddH_2O and immediately used for DNA extraction with the DNeasy PowerSoil Pro Kit (Qiagen, Hilden, Germany) following the instructions of the manufacturer. The absorbance ratios at 260/280 nm and 260/230 nm were checked with a NanoDrop One spectrophotometer (Thermo Fisher Scientific). Thereafter, the DNA was further purified with the Dneasy PowerClean Pro Cleanup Kit (Qiagen) according to the manufacturer's protocol. The resulting DNA concentration was determined using a Qubit dsDNA HS assay Kit in a Qubit 3.0 Fluorometer (Thermo Fisher Scientific). It should be noted that the extraction procedure was successful with the Qiagen soil but not with the Analytik Jena plant kit.

The purified DNA from the fungal mycelium was used to produce a dilution series from 14.8 ng μL^{-1} to 0.00001 ng μL^{-1}. The samples were used for qRT-PCR according to the following conditions: the qRT-PCR reaction mixture contained 10 µL innuMIX qPCR DSGreen Standard master mix (Analytik Jena), 5 µL DNA, 4 µL ddH_2O and 1 µL primer mix (Bc3F and Bc3R) of forward and reverse primer (10 µM). The qRT-PCRs were carried out with a qTower3G (Analytik Jena) and the following conditions: initial denaturation at 95 °C for 2 min, 40 cycles of 1 denaturation at 95 °C for 20 s, 2 annealing at 58 °C for 20 s and 3 elongation at 72 °C for 20 s. The qRT-PCR ended with a melting curve, starting from 60 °C to 95 °C in 15 s with an increase of 5 °C per s. Three technical replicates were analyzed per biological sample. Determination of Ct-values was performed with the qPCRsoft-Software v4 (Analytik Jena).

The Ct values were regressed against the amount of DNA after ln (natural logarithm) transformation of the DNA values. A correlation test was performed using R [32] and Rstudio [33]. Data were plotted, and linear regression was performed (Fig. 3). We obtained a linear relationship ($Ct = -1.598\ \ln(DNA) + 27.43$, $R^2 = 0.9989$, $P < 0.0001$). The equation was used to convert Ct values into corresponding amounts of fungal DNA (in pg) with the following Eq. 1:

$$DNA_{(pg)} = e^{\left(\frac{27.43 - Ctvalue}{1.598}\right)} \quad (1)$$

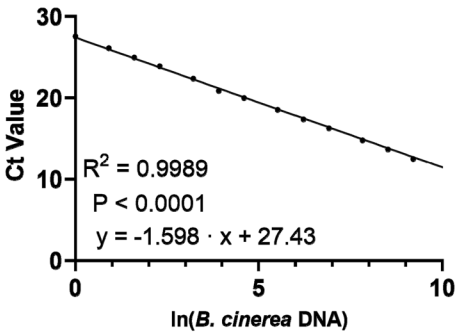

Fig. 3 Calibration curve for the amount of fungal DNA (pg) to Ct values

For all experiments, Ct values were converted into amounts of fungal DNA in pg. These amounts corresponded to the amount of fungal DNA in 25 ng of total (plant + fungal) DNA.

Fungal DNA was extracted from freeze-dried *Botrytis cinerea* mycelium grown in liquid culture. The purified DNA was serially diluted. qRT-PCR was performed using *B. cinerea*-specific primers. For every sample, three technical replicates were analyzed. Mean Ct values of the technical replicates were correlated to the amount of DNA in the PCR reaction. DNA data were ln transformed since the Ct values increase exponentially.

Scanning electron microscopy (SEM) of fungal mycelia on leaf surfaces

Fresh leaf samples (approximately 1 cm × 1 cm) were cut at different positions and time points after inoculation from infected and control leaves with a double-edge razor blade (Wilkinson Sword, Solingen, Germany). Each sample was fixed with conductive double-sided adhesive carbon tabs (Plano, Wetzlar, Germany) on a Standard SEM Pin Stub Mount (diameter 12.7 mm, Phenom-World, Eindhoven, Netherlands). Immediately afterwards, the samples were covered by a 10 nm gold layer (Plano) using the Q150R S/E/ES plus sputter coater (Quorum Technologies, Lewes, United Kingdom). After sputter coating, the edges of the samples were sealed airtight with conductive carbon cement (Plano). The samples were stored in a dust-free SEM sample box for a maximum of two days before the measurements were conducted. SEM images were taken on a Phenom ProX (G5) desktop SEM (Thermo Fisher Scientific). Image acquisition was performed in Back-scattered electron mode (BSE mode) at a voltage of 15 kV and a resolution of 1024 pixels, and magnifications of 350x, 1000x, and 4000x.

Chlorophyll fluorescence imaging

Chlorophyll fluorescence of sections of whole leaves, including inoculated areas, was measured with an IMAGING-PAM (Heinz Walz, Effeltrich, Germany). The measurements were conducted at an intensity of 0.5 µmol m^{-2} s^{-1} PAR, at a modulation frequency of 8 Hz, and at a saturation pulse intensity of 4000 µmol m^{-2} s^{-1} PAR. The emission of blue light was measured at 450 nm and of red light at 650 nm. According to Sekulska-Nalewajko et al. [37], the photosynthetic efficiency of dark-adapted leaves (Fv/Fm) and the quantum yield on non-regulated PSII energy dissipation (Y(NO)) data were used to analyze the impact of *B. cinerea* infection on leaf photosynthesis.

Cross-sections and histochemistry of infected and uninfected leaves

Fresh leaf samples of 1 cm x 1 cm were cut with a razor blade (Wilkinson Sword) from different parts of mock and *B. cinerea*-infected leaves. The samples were transferred individually in 2 cm x 2 cm wells of a sixteen-well plate (Greiner Bio-One International). The wells were then filled with liquid 5% agarose (Duchefa Biochemie), closed with a lid, and solidified at 4 °C overnight. During initial solidification, the samples were pushed down several times with forceps to prevent floating.

The agarose blocks containing the leaf samples were removed from the well plate, orientated for cross-sectioning, and trimmed with a razor blade (Wilkinson Sword). The vibratome VT1200 (Leica Microsystems, Wetzlar, Germany) was used to produce cross sections of 30 µm thickness with a cutting speed of 1 mm sec^{-1} and an amplitude of 0.5 mm. For this purpose, the vibratome was equipped with a double-edge bendable razor blade (Wilkinson Sword). The cross-sections were then submerged in a solution containing 10 µg mL^{-1} Wheat Germ Agglutinin Alexa Fluor 488 conjugate (Thermo Fisher Scientific) and propidium iodide 10 µg mL^{-1} (Thermo Fisher Scientific) in phosphate-buffered saline solution (NaCl 137 mmol L^{-1}, KCl 2.7 mmol L^{-1}, Na_2HPO_4 10 mmol L^{-1}, KH_2PO_4 1.8 mmol L^{-1}) for 15 min. After staining, the cross-sections were washed once with phosphate-buffered saline solution and then transferred to specimen slides, where they were mounted with ROTI-Mount FluorCare (Carl Roth), a medium for fluorescence microscopy. The sections were viewed at 200 × and 400 × magnification with a Zeiss Axio Observer Z1 microscope (Carl Zeiss), using filters with the wavelengths for excitation at 493 nm and emission at 520 nm for WGA Alexa Fluor 488 conjugate and with excitation at 538 nm and emission at 617 nm for propidium iodide. Photos were taken with an AxioCam MRc (Carl Zeiss).

Methyl jasmonate pretreatment

Ten-week-old greenhouse-grown *P.* x *canescens* plants were inserted in a large autoclave bag (Sarstedt, Nümbrecht, Germany) with open ends at the top and the bottom. This setup prevented cross-contamination during spraying. The plants were sprayed with 200 µM methyl jasmonate (Sigma-Aldrich, St. Louis, USA) in ddH_2O or with ddH_2O (control) until runoff (approx. 25 mL) using a 250 mL spray bottle suitable for overhead spraying (Carl Roth). The bags were closed, and the control and MeJA-treated plants were transferred to different greenhouse cells. The bags were removed after four hours, and the plants were incubated for another four hours before inoculation and incubation *with B. cinerea*, as described above.

Statistical analysis

Data are shown as box plots with points representing one biological replicate unless indicated otherwise. The number of biological replicates is indicated in the tables and figure legends. To compare means, the normal distribution of the data sets was tested by visual inspection of residuals. If data were not normally distributed, they were log-transformed to achieve normal distribution. If data in percent included 0 or 1, they were transformed according to Smithson & Verkuilen [38]. Statistical tests were conducted with R [32] and Rstudio [33], using linear generalized mixed models, beta regression [39], or Tukey's post hoc-test in the packages"multcomp" [40] and"car" [41]. Differences between treatments were considered significant when the values of the post hoc tests were $P < 0.05$. Correlations were tested using the build-in cor.test() function of R.

Results

Botrytis cinerea plug-inoculation results in spreading necrosis on the poplar leaves

Leaves of *P.* x *canescens* did not show necrotic symptoms one day after *B. cinerea* inoculation. After 2 dpi, initial dark brownish necroses were observed, which grew in size at 3 and 4 dpi (Fig. 4a). Analyses of the necrotic areas showed significant increases from 2 to 4 dpi (Fig. 4b).

To be able to measure the *B. cinerea* DNA in the leaf disks, *B. cinerea* DNA extracted from pure culture was correlated to Ct values (Fig. 3). We quantified the amount of fungal DNA in infected leaves and mock-inoculated controls with *B. cinerea*-specific primers. *B. cinerea* DNA was detectable at all tested time points and increased significantly until 3 dpi (Fig. 4c). At 4 dpi, no further increase was detected (Fig. 4c). Mock-inoculated leaves also showed minor increases in *B. cinerea* DNA (Fig. 4c). This observation suggests that the fungus was ubiquitously present in leaves of greenhouse-grown poplars and

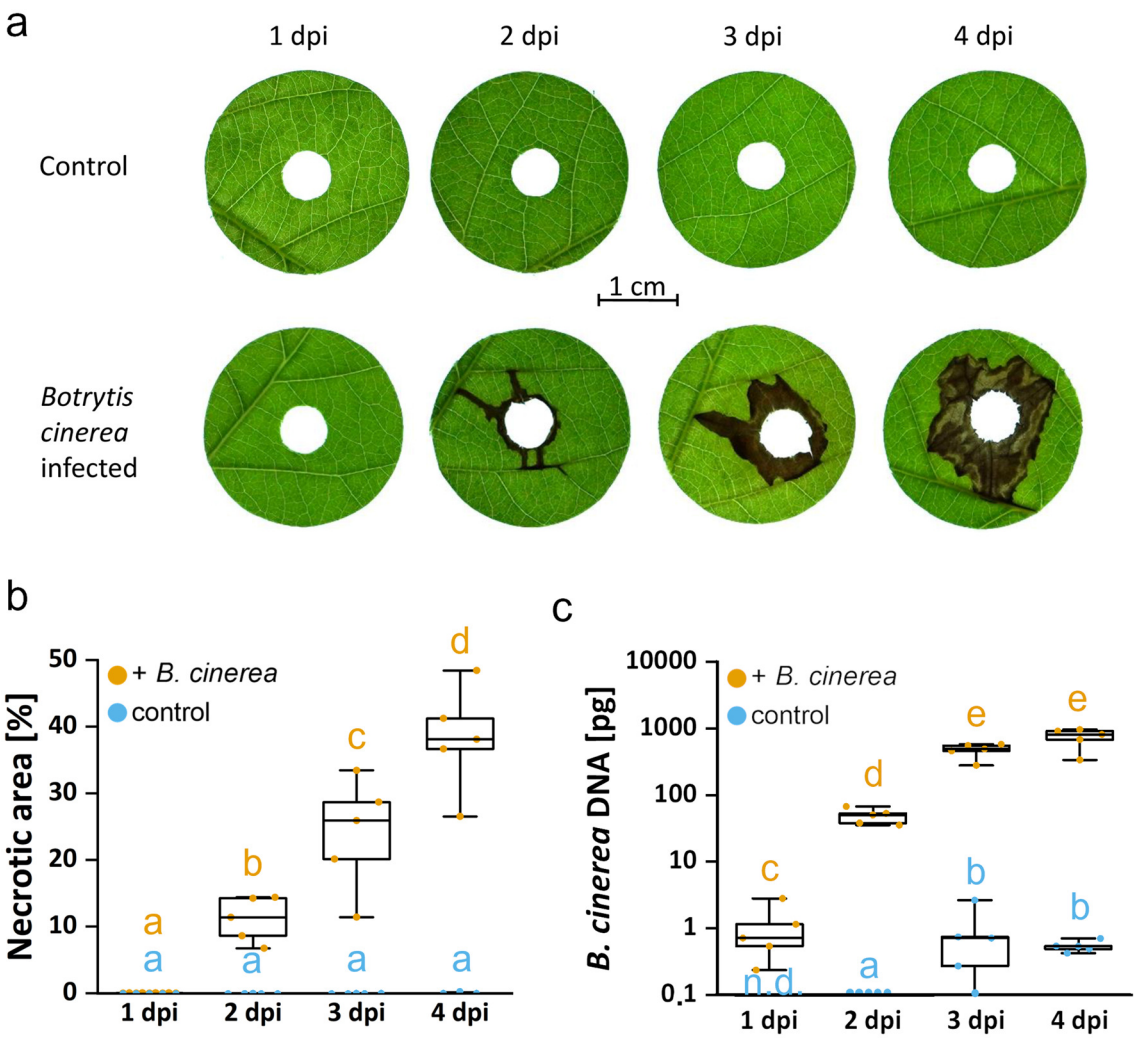

Fig. 4 Time course of disease symptoms **a**, **b** and amount of fungal DNA **c** in poplar leaves in response to *Botrytis cinerea*

that its growth was stimulated by the application of the uninfected plug during the incubation period.

Leaves of *Populus* x *canescens* were inoculated with a seven-day-old *B. cinerea* plug punched out of Potato-Dextrose-Agar plate or were mock inoculated with a plug from a sterile Potato-Dextrose-Agar plate. Leaves were harvested after one, two, three-, and four days post inoculation (dpi) as described in Figs. 1 and 2. a) Visual symptom development, b) increase of the necrotic area, c) and amount of *B. cinerea* DNA within the time course of 4 days. Quantification of necroses was conducted with the pliman package and expressed as percentage of the necrotic area of the leaf disk area (5.44 cm^2). Fungal DNA was extracted from leaf disks (5.44 cm^2), analyzed with *B. cinerea*-specific primers, and converted to the amount of *B. cinerea* DNA using the calibration in Fig. 3. Data are shown as min–max boxplots with the whiskers spanning across the range of the data points. Each point represents one biological replicate (n = 5). Each biological replicate was determined as the mean of three technical replicates. Different letters above the boxplots indicate significant differences at $P < 0.05$ calculated by ANOVA and Tukey post hoc test. n.d. = not detectable.

The infection of *P.* x *canescens* leaves by *B. cinerea* was independently repeated three times to evaluate the reproducibility of the pathosystem. Necrosis developed on the *B. cinerea* inoculated leaves, but the symptomatic areas differed among independent experiments (Fig. 5). This result was probably due to differences in the ambient, semi-controlled glasshouse conditions during the inoculation period or different effects of the conditions on the poplar plants. The necrotic areas were highly correlated with the amount of detected *B. cinerea* DNA (Fig. 5), indicating the proper functioning of the pathosystem also under changing environmental conditions.

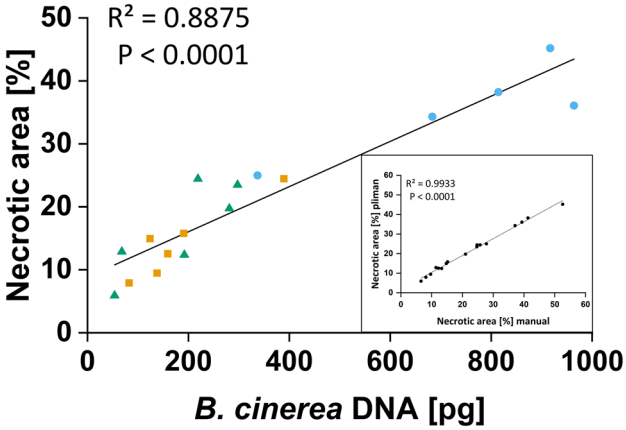

Fig. 5 Relationship of necrotic leaf area and the amount of *Botrytis cinerea* DNA

In three independent experiments, the 4th fully developed leaf of a *Populus* x *canescens* plant was inoculated with a *B. cinerea*-plug from a seven-day-old Potato-Dextrose-Agar plate and harvested after four days of inoculation as described in Figs. 1 and 2. The necrotic area was determined from images using both the pliman package and manually with ImageJ. Necrotic areas were expressed as percentages of the area of the total leaf disk (5.44 cm^2). Different amounts of fungal DNA from different experiments (blue circles, green triangles, orange squares) showed a significant correlation with the necrotic leaf area. Both methods (pliman and manual necrotic area determination) show a highly significant correlation (inset in Fig. 5). Each symbol represents one biological replicate. Each biological replicate was determined as the mean of three technical replicates.

In the initial experiments, we determined the necrotic area on poplar leaves manually, as commonly done in other studies, e.g., [42, 43]. This procedure was very labor-intensive. The recently published R package pliman [34] was used to automatize and speed up the analysis. To test whether pliman delivers reliable results, the necrotic areas found by manual and pliman analyses were compared. Both methods produced similar results and were highly significantly correlated (Inlet Fig. 5). Complete setup and image analysis with pliman took about 20 min, while the manual analysis took approx. three minutes per sample. Thus, pliman outperforms the manual approach by being faster and less laborious when dealing with seven or more samples. The optimized pliman procedure started with reference images for an individual experimental run, which was used to correct for the slight reddish coloration which often appears on poplar leaves.

Inoculation with *Botrytis cinerea* mycelium plugs results in the infection of different poplar species

To test the versatility of the infection system, leaves of poplar species of different sections cultivated under controlled conditions or collected in the Forest Botanical Garden (University of Goettingen, Germany) were inoculated with *B. cinerea* plugs. All tested species from the sections *Populus, Aigeiros, Tacamahaca, Leucoides,* and *Turanga*, except *P. balsamifera*, were successfully infected and showed necroses on day four after inoculation (Fig. 6).

Different poplar species were obtained from greenhouse stocks and the Forest Botanical Garden Göttingen of the University of Goettingen (Germany). Leaves attached to twigs or whole plants were inoculated with a *B. cinerea* plug from a seven-day-old Potato-Dextrose-Agar plate and harvested four days post inoculation, as described in Figs. 1 and 2. *Populus deltoides* and *P. koreana* leaves were additionally damaged by caterpillars during the infection period. Pictures were taken of the full leaves, and brightness was enhanced by 20% for better visualization.

Histological analyses of infected leaves underline the necrotizing lifestyle of Botrytis cinerea

To obtain insights into the response to fungal infection, we analyzed the chlorophyll fluorescence of *B. cinerea*-infected and uninfected *P.* x *canescens* leaves. At 4 dpi, typical necroses were observed below and around the *B. cinerea*-PDA infection plugs but not on control leaves inoculated with pure PDA plugs (Fig. 7, upper row). The maximum quantum yield (Fv/Fm) of photosystem II of control leaves and the non-disturbed tissue of infected leaves were close to 0.8 (dark blue color Fig. 7 middle row). The infected leaves show reduced quantum yield, indicated by the light blue halo surrounding the necrotic area (black). The non-regulated energy dissipation (Y(NO)) was low (orange to yellow) in controls (Fig. 7 bottom row) and increased close to necrotic areas (dark green color in Fig. 7 bottom row). While photosynthetic damage (Fv/Fm) occurred only at the edge of the necrotic area, non-regulated energy dissipation was already observed in a larger area of the infected leaves surrounding the necrotic tissue (Fig. 7, middle and bottom row).

To inspect the presence of *B. cinerea* hyphae outside the necrotic area, leaf cross sections of mock- and *B. cinerea*-inoculated leaves were stained to visualize fungal hyphae and plant cell walls (Fig. 8). Leaf structures were disintegrated in the necrotic areas, and hyphae could be observed all over the broken tissue. No hyphae could be identified in the tissue near the necrosis, away from the necrosis, or mock-inoculated leaves (Fig. 8).

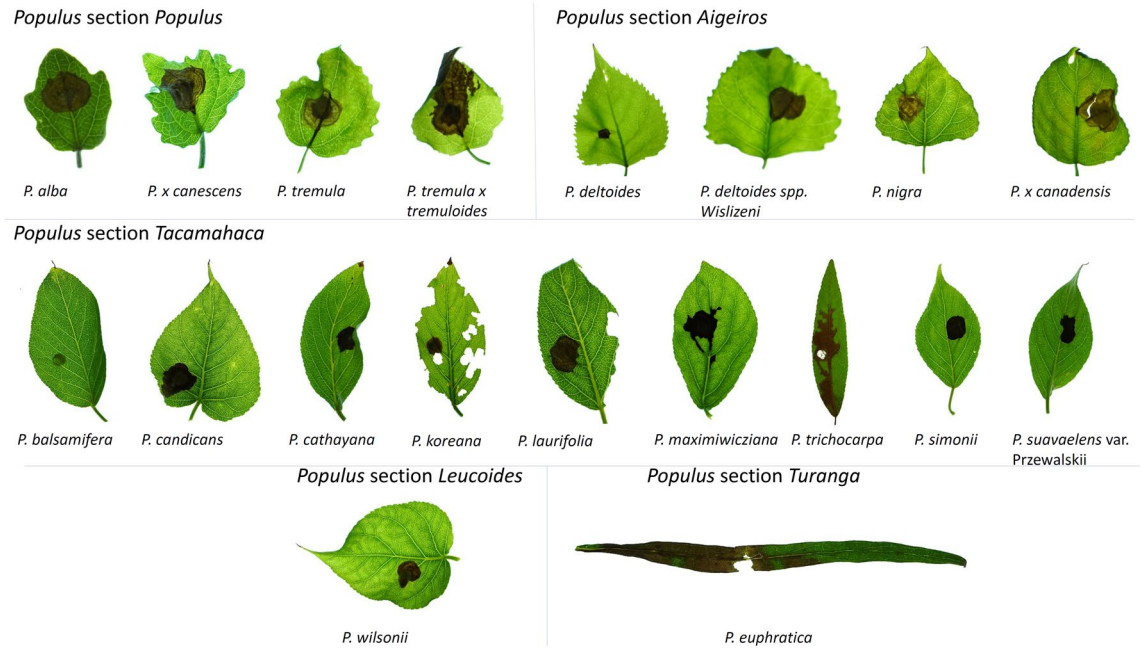

Fig. 6 *Botrytis cinerea*-induced necroses on leaves of poplar species different sections

The 4th fully developed leaf of *P.* x *canescens* was inoculated with a *B. cinerea* plug from a seven-day-old Potato-Dextrose-Agar plate or mock inoculated with a plug from a sterile Potato-Dextrose-Agar plate and harvested four days post-inoculation. Leaf tissues (1 cm × 1 cm) from the positions indicated in the figure were embedded in agarose, trimmed after solidification, and sectioned with a vibratome (thickness 30 µm). The sections were stained with 10 µg mL^{-1} propidium iodide to visualize cell walls (red) and 10 µg mL^{-1} Wheat Germ Agglutinin Alexa Fluor 488 conjugate to visualize the fungus (green). Photos were taken under a fluorescence microscope. V = vascular bundle, T = trichome, H = hyphae.

In addition, scanning electron microscope pictures were taken from inoculated leaves after different time points and at different positions on the leaves. Non-necrotic areas of infected leaves did not show any differences in the epidermal cell patterns compared to healthy

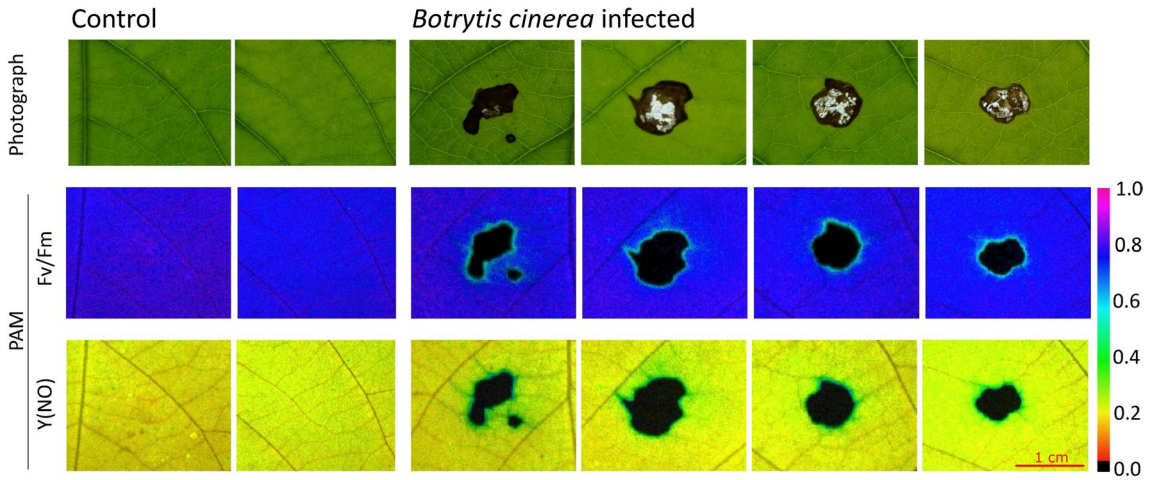

Fig. 7 Images of control and *Botrytis cinerea* infected *Populus* × *canescens* leaves captured by light photography (top row) and pulse amplitude modulation (PAM) fluorometry (middle and bottom rows). Fv/Fm: Photosynthetic efficiency of dark-adapted leaves, Y(NO): quantum yield of non-regulated PSII energy dissipation. Leaves were inspected 4 days post inoculation

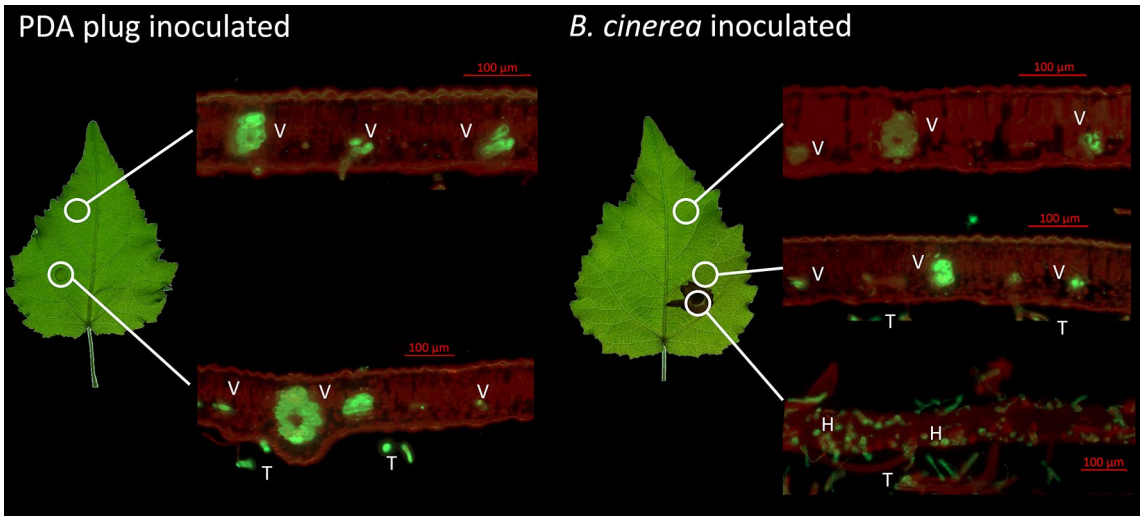

Fig. 8 Fluorescence of leaf cross sections at different positions of mock and *Botrytis cinerea* inoculated *Populus* x *canescens* leaves

leaves (Fig. 9a, b). In necrotic areas of the adaxial side of the leaf, the epidermal cells appeared to be sunken and less turgid, thus, being distinguishable from healthy cells in the direct neighborhood (Fig. 9b). Necrotic tissue showed no clear vital cell patterns, only epidermal ridges (Fig. 9c). At the beginning, mycelium grew from the plug toward the leaves, then, forming a network on the leaf surface, similarly as it does on culture medium. After 2 dpi, hyphae were present on the abaxial side of the leaf directly under necrotic areas, showing fungal trespassing through the leaf (Fig. 9e). Fungal spores (Fig. 9e) and hyphae penetrating the stomatal pores were detected under the necrotic areas on the lower leaf surface (Fig. 9f).

We also tested the ability of fungal spores to induce leaf necrosis on *P. x canescens.* We inoculated the leaves with 1×10^6 spores suspended in water or ¼ PDA. The treatments resulted in irreproducible infection patterns. The spores germinated on ¼ PDA (Fig. 9g), on the leaves (Fig. 9h) and formed hyphal networks (Fig. 9i) and conidia (Fig. 9j). But necrosis did not occur or was only very minor, even after long incubation periods (> 14 dpi). This result shows that the infection is hardly promoted under normal conditions, even when the leaves are kept in high humidity.

Jasmonate-dependency of the infection

Jasmonate is involved in the defense against necrotizing fungi in many plant species [44]. To test whether our bioassay system is capable of capturing jasmonate-responses of poplar leaves, whole *P.* x *canescens* plants were pretreated with methyl jasmonate. After 8 h pretreatment, leaves were plug-inoculated with *B. cinerea*. Mock-inoculated leaves did not show symptoms, whereas inoculated leaves showed visible necroses after 4 dpi. Methyl jasmonate exposed plants showed significantly less necrotic area and fungal DNA than the non-induced plants (Fig. 10).

Ten-week-old greenhouse-grown *Populus* x *canescens* were sprayed with 200 µM methyl jasmonate (MeJA) in ddH_2O or with ddH_2O (control) until runoff (approx. 25 mL). Eight hours after pretreatment, the 4th fully developed leaf was inoculated with a *B. cinerea* plug from a seven-day-old Potato-Dextrose-Agar plate and harvested four days post inoculation. The necrotic area was determined with the pliman method and expressed as percentage of the total leaf disk area (5.44 cm^2). *B. cinerea* growth was quantified by qRT PCR and calibrated with the data in Fig. 3. The figures show min–max boxplots with the whiskers spanning across the range of the data points. Each point represents one biological replicate (n = 6–7). Each biological replicate represents the mean

(See figure on next page.)

Fig. 9 Scanning electron microscopy of *Botrytis cinerea* structures on inoculated *Populus* x *canescens* leaves **a**–**f**, **h**–**j** and light microscopy of *B. cinerea* in liquid culture **g**. **a** Sterile PDA-plug inoculated leaf. **b** *B. cinerea* inoculated leaf. Edge of the necrotic (right) and healthy (left) area after four days. **c**) Collapsed cells of a *B. cinerea* inoculated leaf at 4 dpi (days post inoculation). **d** Mycelium growing from the plug to the leaf at 2 dpi. e) Spore on the abaxial side at 3 dpi. **f** Mycelium growing through a stoma at 3 dpi. g) *B. cinerea* spores germinated 24 h in ¼ strength Potato-Dextrose-Broth, **h** *B. cinerea* spores on inoculated leaf at 12 dpi, **i** germinated *B. cinerea* spores forming a hyphal network on poplar leaf at 12 dpi, **j** *B. cinerea* conidiophores at 12 dpi

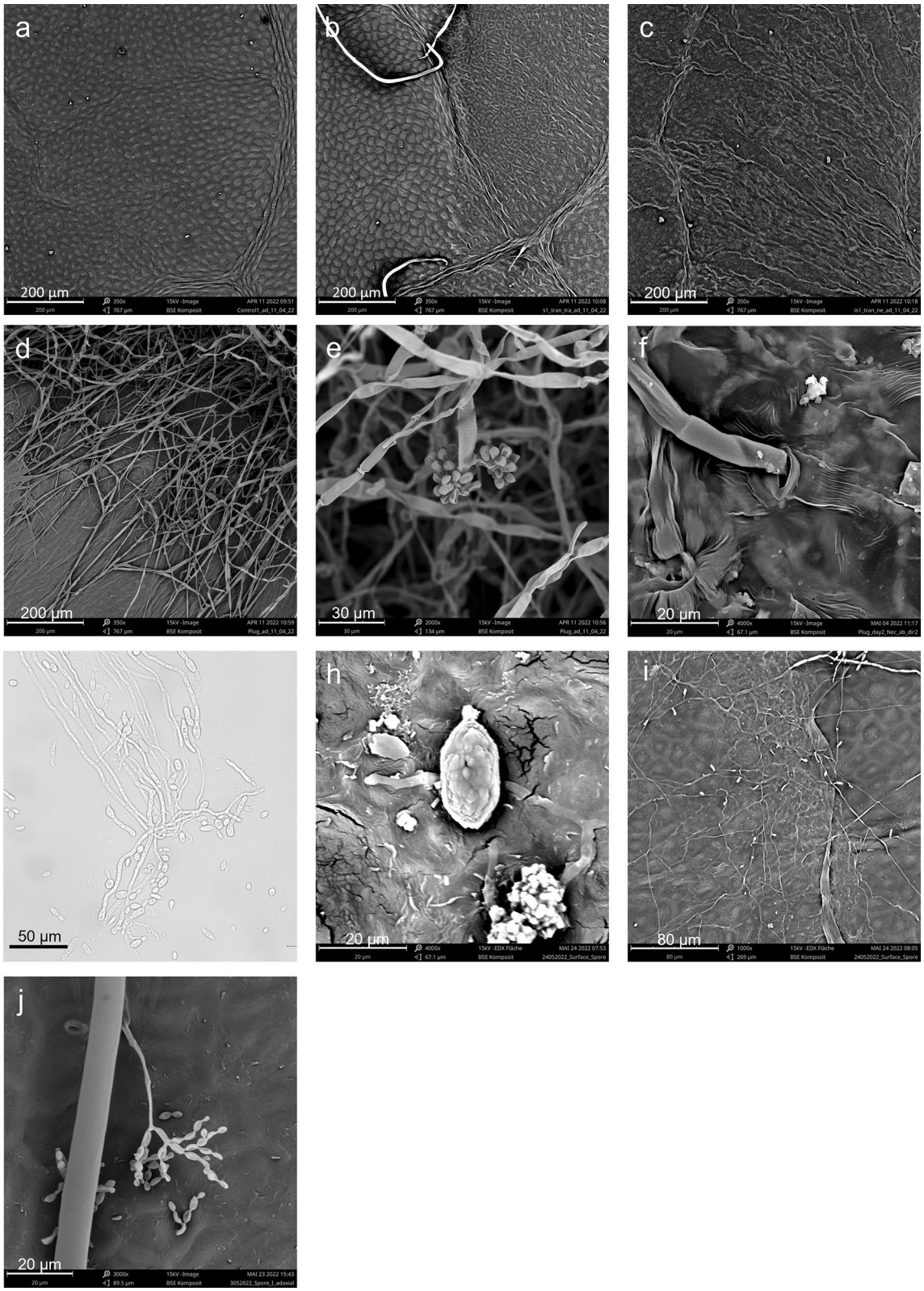

Fig. 9 (See legend on previous page.)

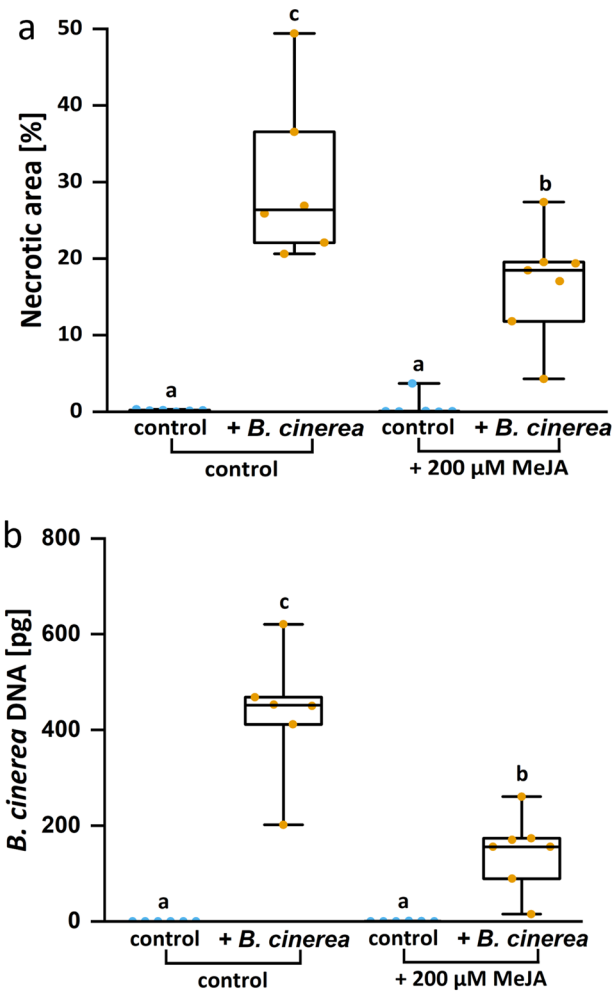

Fig. 10 Leaf necrotic area **a** and *Botrytis cinerea* development **b** in poplar leaves after methyl jasmonate pretreatment

of three technical replicates. Different letters above the box plots indicate significant differences at $P < 0.05$ calculated by ANOVA and Tukey post hoc test.

Discussion

Here, we developed a simple method that leads to the infection of poplar leaves by *B. cinerea* hyphae. We show that under these conditions, a range of phylogenetically divergent poplar species [45] can be infected, whereas *B. cinerea* infections are rare when the leaves were exposed to spores. Within the first days after inoculation, the increase in necrotic area reliably reported the severity of *B. cinerea* poplar leaf infections.

The infection can be performed with basic laboratory materials. While the automated analysis of the necrotic area using pliman is an improvement to individual analyses with imaging software in terms of speed and threshold assignment, it is still facing other problems in phytopathometry, such as the need for expertise in the classification of disease symptoms [21]. The qRT-PCR-based fungal DNA quantification, which we developed here, correlated with the size of the necrotic area. Under our experimental conditions, the increase in fungal DNA leveled off between 3 and 4 dpi. Since we have no evidence for hyphal growth outside the necrotic area in leaf cells, we speculate that the vital fungus continues to grow in newly damaged cells but withdraws from the nutrient-depleted cells at the center of the necrotic area. This proliferation pattern may limit the time scale of the qRT-PCR approach to evaluate the disease incidence. Therefore, we recommend the pliman approach for longer incubation periods, whereas both methods, qRT-PCR and necrotic area determination, achieve accurate *B. cinerea* infection data for up to about 4 dpi.

While spore infection under many different conditions tested here did not lead to homogenous infection patterns, the robustness of the plug infection protocol was demonstrated by several independent repetitions. However, the increase in necrotic tissue varied among different independent runs of the experiments. Since *B. cinerea*-induced infections are favored in the temperature range from 15 °C to 25 °C [46], we speculate that this might have been caused by unattended temperature fluctuations in our greenhouse. It is also conceivable that differences in poplar metabolism under different greenhouse conditions affected fungal proliferation. These possibilities should be clarified by future investigations.

We conducted *B. cinerea* bioassays with different poplar species when the leaves were very young, right after bud break. Young leaves of strawberry plants or eucalypt trees were more susceptible to *B. cinerea* than old leaves [47, 48], while young leaves of bean plants were less susceptible [49]. The disease resistance of poplar leaves may also vary with leaf age and, thus, should be taken into account when using our *B. cinerea* infection protocol.

Our infection system is suitable for inducing strong damage to leaves in controlled experiments using vigorously growing *B. cinerea* hyphae. However, it should be noted that the natural infection caused by *B. cinerea* starts with spores landing on the plant surface [50]. The spores can germinate and penetrate the leaf, where they remain quiescent until favorable conditions prevail for a disease outbreak [5]. This behavior is also true for *B. cinerea* in poplar leaves because we isolated the *B. cinerea* strain, able to induce severe leaf lesions, from healthy-appearing leaves. This finding exemplifies the peculiarity of *B. cinerea* being able to remain symptomless within the host tissue, either in the quiescent stage [5] or by a putatively endophytic lifestyle [51]. In our study, *B. cinerea* also showed symptomless development when germinated from spores on poplar leaves, suggesting adaptation of

this strain to *P.* x *canescens* and vice versa. The latent or asymptomatic infection strategy of *B. cinerea* highlights the importance of its molecular quantification.

The factors that lead to disease outbreaks and occurrence of necroses in poplar are still enigmatic. In *Arabidopsis thaliana*, the phyllosphere microbiome can grant resistance against *B. cinerea* [52]. Our results also hint towards a control of the phyllosphere microbiome on *B. cinerea* because disease outbreak required leaf surface sterilization. Since the microbiome of forest trees show seasonal fluctuations [53], its impact on the severity of *B. cinerea* infections may vary and thus, negatively affect experiments. However, it should also be noted that the ethanol treatment for leaf sterilization can alter leaf surface chemistry and thereby, putatively facilitate fungal infections. Therefore, further studies are necessary to distinguish these possibilities and clarify a potential protective role of the surface microbiome. Inside Arabidopsis leaves, *B. cinerea* secreted toxins induce programmed cell death before fungal proliferation [54, 55]. In the present study, photosynthetic integrity was diminished in areas adjacent to the necroses, although we could not find clear-cut support for fungal presence in these cells. Therefore, we speculate that *B. cinerea* sets off a cell lytic program similar to that in Arabidopsis, feeding on leaking cell contents. *B. cinerea* was also able to grow vertically through the leaf, evading through the open stomata and forming new conidia. Thus, our microscopic results provided novel insights into how *B. cinerea* colonizes poplar leaves.

The reduction of disease severity after methyl jasmonate treatment is in line with findings for other species like Arabidopsis or tomato [56, 57]. In poplar, methyl jasmonate treatment induces phenol-based defenses [58] and recruits a signaling cascade involving JAZ proteins, several transcription factors of the MYB and ERF families, and chitinases [59]. Collectively, these responses are known to play roles in the defense of Arabidopsis against *B. cinerea* [60–62]. The infection protocol described in the present work will enable researchers to investigate controls on this ubiquitous fungus and uncover conditions under which *B. cinerea* escapes the poplar defense systems.

Increasing our knowledge of necrotizing pathogens in tree species is important because fungal diseases threaten the health of our forests [63]. The generalist *B. cinerea* is a dangerous pathogen in climate change-stressed forests, causing increased disease incidences in drought-stressed trees [64]. Our bioassay will be particularly useful for translational research, transferring knowledge from the *B. cinerea* infection system in Arabidopsis [65] to poplar and in tree improvement programs using bioengineering to enhance tree resistance and screening the natural inter- and intra-specific variation of *B. cinerea* resistance in *Populus* sp.

Conclusion

Here, we developed a novel bioassay for the poplar necrotizing pathogen *B. cinerea* and its molecular quantification in leaves. A major benefit of the method is that it is straightforward to use. The setup requires only plates with the *B. cinerea* strain, plastic bags, and photos of the necrotic area as the basis to quantify fungal disease severity. The bioassay is accomplished within 4 dpi, and an initial evaluation of the necrotic area can be done within an hour after image acquisition. The availability of an assay for the interaction of poplar with a necrotizing fungus will stimulate research in many areas, such as ectomycorrhiza-induced resistance [66], abiotic stresses [drought, heat, [67], nutrient stress [68]] or evaluation of new species for wood production [69]. Moreover, it also enables us to uncover molecular signaling pathways to combat necrotizing pathogens in an economically important tree species.

Supplementary Information

The online version contains supplementary material available at https://doi.org/10.1186/s13007-023-01011-3.

Additional file 1: Figure S1. The effect of 70% ethanol poplar leaf surface sterilization on infection severity of *Botrytis cinerea* and mock-PDA plug inoculation at 4 dpi. **Table S1.** Origin of Poplar species challenged with *Botrytis cinerea*.

Acknowledgements

We are grateful to M. Fastenrath for the propagation of *P. euphratica*, to C. Leibecke for helping with plant maintenance, to T. Klein for supporting the DNA extraction and *B. cinerea* identification, and to U. Lipka for help with electron microscopy. We are grateful to V. Meng (Forest Botanical Garden, University of Göttingen) for providing various poplar species. We thank T. Olivoto (Department of Plant Sciences, Federal University of Santa Catarina) for helping fine-tune the pliman analysis for our purpose and J. Ballauff for assistance in statistical analysis.

Author contributions

KHK and SD developed the methodology, performed experiments, and wrote the first draft of the manuscript. KHK supervised the project. ISD worked on fungal sporulation and spore infection. FH conducted scanning electron and fluorescence microscopy. AMW isolated and identified the *Botrytis cinerea* strain used in this study. AP acquired funding, supervised SD, ISD, AMW, and FH, and revised the manuscript. All authors read and approved the final manuscript.

Funding

Open Access funding enabled and organized by Projekt DEAL and the Open Access Publication Funds of the Göttingen University. The work in AP's laboratory is funded by the German Science Foundation (DFG). KHK, SD, and ISD were supported in the framework of the International Research Training Group "PRoTECT" (IRTG 2172, M1, and M2.2), funding No. 273134146.

Availability of data and materials

Sequences are available at NCBI Genbank (https://www.ncbi.nlm.nih.gov/genbank/) under accession numbers ON740896 and ON740897. *B. cinerea*

strain 261.71 from poplar is available in the public collection of DSMZ (https://www.dsmz.de) under the collection number DSM 114993.

Declarations

Ethics approval and consent to participate
Not applicable.

Consent for publication
Not applicable.

Competing interests
The authors declare that they have no competing interests.

Author details
[1]Forest Botany and Tree Physiology, University of Goettingen, 37077 Göttingen, Germany. [2]Department Aquatic Ecosystem Analysis, Helmholtz Center for Environmental Research-UFZ, Magdeburg, Germany. [3]Hessische Landesgesellschaft mbh, Gießen, Germany.

Received: 5 December 2022 Accepted: 21 March 2023
Published online: 29 March 2023

References

1. Williamson B, Tudzynski B, Tudzynski P, Van Kan JAL. *Botrytis cinerea*: the cause of grey mould disease. Mol Plant Pathol. 2007;8:561–80.
2. Elad Y, Pertot I, Cotes Prado AM, Stewart A. Plant hosts of *Botrytis* spp. In: Fillinger S, Elad Y, editors. *Botrytis*—the fungus, the pathogen and its management in agricultural systems. Cham: Springer International Publishing; 2016. p. 413–86.
3. Roca-Couso R, Flores-Félix JD, Rivas R. Mechanisms of action of microbial biocontrol agents against *Botrytis cinerea*. J Fungi. 2021;7:1045.
4. Abbey JA, Percival D, Abbey, Lord, Asiedu SK, Prithiviraj B, Schilder A. Biofungicides as alternative to synthetic fungicide control of grey mould (*Botrytis cinerea*)—prospects and challenges. Biocontrol Sci Technol. 2018;29:207–28.
5. Williamson B. Latency and quiescence in survival and success of fungal plant pathogens Ecology of plant pathogens. Wallingford, UK: Cab International; 1994. p. 187–207.
6. Lilja A, Poteri M, Petäistö R-L, Rikala R, Kurkela T, Kasanen R. Fungal diseases in forest nurseries in Finland. Finn Soc Forest Sci. 2010. https://doi.org/10.14214/sf.147.
7. Mittal RK, Singh P, Wang BSP. *Botrytis*: a hazard to reforestation. Eur J For Res. 1987;17:369–84.
8. Büsgen M. Biologische Studien mit *Botrytis cinerea*. Flora Allg bot Ztg. 1918;111–112:606–20.
9. Hepting GH. Diseases of forest and shade trees of the United States. Washington, DC: U.S. Department of Agriculture Forest Service; 1971.
10. Peace TR. Pathology of trees and shrubs, with special reference to Britain. Oxford: Oxford Univ Press; 1962.
11. Notte A-M, Plaza V, Marambio-Alvarado B, Olivares-Urbina L, Poblete-Morales M, Silva-Moreno E, et al. Molecular identification and characterization of *Botrytis cinerea* associated to the endemic flora of semi-desert climate in Chile. Curr Res Microb Sci. 2021;2:100049.
12. Jeger MJ. The impact of climate change on disease in wild plant populations and communities. Plant Pathol. 2022;71:111–30.
13. Feau N, Joly DL, Hamelin RC. Poplar leaf rusts: model pathogens for a model tree. Can J Bot NRC Res Press. 2007;85:1127–35.
14. Jansson S, Douglas CJ. *Populus*: a model system for plant biology. Annu Rev Plant Biol. 2007;58:435–58.
15. Polle A, Douglas C. The molecular physiology of poplars: paving the way for knowledge-based biomass production. Plant Biol. 2010;12:239–376.
16. Guinet C, Boutigny AL, Vialle A, Hamelin RC, Frey P, Ioos R. Simultaneous monitoring and quantification of *Melampsora allii-populina* and *Melampsora larici-populina* on infected poplar leaves using a duplex real-time PCR assay. Plant Pathol. 2016;65:380–91.
17. Hacquard S, Veneault-Fourrey C, Delaruelle C, Frey P, Martin F, Duplessis S. Validation of *Melampsora larici-populina* reference genes for in planta RT-quantitative PCR expression profiling during time-course infection of poplar leaves. Physiol Mol Plant Pathol. 2011;75:106–12.
18. Gachon C, Saindrenan P. Real-time PCR monitoring of fungal development in *Arabidopsis thaliana* infected by *Alternaria brassicicola* and *Botrytis cinerea*. Plant Physiol Biochem. 2004;42:367–71.
19. Zhang Z, Qin G, Li B, Tian S. Infection assays of tomato and apple fruit by the fungal pathogen *Botrytis cinerea*. Bio-protoc. 2014;4:e1311–e1311.
20. Bai Q, Duan B, Ma J, Fen Y, Sun S, Long Q, et al. Coexpression of *PalbHLH1* and *PalMYB90* genes from *Populus alba* enhances pathogen resistance in poplar by increasing the flavonoid content. Front Plant Sci. 2020;10:101772.
21. Bock CH, Chiang K-S, Del Ponte EM. Plant disease severity estimated visually: a century of research, best practices, and opportunities for improving methods and practices to maximize accuracy. Trop Plant Pathol. 2022;47:25–42.
22. Prins TW, Tudzynski P, von Tiedemann A, Tudzynski B, Ten Have A, Hansen ME, et al. Infection strategies of *Botrytis cinerea* and related necrotrophic pathogens. In: Kronstad JW, editor., et al., Fungal Pathology. Dordrecht: Springer Netherlands; 2000. p. 33–64.
23. Diguta CF, Rousseaux S, Weidmann S, Bretin N, Vincent B, Guilloux-Benatier M, et al. Development of a qPCR assay for specific quantification of *Botrytis cinerea* on grapes: qPCR detection and quantification of *Botrytis cinerea*. FEMS Microbiol Lett. 2010;313:81–7.
24. Müller A, Volmer K, Mishra-Knyrim M, Polle A. Growing poplars for research with and without mycorrhizas. Front Plant Sci. 2013;4:00332.
25. Smith G, Onions AHS, Allsopp D, Eggins HOW. Smith's introduction to industrial mycology. Hoboken: Wiley; 1981.
26. Gams W, van der Aa HA, van der Plaats-Niterink AJ, Samson RA, Stalpers JA. CBS course of mycology CBS course of mycology. Baarn: Centraalbureau voor Schimmelcultures; 1987.
27. Hennebert GL. *Botrytis* and *Botrytis*-like genera. Pers Mol Phylogeny Evol Fungi. 1973;7:183–204.
28. Gardes M, Bruns TD. ITS primers with enhanced specificity for basidiomycetes—application to the identification of mycorrhizae and rusts. Mol Ecol. 1993;2:113–8.
29. White TJ, Bruns T, Lee S, Taylor J. Amplification and direct sequencing of fungal ribosomal RNA genes for phylogenetics. PCR Protocols Guide Methods Appl. 1990;18:315–22.
30. Bonfield JK, Smith KF, Staden R. A new DNA sequence assembly program. Nucleic Acids Res. 1995;23:4992–9.
31. Fernández-Bautista N, Domínguez-Núñez JA, Moreno MMC, Berrocal-Lobo M. Plant tissue trypan blue staining during phytopathogen infection. Bio-protoc. 2016;6:e2078–e2078.
32. R Core Team. R: A language and environment for statistical computing. 2022. https://www.R-project.org/
33. RStudio Team. R Studio: Integrated Development for R. 2020. http://www.rstudio.com/
34. Olivoto T. Lights, camera, pliman! An R package for plant image analysis. Methods Ecol Evol. 2022;13:789–98.
35. The GIMP development team. GIMP. 2022. https://www.gimp.org
36. Suarez MB, Walsh K, Boonham N, O'Neill T, Pearson S, Barker I. Development of real-time PCR (TaqMan®) assays for the detection and quantification of *Botrytis cinerea* in planta. Plant Physiol Biochem. 2005;43:890–9.
37. Sekulska-Nalewajko J, Kornaś A, Gocławski J, Miszalski Z, Kuźniak E. Spatial referencing of chlorophyll fluorescence images for quantitative assessment of infection propagation in leaves demonstrated on the ice plant: *Botrytis cinerea* pathosystem. Plant Methods. 2019;15:18.
38. Smithson M, Verkuilen J. A better lemon squeezer? Maximum-likelihood regression with beta-distributed dependent variables. Psychol Methods. 2006;11:54–71.
39. Cribari-Neto F, Zeileis A. Beta regression in R. J Stat Softw. 2010;34:1–24.
40. Hothorn T, Bretz F, Westfall P. Simultaneous inference in general parametric models. Biom J. 2008;50:346–63.
41. Fox J, Friendly M, Weisberg S. Hypothesis tests for multivariate linear models using the car package. R J. 2013;5:39.
42. Laflamme B, Middleton M, Lo T, Desveaux D, Guttman DS. Image-based quantification of plant immunity and disease. MPMI. 2016;29:919–24.
43. Wang M, Weiberg A, Lin F-M, Thomma BPHJ, Huang H-D, Jin H. Bidirectional cross-kingdom RNAi and fungal uptake of external RNAs confer plant protection. Nat Plants. 2016;2:1–10.

44. Pandey D, Rajendran SRCK, Gaur M, Sajeesh PK, Kumar A. Plant defense signaling and responses against necrotrophic fungal pathogens. J Plant Growth Regul. 2016;35:1159–74.
45. Isebrands JG, Richardson J. Poplars and willows: trees for society and the environment. CABI. 2014. https://doi.org/10.1079/9781780641089.0000.
46. Jarvis WR. Managing diseases in greenhouse crops. St Paul: Aps press; 1992.
47. Caires NP, Rodrigues FA, Furtado GQ. Infection process of *Botrytis cinerea* on Eucalypt leaves. J Phytopathol. 2015;163:604–11.
48. Meng L, Höfte M, Van Labeke M-C. Leaf age and light quality influence the basal resistance against *Botrytis cinerea* in strawberry leaves. Environ Exp Bot. 2019;157:35–45.
49. Deverall BJ, Wood RKS. Infection of bean plants (Vicia faba L) with Botrytis cinerea and B fabae. Ann Appl Biol. 1961;49:461–72.
50. van Kan JAL. Infection strategies of *Botrytis cinerea*. Acta Hortic. 2005. https://doi.org/10.17660/ActaHortic.2005.669.9.
51. van Kan JAL, Shaw MW, Grant-Downton RT. *Botrytis* species: relentless necrotrophic thugs or endophytes gone rogue? Mol Plant Pathol. 2014;15:957–61.
52. Ritpitakphong U, Falquet L, Vimoltust A, Berger A, Métraux J-P, L'Haridon F. The microbiome of the leaf surface of Arabidopsis protects against a fungal pathogen. New Phytol. 2016;210:1033–43.
53. Bao L, Gu L, Sun B, Cai W, Zhang S, Zhuang G, et al. Seasonal variation of epiphytic bacteria in the phyllosphere of *Gingko biloba*, *Pinus bungeana* and *Sabina chinensis*. FEMS Microbiol Ecol. 2020;96:fiaa017.
54. Huo D, Wu J, Kong Q, Zhang GB, Wang YY, Yang HY. Macromolecular toxins secreted by *Botrytis cinerea* induce programmed cell death in Arabidopsis leaves. Russ J Plant Physiol. 2018;65:579–87.
55. Leisen T, Werner J, Pattar P, Safari N, Ymeri E, Sommer F, et al. Multiple knockout mutants reveal a high redundancy of phytotoxic compounds contributing to necrotrophic pathogenesis of *Botrytis cinerea*. PLOS Pathog Public Library Sci. 2022;18:e1010367.
56. Thomma BPHJ, Eggermont K, Broekaert WF, Cammue BPA. Disease development of several fungi on Arabidopsis can be reduced by treatment with methyl jasmonate. Plant Physiol Biochem. 2000;38:421–7.
57. Yu M, Shen L, Fan B, Zhao D, Zheng Y, Sheng J. The effect of MeJA on ethylene biosynthesis and induced disease resistance to *Botrytis cinerea* in tomato. Postharvest Biol Technol. 2009;54:153–8.
58. Hu Z, Zhao L, Yang D, Shen Y, Shen F. Influences of the Populus deltoids seedlings treated with exogenous methyl jasmonate on the growth and development of *Lymantria dispar* larvae. J of For Res. 2006;17:277–80.
59. Luo J, Xia W, Cao P, Xiao Z, Zhang Y, Liu M, et al. Integrated transcriptome analysis reveals plant hormones jasmonic acid and salicylic acid coordinate growth and defense responses upon fungal infection in poplar. Biomolecules. 2019;9:12.
60. El Oirdi M, El Rahman TA, Rigano L, El Hadrami A, Rodriguez MC, Daayf F, et al. *Botrytis cinerea* manipulates the antagonistic effects between immune pathways to promote disease development in tomato. Plant Cell. 2011;23:2405–21.
61. Windram O, Madhou P, McHattie S, Hill C, Hickman R, Cooke E, et al. Arabidopsis defense against *Botrytis cinerea*: chronology and regulation deciphered by high-resolution temporal transcriptomic analysis. Plant Cell. 2012;24:3530–57.
62. Smirnova E, Marquis V, Poirier L, Aubert Y, Zumsteg J, Ménard R, et al. Jasmonic acid oxidase 2 hydroxylates jasmonic acid and represses basal defense and resistance responses against *Botrytis cinerea* infection. Mol Plant. 2017;10:1159–73.
63. Paap T, Wingfield MJ, Burgess TI, Wilson JRU, Richardson DM, Santini A. Invasion frameworks: a forest pathogen perspective. Curr Forestry Rep. 2022;8:74–89.
64. Zhang PG, Sutton JC. High temperature, darkness, and drought predispose black spruce seedlings to gray mold. Can J Bot. 1994;72:135–42.
65. Veloso J, van Kan JAL. Many shades of grey in *Botrytis*–host plant interactions. Trends Plant Sci. 2018;23:613–22.
66. Dreischhoff S, Das IS, Jakobi M, Kasper K, Polle A. Local responses and systemic induced resistance mediated by ectomycorrhizal fungi. Front Plant Sci. 2020;11:590063.
67. Saijo Y, Loo EP. Plant immunity in signal integration between biotic and abiotic stress responses. New Phytol. 2020;225:87–104.
68. Kasper K, Abreu IN, Feussner K, Zienkiewicz K, Herrfurth C, Ischebeck T, et al. Multi-omics analysis of xylem sap uncovers dynamic modulation of poplar defenses by ammonium and nitrate. Plant J. 2022;111:282–303.
69. Polle A, Janz D, Teichmann T, Lipka V. Poplar genetic engineering: promoting desirable wood characteristics and pest resistance. Appl Microbiol Biotechnol. 2013;97:5669–79.

Publisher's Note

Additional information

Fast and easy bioassay for the necrotizing fungus *Botrytis cinerea* on poplar leaves

Steven Dreischhoff[1], Ishani Shankar[1] Das, Felix Häffner[2], Anna Malvine Wolf[3], Andrea Polle[1], Karl Henrik Kasper[1]*

* Correspondence: kkasper@gwdg.de

[1] Forest Botany and Tree Physiology, University of Goettingen, 37077 Göttingen, Germany

[2] Department Aquatic Ecosystem Analysis, Helmholtz Center for Environmental Research-UFZ, 39115 Magedeburg, Germany

[3] Hessische Landesgesellschaft mbh, 35392 Gießen, Germany

Additional Figure

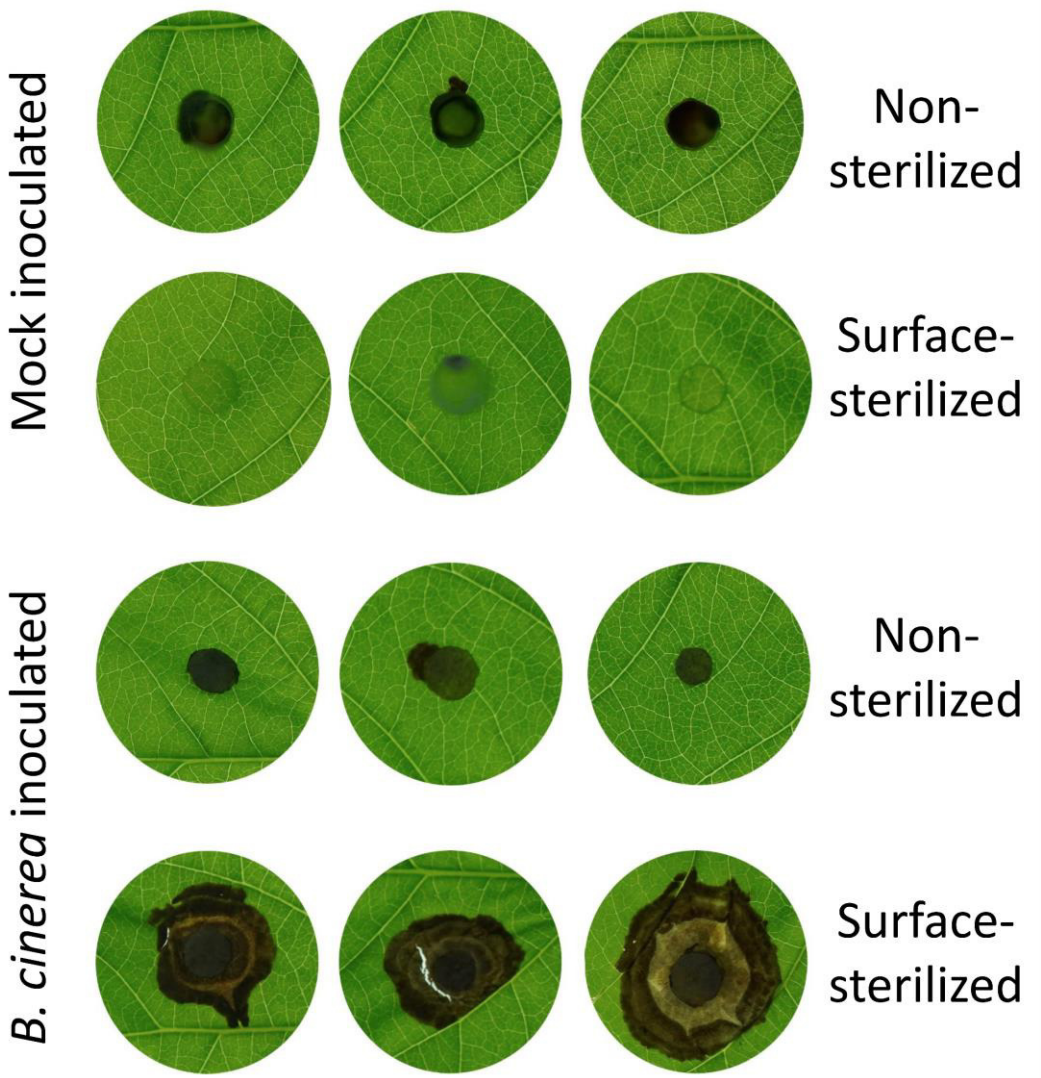

Supplementary Figure S1: The effect of 70% ethanol poplar leaf surface sterilization on infection severity of *Botrytis cinerea* and mock-PDA plug inoculation at 4 dpi.
Leaves of *Populus* x *canescens* were wiped three times with a 70 % ethanol-soaked paper tissue and subsequently inoculated with a sterile Potato-Dextrose-Agar plug (mock treatment) or a *Botrytis cinerea* plug from a seven-day-old Potato-Dextrose-Agar culture. The plugs were 6 mm in diameter. After the harvest, the plugs were removed and leaf disks (Ø=27 mm) were punched out around the previous position of the plugs.

Additional Table

Additional Table S1: Origin of Poplar species challenged with *Botrytis cinerea*.

Species	**Section**	**Origin**
Populus alba	*Populus*	Department of Forest Botany and Tree Physiology, University of Göttingen
P. x *canescens*	*Populus*	INRA 717 1B4, INRA, Nancy, France
P. tremula	*Populus*	NW-FVA[#] Göttingen, formerly Hessische Forstliche Versuchsanstalt Hann Münden-Pappelkamp
P. tremula x *tremuloides*	*Populus*	Department of Forest Botany and Tree Physiology, University of Göttingen
P. deltoides	*Aigeiros*	NW-FVA Göttingen, formerly Hessische Forstliche Versuchsanstalt Hann Münden-Pappelkamp
P. deltoides spp. *Wislizeni*	*Aigeiros*	NW-FVA Göttingen, formerly Hessische Forstliche Versuchsanstalt Hann Münden-Pappelkamp
P. nigra	*Aigeiros*	NW-FVA Göttingen, formerly Hessische Forstliche Versuchsanstalt Hann Münden-Pappelkamp
P. x *canadensis*	*Aigeiros*	NW-FVA Göttingen, formerly Hessische Forstliche Versuchsanstalt Hann Münden-Pappelkamp
P. balsamifera	*Tacamahaca*	NW-FVA Göttingen, formerly Hessische Forstliche Versuchsanstalt Hann Münden-Pappelkamp
P. candicans	*Tacamahaca*	NW-FVA Göttingen, formerly Hessische Forstliche Versuchsanstalt Hann Münden-Pappelkamp
P. cathayana	*Tacamahaca*	NW-FVA Göttingen, formerly Hessische Forstliche Versuchsanstalt Hann Münden-Pappelkamp
P. koreana	*Tacamahaca*	NW-FVA Göttingen, formerly Hessische Forstliche Versuchsanstalt Hann Münden-Pappelkamp
P. laurifolia	*Tacamahaca*	NW-FVA Göttingen, formerly Hessische Forstliche Versuchsanstalt Hann Münden-Pappelkamp
P. maximiwiwicziana	*Tacamahaca*	NW-FVA Göttingen, formerly Hessische Forstliche Versuchsanstalt Hann Münden-Pappelkamp
P. trichocarpa	*Tacamahaca*	NW-FVA Göttingen, formerly Hessische Forstliche Versuchsanstalt Hann Münden-Pappelkamp
P. simonii	*Tacamahaca*	NW-FVA Göttingen, formerly Hessische Forstliche Versuchsanstalt Hann Münden-Pappelkamp
P. suavaelens var. Przewalksii	*Tacamahaca*	NW-FVA Göttingen, formerly Hessische Forstliche Versuchsanstalt Hann Münden-Pappelkamp
P. wilsonii	*Leucoides*	Botanical garden Kiel 2010
P. euphratica	*Turanga*	clone B2 obtained from trees grown in the Ein Avdat region, Israel

[#] Niedersächsische Forstliche Versuchsanstalt

4.4. *B. cinerea* infection experiments with *L. bicolor*-treated poplars

The defense against necrotizing pathogens (like *Botrytis cinerea*) and insects is mediated by JA-dependent signaling (Pieterse et al., 2012). Whether EMF or chitin can also affect the infection with necrotizing pathogens is not known and was therefore investigated here.

WT, *cerk1* KO 19, and *cerk1* KO 20 plants were treated two times over three weeks with living *L. bicolor*, heat-killed *L. bicolor*, the supernatant of the *L. bicolor* liquid culture, chitin or with buffer as a control treatment (3.15), similar as described above (3.15). The treatments did not result in significant differences in mycorrhization rate for WT, *cerk1* KO 19, and *cerk1* KO 20 poplar plants (Figure 39). Most plants had mycorrhization rates of below 2 %. However, some plants had elevated mycorrhization rates, including plants treated with living *L. bicolor*. As mentioned above, the mycorrhization rate could influence the outcome of the experiment. The third leaf was inoculated with *B. cinerea* at the end of the three-week treatment period. There were no significant differences in the necrotic area between all treatments. In addition, genotypes had no significant effect on the necrotic area. The variation within samples of one treatment was relatively high, and the necrotic area was generally low (Figure 40A; compare 4.3). The low necrotic area was also reflected in the low abundance of fungal DNA found in the leaf disks. There was no statistically significant difference in *B. cinerea* DNA abundance between treatments (Figure 40B). Also, the genotypes had no significant differences in *B. cinerea* DNA abundance. Overall, the variation within treatments was high.

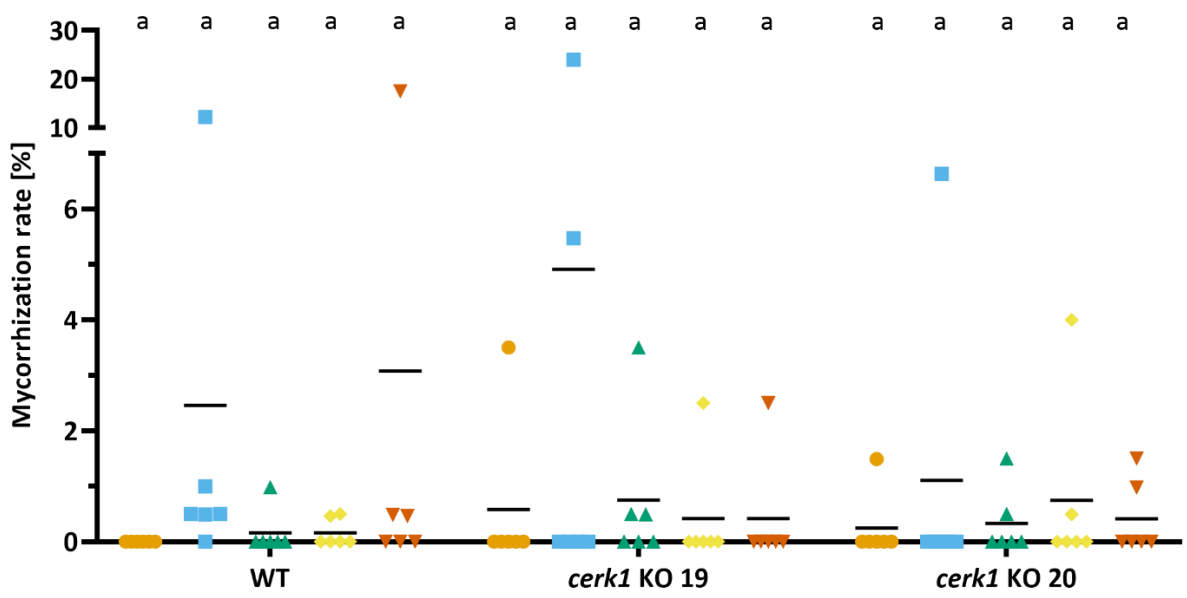

Figure 39 Mycorrhization rate of WT, *cerk1* KO 19, and *cerk1* KO 20 treated with different *L. bicolor* preparations

Greenhouse-grown WT *P.* × *canescens* were treated two times over three weeks buffer (control; orange), *L. bicolor* (*Lb*; blue), heat-killed *L. bicolor* (*Lb*HK; green), the supernatant of *L. bicolor* liquid (*Lb*Su; yellow) culture or 500 µg mL^{-1} chitin (red) for eleven days (3.15). After the harvest, the mycorrhization rate in percent was determined (3.15). The graph shows data points (biological replicates, n = 6) and the mean of one experiment. Different letters above the data points indicate statistically significant differences at $P < 0.05$ calculated by ANOVA and Tukey's post hoc test.

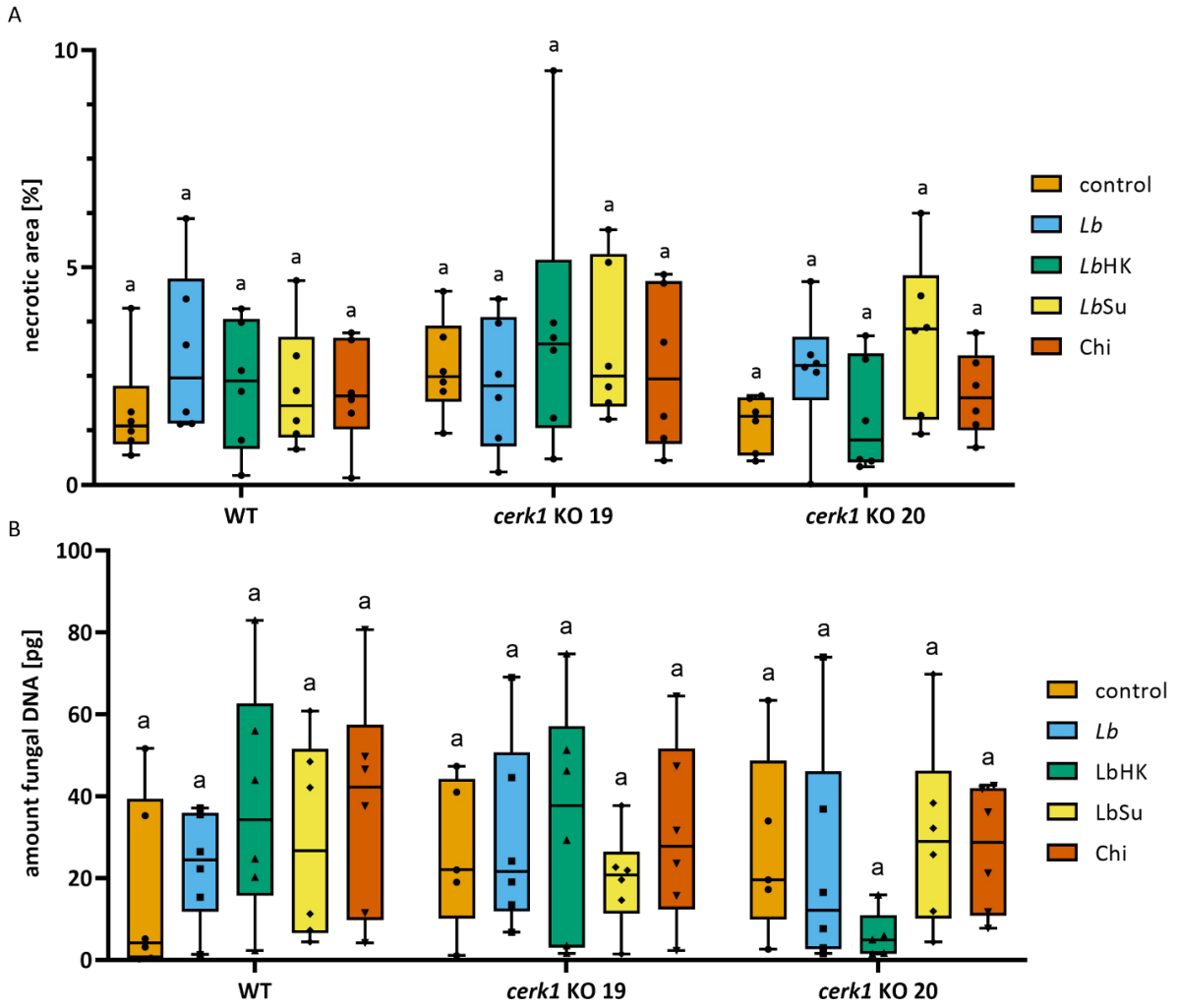

Figure 40 Necrotic area (A) and fungal DNA amount (B) of *B. cinerea* on WT, *cerk1* KO 19, and *cerk1* KO 20 leaves after root application of different *L. bicolor* preparations
Greenhouse-grown WT *P.* × *canescens*, *cerk1* KO 19, and *cerk1* KO 20 were two times three weeks treated with 20 mL of buffer (control; orange), *L. bicolor* OD 0.1 (*Lb*; blue), heat-killed *L. bicolor* OD 2 (*Lb*HK; green), the supernatant of *L. bicolor* liquid culture (*Lb*Su; yellow) or 500 µg mL^{-1} chitin (red; 3.15). After the treatment, the third fully developed leaf was plug-inoculated with *B. cinerea*. The necrotic area and the fungal DNA amount were measured (3.15). The figures show min-max boxplots with the whiskers spanning across the range of the data points. Each point represents one biological replication (n = 5) of one experiment. Different letters above the boxplots indicate statistically significant differences at $P < 0.05$, calculated by ANOVA and Tukey's post hoc test.

The application of *L. bicolor* to soil did not lead to enhanced mycorrhization rates of the inoculated poplar plants (Figure 39). Therefore, *P.* × *canescens* WT and *cerk1* KO 19 plantlets were inoculated under axenic conditions with *L. bicolor* before transferring them to the greenhouse. The mycorrhization rate for *L. bicolor* pre-treated WT plants was higher than for non-*L. bicolor* inoculated plants, as reported above (Figure 34). The colonized plants were then

used to infect leaves with *B. cinerea.* There were no statistical differences in the necrotic area among the treatments and genotypes (Figure 41A). The average necrotic area of mycorrhiza-treated WT plants was bigger than that of control plants but not significantly different. There was more variance between samples for WT plants than *cerk1* KO plants. The DNA abundance reflected a similar picture (Figure 41B). When the necrotic area was correlated to the mycorrhization rate of each plant, a weak positive correlation could be observed, i.e., a higher mycorrhization rate resulted in a bigger necrotic area on the leaves (Figure 42).

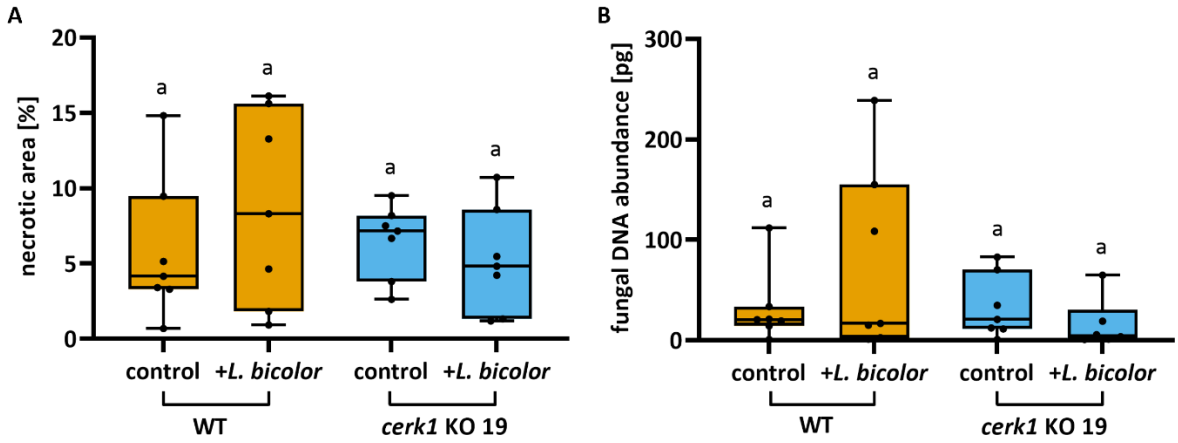

Figure 41 Necrotic area (A) and fungal DNA amount (B) of *B. cinerea* on WT and *cerk1* KO 19 leaves after mycorrhization with *L. bicolor*

WT *P.* × *canescens* and *cerk1* KO 19 plants with or without *L. bicolor* were grown in the greenhouse and irrigated daily nutrient solutions with low nitrogen supply. After ten weeks, the fourth fully expanded leaf was inoculated with *B. cinerea*. The necrotic area and the fungal DNA amount were measured (3.15). The figures show min-max boxplots with the whiskers spanning across the range of the data points. Each point represents one biological replication (n = 7) of one experiment. Different letters above the boxplot indicate statistically significant differences at $P < 0.05$ calculated by ANOVA and Tukey's post hoc test.

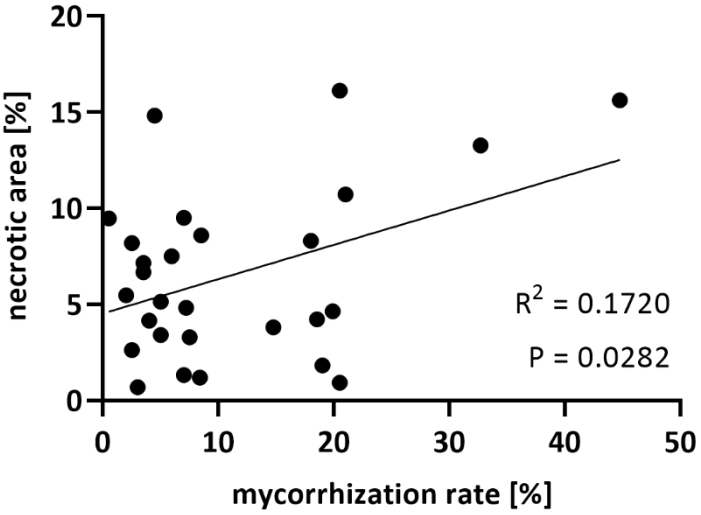

Figure 42 Correlation of mycorrhization rate to the necrotic area
The mycorrhization rate (Figure 27) was correlated to the necrotic area (Figure 41).

The greenhouse experiment suggested that EMF colonization rendered plants slightly more susceptible to *B. cinerea* infections (Figure 42). To validate this result, an independent experiment was conducted under sterile conditions (3.15). *L. bicolor* treated and control plants were inoculated with *B. cinerea* on the leaves. Similarly, as before, mycorrhizal plants showed a trend toward higher necrotic areas than plants non-mycorrhizal plants. This was the case for both WT and the *cerk1* KO 19 line. Because of the variation between samples, no statistically significant difference at $P < 0.05$ was found between mycorrhizal and non-mycorrhizal plants (Figure 43).

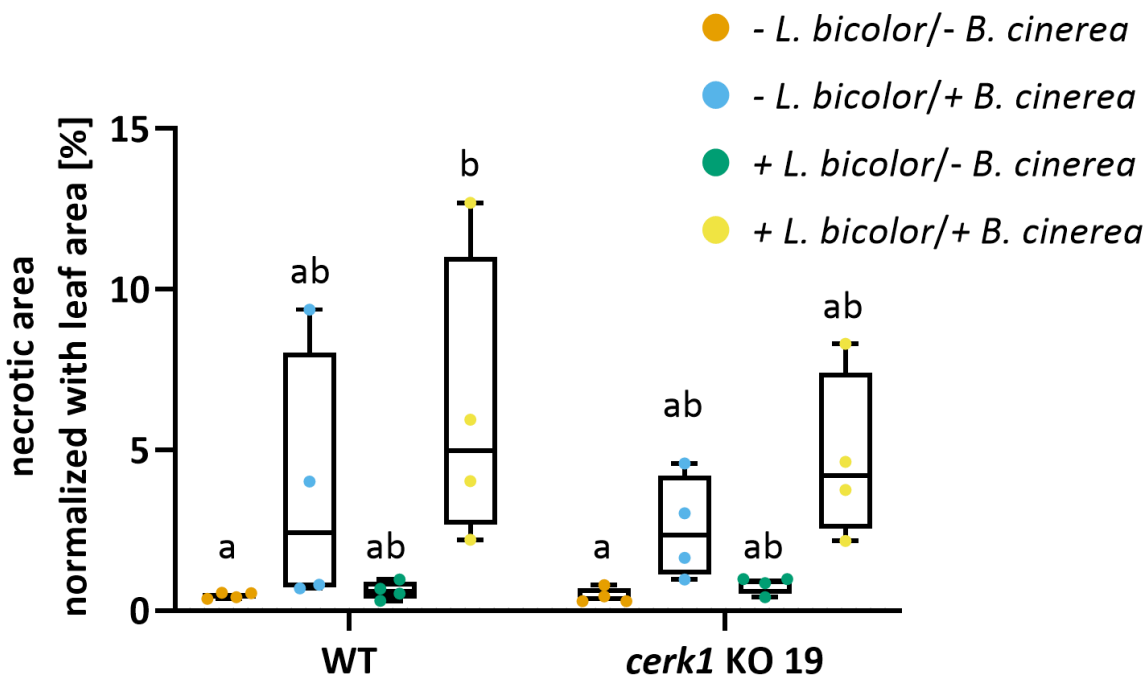

Figure 43 Necrotic area normalized to leaf area of WT and *cerk1* KO 19 in a sterile sandwich system with *L. bicolor*

P. × *canescens* WT and *cerk1* KO 19 were inoculated with *L. bicolor* or not inoculated in a sterile sandwich system (3.3). After ten days, the first fully expanded leaf was inoculated with *B. cinerea* or mock-inoculated. The necrotic area was measured (3.15) and normalized to the leaf area. The figures show min-max boxplots with the whiskers spanning across the range of the data points. Each point represents one biological replication (n = 4) of one experiment. Different letters above the boxplots indicate statistically significant differences at $P < 0.05$, calculated by ANOVA and Tukey's post hoc test.

5. Discussion

5.1. Systemic reprogramming of the defense transcriptome by *Laccaria bicolor*

5.1.1. Initial colonization is necessary for transcriptome changes

The first research question addressed in this thesis is how the systemic defense transcriptome changes in leaves after initial *Laccaria bicolor* contact and in the early phase of colonization on *Populus* × *canescens* roots. During the first two days after *L. bicolor* inoculation, no genes had changed transcript abundances in leaves (Figure 7). Anatomical studies of the colonization of roots by *L. bicolor* and other EMF found that the fungi attach to the root and form a mantle in this initial phase (Brun et al., 1995; Burgess et al., 1996; Wong et al., 1990). Between days two and four, hyphae penetrate the root and grow deeper into the intercellular space (Brun et al., 1995; Burgess et al., 1996; Le Quéré et al., 2005; Ruytinx et al., 2021; Wong et al., 1990). In the present thesis, the first transcript abundance changes were observed after four days. This suggests that only contact between the fungus and the root is insufficient to induce changes in the leaf transcriptome. The number of genes with changed transcript abundances increased from 47 after four days to almost 1500 genes after seven days (Figure 7). This drastic increase might be due to differences in fungal colonization intensity. After four days, *L. bicolor* barely invaded the root, while after seven days, the hyphae grew at least one cell layer deep into the root (Ruytinx et al., 2021; Wong et al., 1990). Altogether, these data suggest that a certain degree of colonization is necessary to induce changes in the leaf transcriptome. During mycorrhizal development, a considerable array of molecules, such as small secreted proteins or terpenoids, is used for communication between the two interaction partners (Felten et al., 2009; Garcia et al., 2015; Wong-Bajracharya et al., 2022). The initiating signals that induce systemic change in the leaf transcriptome appear to require penetration of the root by the fungus.

5.1.2. *L. bicolor* increases JA signaling components

An important result of the transcriptome analysis was that transcripts of six genes involved in the JA biosynthesis exhibited increased transcript abundances, suggesting activation of JA-dependent signaling pathways in the initial phase of colonization. JA signaling is required for the defense against insects and necrotizing pathogens (Kachroo and Kachroo, 2007; Li et al., 2022; Pieterse et al., 2012). Furthermore, the GO term “salicylic acid catabolic process” was enriched. Several studies have shown that JA and SA act antagonistically (Hou and Tsuda,

2022; J. Wang et al., 2020), implying that when JA-dependent defenses are mounted, SA-dependent defenses are down-regulated, potentially, via SA degradation.

Additional evidence for a systemic effect on JA-dependent processes, which are important for ISR, was gained from the analysis of genes associated with GO terms “induced systemic resistance” and “systemic acquired resistance” (Table 1).

Most of the genes identified by this analysis are connected to JA signaling. Genes with increased transcript abundance, like WRKY70 and WRKY11, are involved in suppressing SA signaling (Journot-Catalino et al., 2006; Li et al., 2006, 2004). In addition, genes with decreased transcript abundance (e.g., putative PR1 and NPR1) are SA-responsive in several species (Hou and Tsuda, 2022). These observations may suggest that JA-dependent processes activated in poplar leaves were increased because of antagonistic JA/SA regulation by *L. bicolor*. In *Arabidopsis*, *AtPR1* is a stable marker gene for SA-responsive signaling (Zeier, 2021). In the present experiments, the different transcript abundances of the putative PR1 homologs showed contrasting patterns. In *P. trichocarpa,* there are at least 22 predicted AtPR1 homologs (Duplessis et al., 2009). Not all of them are induced by the same stimulus (Duplessis et al., 2009) and, thus, may exert different functions compared with the *Arabidopsis* gene. The transcript abundance changes of the discussed genes suggest that JA signaling is important for the transcriptome changes in systemic tissues after *L. bicolor* treatment. To further corroborate this suggestion, JAs analyses should be conducted.

L. bicolor produces VOCs that can induce resistance against bacterial pathogens (Hammerbacher et al., 2019; Müller et al., 2013a), recruiting genes that are also important for JA signaling, such as JAZ proteins or WRKY40 transcription factor (Dreischhoff et al., 2020; Godard et al., 2008; Luo et al., 2009). It is, therefore, conceivable that VOCs transmitted via the aerial space might play a role in the systemic effects of *L. bicolor* found here. To test this idea, genes with increased transcript abundance after seven days of a direct contract of *L. bicolor* and poplar from this study were compared with those activated when poplar shared the same air space with *L. bicolor* for seven days but without direct root contact (Jakobi, 2021). This analysis revealed a shared pool of 19 genes (Supplemental Table 8), in which only one gene (PR1) had a documented connection to defense. However, in this and the study by Jakobi (2021), the regulation of PR1 was in opposite directions. Even though VOCs induced flavonol

biosynthesis, they did not induce JA signaling, which makes them unlikely to be the only signaling compound inducing systemic resistance in above-ground tissues at early stages.

5.1.3. Ethylene and other defense pathways

Ethylene can modulate JA signaling, thereby increasing the defense against necrotizing pathogens and reducing resistance against insects (Pieterse et al., 2014b). There is also evidence for ethylene-related processes in the present transcriptome data. The GO term "cellular response to hypoxia" of genes with reduced transcript abundance after four and seven days was mainly driven by ethylene-responsive genes. Ethylene plays a role in hypoxia signaling in aspen and other plants (Hartman et al., 2021; Tan et al., 2021). The decreased transcript abundance of ethylene-related genes might point to an inhibition of ethylene signaling. This assumption is further supported by the transcript abundance increase of *EBF1* and *CTR1*, which are negative regulators of ethylene signaling and increase defense against insects (Huang et al., 2003; Song et al., 2014). However, there were also genes with increased transcript abundances known to be involved in ethylene production in numerous plant species, including *Arabidopsis* (Pattyn et al., 2021). Therefore, based on transcriptome data, clear-cut evidence for a role of ethylene in the systemic effects of *L. bicolor* remains elusive.

It is known that receptor-like kinases (RLK) are important for mycorrhiza establishment in roots (Labbé et al., 2019; Shi et al., 2022), and some even have a double role in mycorrhization and immunity (Gibelin-Viala et al., 2019). RLKs are receptors that can sense molecules outside the cell and transduce the signal into the cell (Dievart et al., 2020). RLKs were only examined in roots for the interaction with mycorrhiza, and there is no information about their role in systemic tissues for the interaction with mycorrhiza. While the exact function of RLK1 and CRK14 is still illusive, transcripts of both RLKs increased after SA treatment (Ohtake et al., 2000; Wrzaczek et al., 2010), and CRK14 transcript levels decreased in SA signaling mutants *sid2* (*salicylic acid induction deficient 2*) and *npr1* (Wrzaczek et al., 2010). The involvement of RLK1 and CRK14 in SA signaling adds to the conception that EMF utilize different components of the ISR and SAR signaling pathways (Cameron et al., 2013). So far, the signal and the receptor establishing systemic ectomycorrhizal-induced resistance are elusive. It is possible that the discussed RLKs play a role in systemic signal recognition or transduction.

An interesting question is whether the transcriptome data contain information on a possible involvement of further phytohormones in systemic *L. bicolor* effects. In this study, the

transcript levels of two homologs of the *CYTOCHROME P450* family gene *AtCYB83B1* were increased. *At*CYB83B1 is involved in auxin signaling and can modulate systemic defenses (Truman et al., 2010). In the leaves of ectomycorrhizal poplar, auxin-responsive genes had increased transcript abundances (Kaling et al., 2018). In roots, *L. bicolor* alters the auxin response locally (Felten et al., 2009; Vayssières et al., 2015). Nevertheless, the role of auxin in systemic responses induced by EMF is unclear.

Overall, similar fractions of all genes in the GO term ISR and SAR had changed transcript abundance in this study. This contributes to the finding of other studies that only parts of SAR and ISR signaling are used to achieve mycorrhiza-induced resistance (Cameron et al., 2013; Dreischhoff et al., 2020; Jung et al., 2012; Pozo and Azcón-Aguilar, 2007).

The analyses revealed that EMF treatment likely results in increased JA signaling. However, the involvement of ethylene is unclear. Measuring the concentrations of JA and its derivatives, ethylene, and other phytohormones in poplar after initial contact with *L. bicolor* is necessary because increased transcript amounts do not necessarily mean increased metabolite concentrations.

5.1.4. *L. bicolor* induces cell wall modification

This study shows that *L. bicolor* changes the transcript abundances of genes involved in the biosynthesis of defense metabolites in leaves. Among these defense compounds are phenolic substances derived from the shikimate pathway (Underwood, 2012), which was transcriptionally activated by *L. bicolor* (Figure 10). Phenolics have been described to be induced by EMF (Baum et al., 2009; Fontana et al., 2009; Gange and West, 1994; Pfabel et al., 2012; Schweiger et al., 2014). Phenolic compounds are precursors for cell wall modifications (Wang et al., 2013). GO term and KEGG analysis revealed that genes involved in cell wall modifications had increased transcript abundances (Figure 11). Notably, six out of seven genes in the phenylalanine biosynthesis which catalyze the formation of chorismate, had increased transcript abundances. In plants, phenylalanine can be produced either via the arogenate pathway or the phenylpyruvate pathway (Qian et al., 2019). Chorismate is the precursor for both pathways, and the availability of phenylalanine is often the limiting factor for the biosynthesis of cell wall components (Adams et al., 2019).

Furthermore, the transcript levels of most genes for monolignol synthesis were increased (Figure 11). Monolignols are components for synthesizing lignin (Wang et al., 2013). It is

known that EMFs induce cell wall modifications in roots during symbiosis (Martin et al., 2016; Sillo et al., 2016), but cell wall modifications in systemic leaves have not been described yet. Increased availability of cell wall components could lead to the remodeling of cell walls and thus potentially enhance the barrier function against various biological attackers (Molina et al., 2021; Underwood, 2012; Y.-F. Wang et al., 2020). In the phase of EMF colonization, defense mechanisms are induced in roots (Plett et al., 2014; Tschaplinski et al., 2014). It is conceivable that in the initial phase of root colonization, defensive responses are activated in leaves, which then decrease over time. These responses could include an initial increase in the biosynthesis of phenolic compounds. This would explain the differences from the study by Kaling et al. (2018), where they found decreased phenolic content at later time points of colonization.

Therefore, anatomical, metabolite, and cell wall composition studies are necessary to validate changes in the cell walls of systemic tissues in response to ectomycorrhizal colonization. Then, it would be possible to gain insights into the induction and time-dependency of secondary metabolite biosynthesis by *L. bicolor*. The accumulation of phenolic is an effect of JA signaling in poplar and other plants, which might suggest that JA could be important in the systemic effects of EMF (An et al., 2006; Park et al., 2019; Tao et al., 2022).

5.1.5. *L. bicolor* possibly induces flavonoid signaling

The transcript levels of numerous genes involved in flavonoid biosynthesis increase in roots during EMF symbiosis formation (Wong et al., 2019). Flavonoids have a defensive capacity and are inducible by JA signaling (Premathilake et al., 2020; Shan et al., 2009; Wang et al., 2019). In addition, plant-derived flavonoids have a signaling function in below-ground interactions between plants and EMF (Garcia et al., 2015; Treutter, 2006). Flavonoids increase spore germination and hyphal growth and trigger the expression of fungal effectors (Garcia et al., 2015; Plett and Martin, 2012). Genes in the flavonoid biosynthesis had increased transcript abundance (Figure 12). It is conceivable that flavonoids have a signaling function in ectomycorrhizal defense induction in above-ground tissues if they were transported to above-ground tissues. There is evidence of flavonoids in poplar xylem sap (Kasper et al., 2022).

Overall, there is no clear picture, under the influence of EMF, if the defenses are activated through flavonoids or specialized metabolites (e.g., anthocyanins) because there is evidence

for reduction (Kaling et al., 2018) but also for an increase of these defense metabolites (Pfabel et al., 2012).

5.1.6. *KTI* is involved in systemic ectomycorrhizal defense induction and downstream of JA signaling

Among the genes responding to EMF colonization under the axenic conditions of this study and those found under outdoor conditions (Kaling et al., 2018), sixteen were shared (Figure 17). Two shared genes (Table 2) are linked to plant defense against biotic stress (Fujita and Inui, 2021; Major and Constabel, 2008). One gene encodes a MAJOR LATEX PROTEIN-LIKE PROTEIN 423 (MLP). MLPs got their name because they were first found in the poppy latex (Nessler et al., 1985), but genes encoding similar proteins can be found in many dicot species (Fujita and Inui, 2021). The exact function of MLPs is still unclear, but they are responsive to drought stress and pathogen infections (Chen and Dai, 2010; Deng et al., 2011; Song et al., 2020; Yuan et al., 2020). There is evidence that other ectomycorrhizal fungi besides *L. bicolor* induce *MLPs* (Sillo et al., 2022). Furthermore, *MLPs* are induced by arbuscular mycorrhiza and increase resistance against nematodes (Balestrini et al., 2019).

The second gene is a putative *KUNITZ FAMILY TRYPSIN AND PROTEASE INHIBITOR* (*KTI*). KTIs accumulate after wounding and are involved in the defense against insects by interfering with digestion (Haruta et al., 2001; Major and Constabel, 2008; McManus and Burgess, 1995; Srinivasan et al., 2005). Thereby, KTIs may not directly diminish feeding on the plant but affect the fitness of the insect by reducing its reproduction (Kaling et al., 2018). KTIs also have antimicrobial and antifungal activity (Alencar de Barros et al., 2021; de Oliveira et al., 2018; Zhang et al., 2020). In *Medicago sativa, KTIs* are induced by arbuscular mycorrhiza to promote resistance against aphids (Y. Li et al., 2019). MeJA treatment induces KTIs in several species like tomato or aspen (Bolter, 1993; Haruta et al., 2001). In *Nicotiana attenuata,* the transcription factors *Na*WRKY3 and *Na*WRKY6 regulate KTIs (Yin et al., 2021). Silencing of *Na*WRKY3 and *Na*WRKY6 results in increased susceptibility toward an insect herbivore and decreased production of JA and JA-derivatives (Skibbe et al., 2008; Zavala et al., 2004). In addition, KTI levels are less inducible after silencing *Na*AOC (ALLENE OXIDE CYCLASE), an enzyme essential for JA biosynthesis (Wasternack and Feussner, 2018; Yin et al., 2021). Paschold and colleagues (2007) silenced the JA-Ile co-receptor *Na*COI1 making the plants

insensitive to JA treatment and unable to induce protease inhibitors after herbivore attack. These findings support that *KTI* is downstream of JA signaling.

Since the transcriptomic data in this thesis suggested that JA, SA, and ethylene might be involved in mounting the defenses, MeJA, BTH (a relatively stable SA analog, (Kunz et al., 1997)), and ACC (ethylene precursor) were applied to *P.* × *canescens* plants to dissect their possible involvement in *KTI* induction. No marker gene was affected explicitly by one phytohormone. Thus, the marker genes cannot be used to determine whether the phytohormone application was successful. The transcript abundance of a marker gene needs to be altered for a specific stimulus to disentangle signaling pathways (Beyer et al., 2021).

KTI transcript abundance was increased after MeJA treatment, similarly as observed for *P. nigra* × *P. deltoides*, *P. deltoides* × *P. trichocarpa,* and *P.* × *euramericana* (Chen et al., 2021; Luo et al., 2019). This response was consistently found under axenic as well as under greenhouse conditions. After BTH treatment, *KTI* transcript levels were reduced (Figure 18A+B), suggesting that activation of SA-mediated defenses might have led to repression of JA-mediated responses, while there is no evidence that ethylene played a role in *KTI* regulation.

Whether EMF modulate JA levels in leaves or along the transport route is still unclear. So far, increased JA or JA derivatives levels were not detected in plants treated with EMF (Luo et al., 2011; Vishwanathan et al., 2020). *L. bicolor* can modulate the sensitivity toward MeJA in roots (Basso et al., 2020). AMF colonization affects the sensitivity toward JA or its derivatives in above-ground tissues (Jung et al., 2012). Therefore, it is conceivable that *L. bicolor* also changes the sensitivity for JAs in leaves. This idea is supported by the present data because the combination of MeJA and *L. bicolor* treatment reduced the KTI induction (Figure 19). The modulation of JA sensitivity would not require changes in the abundance of JAs. Nevertheless, it would be worthwhile to repeat the experiments and use roots and leaves to measure KTI induction and JA levels. To better understand the potential roles of SA and ET, additional work is required to establish reliable marker genes. Components downstream of JA biosynthesis, like the *MYC2* transcription factor (Liao et al., 2020), might be a more reliable marker for MeJA treatment than AOS. Since ACC is the ethylene precursor, ACC oxidase is needed to produce ethylene (Wang et al., 2002). It might be a better marker than *ERF1* for the effects of ACC, as shown for wood formation (Andersson-Gunnerås et al., 2003). Possibly WRKY89 or WRKY18,

used by Ullah et al. (2022), or WRKY73 (Duan et al., 2015) might be better transcriptional markers for SA-induced signaling by BTH than PR1.

Even though the results of both phytohormone application experiments should be considered carefully, the results suggest that MeJA induces *KTI*. This finding agrees with the literature and indicates that *KTI* acts downstream of JA signaling. It adds to the findings of the transcriptome analysis that JA is a key factor in EMF-induced systemic defense.

5.2. CERK1 is a component of *L. bicolor*-induced systemic resistance

5.2.1. WT and *cerk1* KO lines growth have similar physiological parameters

Vishwanathan et al. (2020) treated *Arabidopsis* roots with different *L. bicolor*-derived preparations and chitin. Consequently, *Trichoplusia ni* gained less weight while feeding on treated plants. The effect was abolished in KO mutants of the chitin receptor *cerk1*. The obvious question was whether CERK1 and chitin are involved in inducing systemic effects in the host interaction of *L. bicolor* and poplar. This question was addressed with *cerk1* KO poplar.

Plants only have limited resources, and thus there is the common conception of a growth-defense trade-off, meaning when defenses are activated, growth is slowed down (Figueroa-Macías et al., 2021). CERK1 is an important receptor for pathogen attack and is directly involved in defense activation (Miya et al., 2007). Thus, it was conceivable that *cerk1* KO plants have a growth-defense trade-off. Therefore, plant growth and physiological performance were characterized under greenhouse conditions. With foliar ROS burst and MAP kinase assays (Petutschnig et al., 2010), it was confirmed that the cerk1 KO lines did not respond to chitin (Figure 19 & Figure 20). Furthermore, the growth rates of WT and *cerk1* KO were similar (Figure 22, Figure 23, and Figure 29).

The analyses during the time course of mycorrhization under axenic conditions showed that transcripts of genes involved in the biosynthesis of phenolic compounds and flavonoids were increased. To test whether there were differences between the cerk1 KO lines and the WT, the contents of metabolites such as anthocyanin, flavone photosynthetic pigments, and nitrogen were evaluated with a non-destructive method (Cerovic et al., 2012). Variable results of the nitrogen balance index revealed that plant nutrition should be better controlled in future experiments. Here, usually, conditions, which favor EMF colonization, i.e., low nitrogen supply, were applied. Nitrogen supply influences foliar defenses (Kasper et al., 2022) and thus may have confounded mycorrhizal effects. It should also be noted that the temperature in the greenhouse fluctuated and reached values up to 31 °C. This may have also caused stress, resulting in low rates of photosynthesis compared with other studies (Kasper et al., 2022; Sharmin et al., 2021). Since the greenhouse plants were obviously stressed, it may not be too surprising that preliminary feeding assays with *Helicoverpa armigera* did not reveal differences between the *cerk1* KO lines and the WT. Experiments with this generalist herbivore

are often conducted with the first instar stage on young seedlings with soft leaves (Johnson and Zalucki, 2005; Sharma et al., 2005). Here, the poplar leaves were mature and covered by leaf hairs, which was not a proper diet for the larvae since some lost weight compared to the start. Due to time constraints, the establishment of the conditions for feeding experiments was not possible.

Although the overall performance of the *cerk1* KO lines was unaffected compared with the WT, some differences were observed. In all experiments under greenhouse conditions, only the *cerk1* KO plants and not the WT developed small red spots on the leaves (Figure 25). Red leaves are often associated with higher contents of anthocyanin (van den Berg and Perkins, 2005). Anthocyanin accumulation is a response to various stresses, including nutrient availability (Liang and He, 2018) or high light and UV stress (Merzlyak and Chivkunova, 2000). Since the red spots were small and occurred irregularly on the leaves, the anthocyanin index of the leaves of *cerk1* KO plants was not elevated compared to WT. Local pigment accumulations have been associated with plant stress (Petrussa et al., 2013). Whether the *cerk1* KO plants experience higher stress than WT plants under greenhouse conditions while interacting with microbes or whether the speckles occur spontaneously should be clarified in future studies.

A further interesting difference between the WT and the *cerk1* KO lines was observed for *L. bicolor* colonization in the greenhouse. *L. bicolor*-treated *cerk1* KO plants had a lower mycorrhization rate than WT plants (Figure 27). This observation suggests that CERK1 takes part in establishing the EMF symbiosis, similarly as reported for rice OsCERK1, which is involved in arbuscular mycorrhiza establishment (Huang et al., 2020). Once the symbiosis was established, mantle and Hartig net structures were present (Figure 28). Further experiments determining the time course of mycorrhization of the *cerk1* KO lines and systematic studies examining the mantle thickness and depth of the Hartig net would be interesting and are required to better understand the plant´s components involved in EMF formation.

5.2.2. Loss of function of CERK1 yields reduced *KTI* and *MLP423* transcript abundances in EMF-exposed plants

A critical experiment is to test the role of CERK1 in systemic defense by EMF. As a marker for the defense induction, the transcript abundances of *KTI* and *MLP423* in *P.* × *canescens* leaves were measured (Figure 32). In WT plants, the transcript abundances of both genes were significantly increased, while transcript abundances of *KTI* and MLP423 were less increased in *cerk1* KO plants after *L. bicolor* treatment. These findings may suggest that CERK1 is a part of the signaling processes involved in systemic defense induction. A potential mechanism could be that CERK1 participates in mycorrhiza formation in poplar and that delayed colonization of *cerk1* also delayed the KTI defense response. The fact that KTI induction was not entirely abolished indicates that additional signaling pathways were involved in mounting EMF systemic responses. This might have been expected since the interaction of crop plants with arbuscular mycorrhiza required additional receptors to CERK1 (Gutjahr et al., 2015; Maillet et al., 2020).

Cerk1 line 19 showed less transcript reduction after *L. bicolor* treatment than *cerk1* line 20. This may have several reasons. For instance, the variation between the experiments was high and different numbers of replicates were available (line 19, five experiments, line 20, three experiments, each with six plants). Further, the editing events in the *cerk1* KO lines 19 and 20 are different and chimeric (Supplemental Table 1).

In contrast to KTI, the *MLP423* transcript abundance did not differ between the non-inoculated and *L. bicolor*-treated WT plants after 14 days. *MLP423* is a stress-responsive gene (Song et al., 2020; Yuan et al., 2020), and it is possible that the observed induction by *L. bicolor* after one week disappears when the mycorrhization is fully established.

In this thesis, the focus was on systemic effects induced by *L. bicolor* in leaves. It would be very interesting to investigate the responses in WT and *cerk1* KO roots to *L. bicolor*. Thereby, it would be possible to test if CERK1 was required to trigger the common defenses in roots during the initial phase of mycorrhization. Even though the experiments have considerable variation, the data suggest that CERK1 participates but is probably not the only component to modulate systemic ectomycorrhizal defense changes.

5.2.3. Chitin likely plays no role in ectomycorrhizal systemic effects

In a previous study, chitin supplied to the soil was sufficient to induce a systemic response in *Arabidopsis* leaves, which eventually had a negative effect on the fitness of leaf-feeding herbivores (Vishwanathan et al., 2020). In the present thesis, *KTI* and *MLP423* were used as markers for EMF-induced systemic effects. Neither chitin nor heat-killed *L. bicolor* caused significant increases in the transcript levels of *KTI* after root application to poplars grown under greenhouse conditions. Heat-killed *L. bicolor* caused elevated *MLP423* average transcript abundance (Figure 35). This could indicate that this preparation contained components that can induce certain genes systemically. There is no evidence for a direct effect of secreted *L. bicolor* proteins because the supernatant from *L. bicolor* cultures did not induce *MLP423* or *KTI* transcript abundances. If a protein induces systemic effects, it may be only induced during symbiosis development with the plant, as shown for small secreted proteins of *L. bicolor* (Martin et al., 2016; Ruytinx et al., 2021).

The greenhouse experiments described here are suitable for analyzing the effects in a biological context and estimating whether the observed effects can be biologically relevant. Axenic conditions are suitable for studying signaling and induction of pathways because disturbances that could influence these events are minimized. Therefore, the chitin responses were tested in an axenic setup. Under these conditions, *MLP* and *KTI* transcript abundances varied over time, but there was no significant change in transcript abundance after chitin treatment, regardless of the amount of chitin applied (Figure 37 & Figure 38). Unexpectedly, after longer time periods of chitin exposure (one day), the level of KTI in leaves was decreased compared with untreated controls. This observation was surprising since chitin is used in agriculture to improve plant resistance against various biological threats (Sharp, 2013). Furthermore, chitin agar, similar to the agar used in this study, affected growth and triggered an immune response in *Physcomitrium patens* (Galotto et al., 2020). However, there is evidence that chitin also causes decreases in gene expression, for instance, transcription factors and ubiquitin ligases in *Arabidopsis* (Libault et al., 2007). It cannot be ruled out that the chitin application to the root elicits local responses in poplar roots, which differentially affect gene expression in systemic tissues. It is recommended that future studies should check for signs of chitin perception, like callose deposition in the roots (Millet et al., 2010), and analyze defense genes and metabolites in roots. It was reported that, e.g., in tomatoes, chitin-related components can induce jasmonate signaling and accumulation (Bohland et al., 1997;

Doares et al., 1995; Sharp, 2013). In this study, exposure to increasing amounts of chitin did not induce *AOS* transcription in leaves (Figure 38). Since *AOS* was not induced, probably no jasmonates accumulated, which could explain why there was no increased *KTI* transcript abundance.

The results show that chitin application to poplar roots may be insufficient for a systemic effect. This observation adds to the finding from the transcriptome analysis that a certain degree of colonization might be necessary to change leaf transcript abundances. Another possibility is that not chitin but related compounds such as LCOs are required to induce the systemic effects. In *Arabidopsis*, chitin is sensed by *At*CERK1 together with the coreceptors *At*LYK4 and *At*LYK5 (LYSM-CONTAINING RECEPTOR-LIKE KINASE). LYK receptors also recognize lipochitooligosaccharides (LCO) in most land plants (Choi et al., 2018; MacLean et al., 2017). LCO and chitin oligomers are part of Myc factors, which are used by arbuscular mycorrhizas for communication with their host (Maillet et al., 2011; Sun et al., 2015). In poplar, LCO produced by *L. bicolor* and other EMF also activate the common symbiosis pathway (Cope et al., 2021, 2019). The common symbiosis pathway is involved in symbiosis development by AMF and rhizobia and uses calcium spiking as a secondary messenger (Oldroyd, 2013). Silencing components of the common symbiosis pathway in poplar reduced colonization by *L. bicolor* (Cope et al., 2019). Possibly not chitin, but LCO derived from EMF are the component inducing systemic effects in poplar.

However, it cannot be ruled out that chitin influences the defense against insects without inducing KTI or MPL. Therefore, transcriptome analysis can help to assess whether chitin can induce responses in systemic leaves. Although each of the chitin treatments was not repeated independently, together, three experimental approaches had similar outcomes, thus, making it unlikely that KTI is triggered in systemic leaves in response to chitin. Whether soil treatment with chitin can affect insect fitness requires experiments.

Summarized, the results of this thesis indicate that CERK1 participates in modulating systemic mycorrhizal defense signaling, but chitin is unlikely to be sufficient for the systemic effect. In addition, CERK1 in poplar could be involved in symbiosis formation.

5.3. *L. bicolor* increases susceptibility to *B. cinerea*

The systemic defense elicited by EMF has mainly been reported to be effective against insects (Dreischhoff et al., 2020). One study reported increased susceptibility to foliar necrotizing pathogens in ectomycorrhizal Norway spruce (Velmala et al., 2018). The defense against insects, modulated by ABA, is antagonistic to the defense against necrotizing pathogens, which is modulated by ethylene (Pieterse et al., 2012). The transcriptome analysis of this thesis revealed that *L. bicolor* influences transcript levels of ethylene biosynthesis and signaling in systemic leaves, but the consequences of these alterations are unknown. Therefore, a pathogen bioassay was established (Dreischhoff et al., under revision, chapter 4.3), and this assay was applied to test the response of *L. bicolor*-treated WT and *cerk1* KO poplars to the necrotizing fungus *B. cinerea.* Since the bioassay was only available at the end of this thesis, just a few preliminary experiments could be performed.

Knockout of *cerk1* did not affect the symptoms of *B. cinerea* in comparison with the WT (Figure 40 & Figure 41). At first sight, it might be unintuitive that the *cerk1* KO poplar lines did not develop more severe symptoms and accumulate more fungal DNA than WT despite a missing receptor for fungal components. However, the *B. cinerea* strain used in this study is living as an endophyte in poplar, most of the time not causing any symptoms. This behavior has been described before for other *B. cinerea* isolates (van Kan et al., 2014). When the fungus lives endophytically, it must overcome the host defenses to colonize the plants, potentially evading CERK1 recognition. The existence of such a mechanism was shown for other endophytic fungal species (Lahrmann and Zuccaro, 2012; Mattoo and Nonzom, 2021). In addition, in the original publication where *At*CERK1 was described for the first time, Miya et al. (2007) used the necrotizing fungus *Alternaria brassicicola* to characterize the mutant. In their experiments, the difference in lesion size on *Atcerk1* KO was significant compared with the WT plants, but the values show that the absolute difference was small. It might be that the effect of *cerk1* KO is also small and, thus, may not be detectable under the environmental conditions in the greenhouse where these experiments were conducted. *B. cinerea* colonization and symptom development varied among independent experiments (Dreischhoff et al. under revision, chapter 5.3). In the experiments with the cerk1 lines reported here, the infection (Figure 40) was not very strong, which may preclude the detection of moderate differences in fungal growth (compare 4.3).

Further, the impact of mycorrhizal colonization on the development of *B. cinerea* infections was assessed (Figure 40 & Figure 41). When mycorrhizal WT and *cerk1* KO 19 poplars were inoculated with *B. cinerea*, no direct effect of mycorrhization on the necrotic area and *B. cinerea* DNA was observed (Figure 41), but a weak correlation of necrotic area and mycorrhization rate was noticeable (Figure 42). This trend was also observed when WT poplars were inoculated with *B. cinerea* in axenic conditions (Figure 43). This finding resembles the observation that ectomycorrhizal Norway spruce was also more susceptible to necrotizing pathogens than non-mycorrhizal spruce (Velmala et al., 2018). The results of this thesis may indicate a shift in the balance between insect and necrotizing pathogen defense, which is mediated by ABA (Pieterse et al., 2012). There are indications that ABA is locally essential for establishing ectomycorrhizal symbiosis (Abdulsalam et al., 2021; Hill et al., 2022; Jin et al., 2019). ABA metabolism in leaves may be affected under these conditions because Kaling et al. (2018) found increased transcript abundance for genes involved in ABA-mediated signaling pathways in the leaves of ectomycorrhizal poplar. If EMF systemically induce ABA-modulated defenses, it would explain why EMF-treated poplars are more susceptible to the necrotizing pathogen *B. cinerea*.

Overall, the experiments provide only initial evidence about the performance of *B. cinerea* on leaves of ectomycorrhizal poplars. They suggest that *L. bicolor* does not induce resistance but increases the susceptibility toward *B. cinerea* infection. It could be speculated that the induction of ABA-dependent signaling caused this effect. These preliminary data need to be validated by further repetitions of the infection experiments. If it is possible to validate the increased susceptibility of mycorrhizal poplar, transcriptome, and metabolome, studies of *B. cinerea*-infected mycorrhizal poplar can give insights into the processes which change in mycorrhizal poplar upon infection.

5.4. Conclusion and outlook

The phenomenon of ectomycorrhizal defense induction against insects has frequently been reported (Dreischhoff et al., 2020), but the systemic processes leading to the defense are still elusive. This thesis aimed to contribute to understanding the systemic effects in poplar leaves that occur in response to mycorrhizal root colonization with *L. bicolor.*

Summarized, the findings of this study show that early on, *L. bicolor* rewrites the transcriptional program in systemic tissues. A certain degree of colonization seems necessary to achieve the systemic changes because changes in the leaf transcriptome were only observed after four days, when EMF usually start to penetrate the root (Ruytinx et al., 2021; Wong et al., 1990). It would be interesting to trace the transcriptional profile of leaves further over time because, in roots, the pattern of transcript abundances changes throughout the symbiosis development (Duplessis et al., 2005; Felten et al., 2009; Le Quéré et al., 2005). Different gene induction patterns could explain the variability of the results of this thesis.

The induction of JA-dependent signaling processes potentially leads to cell wall remodeling and terpenoid biosynthesis, which may act as systemic signals for ectomycorrhizal defense induction similar to signaling through sesquiterpenes in roots (Ditengou et al., 2015). The involvement of other phytohormones besides JA is unclear. Positive and negative regulators of ethylene signaling had increased transcript abundances. Furthermore, components of SAR were involved. This adds to the conception that EMF induce various components of known defense signaling pathways (Figure 44). Even though EMF-induced defense has mainly been reported for insects (Dreischhoff et al., 2020) and the defense against insects is modulated by ABA (Pieterse et al., 2012), no ABA-signaling elements were found in the transcriptome analysis. However, the trend of increased susceptibility of EMF-treated poplar to *B. cinerea* could indicate involvement of ABA signaling.

This thesis demonstrates the experimental challenges when working simultaneously with mycorrhizal fungi, plants, and foliar pests (herbivores, fungal pathogens). Therefore, marker genes are a valuable tool for getting an easy read-out for responses to certain stimuli. Marker genes are widely used to study signaling processes in response to phytohormones, especially the SA-JA antagonism (Beyer et al., 2021; Thaler et al., 2012; Ullah et al., 2022). Here, the transcriptome analysis revealed *KTI* and *MLP423* to be involved in systemic effects induced by EMF. However, their expression levels were variable and not always induced in mycorrhizal

plants, which renders them unsuitable as marker genes. Although they cannot be used to report ectomycorrhizal defense induction, the role of KTI and MLP423 in EMF-induced defense should be clarified. Chitin did not cause transcript abundance changes in KTI and MLP423.

However, the chitin receptor CERK1 is likely involved in the induction of mycorrhizal defense since *KTI,* and *MLP423* transcript abundances were reduced in *cerk1* KO lines. Since the increase in the transcript abundances after *L. bicolor* treatment was not completely abolished, it is likely that other components besides CERK1 play a role. Experiments with insects on mycorrhizal *cerk1* KO poplars similar to the experiments by Kaling et al. (2018) and utilizing the newly developed bioassay for poplar with *B. cinerea* are vital for examining the role of CERK1 in establishing a mycorrhiza-induced resistance and validating the findings of this study. Furthermore, it is necessary to study other potential components besides and downstream of CERK1 in roots and systemic tissues to trace the signal transduction pathway to systemic tissues. Furthermore, the role of CERK1 in mycorrhiza development, as shown for AMF symbiosis (Miyata et al., 2014), needs to be assessed because a reduction in mycorrhizae could explain the reduced systemic effects in *KTI* and *MLP* transcript abundances. As vital as finding plant components inducing the systemic effects is, finding the fungal signals required for the systemic effect is necessary. Other components, such as small secreted proteins or LCO produced by *L. bicolor*, could be initial signals that induce the systemic effect. Disentangling the signaling processes involved in systemic ectomycorrhizal defense induction and the initial signal can open new breeding or plant protection opportunities in the face of climate change.

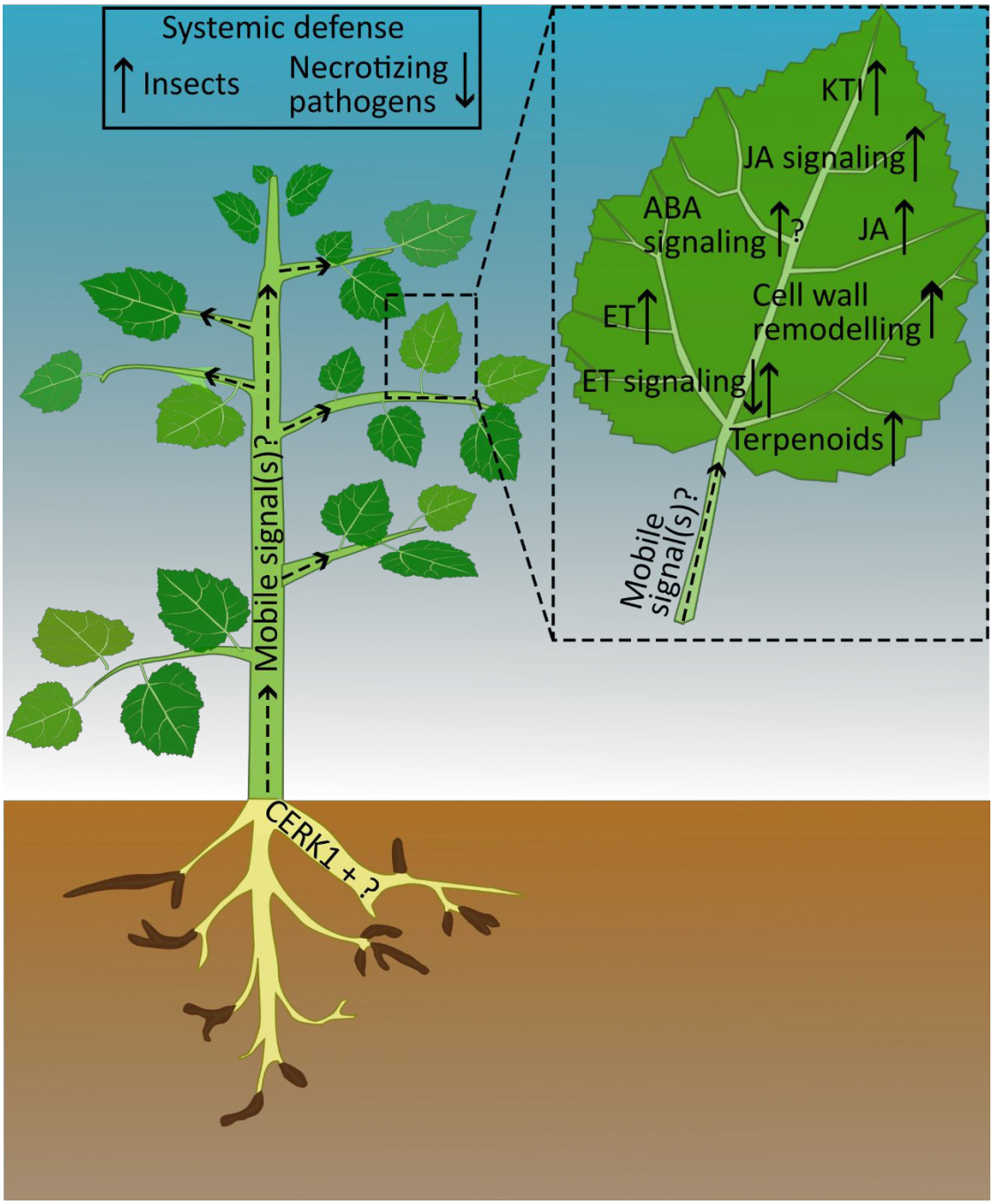

Figure 44 Defense-related processes affected by *L. bicolor* described in this study
Schematic figure of an ectomycorrhizal plant. CERK1 is involved in the systemic effects of ectomycorrhiza colonization, but there are probably additional components necessary. Subsequently, there must be signal(s) that travel in the plant to systemic tissues and induce various processes in leaves. These processes are depicted in the enlarged leaf on the right. As a result of these processes, systemic defenses against insects are increased, and defenses against necrotizing pathogens are decreased (box on top). Upward arrows indicate an increase and downward arrows indicate a decrease. Dashed lines and question marks indicate speculative relationships. ABA = Abscisic acid, CERK1 = CHITIN ELICITOR RECEPTOR KINASE 1, ET = Ethylene, JA = Jasmonic acid, KTI = Kunitz trypsin inhibitor.

6. References

Abdulsalam, O., Wagner, K., Wirth, S., Kunert, M., David, A., Kallenbach, M., Boland, W., Kothe, E., Krause, K., 2021. Phytohormones and volatile organic compounds, like geosmin, in the ectomycorrhiza of *Tricholoma vaccinum* and Norway spruce (*Picea abies*). Mycorrhiza 31, 173–188. https://doi.org/10.1007/s00572-020-01005-2

Adams, Z.P., Ehlting, J., Edwards, R., 2019. The regulatory role of shikimate in plant phenylalanine metabolism. J. Theor. Biol. 462, 158–170. https://doi.org/10.1016/j.jtbi.2018.11.005

Adolfsson, L., Nziengui, H., Abreu, I.N., Šimura, J., Beebo, A., Herdean, A., Aboalizadeh, J., Široká, J., Moritz, T., Novák, O., Ljung, K., Schoefs, B., Spetea, C., 2017. Enhanced secondary- and hormone metabolism in leaves of arbuscular mycorrhizal *Medicago truncatula*. Plant Physiol. 175, 392–411. https://doi.org/10.1104/pp.16.01509

Albrecht, C., Asselin, A., Piché, Y., Lapeyrie, F., 1994a. Chitinase activities are induced in *Eucalyptus globulus* roots by ectomycorrhizal or pathogenic fungi, during early colonization. Physiol. Plant. 91, 104–110. https://doi.org/10.1111/j.1399-3054.1994.tb00665.x

Albrecht, C., Burgess, T., Dell, B., Lapeyrie, F., 1994b. Chitinase and peroxidase activities are induced in eucalyptus roots according to aggressiveness of Australian ectomycorrhizal strains of *Pisolithus* sp. New Phytol. 127, 217–222. https://doi.org/10.1111/j.1469-8137.1994.tb04273.x

Albrecht, C., Laurent, P., Lapeyrie, F., 1994c. Eucalyptus root and shoot chitinases, induced following root colonization by pathogenic versus ectomycorrhizal fungi, compared on one- and two-dimensional activity gels. Plant Sci. 100, 157–164. https://doi.org/10.1016/0168-9452(94)90071-X

Alencar de Barros, K.M., Sardi, J. de C.O., Maria-Neto, S., Macedo, A.J., Ramalho, S.R., Lourenço de Oliveira, D.G., Pontes, G.S., Weber, S.S., Ramalho de Oliveira, C.F., Macedo, M.L.R., 2021. A new Kunitz trypsin inhibitor from *Erythrina poeppigiana* exhibits antimicrobial and antibiofilm properties against bacteria. Biomed. Pharmacother. 144, 112198. https://doi.org/10.1016/j.biopha.2021.112198

Almario, J., Fabiańska, I., Saridis, G., Bucher, M., 2022. Unearthing the plant–microbe *quid pro quo* in root associations with beneficial fungi. New Phytol. 234, 1967–1976. https://doi.org/10.1111/nph.18061

Ament, K., Kant, M.R., Sabelis, M.W., Haring, M.A., Schuurink, R.C., 2004. Jasmonic acid is a key regulator of spider mite-induced volatile terpenoid and methyl salicylate emission in tomato. Plant Physiol 135, 2025–2037. https://doi.org/10.1104/pp.104.048694

An, Y., Shen, Y., Wu, L., Zhang, Z., 2006. A change of phenolic acids content in poplar leaves induced by methyl salicylate and methyl jasmonate. J. For. Res. 17, 107–110. https://doi.org/10.1007/s11676-006-0025-1

Andersson-Gunnerås, S., Hellgren, J.M., Björklund, S., Regan, S., Moritz, T., Sundberg, B., 2003. Asymmetric expression of a poplar ACC oxidase controls ethylene production during gravitational induction of tension wood. Plant J. 34, 339–349. https://doi.org/10.1046/j.1365-313X.2003.01727.x

Backer, R., Naidoo, S., van den Berg, N., 2019. The NONEXPRESSOR OF PATHOGENESIS-RELATED GENES 1 (NPR1) and related family: mechanistic insights in plant disease resistance. Front. Plant Sci. 10, 102. https://doi.org/10.3389/fpls.2019.00102

Balestrini, R., Rosso, L.C., Veronico, P., Melillo, M.T., De Luca, F., Fanelli, E., Colagiero, M., di Fossalunga, A.S., Ciancio, A., Pentimone, I., 2019. Transcriptomic responses to water

deficit and nematode infection in mycorrhizal tomato roots. Front. Microbiol. 10, 1807. https://doi.org/10.3389/fmicb.2019.01807

Balint-Kurti, P., 2019. The plant hypersensitive response: concepts, control and consequences. Mol. Plant Pathol. 20, 1163–1178. https://doi.org/10.1111/mpp.12821

Barsoum, M., Sabelleck, B., Spanu, P.D., Panstruga, R., 2019. Rumble in the effector jungle: Candidate effector proteins in interactions of plants with powdery mildew and rust fungi. Crit. Rev. Plant Sci. 38, 255–279. https://doi.org/10.1080/07352689.2019.1653514

Basso, V., Kohler, A., Miyauchi, S., Singan, V., Guinet, F., Šimura, J., Novák, O., Barry, K.W., Amirebrahimi, M., Block, J., Daguerre, Y., Na, H., Grigoriev, I.V., Martin, F., Veneault-Fourrey, C., 2020. An ectomycorrhizal fungus alters sensitivity to jasmonate, salicylate, gibberellin, and ethylene in host roots. Plant Cell Environ. 43, 1047–1068. https://doi.org/10.1111/pce.13702

Bates, D., Mächler, M., Bolker, B., Walker, S., 2015. Fitting linear mixed-effects models using lme4. J. Stat. Softw. 67, 1–48. https://doi.org/10.18637/jss.v067.i01

Baum, C., Toljander, Y.K., Eckhardt, K.-U., Weih, M., 2009. The significance of host-fungus combinations in ectomycorrhizal symbioses for the chemical quality of willow foliage. Plant Soil 323, 213–224. https://doi.org/10.1007/s11104-009-9928-x

Beckers, G.J.M., Jaskiewicz, M., Liu, Y., Underwood, W.R., He, S.Y., Zhang, S., Conrath, U., 2009. Mitogen-activated protein kinases 3 and 6 are required for full priming of stress responses in *Arabidopsis thaliana*. Plant Cell 21, 944–953. https://doi.org/10.1105/tpc.108.062158

Begheldo, M., Nonis, A., Trevisan, S., Ruperti, B., Quaggiotti, S., 2015. The dynamic regulation of microRNAs circuits in plant adaptation to abiotic stresses: a survey on molecular, physiological and methodological aspects. Environ. Exp. Bot., Plant signalling mechanisms in response to the environment 114, 65–79. https://doi.org/10.1016/j.envexpbot.2014.05.011

Benjamini, Y., Hochberg, Y., 1995. Controlling the false discovery rate: a practical and powerful approach to multiple testing. J. R. Stat. Soc. Ser. B Methodol. 57, 289–300. https://doi.org/10.1111/j.2517-6161.1995.tb02031.x

Berardini, T.Z., Reiser, L., Li, D., Mezheritsky, Y., Muller, R., Strait, E., Huala, E., 2015. The *Arabidopsis* information resource: making and mining the "gold standard" annotated reference plant genome. Genesis 53, 474–485. https://doi.org/10.1002/dvg.22877

Beyer, S.F., Bel, P.S., Flors, V., Schultheiss, H., Conrath, U., Langenbach, C.J.G., 2021. Disclosure of salicylic acid and jasmonic acid-responsive genes provides a molecular tool for deciphering stress responses in soybean. Sci. Rep. 11, 20600. https://doi.org/10.1038/s41598-021-00209-6

Bi, K., Liang, Y., Mengiste, T., Sharon, A., 2023. Killing softly: a roadmap of *Botrytis cinerea* pathogenicity. Trends Plant Sci. 28, 211–222. https://doi.org/10.1016/j.tplants.2022.08.024

Boeckler, G.A., Towns, M., Unsicker, S.B., Mellway, R.D., Yip, L., Hilke, I., Gershenzon, J., Constabel, C.P., 2014. Transgenic upregulation of the condensed tannin pathway in poplar leads to a dramatic shift in leaf palatability for two tree-feeding Lepidoptera. J. Chem. Ecol. 40, 150–158. https://doi.org/10.1007/s10886-014-0383-7

Bohland, C., Balkenhohl, T., Loers, G., Feussner, I., Grambow, H.J., 1997. Differential induction of lipoxygenase isoforms in wheat upon treatment with rust fungus elicitor, chitin oligosaccharides, chitosan, and methyl jasmonate. Plant Physiol. 114, 679–685. https://doi.org/10.1104/pp.114.2.679

Boller, T., Felix, G., 2009. A renaissance of elicitors: perception of microbe-associated molecular patterns and danger signals by pattern-recognition receptors. Annu. Rev. Plant Biol. 60, 379–406. https://doi.org/10.1146/annurev.arplant.57.032905.105346

Bolter, C.J., 1993. Methyl jasmonate induces papain inhibitor(s) in tomato leaves. Plant Physiol. 103, 1347–1353. https://doi.org/10.1104/pp.103.4.1347

Bonfante, P., Anca, I.-A., 2009. Plants, mycorrhizal fungi, and bacteria: a network of interactions. Annu. Rev. Microbiol. 63, 363–383. https://doi.org/10.1146/annurev.micro.091208.073504

Bouffaud, M.-L., Herrmann, S., Tarkka, M.T., Bönn, M., Feldhahn, L., Buscot, F., 2020. Oak displays common local but specific distant gene regulation responses to different mycorrhizal fungi. BMC Genomics 21. https://doi.org/10.1186/s12864-020-06806-5

Breitenbach, H.H., Wenig, M., Wittek, F., Jordá, L., Maldonado-Alconada, A.M., Sarioglu, H., Colby, T., Knappe, C., Bichlmeier, M., Pabst, E., 2014. Contrasting roles of the apoplastic aspartyl protease APOPLASTIC, *ENHANCED DISEASE SUSCEPTIBILITY1*-DEPENDENT1 and LEGUME LECTIN-LIKE PROTEIN1 in *Arabidopsis* systemic acquired resistance. Plant Physiol. 165, 791–809. https://doi.org/10.1104/pp.114.239665

Brun, A., Chalot, M., Finlay, R.D., Söderström, B., 1995. Structure and function of the ectomycorrhizal association between *Paxillus involutus* (Batsch) Fr. and *Betula pendula* Roth. New Phytol. 129, 487–493. https://doi.org/10.1111/j.1469-8137.1995.tb04319.x

Brundrett, M.C., 2009. Mycorrhizal associations and other means of nutrition of vascular plants: Understanding the global diversity of host plants by resolving conflicting information and developing reliable means of diagnosis. Plant Soil 320, 37–77. https://doi.org/10.1007/s11104-008-9877-9

Brundrett, M.C., Tedersoo, L., 2018. Evolutionary history of mycorrhizal symbioses and global host plant diversity. New Phytol 220, 1108–1115. https://doi.org/10.1111/nph.14976

Burgess, T., Dell, B., Malajczuk, N., 1996. *In vitro* synthesis of *Pisolithus-Eucalyptus* ectomycorrhizae: synchronization of lateral tip emergence and ectomycorrhizal development. Mycorrhiza 6, 189–196. https://doi.org/10.1007/s005720050125

Büsgen, M., 1918. Biologische Studien mit *Botrytis cinerea*. Flora Allg. Bot. Ztg. 111–112, 606–620. https://doi.org/10.1016/S0367-1615(17)32864-1

Camacho, C., Coulouris, G., Avagyan, V., Ma, N., Papadopoulos, J., Bealer, K., Madden, T.L., 2009. BLAST+: architecture and applications. BMC Bioinformatics 10, 421. https://doi.org/10.1186/1471-2105-10-421

Cameron, D.D., Neal, A.L., van Wees, S.C.M., Ton, J., 2013. Mycorrhiza-induced resistance: more than the sum of its parts? Trends Plant Sci. 18, 539–545. https://doi.org/10.1016/j.tplants.2013.06.004

Cerovic, Z.G., Masdoumier, G., Ghozlen, N.B., Latouche, G., 2012. A new optical leaf-clip meter for simultaneous non-destructive assessment of leaf chlorophyll and epidermal flavonoids. Physiol. Plant. 146, 251–260. https://doi.org/10.1111/j.1399-3054.2012.01639.x

Chaudhry, S., Sidhu, G.P.S., 2022. Climate change regulated abiotic stress mechanisms in plants: a comprehensive review. Plant Cell Rep. 41, 1–31. https://doi.org/10.1007/s00299-021-02759-5

Chen, J.-Y., Dai, X.-F., 2010. Cloning and characterization of the *Gossypium hirsutum* major latex protein gene and functional analysis in *Arabidopsis thaliana*. Planta 231, 861–873. https://doi.org/10.1007/s00425-009-1092-2

Chen, Q., Zhang, R., Li, D., Wang, F., 2021. Integrating transcriptome and coexpression network analyses to characterize salicylic acid- and jasmonic acid-related genes in tolerant poplars infected with rust. Int. J. Mol. Sci. 22, 5001. https://doi.org/10.3390/ijms22095001

Chen, S., Zhou, Y., Chen, Y., Gu, J., 2018. fastp: an ultra-fast all-in-one FASTQ preprocessor. Bioinformatics 34, i884–i890. https://doi.org/10.1093/bioinformatics/bty560

Chen, Y.-C., Holmes, E.C., Rajniak, J., Kim, J.-G., Tang, S., Fischer, C.R., Mudgett, M.B., Sattely, E.S., 2018. *N*-hydroxy-pipecolic acid is a mobile metabolite that induces systemic disease resistance in *Arabidopsis*. Proc. Natl. Acad. Sci. 115, E4920–E4929. https://doi.org/10.1073/pnas.1805291115

Chini, A., Fonseca, S., Fernández, G., Adie, B., Chico, J.M., Lorenzo, O., García-Casado, G., López-Vidriero, I., Lozano, F.M., Ponce, M.R., Micol, J.L., Solano, R., 2007. The JAZ family of repressors is the missing link in jasmonate signalling. Nature 448, 666–671. https://doi.org/10.1038/nature06006

Choi, J., Summers, W., Paszkowski, U., 2018. Mechanisms underlying establishment of arbuscular mycorrhizal symbioses. Annu. Rev. Phytopathol. 56, 135–160. https://doi.org/10.1146/annurev-phyto-080516-035521

Conrath, U., Beckers, G.J.M., Flors, V., García-Agustín, P., Jakab, G., Mauch, F., Newman, M.-A., Pieterse, C.M.J., Poinssot, B., Pozo, M.J., Pugin, A., Schaffrath, U., Ton, J., Wendehenne, D., Zimmerli, L., Mauch-Mani, B., 2006. Priming: getting ready for battle. MPMI 19, 1062–1071. https://doi.org/10.1094/MPMI-19-1062

Conrath, U., Beckers, G.J.M., Langenbach, C.J.G., Jaskiewicz, M.R., 2015. Priming for enhanced defense. Annu. Rev. Phytopathol. 53, 97–119. https://doi.org/10.1146/annurev-phyto-080614-120132

Cope, K.R., Bascaules, A., Irving, T.B., Venkateshwaran, M., Maeda, J., Garcia, K., Rush, T.A., Ma, C., Labbé, J., Jawdy, S., Steigerwald, E., Setzke, J., Fung, E., Schnell, K.G., Wang, Y., Schleif, N., Bücking, H., Strauss, S.H., Maillet, F., Jargeat, P., Bécard, G., Puech-Pagès, V., Ané, J.-M., 2019. The ectomycorrhizal fungus *Laccaria bicolor* produces lipochitooligosaccharides and uses the common symbiosis pathway to colonize *Populus* roots. Plant Cell 31, 2386–2410. https://doi.org/10.1105/tpc.18.00676

Cope, K.R., Irving, T.B., Chakraborty, S., Ané, J.-M., 2021. Perception of lipo-chitooligosaccharides by the bioenergy crop *Populus*. Plant Signal. Behav. 16, 1903758. https://doi.org/10.1080/15592324.2021.1903758

Cribari-Neto, F., Zeileis, A., 2010. Beta regression in R. J. Stat. Softw. 34, 1–24. https://doi.org/10.18637/jss.v034.i02

Cui, H., Tsuda, K., Parker, J.E., 2015. Effector-triggered immunity: from pathogen perception to robust defense. Annu. Rev. Plant Biol. 66, 487–511. https://doi.org/10.1146/annurev-arplant-050213-040012

de Freitas Pereira, M., Veneault-Fourrey, C., Vion, P., Guinet, F., Morin, E., Barry, K.W., Lipzen, A., Singan, V., Pfister, S., Na, H., Kennedy, M., Egli, S., Grigoriev, I., Martin, F., Kohler, A., Peter, M., 2018. Secretome analysis from the ectomycorrhizal ascomycete *Cenococcum geophilum*. Front. Microbiol. 9, 141. https://doi.org/10.3389/fmicb.2018.00141

De Kesel, J., Conrath, U., Flors, V., Luna, E., Mageroy, M.H., Mauch-Mani, B., Pastor, V., Pozo, M.J., Pieterse, C.M.J., Ton, J., Kyndt, T., 2021. The induced resistance lexicon: do's and don'ts. Trends Plant Sci. 26, 685–691. https://doi.org/10.1016/j.tplants.2021.01.001

de Oliveira, C.F.R., Oliveira, C.T., Taveira, G.B., de Oliveira Mello, E., Gomes, V.M., Macedo, M.L.R., 2018. Characterization of a Kunitz trypsin inhibitor from *Enterolobium*

timbouva with activity against *Candida* species. Int. J. Biol. Macromol. 119, 645–653. https://doi.org/10.1016/j.ijbiomac.2018.07.034

de Sá, C.S.B., Campos, M.A.S., 2020. Arbuscular mycorrhizal fungi decrease *Meloidogyne enterolobii* infection of Guava seedlings. J. Helminthol. 94, e183. https://doi.org/10.1017/S0022149X20000668

Deng, W., Bian, W.P., Xian, Z.Q., Yang, Y.W., Li, Z.G., 2011. Molecular cloning and characterization of a pathogenrelated protein PR10 gene in pyrethrum (*Chrysanthemum cinerariaefolium*) flower response to insect herbivore. Afr. J. Biotechnol. 10, 19514–19521. https://doi.org/10.5897/AJB11.1051

Di Battista, C., Selosse, M.-A., Bouchard, D., Stenström, E., Le Tacon, F., 1996. Variations in symbiotic efficiency, phenotypic characters and ploidy level among different isolates of the ectomycorrhizal basidiomycete *Laccaria bicolor* strain S 238. Mycol. Res. 100, 1315–1324. https://doi.org/10.1016/S0953-7562(96)80058-X

Dievart, A., Gottin, C., Périn, C., Ranwez, V., Chantret, N., 2020. Origin and diversity of plant receptor-like kinases. Annu. Rev. Plant Biol. 71, 131–156. https://doi.org/10.1146/annurev-arplant-073019-025927

Diguta, C.F., Rousseaux, S., Weidmann, S., Bretin, N., Vincent, B., Guilloux-Benatier, M., Alexandre, H., 2010. Development of a qPCR assay for specific quantification of *Botrytis cinerea* on grapes: qPCR detection and quantification of *Botrytis cinerea*. FEMS Microbiol. Lett. 313, 81–87. https://doi.org/10.1111/j.1574-6968.2010.02127.x

Ding, Y., Sun, T., Ao, K., Peng, Y., Zhang, Yaxi, Li, X., Zhang, Yuelin, 2018. Opposite roles of salicylic acid receptors NPR1 and NPR3/NPR4 in transcriptional regulation of plant Immunity. Cell 173, 1454-1467.e15. https://doi.org/10.1016/j.cell.2018.03.044

Ditengou, F.A., Müller, A., Rosenkranz, M., Felten, J., Lasok, H., Doorn, M.M. van, Legué, V., Palme, K., Schnitzler, J.-P., Polle, A., 2015. Volatile signalling by sesquiterpenes from ectomycorrhizal fungi reprogrammes root architecture. Nat. Commun. 6, 1–9. https://doi.org/10.1038/ncomms7279

Divekar, P.A., Rani, V., Majumder, S., Karkute, S.G., Molla, K.A., Pandey, K.K., Behera, T.K., Govindharaj, G.-P.-P., 2022. Protease inhibitors: an induced plant defense mechanism against herbivores. J. Plant Growth Regul. https://doi.org/10.1007/s00344-022-10767-2

Doares, S.H., Syrovets, T., Weiler, E.W., Ryan, C.A., 1995. Oligogalacturonides and chitosan activate plant defensive genes through the octadecanoid pathway. Proc. Natl. Acad. Sci. U. S. A. 92, 4095–4098. https://doi.org/10.1073/pnas.92.10.4095

Doré, J., Perraud, M., Dieryckx, C., Kohler, A., Morin, E., Henrissat, B., Lindquist, E., Zimmermann, S.D., Girard, V., Kuo, A., Grigoriev, I.V., Martin, F., Marmeisse, R., Gay, G., 2015. Comparative genomics, proteomics and transcriptomics give new insight into the exoproteome of the basidiomycete *Hebeloma cylindrosporum* and its involvement in ectomycorrhizal symbiosis. New Phytol. 208, 1169–1187. https://doi.org/10.1111/nph.13546

Dreischhoff, S., Das, I.S., Häffner, F., Wolf, A.M., Polle, A., Kasper, K., under revision. Fast and easy bioassay for the necrotizing fungus *Botrytis cinerea* on poplar leaves.

Dreischhoff, S., Das, I.S., Jakobi, M., Kasper, K., Polle, A., 2020. Local responses and systemic induced resistance mediated by ectomycorrhizal fungi. Front. Plant Sci. 11, 590063. https://doi.org/10.3389/fpls.2020.590063

Duan, Y., Jiang, Y., Ye, S., Karim, A., Ling, Z., He, Y., Yang, S., Luo, K., 2015. PtrWRKY73, a salicylic acid-inducible poplar WRKY transcription factor, is involved in disease resistance in

Arabidopsis thaliana. Plant Cell Rep. 34, 831–841. https://doi.org/10.1007/s00299-015-1745-5

Duplessis, S., Courty, P.-E., Tagu, D., Martin, F., 2005. Transcript patterns associated with ectomycorrhiza development in *Eucalyptus globulus* and *Pisolithus microcarpus*. New Phytol. 165, 599–611. https://doi.org/10.1111/j.1469-8137.2004.01248.x

Duplessis, S., Major, I., Martin, F., Séguin, A., 2009. Poplar and pathogen interactions: insights from *Populus* genome-wide analyses of resistance and defense gene families and gene expression profiling. Crit. Rev. Plant Sci. 28, 309–334. https://doi.org/10.1080/07352680903241063

Durrant, W.E., Dong, X., 2004. Systemic acquired resistance. Annu. Rev. Phytopathol. 42, 185–209. https://doi.org/10.1146/annurev.phyto.42.040803.140421

Eimil-Fraga, C., Proupín-Castiñeiras, X., Rodríguez-Añón, J.A., Rodríguez-Soalleiro, R., 2019. Effects of shoot size and genotype on energy properties of poplar biomass in short rotation crops. Energies 12, 2051. https://doi.org/10.3390/en12112051

Elad, Y., Pertot, I., 2014. Climate change impacts on plant pathogens and plant diseases. J. Crop Improv. 28, 99–139. https://doi.org/10.1080/15427528.2014.865412

Farmer, E.E., Ryan, C.A., 1990. Interplant communication: airborne methyl jasmonate induces synthesis of proteinase inhibitors in plant leaves. Proc. Natl. Acad. Sci. 87, 7713–7716. https://doi.org/10.1073/pnas.87.19.7713

Felix, G., Duran, J.D., Volko, S., Boller, T., 1999. Plants have a sensitive perception system for the most conserved domain of bacterial flagellin. Plant J. 18, 265–276. https://doi.org/10.1046/j.1365-313X.1999.00265.x

Felix, G., Regenass, M., Boller, T., 1993. Specific perception of subnanomolar concentrations of chitin fragments by tomato cells: induction of extracellular alkalinization, changes in protein phosphorylation, and establishment of a refractory state. Plant J. 4, 307–316. https://doi.org/10.1046/j.1365-313X.1993.04020307.x

Felten, J., Kohler, A., Morin, E., Bhalerao, R.P., Palme, K., Martin, F., Ditengou, F.A., Legué, V., 2009. The ectomycorrhizal fungus *Laccaria bicolor* stimulates lateral root formation in poplar and *Arabidopsis* through auxin transport and signaling. Plant Physiol. 151, 1991–2005. https://doi.org/10.1104/pp.109.147231

Fernández, I., Cosme, M., Stringlis, I.A., Yu, K., de Jonge, R., Van Wees, S.C.M., Pozo, M.J., Pieterse, C.M.J., van der Heijden, M.G.A., 2019. Molecular dialogue between arbuscular mycorrhizal fungi and the nonhost plant *Arabidopsis thaliana* switches from initial detection to antagonism. New Phytol. 223, 867–881. https://doi.org/10.1111/nph.15798

Feys, B.J., Benedetti, C.E., Penfold, C.N., Turner, J.G., 1994. *Arabidopsis* mutants selected for resistance to the phytotoxin coronatine are male sterile, insensitive to methyl jasmonate, and resistant to a bacterial pathogen. Plant Cell 6, 751–759. https://doi.org/10.1105/tpc.6.5.751

Figueroa-Macías, J.P., García, Y.C., Núñez, M., Díaz, K., Olea, A.F., Espinoza, L., 2021. Plant growth-defense trade-offs: molecular processes leading to physiological changes. Int. J. Mol. Sci. 22, 693. https://doi.org/10.3390/ijms22020693

Fontana, A., Reichelt, M., Hempel, S., Gershenzon, J., Unsicker, S.B., 2009. The effects of arbuscular mycorrhizal fungi on direct and indirect defense metabolites of *Plantago lanceolata* L. J Chem Ecol 35, 833–843. https://doi.org/10.1007/s10886-009-9654-0

Fox, J., Weisberg, S., 2019. An R companion to applied regression, Third edition. Sage, Thousand Oaks. https://socialsciences.mcmaster.ca/jfox/Books/Companion/.

Foyer, C.H., Noctor, G., 2005. Oxidant and antioxidant signalling in plants: a re-evaluation of the concept of oxidative stress in a physiological context. Plant Cell Environ. 28, 1056–1071. https://doi.org/10.1111/j.1365-3040.2005.01327.x

Frost, C.J., Mescher, M.C., Carlson, J.E., De Moraes, C.M., 2008. Plant defense priming against herbivores: Getting ready for a different battle. Plant Physiol. 146, 818–824. https://doi.org/10.1104/pp.107.113027

Fujita, K., Inui, H., 2021. Biological functions of major latex-like proteins in plants. Plant Sci. 306, 110856. https://doi.org/10.1016/j.plantsci.2021.110856

Gallou, A., Lucero Mosquera, H.P., Cranenbrouck, S., Suárez, J.P., Declerck, S., 2011. Mycorrhiza induced resistance in potato plantlets challenged by *Phytophthora infestans*. Physiol Mol Plant Path 76, 20–26. https://doi.org/10.1016/j.pmpp.2011.06.005

Galotto, G., Abreu, I., Sherman, C., Liu, B., Gonzalez-Guerrero, M., Vidali, L., 2020. Chitin triggers calcium-mediated immune response in the plant model *Physcomitrella patens*. Mol. Plant-Microbe Interactions® 33, 911–920. https://doi.org/10.1094/MPMI-03-20-0064-R

Gange, A.C., West, H.M., 1994. Interactions between arbuscular mycorrhizal fungi and foliar-feeding insects in *Plantago lanceolata* L. New Phytol. 128, 79–87. https://doi.org/10.1111/j.1469-8137.1994.tb03989.x

Garcia, K., Delaux, P.-M., Cope, K.R., Ané, J.-M., 2015. Molecular signals required for the establishment and maintenance of ectomycorrhizal symbioses. New Phytol. 208, 79–87. https://doi.org/10.1111/nph.13423

Genre, A., Lanfranco, L., Perotto, S., Bonfante, P., 2020. Unique and common traits in mycorrhizal symbioses. Nat. Rev. Microbiol. 18, 649–660. https://doi.org/10.1038/s41579-020-0402-3

Gergs, A., Baden, C.U., 2021. A dynamic energy budget approach for the prediction of development times and variability in *Spodoptera frugiperda* rearing. Insects 12, 300. https://doi.org/10.3390/insects12040300

Ghorbanpour, M., Omidvari, M., Abbaszadeh-Dahaji, P., Omidvar, R., Kariman, K., 2018. Mechanisms underlying the protective effects of beneficial fungi against plant diseases. Biol. Control 117, 147–157. https://doi.org/10.1016/j.biocontrol.2017.11.006

Gibelin-Viala, C., Amblard, E., Puech-Pages, V., Bonhomme, M., Garcia, M., Bascaules-Bedin, A., Fliegmann, J., Wen, J., Mysore, K.S., le Signor, C., Jacquet, C., Gough, C., 2019. The *Medicago truncatula* LysM receptor-like kinase LYK9 plays a dual role in immunity and the arbuscular mycorrhizal symbiosis. New Phytol. 223, 1516–1529. https://doi.org/10.1111/nph.15891

Godard, K.-A., White, R., Bohlmann, J., 2008. Monoterpene-induced molecular responses in *Arabidopsis thaliana*. Phytochemistry 69, 1838–1849. https://doi.org/10.1016/j.phytochem.2008.02.011

Gómez-Gómez, L., Bauer, Z., Boller, T., 2001. Both the extracellular leucine-rich repeat domain and the kinase activity of FLS2 are required for flagellin binding and signaling in *Arabidopsis*. Plant Cell 13, 1155–1163. https://doi.org/10.1105/tpc.13.5.1155

Gordon, H., Fellenberg, C., Lackus, N.D., Archinuk, F., Sproule, A., Nakamura, Y., Köllner, T.G., Gershenzon, J., Overy, D.P., Constabel, C.P., 2022. CRISPR/Cas9 disruption of *UGT71L1* in poplar connects salicinoid and salicylic acid metabolism and alters growth and morphology. Plant Cell 34, 2925–2947. https://doi.org/10.1093/plcell/koac135

GraphPad Software, 2022. GraphPad Prism. https://www.graphpad.com

Gutjahr, C., Gobbato, E., Choi, J., Riemann, M., Johnston, M.G., Summers, W., Carbonnel, S., Mansfield, C., Yang, S.-Y., Nadal, M., Acosta, I., Takano, M., Jiao, W.-B., Schneeberger, K., Kelly, K.A., Paszkowski, U., 2015. Rice perception of symbiotic arbuscular mycorrhizal fungi requires the karrikin receptor complex. Science 350, 1521–1524. https://doi.org/10.1126/science.aac9715

Gutsche, N., Thurow, C., Zachgo, S., Gatz, C., 2015. Plant-specific CC-type glutaredoxins: functions in developmental processes and stress responses. Biol. Chem. 396, 495–509. https://doi.org/10.1515/hsz-2014-0300

Hammerbacher, A., Coutinho, T.A., Gershenzon, J., 2019. Roles of plant volatiles in defence against microbial pathogens and microbial exploitation of volatiles. Plant Cell Env. 42, 2827–2843. https://doi.org/10.1111/pce.13602

Hartman, S., Sasidharan, R., Voesenek, L.A.C.J., 2021. The role of ethylene in metabolic acclimations to low oxygen. New Phytol. 229, 64–70. https://doi.org/10.1111/nph.16378

Hartmann, M., Zeier, T., Bernsdorff, F., Reichel-Deland, V., Kim, D., Hohmann, M., Scholten, N., Schuck, S., Bräutigam, A., Hölzel, T., Ganter, C., Zeier, J., 2018. Flavin monooxygenase-generated *N*-hydroxypipecolic acid is a critical element of plant systemic immunity. Cell 173, 456-469.e16. https://doi.org/10.1016/j.cell.2018.02.049

Haruta, M., Major, I.T., Christopher, M.E., Patton, J.J., Constabel, C.P., 2001. A Kunitz trypsin inhibitor gene family from trembling aspen (*Populus tremuloides* Michx.): cloning, functional expression, and induction by wounding and herbivory. Plant Mol. Biol. 46, 347–359. https://doi.org/10.1023/A:1010654711619

Hazard, C., Kruitbos, L., Davidson, H., Mbow, F.T., Taylor, A.F.S., Johnson, D., 2017. Strain identity of the ectomycorrhizal fungus *Laccaria bicolor* Is more important than richness in regulating plant and fungal performance under nutrient rich conditions. Front. Microbiol. 8, 1874. https://doi.org/10.3389/fmicb.2017.01874

Heil, M., Ton, J., 2008. Long-distance signalling in plant defence. Trends Plant Sci. 13, 264–272. https://doi.org/10.1016/j.tplants.2008.03.005

Herrmann, K.M., Weaver, L.M., 1999. The shikimate pathway. Annu. Rev. Plant Biol. 50, 473. https://doi.org/10.1146/annurev.arplant.50.1.473

Hewitt, E.J., 1952. Sand and water culture methods used in the study of plant nutrition., in: Technical communication / Commonwealth Bureau of Horticulture and Plantation Crops. Commonwealth Agricultural Bureaux, Farnham Royal, United Kingdom., pp. 479–534.

Hill, R.A., Wong-Bajracharya, J., Anwar, S., Coles, D., Wang, M., Lipzen, A., Ng, V., Grigoriev, I.V., Martin, F., Anderson, I.C., Cazzonelli, C.I., Jeffries, T., Plett, K.L., Plett, J.M., 2022. Abscisic acid supports colonization of *Eucalyptus grandis* roots by the mutualistic ectomycorrhizal fungus *Pisolithus microcarpus*. New Phytol. 233, 966–982. https://doi.org/10.1111/nph.17825

Hossain, Md.M., Sultana, F., Kubota, M., Hyakumachi, M., 2008. Differential inducible defense mechanisms against bacterial speck pathogen in *Arabidopsis thaliana* by plant-growth-promoting-fungus *Penicillium* sp. GP16-2 and its cell free filtrate. Plant Soil 304, 227–239. https://doi.org/10.1007/s11104-008-9542-3

Hothorn, T., Bretz, F., Westfall, P., 2008. Simultaneous inference in general parametric models. Biom. J. 50, 346–363. https://doi.org/10.1002/bimj.200810425

Hou, S., Tsuda, K., 2022. Salicylic acid and jasmonic acid crosstalk in plant immunity. Essays Biochem. 66, 647–656. https://doi.org/10.1042/EBC20210090

Huang, R., Li, Z., Mao, C., Zhang, H., Sun, Z., Li, H., Huang, C., Feng, Y., Shen, X., Bucher, M., Zhang, Z., Lin, Y., Cao, Y., Duanmu, D., 2020. Natural variation at OsCERK1 regulates arbuscular mycorrhizal symbiosis in rice. New Phytol. 225, 1762–1776. https://doi.org/10.1111/nph.16158

Huang, Y., Li, H., Hutchison, C.E., Laskey, J., Kieber, J.J., 2003. Biochemical and functional analysis of CTR1, a protein kinase that negatively regulates ethylene signaling in *Arabidopsis*. Plant J. 33, 221–233. https://doi.org/10.1046/j.1365-313X.2003.01620.x

Hunter, C., Stewart, J.J., Gleason, S.M., Pilon, M., 2022. Age dependent partitioning patterns of essential nutrients induced by copper feeding status in leaves and stems of poplar. Front. Plant Sci. 13, 930344. https://doi.org/10.3389/fpls.2022.930344

Irmisch, S., McCormick, A.C., Boeckler, G.A., Schmidt, A., Reichelt, M., Schneider, B., Block, K., Schnitzler, J.-P., Gershenzon, J., Unsicker, S.B., Köllner, T.G., 2013. Two herbivore-induced cytochrome P450 Enzymes CYP79D6 and CYP79D7 catalyze the formation of volatile aldoximes involved in poplar defense. Plant Cell 25, 4737–4754. https://doi.org/10.1105/tpc.113.118265

Irmisch, S., McCormick, A.C., Günther, J., Schmidt, A., Boeckler, G.A., Gershenzon, J., Unsicker, S.B., Köllner, T.G., 2014. Herbivore-induced poplar cytochrome P450 enzymes of the CYP71 family convert aldoximes to nitriles which repel a generalist caterpillar. Plant J 80, 1095–1107. https://doi.org/10.1111/tpj.12711

Jakobi, M., 2021. Down-stream molecular responses to volatile signaling in roots (Doctoral thesis). University of Göttingen, Göttingen, Germany. https://doi.org/10.53846/goediss-8610

Jashni, M.K., Mehrabi, R., Collemare, J., Mesarich, C.H., de Wit, P.J.G.M., 2015. The battle in the apoplast: further insights into the roles of proteases and their inhibitors in plant–pathogen interactions. Front. Plant Sci. 6, 584. https://doi.org/10.3389/fpls.2015.00584

Jiang, D., Tan, M., Wu, S., Zheng, L., Wang, Q., Wang, G., Yan, S., 2021. Defense responses of arbuscular mycorrhizal fungus-colonized poplar seedlings against gypsy moth larvae: a multiomics study. Hortic. Res. 8, 245. https://doi.org/10.1038/s41438-021-00671-3

Jin, W., Peng, L., Zhang, X., Sun, H., Yuan, Z., 2019. Effects of endophytic and ectomycorrhizal basidiomycetes on *Quercus virginiana* seedling growth and nutrient absorption. J. Sustain. For. 38, 457–470. https://doi.org/10.1080/10549811.2019.1570467

Johnson, M.-L., Zalucki, M.P., 2005. Foraging behaviour of *Helicoverpa armigera* first instar larvae on crop plants of different developmental stages. J. Appl. Entomol. 129, 239–245. https://doi.org/10.1111/j.1439-0418.2005.00958.x

Jones, J.D.G., Dangl, J.L., 2006. The plant immune system. Nature 444, 323–329. https://doi.org/10.1038/nature05286

Jost, R., Altschmied, L., Bloem, E., Bogs, J., Gershenzon, J., Hähnel, U., Hänsch, R., Hartmann, T., Kopriva, S., Kruse, C., Mendel, R.R., Papenbrock, J., Reichelt, M., Rennenberg, H., Schnug, E., Schmidt, A., Textor, S., Tokuhisa, J., Wachter, A., Wirtz, M., Rausch, T., Hell, R., 2005. Expression profiling of metabolic genes in response to methyl jasmonate reveals regulation of genes of primary and secondary sulfur-related pathways in *Arabidopsis thaliana*. Photosynth. Res. 86, 491–508. https://doi.org/10.1007/s11120-005-7386-8

Journot-Catalino, N., Somssich, I.E., Roby, D., Kroj, T., 2006. The transcription factors WRKY11 and WRKY17 act as negative regulators of basal resistance in *Arabidopsis thaliana*. Plant Cell 18, 3289–3302. https://doi.org/10.1105/tpc.106.044149

Jung, H.W., Tschaplinski, T.J., Wang, L., Glazebrook, J., Greenberg, J.T., 2009. Priming in systemic plant immunity. Science 324, 89–91. https://doi.org/10.1126/science.1170025

Jung, S.C., Martinez-Medina, A., Lopez-Raez, J.A., Pozo, M.J., 2012. Mycorrhiza-induced resistance and priming of plant defenses. J. Chem. Ecol. 38, 651–664. https://doi.org/10.1007/s10886-012-0134-6

Kachroo, A., Kachroo, P., 2007. Salicylic acid-, jasmonic acid-and ethylenemediated regulation of plant defense signaling, in: Genetic Engineering. Springer, Boston, USA, pp. 55-83 https://doi.org/10.1007/978-0-387-34504–8_4.

Kadam, S.B., Pable, A.A., Barvkar, V.T., 2020. Mycorrhiza induced resistance (MIR): a defence developed through synergistic engagement of phytohormones, metabolites and rhizosphere. Funct. Plant Biol. 47, 880–890. https://doi.org/10.1071/FP20035

Kaling, M., Schmidt, A., Moritz, F., Rosenkranz, M., Witting, M., Kasper, K., Janz, D., Schmitt-Kopplin, P., Schnitzler, J.-P., Polle, A., 2018. Mycorrhiza-triggered transcriptomic and metabolomic networks impinge on herbivore fitness. Plant Physiol. 176, 2639–2656. https://doi.org/10.1104/pp.17.01810

Kamble, V.R., Agre, D.G., 2014. New report on AMF colonization in root parasite *Striga gesnerioides* and its host *Lepidagathis hamiltoniana* from high altitude region of Maharashtra. Int. Multidiscip. Res. J. 3, 27–31.

Kanehisa, M., Goto, S., 2000. KEGG: Kyoto Encyclopedia of Genes and Genomes. Nucleic Acids Res. 28, 27–30. https://doi.org/10.1093/nar/28.1.27

Kang, H., Chen, X., Kemppainen, M., Pardo, A.G., Veneault-Fourrey, C., Kohler, A., Martin, F.M., 2020. The small secreted effector protein MiSSP7.6 of *Laccaria bicolor* is required for the establishment of ectomycorrhizal symbiosis. Environ. Microbiol. 1462-2920.14959. https://doi.org/10.1111/1462-2920.14959

Kasper, K., 2020. Impact of nitrogen nutrition and ectomycorrhizal interaction on *Populus x canescens* xylem sap composition and defense (Doctoral thesis). University of Göttingen, Göttingen, Germany. https://doi.org/10.53846/goediss-8259

Kasper, K., Abreu, I.N., Feussner, K., Zienkiewicz, K., Herrfurth, C., Ischebeck, T., Janz, D., Majcherczyk, A., Schmitt, K., Valerius, O., Braus, G.H., Feussner, I., Polle, A., 2022. Multi-omics analysis of xylem sap uncovers dynamic modulation of poplar defenses by ammonium and nitrate. Plant J. 111, 282–303. https://doi.org/10.1111/tpj.15802

Kazan, K., Manners, J.M., 2009. Linking development to defense: auxin in plant–pathogen interactions. Trends Plant Sci. 14, 373–382. https://doi.org/10.1016/j.tplants.2009.04.005

Kebert, M., Kostić, S., Zlatković, M., Stojnic, S., Čapelja, E., Zorić, M., Kiprovski, B., Budakov, D., Orlović, S., 2022. Ectomycorrhizal fungi modulate biochemical response against powdery mildew disease in *Quercus robur* L. Forests 13, 1491. https://doi.org/10.3390/f13091491

Kim, D., Langmead, B., Salzberg, S.L., 2015. HISAT: a fast spliced aligner with low memory requirements. Nat. Methods 12, 357–360. https://doi.org/10.1038/nmeth.3317

Kohout, P., 2017. Biogeography of ericoid mycorrhiza, in: Biogeography of Mycorrhizal Symbiosis, Ecological Studies. Springer International Publishing, Cham, Germany, pp. 179–193. https://doi.org/10.1007/978-3-319-56363-3_9

Kulmann, C., 2005. Lokalisation und Regulation der sauren Invertase in mykorrhizierten Kurzwurzeln (Doctoral thesis). University of Bremen, Bremen, Germany. http://nbn-resolving.de/urn:nbn:de:gbv:46-diss000103255.

Kumar, S., Abedin, M., Singh, A.K., Das, S., 2020. Role of phenolic compounds in plant-defensive mechanisms, in: Plant Phenolics in Sustainable Agriculture. Springer, Singapore, Singapore, pp. 517-532 https://doi.org/10.1007/978-981-15-4890–1_22.

Kunz, W., Schurter, R., Maetzke, T., 1997. The chemistry of benzothiadiazole plant activators. Pestic. Sci. 50, 275–282. https://doi.org/10.1002/(SICI)1096-9063(199708)50:4<275::AID-PS593>3.0.CO;2-7

Labbé, J., Muchero, W., Czarnecki, O., Wang, J., Wang, X., Bryan, A.C., Zheng, K., Yang, Y., Xie, M., Zhang, J., Wang, D., Meidl, P., Wang, H., Morrell-Falvey, J.L., Cope, K.R., Maia, L.G.S., Ané, J.-M., Mewalal, R., Jawdy, S.S., Gunter, L.E., Schackwitz, W., Martin, J., Le Tacon, F., Li, T., Zhang, Z., Ranjan, P., Lindquist, E., Yang, X., Jacobson, D.A., Tschaplinski, T.J., Barry, K., Schmutz, J., Chen, J.-G., Tuskan, G.A., 2019. Mediation of plant–mycorrhizal interaction by a lectin receptor-like kinase. Nat. Plants 5, 676–680. https://doi.org/10.1038/s41477-019-0469-x

Lahrmann, U., Zuccaro, A., 2012. Opprimo ergo sum—evasion and suppression in the root endophytic fungus *Piriformospora indica*. MPMI 25, 727–737. https://doi.org/10.1094/MPMI-11-11-0291

Langenfeld-Heyser, R., Gao, J., Ducic, T., Tachd, Ph., Lu, C.F., Fritz, E., Gafur, A., Polle, A., 2007. *Paxillus involutus* mycorrhiza attenuate NaCl-stress responses in the salt-sensitive hybrid poplar *Populus* × *canescens*. Mycorrhiza 17, 121–131. https://doi.org/10.1007/s00572-006-0084-3

Larrieu, A., Vernoux, T., 2016. Q&A: how does jasmonate signaling enable plants to adapt and survive? BMC Biol. 14, 79. https://doi.org/10.1186/s12915-016-0308-8

Le Marquer, M., Bécard, G., Frei dit Frey, N., 2019. Arbuscular mycorrhizal fungi possess a CLAVATA3/embryo surrounding region-related gene that positively regulates symbiosis. New Phytol. 222, 1030–1042. https://doi.org/10.1111/nph.15643

Le Quéré, A., Wright, D.P., Söderström, B., Tunlid, A., Johansson, T., 2005. Global patterns of gene regulation associated with the development of ectomycorrhiza between birch (*Betula pendula* Roth.) and *Paxillus involutus* (Batsch) Fr. MPMI 18, 659–673. https://doi.org/10.1094/MPMI-18-0659

Lefevere, H., Bauters, L., Gheysen, G., 2020. Salicylic acid biosynthesis in plants. Front. Plant Sci. 11, 338. https://doi.org/10.3389/fpls.2020.00338

Lemoine, M., 1973. Amélioration des peupliers de la section Leuce sur sols hydromorphes (Doctoral thesis). University of Nancy, Nancy, France.

Leple, J.C., Brasileiro, A.C.M., Michel, M.F., Delmotte, F., Jouanin, L., 1992. Transgenic poplars: expression of chimeric genes using four different constructs. Plant Cell Rep. 11, 137–141. https://doi.org/10.1007/BF00232166

Li, C., Xu, M., Cai, X., Han, Z., Si, J., Chen, D., 2022. Jasmonate signaling pathway modulates plant defense, growth, and their trade-offs. Int. J. Mol. Sci. 23, 3945. https://doi.org/10.3390/ijms23073945

Li, J., Brader, G., Kariola, T., Tapio Palva, E., 2006. WRKY70 modulates the selection of signaling pathways in plant defense. Plant J. 46, 477–491. https://doi.org/10.1111/j.1365-313X.2006.02712.x

Li, J., Brader, G., Palva, E.T., 2004. The WRKY70 transcription factor: a node of convergence for jasmonate-mediated and salicylate-mediated signals in plant defense. Plant Cell 16, 319–331. https://doi.org/10.1105/tpc.016980

Li, N., Han, X., Feng, D., Yuan, D., Huang, L.-J., 2019. Signaling crosstalk between salicylic acid and ethylene/jasmonate in plant defense: do we understand what they are whispering? Int. J. Mol. Sci. 20, 671. https://doi.org/10.3390/ijms20030671

Li, Y., Nan, Z., Duan, T., 2019. *Rhizophagus intraradices* promotes alfalfa (*Medicago sativa*) defense against pea aphids (*Acyrthosiphon pisum*) revealed by RNA-seq analysis. Mycorrhiza 29, 623–635. https://doi.org/10.1007/s00572-019-00915-0

Liang, J., He, J., 2018. Protective role of anthocyanins in plants under low nitrogen stress. Biochem. Biophys. Res. Commun. 498, 946–953. https://doi.org/10.1016/j.bbrc.2018.03.087

Liao, Y., Cui, R., Xu, X., Cheng, Q., Li, X., 2020. Jasmonic acid-and ethylene-induced mitochondrial alternative oxidase stimulates *Marssonina brunnea* defense in poplar. Plant Cell Physiol. 61, 2031–2042. https://doi.org/10.1093/pcp/pcaa117

Liao, Y., Smyth, G.K., Shi, W., 2014. featureCounts: an efficient general purpose program for assigning sequence reads to genomic features. Bioinformatics 30, 923–930.

Libault, M., Wan, J., Czechowski, T., Udvardi, M., Stacey, G., 2007. Identification of 118 *Arabidopsis* transcription factor and 30 ubiquitin-ligase genes responding to chitin, a plant-defense elicitor. MPMI 20, 900–911. https://doi.org/10.1094/MPMI-20-8-0900

Liew, O.W., Chong, P.C.J., Li, B., Asundi, A.K., 2008. Signature optical cues: emerging technologies for monitoring plant health. Sensors 8, 3205–3239. https://doi.org/10.3390/s8053205

Ligat, L., Lauber, E., Albenne, C., Clemente, H.S., Valot, B., Zivy, M., Pont-Lezica, R., Arlat, M., Jamet, E., 2011. Analysis of the xylem sap proteome of *Brassica oleracea* reveals a high content in secreted proteins. PROTEOMICS 11, 1798–1813. https://doi.org/10.1002/pmic.201000781

Lin, Z., Zhong, S., Grierson, D., 2009. Recent advances in ethylene research. J. Exp. Bot. 60, 3311–3336. https://doi.org/10.1093/jxb/erp204

Lindroth, R.L., St. Clair, S.B., 2013. Adaptations of quaking aspen (*Populus tremuloides* Michx.) for defense against herbivores. For. Ecol. Manag. 299, 14–21. https://doi.org/10.1016/j.foreco.2012.11.018

Liu, R., Dai, M., Wu, X., Li, M., Liu, X., 2012. Suppression of the root-knot nematode [*Meloidogyne incognita* (Kofoid & White) Chitwood] on tomato by dual inoculation with arbuscular mycorrhizal fungi and plant growth-promoting rhizobacteria. Mycorrhiza 22, 289–296. https://doi.org/10.1007/s00572-011-0397-8

Liu, Y., Sun, T., Sun, Y., Zhang, Y., Radojičić, A., Ding, Y., Tian, H., Huang, X., Lan, J., Chen, S., 2020. Diverse roles of the salicylic acid receptors NPR1 and NPR3/NPR4 in plant immunity. Plant Cell 32, 4002–4016. https://doi.org/in

Lorenzo, O., Piqueras, R., Sánchez-Serrano, J.J., Solano, R., 2003. ETHYLENE RESPONSE FACTOR1 integrates signals from ethylene and jasmonate pathways in plant defense. Plant Cell 15, 165–178. https://doi.org/10.1105/tpc.007468

Loreto, F., Schnitzler, J.-P., 2010. Abiotic stresses and induced BVOCs. Trends Plant Sci. 15, 154–166. https://doi.org/10.1016/j.tplants.2009.12.006

Love, M.I., Huber, W., Anders, S., 2014. Moderated estimation of fold change and dispersion for RNA-seq data with DESeq2. Genome Biol. 15, 550. https://doi.org/10.1186/s13059-014-0550-8

Lugtenberg, B., Kamilova, F., 2009. Plant-growth-promoting rhizobacteria. Annu. Rev. Microbiol. 63, 541–556. https://doi.org/10.1146/annurev.micro.62.081307.162918

Luo, J., Xia, W., Cao, P., Xiao, Z., Zhang, Y., Liu, M., Zhan, C., Wang, N., 2019. Integrated transcriptome analysis reveals plant hormones jasmonic acid and salicylic acid coordinate growth and defense responses upon fungal infection in poplar. Biomolecules 9, 12. https://doi.org/10.3390/biom9010012

Luo, Z.-B., Janz, D., Jiang, X., Goebel, C., Wildhagen, H., Tan, Y., Rennenberg, H., Feussner, I., Polle, A., 2009. Upgrading toot physiology for stress tolerance by ectomycorrhizas: insights from metabolite and transcriptional profiling into reprogramming for stress anticipation. Plant Physiol. 151, 1902–1917. https://doi.org/10.1104/pp.109.143735

Luo, Z.-B., Li, K., Gai, Y., Göbel, C., Wildhagen, H., Jiang, X., Feußner, I., Rennenberg, H., Polle, A., 2011. The ectomycorrhizal fungus (*Paxillus involutus*) modulates leaf physiology of poplar towards improved salt tolerance. Environ. Exp. Bot. 72, 304–311. https://doi.org/10.1016/j.envexpbot.2011.04.008

Lyons, E., Freeling, M., 2008. How to usefully compare homologous plant genes and chromosomes as DNA sequences. Plant J. 53, 661–673. https://doi.org/10.1111/j.1365-313X.2007.03326.x

MacLean, A.M., Bravo, A., Harrison, M.J., 2017. Plant signaling and metabolic pathways enabling arbuscular mycorrhizal symbiosis. Plant Cell 29, 2319–2335. https://doi.org/10.1105/tpc.17.00555

Mader, M., Paslier, M.-C.L., Bounon, R., Bérard, A., Rampant, P.F., Fladung, M., Leplé, J.-C., Kersten, B., 2016. Whole-genome draft assembly of *Populus tremula* x *P. alba* clone INRA 717-1B4. Silvae Genet. 65, 74–79. https://doi.org/10.1515/sg-2016-0019

Maillet, F., Fournier, J., Mendis, H.C., Tadege, M., Wen, J., Ratet, P., Mysore, K.S., Gough, C., Jones, K.M., 2020. *Sinorhizobium meliloti* succinylated high-molecular-weight succinoglycan and the *Medicago truncatula* LysM receptor-like kinase MtLYK10 participate independently in symbiotic infection. Plant J. 102, 311–326. https://doi.org/10.1111/tpj.14625

Maillet, F., Poinsot, V., André, O., Puech-Pagès, V., Haouy, A., Gueunier, M., Cromer, L., Giraudet, D., Formey, D., Niebel, A., Martinez, E.A., Driguez, H., Bécard, G., Dénarié, J., 2011. Fungal lipochitooligosaccharide symbiotic signals in arbuscular mycorrhiza. Nature 469, 58–63. https://doi.org/10.1038/nature09622

Major, I.T., Constabel, C.P., 2008. Functional analysis of the Kunitz trypsin inhibitor family in poplar reveals biochemical diversity and multiplicity in defense against herbivores. Plant Physiol. 146, 888–903. https://doi.org/10.1104/pp.107.106229

Manninen, A.-M., Holopainen, T., Holopainen, J.K., 1998. Susceptibility of ectomycorrhizal and non-mycorrhizal Scots pine (*Pinus sylvestris*) seedlings to a generalist insect herbivore, *Lygus rugulipennis*, at two nitrogen availability levels. New Phytol. 140, 55–63. https://doi.org/10.1046/j.1469-8137.1998.00246.x

Marshall, O.J., 2004. PerlPrimer: cross-platform, graphical primer design for standard, bisulphite and real-time PCR. Bioinforma. Oxf. Engl. 20, 2471–2472. https://doi.org/10.1093/bioinformatics/bth254

Martin, F., Aerts, A., Ahrén, D., Brun, A., Danchin, E.G.J., Duchaussoy, F., Gibon, J., Kohler, A., Lindquist, E., Pereda, V., Salamov, A., Shapiro, H.J., Wuyts, J., Blaudez, D., Buée, M., Brokstein, P., Canbäck, B., Cohen, D., Courty, P.E., Coutinho, P.M., Delaruelle, C., Detter, J.C., Deveau, A., DiFazio, S., Duplessis, S., Fraissinet-Tachet, L., Lucic, E., Frey-Klett, P., Fourrey, C., Feussner, I., Gay, G., Grimwood, J., Hoegger, P.J., Jain, P., Kilaru, S., Labbé, J., Lin, Y.C., Legué, V., Le Tacon, F., Marmeisse, R., Melayah, D., Montanini, B., Muratet, M., Nehls, U., Niculita-Hirzel, H., Secq, M.P.O.-L., Peter, M., Quesneville, H., Rajashekar, B., Reich, M., Rouhier, N., Schmutz, J., Yin, T., Chalot, M., Henrissat, B., Kües, U., Lucas, S., Van de Peer, Y., Podila, G.K., Polle, A., Pukkila, P.J., Richardson, P.M., Rouzé, P., Sanders, I.R., Stajich, J.E., Tunlid, A., Tuskan, G., Grigoriev, I.V., 2008. The genome of *Laccaria bicolor* provides insights into mycorrhizal symbiosis. Nature 452, 88–92. https://doi.org/10.1038/nature06556

Martin, F., Kohler, A., Murat, C., Veneault-Fourrey, C., Hibbett, D.S., 2016. Unearthing the roots of ectomycorrhizal symbioses. Nat. Rev. Microbiol. 14, 760–773. https://doi.org/10.1038/nrmicro.2016.149

Martin, F.M., Harrison, M.J., Lennon, S., Lindahl, B., Öpik, M., Polle, A., Requena, N., Selosse, M.-A., 2018. Cross-scale integration of mycorrhizal function. New Phytol. 220, 941–946. https://doi.org/10.1111/nph.15493

Mathys, J., De Cremer, K., Timmermans, P., Van Kerkhove, S., Lievens, B., Vanhaecke, M., Cammue, B., De Coninck, B., 2012. Genome-Wide Characterization of ISR Induced in *Arabidopsis thaliana* by *Trichoderma hamatum* T382 Against *Botrytis cinerea* Infection. Front. Plant Sci. 3. https://doi.org/10.3389/fpls.2012.00108

Mattoo, A.J., Nonzom, S., 2021. Endophytic fungi: understanding complex cross-talks. Symbiosis 83, 237–264. https://doi.org/10.1007/s13199-020-00744-2

Matzner, E., Khannah, P.K., Meiwes, K.J., Lindheim, M., Prenzel, J., Ulrich, B., 1982. Elementflüsse in Waldökosystemen im Solling — Datendokumentation. Gött. Bodenkd. Berichte. https://pascal-francis.inist.fr/vibad/index.php?action=getRecordDetail&idt=8950691

Mauch-Mani, B., Baccelli, I., Luna, E., Flors, V., 2017. Defense priming: an adaptive part of induced resistance. Annu. Rev. Plant Biol. 68, 485–512. https://doi.org/10.1146/annurev-arplant-042916-041132

McManus, M.T., Burgess, E.P.J., 1995. Effects of the soybean (Kunitz) trypsin inhibitor on growth and digestive proteases of larvae of *Spodoptera litura*. J. Insect Physiol. 41, 731–738. https://doi.org/10.1016/0022-1910(95)00043-T

Merzlyak, M.N., Chivkunova, O.B., 2000. Light-stress-induced pigment changes and evidence for anthocyanin photoprotection in apples. J. Photochem. Photobiol. B 55, 155–163. https://doi.org/10.1016/S1011-1344(00)00042-7

Miedes, E., Vanholme, R., Boerjan, W., Molina, A., 2014. The role of the secondary cell wall in plant resistance to pathogens. Front. Plant Sci. 5, 358. https://doi.org/10.3389/fpls.2014.00358

Millet, Y.A., Danna, C.H., Clay, N.K., Songnuan, W., Simon, M.D., Werck-Reichhart, D., Ausubel, F.M., 2010. Innate immune responses activated in *Arabidopsis* roots by microbe-associated molecular patterns. Plant Cell 22, 973–990. https://doi.org/10.1105/tpc.109.069658

Miransari, M., 2011. Interactions between arbuscular mycorrhizal fungi and soil bacteria. Appl. Microbiol. Biotechnol. 89, 917–930. https://doi.org/10.1007/s00253-010-3004-6

Miya, A., Albert, P., Shinya, T., Desaki, Y., Ichimura, K., Shirasu, K., Narusaka, Y., Kawakami, N., Kaku, H., Shibuya, N., 2007. CERK1, a LysM receptor kinase, is essential for chitin elicitor signaling in *Arabidopsis*. Proc. Natl. Acad. Sci. 104, 19613–19618. https://doi.org/10.1073/pnas.0705147104

Miyata, K., Kozaki, T., Kouzai, Y., Ozawa, K., Ishii, K., Asamizu, E., Okabe, Y., Umehara, Y., Miyamoto, A., Kobae, Y., 2014. The bifunctional plant receptor, OsCERK1, regulates both chitin-triggered immunity and arbuscular mycorrhizal symbiosis in rice. Plant Cell Physiol. 55, 1864–1872. https://doi.org/10.1093/pcp/pcu129

Mohnike, L., Huang, W., Worbs, B., Feussner, K., Zhang, Y., Feussner, I., 2023. *N*-hydroxy pipecolic acid methyl ester is involved in *Arabidopsis* immunity. J. Exp. Bot. 74, 458–471. https://doi.org/10.1093/jxb/erac422

Mohnike, L., Rekhter, D., Huang, W., Feussner, K., Tian, H., Herrfurth, C., Zhang, Y., Feussner, I., 2021. The glycosyltransferase UGT76B1 modulates *N*-hydroxy-pipecolic acid

homeostasis and plant immunity. Plant Cell 33, 735–749. https://doi.org/10.1093/plcell/koaa045

Molina, A., Miedes, E., Bacete, L., Rodríguez, T., Mélida, H., Denancé, N., Sánchez-Vallet, A., Rivière, M.-P., López, G., Freydier, A., Barlet, X., Pattathil, S., Hahn, M., Goffner, D., 2021. *Arabidopsis* cell wall composition determines disease resistance specificity and fitness. Proc. Natl. Acad. Sci. 118, e2010243118. https://doi.org/10.1073/pnas.2010243118

Mueller, G.M., Gardes, M., 1991. Intra- and interspecific relations within *Laccaria bicolor sensu lato*. Mycol. Res. 95, 592–601. https://doi.org/10.1016/S0953-7562(09)80073-7

Muhr, M., 2022. Characterization of *Populus* x *canescens* LysM receptor-like kinases CERK1-1 and CERK1-2 and their role in chitin signaling (Doctoral thesis). University of Göttingen, Germany, Göttingen. https://doi.org/10.53846/goediss-9128

Müller, A., Faubert, P., Hagen, M., zu Castell, W., Polle, A., Schnitzler, J.-P., Rosenkranz, M., 2013a. Volatile profiles of fungi – Chemotyping of species and ecological functions. Fungal Genet. Biol. 54, 25–33. https://doi.org/10.1016/j.fgb.2013.02.005

Müller, A., Volmer, K., Mishra-Knyrim, M., Polle, A., 2013b. Growing poplars for research with and without mycorrhizas. Front. Plant Sci. 4, 332. https://doi.org/10.3389/fpls.2013.00332

Murashige, T., Skoog, F., 1962. A revised medium for rapid growth and bio assays with tobacco tissue cultures. Physiol. Plant. 15, 473–497. https://doi.org/10.1111/j.1399-3054.1962.tb08052.x

Nehls, U., Plassard, C., 2018. Nitrogen and phosphate metabolism in ectomycorrhizas. New Phytol. 220, 1047–1058. https://doi.org/10.1111/nph.15257

Nerg, A.-M., Kasurinen, A., Holopainen, T., Julkunen-Tiitto, R., Neuvonen, S., Holopainen, J.K., 2008. The significance of ectomycorrhizas in chemical quality of silver birch foliage and above-ground insect herbivore performance. J. Chem. Ecol. 34, 1322–1330. https://doi.org/10.1007/s10886-008-9542-z

Nessler, C.L., Allen, R.D., Galewsky, S., 1985. Identification and characterization of latex-specific proteins in opium poppy. Plant Physiol. 79, 499–504. https://doi.org/10.1104/pp.79.2.499

Ngou, B.P.M., Ahn, H.-K., Ding, P., Jones, J.D.G., 2021. Mutual potentiation of plant immunity by cell-surface and intracellular receptors. Nature 592, 110–115. https://doi.org/10.1038/s41586-021-03315-7

Notaguchi, M., Okamoto, S., 2015. Dynamics of long-distance signaling via plant vascular tissues. Front. Plant Sci. 6, 161. https://doi.org/10.3389/fpls.2015.00161

Ohtake, Y., Takahashi, T., Komeda, Y., 2000. Salicylic acid induces the expression of a number of receptor-like kinase genes in *Arabidopsis thaliana*. Plant Cell Physiol. 41, 1038–1044. https://doi.org/10.1093/pcp/pcd028

Okamoto, S., Shinohara, H., Mori, T., Matsubayashi, Y., Kawaguchi, M., 2013. Root-derived CLE glycopeptides control nodulation by direct binding to HAR1 receptor kinase. Nat. Commun. 4, 2191. https://doi.org/10.1038/ncomms3191

Oldroyd, G.E.D., 2013. Speak, friend, and enter: signalling systems that promote beneficial symbiotic associations in plants. Nat. Rev. Microbiol. 11, 252–263. https://doi.org/10.1038/nrmicro2990

Ostin, A., Kowalyczk, M., Bhalerao, R.P., Sandberg, G., 1998. Metabolism of indole-3-acetic acid in *Arabidopsis*. Plant Physiol. 118, 285–296. https://doi.org/10.1104/pp.118.1.285

Papp, N., 2005. Antimicrobial activity of extracts of five Hungarian *Euphorbia* species and some plant metabolits. Acta Bot. Hung. 46, 363–371. https://doi.org/10.1556/abot.46.2004.3-4.8

Park, C.H., Yeo, H.J., Park, Y.E., Chun, S.W., Chung, Y.S., Lee, S.Y., Park, S.U., 2019. Influence of chitosan, salicylic acid and jasmonic acid on phenylpropanoid accumulation in germinated buckwheat (*Fagopyrum esculentum* Moench). Foods 8, 153. https://doi.org/10.3390/foods8050153

Park, S.-W., Kaimoyo, E., Kumar, D., Mosher, S., Klessig, D.F., 2007. Methyl salicylate is a critical mobile signal for plant systemic acquired resistance. Science 318, 113–116. https://doi.org/10.1126/science.1147113

Paschold, A., Halitschke, R., Baldwin, I.T., 2007. Co(i)-ordinating defenses: NaCOI1 mediates herbivore- induced resistance in *Nicotiana attenuata* and reveals the role of herbivore movement in avoiding defenses. Plant J. 51, 79–91. https://doi.org/10.1111/j.1365-313X.2007.03119.x

Pattyn, J., Vaughan-Hirsch, J., Van de Poel, B., 2021. The regulation of ethylene biosynthesis: a complex multilevel control circuitry. New Phytol. 229, 770–782. https://doi.org/10.1111/nph.16873

Pearce, G., Strydom, D., Johnson, S., Ryan, C.A., 1991. A polypeptide from tomato leaves induces wound-inducible proteinase inhibitor proteins. Science 253, 895–897. https://doi.org/10.1126/science.253.5022.895

Petrussa, E., Braidot, E., Zancani, M., Peresson, C., Bertolini, A., Patui, S., Vianello, A., 2013. Plant flavonoids—biosynthesis, transport and involvement in stress responses. Int. J. Mol. Sci. 14, 14950–14973. https://doi.org/10.3390/ijms140714950

Petutschnig, E.K., Jones, A.M.E., Serazetdinova, L., Lipka, U., Lipka, V., 2010. The lysin motif receptor-like kinase (LysM-RLK) CERK1 is a major chitin-binding protein in *Arabidopsis thaliana* and subject to chitin-induced phosphorylation. J. Biol. Chem. 285, 28902–28911. https://doi.org/10.1074/jbc.M110.116657

Pfabel, C., Eckhardt, K.-U., Baum, C., Struck, C., Frey, P., Weih, M., 2012. Impact of ectomycorrhizal colonization and rust infection on the secondary metabolism of poplar (*Populus trichocarpa* × *deltoides*). Tree Physiol. 32, 1357–1364. https://doi.org/10.1093/treephys/tps093

Pfaffl, M.W., 2001. A new mathematical model for relative quantification in real-time RT–PCR. Nucleic Acids Res. 29, e45. https://doi.org/10.1093/nar/29.9.e45

Philippe, R.N., Bohlmann, J., 2007. Poplar defense against insect herbivores. Can. J. Bot. 85, 1111–1126. https://doi.org/10.1139/B07-109

Pieterse, C.M., Zamioudis, C., Berendsen, R.L., Weller, D.M., Van Wees, S.C., Bakker, P.A., 2014a. Induced systemic resistance by beneficial microbes. Annu. Rev. Phytopathol. 52, 347–375. https://doi.org/10.1146/annurev-phyto-082712-102340

Pieterse, C.M., Zamioudis, C., Does, D., Van Wees, S.C., 2014b. Signalling networks involved in induced resistance, in: Induced Resistance for Plant Defense. John Wiley & Sons, New York, USA, pp. 58–80. https://doi.org/10.1002/9781118371848.ch4

Pieterse, C.M.J., Van der Does, D., Zamioudis, C., Leon-Reyes, A., Van Wees, S.C.M., 2012. Hormonal modulation of plant immunity. Annu. Rev. Cell Dev. Biol. 28, 489–521. https://doi.org/10.1146/annurev-cellbio-092910-154055

Pineda, A., Dicke, M., Pieterse, C.M.J., Pozo, M.J., 2013. Beneficial microbes in a changing environment: are they always helping plants to deal with insects? Funct. Ecol. 27, 574–586. https://doi.org/10.1111/1365-2435.12050

Plett, J.M., Martin, F., 2012. Poplar root exudates contain compounds that induce the expression of MiSSP7 in *Laccaria bicolor*. Plant Signal. Behav. 7, 12–15. https://doi.org/10.4161/psb.7.1.18357

Plett, J.M., Tisserant, E., Brun, A., Morin, E., Grigoriev, I.V., Kuo, A., Martin, F., Kohler, A., 2014. The mutualist *Laccaria bicolor* expresses a core gene regulon during the colonization of diverse host plants and a variable regulon to counteract host-specific defenses. MPMI 28, 261–273. https://doi.org/10.1094/MPMI-05-14-0129-FI

Polle, A., Chen, S.L., Eckert, C., Harfouche, A., 2019. Engineering drought resistance in forest trees. Front. Plant Sci. 9, 1875. https://doi.org/10.3389/fpls.2018.01875

Polle, A., Douglas, C., 2010. The molecular physiology of poplars: paving the way for knowledge-based biomass production. Plant Biol. 12, 239–376. https://doi.org/10.1111/j.1438-8677.2009.00318.x

Pozo, M.J., Azcón-Aguilar, C., 2007. Unraveling mycorrhiza-induced resistance. Curr. Opin. Plant Biol. 10, 393–398. https://doi.org/10.1016/j.pbi.2007.05.004

Premathilake, A.T., Ni, J., Shen, J., Bai, S., Teng, Y., 2020. Transcriptome analysis provides new insights into the transcriptional regulation of methyl jasmonate-induced flavonoid biosynthesis in pear calli. BMC Plant Biol. 20, 388. https://doi.org/10.1186/s12870-020-02606-x

Pruitt, R.N., Gust, A.A., Nürnberger, T., 2021. Plant immunity unified. Nat. Plants 7, 382–383. https://doi.org/10.1038/s41477-021-00903-3

Qian, Y., Lynch, J.H., Guo, L., Rhodes, D., Morgan, J.A., Dudareva, N., 2019. Completion of the cytosolic post-chorismate phenylalanine biosynthetic pathway in plants. Nat. Commun. 10, 15. https://doi.org/10.1038/s41467-018-07969-2

R Core Team, 2022. R: a language and environment for statistical computing. https://www.R-project.org/

Reina-Pinto, J.J., Yephremov, A., 2009. Surface lipids and plant defenses. Plant Physiol. Biochem., Plant Lipids 47, 540–549. https://doi.org/10.1016/j.plaphy.2009.01.004

Rennenberg, H., Wildhagen, H., Ehlting, B., 2010. Nitrogen nutrition of poplar trees. Plant Biol. 12, 275–291. https://doi.org/10.1111/j.1438-8677.2009.00309.x

Roca-Couso, R., Flores-Félix, J.D., Rivas, R., 2021. Mechanisms of action of microbial biocontrol agents against *Botrytis cinerea*. J. Fungi 7, 1045. https://doi.org/10.3390/jof7121045

Rosenkranz, M., Shi, H., Ballauff, J., Schnitzler, J.-P., Polle, A., 2022. Reactive oxygen species (ROS) in mycorrhizal fungi and symbiotic interactions with plants, in: Advances in Botanical Research. Academic Press, New York, USA. https://doi.org/10.1016/bs.abr.2022.11.001

Rowen, E., Gutensohn, M., Dudareva, N., Kaplan, I., 2017. Carnivore attractant or plant elicitor? Multifunctional roles of methyl salicylate lures in tomato defense. J. Chem. Ecol. 43, 573–585. https://doi.org/10.1007/s10886-017-0856-6

RStudio Team, 2020. RStudio: integrated Development for R. http://www.rstudio.com/

Ruan, J., Zhou, Y., Zhou, M., Yan, J., Khurshid, M., Weng, W., Cheng, J., Zhang, K., 2019. Jasmonic acid signaling pathway in plants. Int. J. Mol. Sci. 20, 2479. https://doi.org/10.3390/ijms20102479

Ruytinx, J., Miyauchi, S., Hartmann-Wittulsky, S., de Freitas Pereira, M., Guinet, F., Churin, J.-L., Put, C., Le Tacon, F., Veneault-Fourrey, C., Martin, F., Kohler, A., 2021. A transcriptomic atlas of the ectomycorrhizal fungus *Laccaria bicolor*. Microorganisms 9, 2612. https://doi.org/10.3390/microorganisms9122612

Sauter, M., Hager, A., 1989. The mycorrhizal fungus *Amanita muscaria* induces chitinase activity in roots and in suspension-cultured cells of its host *Picea abies*. Planta 179, 61–66. https://doi.org/10.1007/BF00395771

Schachtman, D.P., Goodger, J.Q.D., 2008. Chemical root to shoot signaling under drought. Trends Plant Sci. 13, 281–287. https://doi.org/10.1016/j.tplants.2008.04.003

Schädler, M., Ballhorn, D.J., 2017. Beneficial soil microbiota as mediators of the plant defensive phenotype and aboveground plant-herbivore interactions, in: Progress in Botany. Springer International Publishing, Cham, Germany, pp. 305–343. https://doi.org/10.1007/124_2016_13

Schindelin, J., Arganda-Carreras, I., Frise, E., Kaynig, V., Longair, M., Pietzsch, T., Preibisch, S., Rueden, C., Saalfeld, S., Schmid, B., Tinevez, J.-Y., White, D.J., Hartenstein, V., Eliceiri, K., Tomancak, P., Cardona, A., 2012. Fiji: an open-source platform for biological-image analysis. Nat. Methods 9, 676–682. https://doi.org/10.1038/nmeth.2019

Schoenherr, A.P., Rizzo, E., Jackson, N., Manosalva, P., Gomez, S.K., 2019. Mycorrhiza-induced resistance in potato involves priming of defense responses against cabbage looper (Noctuidae: Lepidoptera). Environ. Entomol. 48, 370–381. https://doi.org/10.1093/ee/nvy195

Schulz-Bohm, K., Martín-Sánchez, L., Garbeva, P., 2017. Microbial nolatiles: small molecules with an important role in intra- and inter-kingdom interactions. Front. Microbiol. 8, 2484. https://doi.org/10.3389/fmicb.2017.02484

Schweiger, R., Baier, M.C., Persicke, M., Müller, C., 2014. High specificity in plant leaf metabolic responses to arbuscular mycorrhiza. Nat. Commun. 5, 3886. https://doi.org/10.1038/ncomms4886

Shabala, S., White, R.G., Djordjevic, M.A., Ruan, Y.-L., Mathesius, U., Shabala, S., White, R.G., Djordjevic, M.A., Ruan, Y.-L., Mathesius, U., 2015. Root-to-shoot signalling: integration of diverse molecules, pathways and functions. Funct. Plant Biol. 43, 87–104. https://doi.org/10.1071/FP15252

Shafiei, F., Shahidi-Noghabi, S., Sedaghati, E., 2022. The impact of arbuscular mycorrhizal fungi on tomato plant resistance against *Tuta absoluta* (Meyrick) in greenhouse conditions. J. Asia-Pac. Entomol. 25, 101971. https://doi.org/10.1016/j.aspen.2022.101971

Shah, J., Zeier, J., 2013. Long-distance communication and signal amplification in systemic acquired resistance. Front. Plant Sci. 4, 30. https://doi.org/10.3389/fpls.2013.00030

Shan, X., Zhang, Y., Peng, W., Wang, Z., Xie, D., 2009. Molecular mechanism for jasmonate-induction of anthocyanin accumulation in *Arabidopsis*. J. Exp. Bot. 60, 3849–3860. https://doi.org/10.1093/jxb/erp223

Sharma, H., Pampapathy, G., Kumar, R., 2005. Standardization of cage techniques to screen chickpeas for resistance to *Helicoverpa armigera* (Lepidoptera: Noctuidae) in greenhouse and field conditions. J. Econ. Entomol. 98, 210–216.

Sharmin, S., Lipka, U., Polle, A., Eckert, C., 2021. The influence of transpiration on foliar accumulation of salt and nutrients under salinity in poplar (*Populus* × *canescens*). PLOS ONE 16, e0253228. https://doi.org/10.1371/journal.pone.0253228

Sharp, R.G., 2013. A review of the applications of chitin and its derivatives in agriculture to modify plant-microbial interactions and improve crop yields. Agronomy 3, 757–793. https://doi.org/10.3390/agronomy3040757

Sheard, L.B., Tan, X., Mao, H., Withers, J., Ben-Nissan, G., Hinds, T.R., Kobayashi, Y., Hsu, F.-F., Sharon, M., Browse, J., He, S.Y., Rizo, J., Howe, G.A., Zheng, N., 2010. Jasmonate perception by inositol-phosphate-potentiated COI1–JAZ co-receptor. Nature 468, 400–405. https://doi.org/10.1038/nature09430

Shi, J., Zhao, B., Jin, R., Hou, L., Zhang, X., Dai, H., Yu, N., Wang, E., 2022. A phosphate starvation response-regulated receptor-like kinase, OsADK1, is required for mycorrhizal symbiosis and phosphate starvation responses. New Phytol. n/a. https://doi.org/10.1111/nph.18546

Shi, W.-G., Li, H., Liu, T.-X., Polle, A., Peng, C.-H., Luo, Z.-B., 2015. Exogenous abscisic acid alleviates zinc uptake and accumulation in *Populus* × *canescens* exposed to excess zinc. Plant Cell Environ. 38, 207–223. https://doi.org/10.1111/pce.12434

Sillo, F., Brunetti, C., Marroni, F., Vita, F., dos Santos Nascimento, L.B., Vizzini, A., Mello, A., Balestrini, R., 2022. Systemic effects of *Tuber melanosporum* inoculation in two *Corylus avellana* genotypes. Tree Physiol. 42, 1463–1480. https://doi.org/10.1093/treephys/tpac012

Sillo, F., Fangel, J.U., Henrissat, B., Faccio, A., Bonfante, P., Martin, F., Willats, W.G.T., Balestrini, R., 2016. Understanding plant cell-wall remodelling during the symbiotic interaction between *Tuber melanosporum* and *Corylus avellana* using a carbohydrate microarray. Planta 244, 347–359. https://doi.org/10.1007/s00425-016-2507-5

Sivaprakasam Padmanaban, P.B., Rosenkranz, M., Zhu, P., Kaling, M., Schmidt, A., Schmitt-Kopplin, P., Polle, A., Schnitzler, J.-P., 2022. Mycorrhiza-tree-herbivore interactions: alterations in poplar metabolome and volatilome. Metabolites 12, 93. https://doi.org/10.3390/metabo12020093

Skibbe, M., Qu, N., Galis, I., Baldwin, I.T., 2008. Induced plant defenses in the natural environment: *Nicotiana attenuata* WRKY3 and WRKY6 coordinate responses to herbivory. Plant Cell 20, 1984–2000. https://doi.org/10.1105/tpc.108.058594

Smith, S.E., Read, D.J., 2008. Mycorrhizal symbiosis. Academic press, New York, USA. https://doi.org/10.1016/B978-0-12-370526-6.X5001-6.

Smithson, M., Verkuilen, J., 2006. A better lemon squeezer? Maximum-likelihood regression with beta-distributed dependent variables. Psychol. Methods 11, 54–71. https://doi.org/10.1037/1082-989X.11.1.54

Song, L., Wang, J., Jia, H., Kamran, A., Qin, Y., Liu, Y., Hao, K., Han, F., Zhang, C., Li, B., Li, Y., Shen, L., Wang, F., Wu, Y., Yang, J., 2020. Identification and functional characterization of NbMLP28, a novel MLP-like protein 28 enhancing potato virus Y resistance in *Nicotiana benthamiana*. BMC Microbiol. 20, 55. https://doi.org/10.1186/s12866-020-01725-7

Song, S., Huang, H., Gao, H., Wang, J., Wu, D., Liu, X., Yang, S., Zhai, Q., Li, C., Qi, T., 2014. Interaction between MYC2 and ETHYLENE INSENSITIVE3 modulates antagonism between jasmonate and ethylene signaling in *Arabidopsis*. Plant Cell 26, 263–279. https://doi.org/10.1105/tpc.113.120394

Song, Y.Y., Ye, M., Li, C.Y., Wang, R.L., Wei, X.C., Luo, S.M., Zeng, R.S., 2013. Priming of anti-herbivore defense in tomato by arbuscular mycorrhizal fungus and involvement of the jasmonate pathway. J. Chem. Ecol. 39, 1036–1044. https://doi.org/10.1007/s10886-013-0312-1

Spoel, S.H., Dong, X., 2012. How do plants achieve immunity? Defence without specialized immune cells. Nat. Rev. Immunol. 12, 89–100. https://doi.org/10.1038/nri3141

Srinivasan, A., Giri, A.P., Harsulkar, A.M., Gatehouse, J.A., Gupta, V.S., 2005. A Kunitz trypsin inhibitor from chickpea (*Cicer arietinum* L.) that exerts anti-metabolic effect on podborer (*Helicoverpa armigera*) larvae. Plant Mol. Biol. 57, 359–374. https://doi.org/10.1007/s11103-004-7925-2

Steinkellner, S., Hage-Ahmed, K., García-Garrido, J.M., Illana, A., Ocampo, J.A., Vierheilig, H., 2012. A comparison of wild-type, old and modern tomato cultivars in the interaction

with the arbuscular mycorrhizal fungus *Glomus mosseae* and the tomato pathogen *Fusarium oxysporum* f. sp. *lycopersici*. Mycorrhiza 22, 189–194. https://doi.org/10.1007/s00572-011-0393-z

Stettler, R.F., 1996. Biology of *Populus* and its implications for management and conservation. NRC Research Press, Ottawa, Canada.

Stimm, B., Weisgerber, H., 2014. *Populus* x *canescens*, in: Enzyklopädie der Holzgewächse: Handbuch und Atlas der Dendrologie. John Wiley & Sons, Ltd, Hoboken, USA, pp. 1–14. https://doi.org/10.1002/9783527678518.ehg2008001

Strijkstra, G.-J., 2021. Modification of lipid biosynthesis in *Populus x canescens* and characterization of transgenic lines (Doctoral thesis). University of Göttingen, Göttingen, Germany. https://doi.org/10.53846/goediss-8459

Suarez, M.B., Walsh, K., Boonham, N., O'Neill, T., Pearson, S., Barker, I., 2005. Development of real-time PCR (TaqMan®) assays for the detection and quantification of *Botrytis cinerea* in planta. Plant Physiol. Biochem. 43, 890–899. https://doi.org/10.1016/j.plaphy.2005.07.003

Sun, J., Miller, J.B., Granqvist, E., Wiley-Kalil, A., Gobbato, E., Maillet, F., Cottaz, S., Samain, E., Venkateshwaran, M., Fort, S., Morris, R.J., Ané, J.-M., Dénarié, J., Oldroyd, G.E.D., 2015. Activation of symbiosis signaling by arbuscular mycorrhizal fungi in legumes and rice. Plant Cell 27, 823–838. https://doi.org/10.1105/tpc.114.131326

Sun, J.-Q., Jiang, H.-L., Li, C.-Y., 2011. Systemin/jasmonate-mediated systemic defense signaling in tomato. Mol. Plant 4, 607–615. https://doi.org/10.1093/mp/ssr008

Sun, T., Zhang, Y., 2021. Short- and long-distance signaling in plant defense. Plant J. 105, 505–517. https://doi.org/10.1111/tpj.15068

Tan, X., Liu, M., Du, N., Zwiazek, J.J., 2021. Ethylene enhances root water transport and aquaporin expression in trembling aspen (*Populus tremuloides*) exposed to root hypoxia. BMC Plant Biol. 21, 227. https://doi.org/10.1186/s12870-021-02995-7

Tao, X., Wu, Q., Li, J., Huang, S., Cai, L., Mao, L., Luo, Z., Li, L., Ying, T., 2022. Exogenous methyl jasmonate regulates phenolic compounds biosynthesis during postharvest tomato ripening. Postharvest Biol. Technol. 184, 111760. https://doi.org/10.1016/j.postharvbio.2021.111760

Tarkka, M.T., Herrmann, S., Wubet, T., Feldhahn, L., Recht, S., Kurth, F., Mailänder, S., Bönn, M., Neef, M., Angay, O., Bacht, M., Graf, M., Maboreke, H., Fleischmann, F., Grams, T.E.E., Ruess, L., Schädler, M., Brandl, R., Scheu, S., Schrey, S.D., Grosse, I., Buscot, F., 2013. OakContigDF159.1, a reference library for studying differential gene expression in *Quercus robur* during controlled biotic interactions: use for quantitative transcriptomic profiling of oak roots in ectomycorrhizal symbiosis. New Phytol. 199, 529–540. https://doi.org/10.1111/nph.12317

Tena, G., Asai, T., Chiu, W.-L., Sheen, J., 2001. Plant mitogen-activated protein kinase signaling cascades. Curr. Opin. Plant Biol. 4, 392–400. https://doi.org/10.1016/S1369-5266(00)00191-6

Thaler, J.S., Humphrey, P.T., Whiteman, N.K., 2012. Evolution of jasmonate and salicylate signal crosstalk. Trends Plant Sci. 17, 260–270. https://doi.org/10.1016/j.tplants.2012.02.010

Thieme, C.J., Rojas-Triana, M., Stecyk, E., Schudoma, C., Zhang, W., Yang, L., Miñambres, M., Walther, D., Schulze, W.X., Paz-Ares, J., Scheible, W.-R., Kragler, F., 2015. Endogenous *Arabidopsis* messenger RNAs transported to distant tissues. Nat. Plants 1, 1–9. https://doi.org/10.1038/nplants.2015.25

Thines, B., Katsir, L., Melotto, M., Niu, Y., Mandaokar, A., Liu, G., Nomura, K., He, S.Y., Howe, G.A., Browse, J., 2007. JAZ repressor proteins are targets of the SCF^{COI1} complex during jasmonate signalling. Nature 448, 661–665. https://doi.org/10.1038/nature05960

Thompson, V., 2022. Insect-plant-fungus interactions in mycorrhizal associations, with a focus on spittlebugs and ectomycorrhizal host plants. Ecol. Entomol. 47, 915–929. https://doi.org/10.1111/een.13192

Thorpe, M.R., Ferrieri, A.P., Herth, M.M., Ferrieri, R.A., 2007. ^{11}C-imaging: methyl jasmonate moves in both phloem and xylem, promotes transport of jasmonate, and of photoassimilate even after proton transport is decoupled. Planta 226, 541–551. https://doi.org/10.1007/s00425-007-0503-5

Tiku, A.R., 2020. Antimicrobial compounds (phytoanticipins and phytoalexins) and their role in plant defense, in: Co-Evolution of Secondary Metabolites. Springer International Publishing, Cham, Germany, pp. 845–868. https://doi.org/10.1007/978-3-319-96397-6_63

Treutter, D., 2006. Significance of flavonoids in plant resistance: a review. Environ. Chem. Lett. 4, 147–157. https://doi.org/10.1007/s10311-006-0068-8

Truman, W.M., Bennett, M.H., Turnbull, C.G.N., Grant, M.R., 2010. *Arabidopsis* auxin mutants are compromised in systemic acquired resistance and exhibit aberrant accumulation of various indolic compounds. Plant Physiol. 152, 1562–1573. https://doi.org/10.1104/pp.109.152173

Trusov, Y., Sewelam, N., Rookes, J.E., Kunkel, M., Nowak, E., Schenk, P.M., Botella, J.R., 2009. Heterotrimeric G proteins-mediated resistance to necrotrophic pathogens includes mechanisms independent of salicylic acid-, jasmonic acid/ethylene- and abscisic acid-mediated defense signaling. Plant J. 58, 69–81. https://doi.org/10.1111/j.1365-313X.2008.03755.x

Tschaplinski, T.J., Plett, J.M., Engle, N.L., Deveau, A., Cushman, K.C., Martin, M.Z., Doktycz, M.J., Tuskan, G.A., Brun, A., Kohler, A., Martin, F., 2014. *Populus trichocarpa* and *Populus deltoides* exhibit different metabolomic responses to colonization by the symbiotic fungus *Laccaria bicolor*. Mol. Plant-Microbe Interactions® 27, 546–556. https://doi.org/10.1094/MPMI-09-13-0286-R

Turner, J.G., Ellis, C., Devoto, A., 2002. The jasmonate signal pathway. Plant Cell 14, S153–S164. https://doi.org/10.1105/tpc.000679

Tuskan, G.A., DiFazio, S., Jansson, S., Bohlmann, J., Grigoriev, I., Hellsten, U., Putnam, N., Ralph, S., Rombauts, S., Salamov, A., Schein, J., Sterck, L., Aerts, A., Bhalerao, R.R., Bhalerao, R.P., Blaudez, D., Boerjan, W., Brun, A., Brunner, A., Busov, V., Campbell, M., Carlson, J., Chalot, M., Chapman, J., Chen, G.-L., Cooper, D., Coutinho, P.M., Couturier, J., Covert, S., Cronk, Q., Cunningham, R., Davis, J., Degroeve, S., Déjardin, A., dePamphilis, C., Detter, J., Dirks, B., Dubchak, I., Duplessis, S., Ehlting, J., Ellis, B., Gendler, K., Goodstein, D., Gribskov, M., Grimwood, J., Groover, A., Gunter, L., Hamberger, B., Heinze, B., Helariutta, Y., Henrissat, B., Holligan, D., Holt, R., Huang, W., Islam-Faridi, N., Jones, S., Jones-Rhoades, M., Jorgensen, R., Joshi, C., Kangasjärvi, J., Karlsson, J., Kelleher, C., Kirkpatrick, R., Kirst, M., Kohler, A., Kalluri, U., Larimer, F., Leebens-Mack, J., Leplé, J.-C., Locascio, P., Lou, Y., Lucas, S., Martin, F., Montanini, B., Napoli, C., Nelson, D.R., Nelson, C., Nieminen, K., Nilsson, O., Pereda, V., Peter, G., Philippe, R., Pilate, G., Poliakov, A., Razumovskaya, J., Richardson, P., Rinaldi, C., Ritland, K., Rouzé, P., Ryaboy, D., Schmutz, J., Schrader, J., Segerman, B., Shin, H., Siddiqui, A., Sterky, F., Terry, A., Tsai, C.-J., Uberbacher, E., Unneberg, P., Vahala, J., Wall, K., Wessler, S., Yang, G., Yin, T., Douglas, C., Marra, M., Sandberg, G., Van de Peer, Y., Rokhsar, D., 2006. The

genome of black cottonwood, *Populus trichocarpa* (Torr. & Gray). Science 313, 1596–1604. https://doi.org/10.1126/science.1128691

Ullah, C., Schmidt, A., Reichelt, M., Tsai, C.-J., Gershenzon, J., 2022. Lack of antagonism between salicylic acid and jasmonate signalling pathways in poplar. New Phytol. 235, 701–717. https://doi.org/10.1111/nph.18148

Underwood, W., 2012. The plant cell wall: a dynamic barrier against pathogen invasion. Front. Plant Sci. 3, 85. https://doi.org/10.3389/fpls.2012.00085

Urban, J., 2006. Occurrence, bionomics and harmfulness of *Chrysomela populi* L. (Coleoptera, Chrysomelidae). J For. Sci 52, 255–284. https://doi.org/10.17221/4509-JFS

Vallad, G.E., Goodman, R.M., 2004. Systemic acquired resistance and induced systemic resistance in conventional agriculture. Crop Sci. 44, 1920–1934. https://doi.org/10.2135/cropsci2004.1920

van den Berg, A.K., Perkins, T.D., 2005. Nondestructive estimation of anthocyanin content in autumn sugar maple leaves. HortScience 40, 685–686. https://doi.org/10.21273/HORTSCI.40.3.685

Van der Ent, S., Van Hulten, M., Pozo, M.J., Czechowski, T., Udvardi, M.K., Pieterse, C.M.J., Ton, J., 2009. Priming of plant innate immunity by rhizobacteria and β-aminobutyric acid: differences and similarities in regulation. New Phytol. 183, 419–431. https://doi.org/10.1111/j.1469-8137.2009.02851.x

van der Heijden, M.G.A., Martin, F.M., Selosse, M.-A., Sanders, I.R., 2015. Mycorrhizal ecology and evolution: the past, the present, and the future. New Phytol. 205, 1406–1423. https://doi.org/10.1111/nph.13288

van Kan, J.A.L., Shaw, M.W., Grant-Downton, R.T., 2014. *Botrytis* species: relentless necrotrophic thugs or endophytes gone rogue? Mol. Plant Pathol. 15, 957–961. https://doi.org/10.1111/mpp.12148

van Loon, L.C., Rep, M., Pieterse, C.M.J., 2006. Significance of inducible defense-related proteins in infected plants. Annu. Rev. Phytopathol. 44, 135–162. https://doi.org/10.1146/annurev.phyto.44.070505.143425

van Schie, C.C.N., Haring, M.A., Schuurink, R.C., 2007. Tomato linalool synthase is induced in trichomes by jasmonic acid. Plant Mol. Biol. 64, 251–263. https://doi.org/10.1007/s11103-007-9149-8

Vandenkoornhuyse, P., Quaiser, A., Duhamel, M., Le Van, A., Dufresne, A., 2015. The importance of the microbiome of the plant holobiont. New Phytol. 206, 1196–1206. https://doi.org/10.1111/nph.13312

Vayssières, A., Pěnčík, A., Felten, J., Kohler, A., Ljung, K., Martin, F., Legué, V., 2015. Development of the poplar-*Laccaria bicolor* ectomycorrhiza modifies root auxin metabolism, signaling, and response. Plant Physiol. 169, 890–902. https://doi.org/10.1104/pp.114.255620

Velmala, S.M., Vuorinen, I., Uimari, A., Piri, T., Pennanen, T., 2018. Ectomycorrhizal fungi increase the vitality of Norway spruce seedlings under the pressure of *Heterobasidion* root rot in vitro but may increase susceptibility to foliar necrotrophs. Fungal Biol. 122, 101–109. https://doi.org/10.1016/j.funbio.2017.11.001

Vincent, D., Kohler, A., Claverol, S., Solier, E., Joets, J., Gibon, J., Lebrun, M.-H., Plomion, C., Martin, F., 2012. Secretome of the free-living mycelium from the ectomycorrhizal basidiomycete *Laccaria bicolor*. J. Proteome Res. 11, 157–171. https://doi.org/10.1021/pr200895f

Vishwanathan, K., Zienkiewicz, K., Liu, Y., Janz, D., Feussner, I., Polle, A., Haney, C.H., 2020. Ectomycorrhizal fungi induce systemic resistance against insects on a nonmycorrhizal

plant in a CERK1-dependent manner. New Phytol. 228, 728–740. https://doi.org/10.1111/nph.16715

Vlot, A.C., Dempsey, D.A., Klessig, D.F., 2009. Salicylic acid, a multifaceted hormone to combat disease. Annu. Rev. Phytopathol. 47, 177–206. https://doi.org/10.1146/annurev.phyto.050908.135202

Wan, Z., Li, Y., Liu, M., Chen, Y., Yin, T., 2015. Natural infectious behavior of the urediniospores of *Melampsora larici-populina* on poplar leaves. J. For. Res. 26, 225–231. https://doi.org/10.1007/s11676-015-0021-4

Wang, B., Yeun, L.H., Xue, J.-Y., Liu, Y., Ané, J.-M., Qiu, Y.-L., 2010. Presence of three mycorrhizal genes in the common ancestor of land plants suggests a key role of mycorrhizas in the colonization of land by plants. New Phytol. 186, 514–525. https://doi.org/10.1111/j.1469-8137.2009.03137.x

Wang, J., Song, L., Gong, X., Xu, J., Li, M., 2020. Functions of jasmonic acid in plant regulation and response to abiotic stress. Int. J. Mol. Sci. 21, 1446. https://doi.org/10.3390/ijms21041446

Wang, K.L.-C., Li, H., Ecker, J.R., 2002. Ethylene biosynthesis and signaling networks. Plant Cell 14, 131–151. https://doi.org/10.1105/tpc.001768

Wang, Y., Chantreau, M., Sibout, R., Hawkins, S., 2013. Plant cell wall lignification and monolignol metabolism. Front. Plant Sci. 4, 220. https://doi.org/10.3389/fpls.2013.00220

Wang, Y., Li, X., Fan, B., Zhu, C., Chen, Z., 2021. Regulation and function of defense-related callose deposition in plants. Int. J. Mol. Sci. 22, 2393. https://doi.org/10.3390/ijms22052393

Wang, Y., Liu, W., Jiang, H., Mao, Z., Wang, N., Jiang, S., Xu, H., Yang, G., Zhang, Z., Chen, X., 2019. The R2R3-MYB transcription factor MdMYB24-like is involved in methyl jasmonate-induced anthocyanin biosynthesis in apple. Plant Physiol. Biochem. 139, 273–282. https://doi.org/10.1016/j.plaphy.2019.03.031

Wang, Y.-F., Baloch, A.M., Deng, J., Baloch, A.W., Hou, X., Miao, R., Zhang, R.-S., 2020. Influence of *Trichoderma inoculation* on four crucial defense-related enzymes and leaf soluble protein level of poplar. Pak. J. Bot. 52, 879–884. https://doi.org/0.30848/PJB2020-3(11)

Wani, S.H., Anand, S., Singh, B., Bohra, A., Joshi, R., 2021. WRKY transcription factors and plant defense responses: latest discoveries and future prospects. Plant Cell Rep. 40, 1071–1085. https://doi.org/10.1007/s00299-021-02691-8

Wasternack, C., Feussner, I., 2018. The oxylipin pathways: biochemistry and function. Annu. Rev. Plant Biol. 69, 363–386. https://doi.org/10.1146/annurev-arplant-042817-040440

Werner, S., Polle, A., Brinkmann, N., 2016. Belowground communication: impacts of volatile organic compounds (VOCs) from soil fungi on other soil-inhabiting organisms. Appl. Microbiol. Biotechnol. 100, 8651–8665. https://doi.org/10.1007/s00253-016-7792-1

Wiermer, M., Feys, B.J., Parker, J.E., 2005. Plant immunity: the EDS1 regulatory node. Curr. Opin. Plant Biol., Biotic interactions 8, 383–389. https://doi.org/10.1016/j.pbi.2005.05.010

Wink, M., 2018. Plant secondary metabolites modulate insect behavior-steps toward addiction? Front. Physiol. 9, 364. https://doi.org/10.3389/fphys.2018.00364

Wong, J.W.H., Lutz, A., Natera, S., Wang, M., Ng, V., Grigoriev, I., Martin, F., Roessner, U., Anderson, I.C., Plett, J.M., 2019. The influence of contrasting microbial lifestyles on the

pre-symbiotic metabolite responses of *Eucalyptus grandis* roots. Front. Ecol. Evol. 7, 10. https://doi.org/10.3389/fevo.2019.00010

Wong, K.K.Y., Piché, Y., Fortin, J.A., 1990. Differential development of root colonization among four closely related genotypes of ectomycorrhizal *Laccaria bicolor*. Mycol. Res. 94, 876–884. https://doi.org/10.1016/S0953-7562(09)81300-2

Wong-Bajracharya, J., Singan, V.R., Monti, R., Plett, K.L., Ng, V., Grigoriev, I.V., Martin, F.M., Anderson, I.C., Plett, J.M., 2022. The ectomycorrhizal fungus *Pisolithus microcarpus* encodes a microRNA involved in cross-kingdom gene silencing during symbiosis. Proc. Natl. Acad. Sci. 119, e2103527119. https://doi.org/10.1073/pnas.2103527119

Wrzaczek, M., Brosché, M., Salojärvi, J., Kangasjärvi, S., Idänheimo, N., Mersmann, S., Robatzek, S., Karpiński, S., Karpińska, B., Kangasjärvi, J., 2010. Transcriptional regulation of the CRK/DUF26 group of Receptor-like protein kinases by ozone and plant hormones in *Arabidopsis*. BMC Plant Biol. 10, 95. https://doi.org/10.1186/1471-2229-10-95

Xiao, L., Du, Q., Fang, Y., Quan, M., Lu, W., Wang, D., Si, J., El-Kassaby, Y.A., Zhang, D., 2021. Genetic architecture of the metabolic pathway of salicylic acid biosynthesis in *Populus*. Tree Physiol. 41, 2198–2215. https://doi.org/10.1093/treephys/tpab068

Xie, D.-X., Feys, B.F., James, S., Nieto-Rostro, M., Turner, J.G., 1998. COI1: an *Arabidopsis* gene required for jasmonate-regulated defense and fertility. Science 280, 1091–1094. https://doi.org/10.1126/science.280.5366.1091

Xu, J., Tian, Y.-S., Xing, X.-J., Peng, R.-H., Zhu, B., Gao, J.-J., Yao, Q.-H., 2016. Over-expression of AtGSTU19 provides tolerance to salt, drought and methyl viologen stresses in *Arabidopsis*. Physiol. Plant. 156, 164–175. https://doi.org/10.1111/ppl.12347

Yan, L., Zhu, J., Zhao, X., Shi, J., Jiang, C., Shao, D., 2019. Beneficial effects of endophytic fungi colonization on plants. Appl. Microbiol. Biotechnol. 103, 3327–3340. https://doi.org/10.1007/s00253-019-09713-2

Yan, Y., Stolz, S., Chételat, A., Reymond, P., Pagni, M., Dubugnon, L., Farmer, E.E., 2007. A downstream mediator in the growth repression limb of the jasmonate pathway. Plant Cell 19, 2470–2483. https://doi.org/10.1105/tpc.107.050708

Yin, M., Song, N., Chen, S., Wu, J., 2021. NaKTI2, a Kunitz trypsin inhibitor transcriptionally regulated by NaWRKY3 and NaWRKY6, is required for herbivore resistance in *Nicotiana attenuata*. Plant Cell Rep. 40, 97–109. https://doi.org/10.1007/s00299-020-02616-x

Yu, X., Zhang, W., Zhang, Y., Zhang, Xiaojia, Lang, D., Zhang, Xinhui, 2018. The roles of methyl jasmonate to stress in plants. Funct. Plant Biol. 46, 197–212. https://doi.org/10.1071/FP18106

Yuan, G., He, S., Bian, S., Han, X., Liu, K., Cong, P., Zhang, C., 2020. Genome-wide identification and expression analysis of major latex protein (MLP) family genes in the apple (*Malus domestica* Borkh.) genome. Gene 733, 144275. https://doi.org/10.1016/j.gene.2019.144275

Yuan, M., Jiang, Z., Bi, G., Nomura, K., Liu, M., Wang, Y., Cai, B., Zhou, J.-M., He, S.Y., Xin, X.-F., 2021. Pattern-recognition receptors are required for NLR-mediated plant immunity. Nature 592, 105–109. https://doi.org/10.1038/s41586-021-03316-6

Yuan, P., Jauregui, E., Du, L., Tanaka, K., Poovaiah, B., 2017. Calcium signatures and signaling events orchestrate plant–microbe interactions. Curr. Opin. Plant Biol. 38, 173–183. https://doi.org/10.1016/j.pbi.2017.06.003

Zavala, J.A., Patankar, A.G., Gase, K., Hui, D., Baldwin, I.T., 2004. Manipulation of endogenous trypsin proteinase inhibitor production in *Nicotiana attenuata* demonstrates their

function as antiherbivore defenses. Plant Physiol. 134, 1181–1190. https://doi.org/10.1104/pp.103.035634

Zeier, J., 2021. Metabolic regulation of systemic acquired resistance. Curr. Opin. Plant Biol., Biotic interactions 62, 102050. https://doi.org/10.1016/j.pbi.2021.102050

Zhang, X., Dong, W., Sun, J., Feng, F., Deng, Y., He, Z., Oldroyd, G.E.D., Wang, E., 2015. The receptor kinase CERK1 has dual functions in symbiosis and immunity signalling. Plant J. 81, 258–267. https://doi.org/10.1111/tpj.12723

Zhang, X., Guo, K., Dong, Z., Chen, Z., Zhu, H., Zhang, Y., Xia, Q., Zhao, P., 2020. Kunitz-type protease inhibitor BmSPI51 plays an antifungal role in the silkworm cocoon. Insect Biochem. Mol. Biol. 116, 103258. https://doi.org/10.1016/j.ibmb.2019.103258

Zhang, Z., Xin, W., Wang, S., Zhang, X., Dai, H., Sun, R., Frazier, T., Zhang, B., Wang, Q., 2015. Xylem sap in cotton contains proteins that contribute to environmental stress response and cell wall development. Funct. Integr. Genomics 15, 17–26. https://doi.org/10.1007/s10142-014-0395-y

Zhou, Y., Zhou, B., Pache, L., Chang, M., Khodabakhshi, A.H., Tanaseichuk, O., Benner, C., Chanda, S.K., 2019. Metascape provides a biologist-oriented resource for the analysis of systems-level datasets. Nat. Commun. 10, 1523. https://doi.org/10.1038/s41467-019-09234-6

Zhu-Salzman, K., Zeng, R., 2015. Insect response to plant defensive protease inhibitors. Annu. Rev. Entomol. 60, 233–252. https://doi.org/10.1146/annurev-ento-010814-020816

Zipfel, C., 2014. Plant pattern-recognition receptors. Trends Immunol. 35, 345–351. https://doi.org/10.1016/j.it.2014.05.004

Zipfel, C., 2009. Early molecular events in PAMP-triggered immunity. Curr. Opin. Plant Biol., Biotic Interactions 12, 414–420. https://doi.org/10.1016/j.pbi.2009.06.003

7. Supplement

7.1. List of supplemental tables

7.2. Supplemental Tables

Supplemental Table 1 Editing by CRISPR/CAS9 of poplar *cerk1* KO lines 19 and 20
The cerk1 KO lines were generated by Muhr, 2022.

Gene	*CERK1-like1* (Potri.002G226600)	
	1st allele	2nd allele
Line	Editing	Editing
19	113 bp deletion (premature stop codon)	112 bp deletion (premature stop codon)
20	18 bp deletion (premature stop codon) + 275 bp insertion (premature stop codon)	20 bp deletion (premature stop codon)

Gene	*CERK1-like2* (Potri.014G156400)	
	1st allele	2nd allele
Line	Editing	Editing
19	112 bp inverted (premature stop codon) + 114 bp deletion (deletion of LysM1 domain) + 5 bp deletion (premature stop codon)	2 bp deletion (premature stop codon) + 4 bp deletion (premature stop codon) + 5 bp deletion (premature stop codon) + 7 bp deletion (premature stop codon) + 112 bp deletion (premature stop codon)
20	7 bp deletion (premature stop codon)	1 bp deletion (premature stop codon) + 3 bp deletion (premature stop codon) + 39 bp deletion (premature stop codon)

Supplemental Table 2 Composition of Murashig & Skoog medium for plant propagation
All compounds were mixed from stock solutions in 1 L ddH_2O, and pH was adjusted to 5.7 with KOH before adding Gelrite. Thereafter, the media was autoclaved at 121 °C for 20 min at 2.2 bar. The concentrations are given as final concentrations [g/L]. The recipe was adapted from Müller et al. (2013b). Suppliers: Merck, Darmstadt, Germany; Carl Roth, Darmstadt, Germany; Duchefa Biochemie, Haarlem, Netherlands.

Compound	Final concentration [g/L]	Supplier
Macro		
NH_4NO_3	1.6500	Carl Roth
KNO_3	1.9000	Carl Roth
$CaCl_2$ x 2 H_2O	0.4400	Carl Roth
$MgSO_4$ x 7 H_2O	0.3700	Carl Roth
KH_2PO_4	0.1700	Carl Roth
Micro		
H_3BO_3	$62x10^{-4}$	Carl Roth
$MnSO_4$ x H_2O	0.0100	Merck
$ZnSO_2$ x 7 H_2O	$86x10^{-4}$	Merck
KJ	$83x10^{-5}$	Merck
Na_2MoO_4 x 2 H_2O	$2.5x10^{-4}$	Merck
$CuSO_4$ 5 H_2O	$2.5x10^{-5}$	Merck
$CoCl_2$ x 6 H_2O	$2.5x10^{-5}$	Merck
Vitamins		
Nicotine acid	$5x10^{-4}$	Merck
Pyridoxin – HCl	$6x10^{-4}$	Duchefa Biochemie
Thiamin – HCl	$1x10^{-4}$	Merck
Glycin	0.0020	Carl Roth
myo inositol	0.1000	Duchefa Biochemie
$C_{10}H_{12}FeN_2NaO_8$	$36.7x10^{-3}$	Carl Roth
Saccarose	20	Duchefa Biochemie
Gelrite	5	Duchefa Biochemie

Supplemental Table 3 Composition of modified-Melin-Norkrans-Sucrose medium for *L. bicolor* propagation

All compounds (except Thiamin HCl and $FeCl_3$ x $6H_2O$) were mixed from stock solutions in 1 L ddH_2O, and pH was adjusted to 5.5 with KOH before adding micro agar. Thereafter, the media was autoclaved at 121 °C for 20 min at 2.2 bar. After cooling the medium to about 60 °C, sterile filtered Thiamin HCL and $FeCl_3$ x $6H_2O$ were added. The concentrations are given as final concentrations [g/L]. The recipe was adapted from Kulmann (2005). Suppliers: Merck, Darmstadt, Germany; Carl Roth, Darmstadt, Germany; Sigma-Aldrich, Taufkirchen, Germany; Duchefa Biochemie, Haarlem, Netherlands.

Compound	**Final concentration [g/L]**	**Supplier**
Macro		
$(NH_4)_2SO_4$	0.2500	Sigma-Aldrich
KH_2PO_4	0.5000	Carl Roth
$MgSO_4$ x $7H_2O$	0.1500	Carl Roth
$CaCl_2$ x $2H_2O$	0.5000	Carl Roth
NaCl	0,2500	Carl Roth
Micro		
$MnSO_4$ x H_2O	0.1100	Merck
$ZnSO_4$ x $7H_2O$	0.2200	Merck
$CuSO_4$ x $5H_2O$	0.0490	Merck
$(NH_4)_6MO_7O_{24}$ x $4H_2O$	0.0230	Merck
Thiamin HCl	0.0001	Duchefa Biochemie
$FeCl_3$ x $6H_2O$	0.0100	Carl Roth
Saccharose	10 or 2	Duchefa Biochemie
Micro Agar	20	Duchefa Biochemie

Supplemental Table 4 Composition of nutrient solutions with low nitrogen supply for plant irrigation

All compounds were mixed in 100 L distilled H_2O. The recipe was adapted from Langenfeld-Heyer et al. (2007) and Matzner et al. (1982). Suppliers: Merck, Darmstadt, Germany; Carl Roth, Darmstadt, Germany.

Compound	Finale concentration [µM]	Supplier
NH_4NO_3	300	Carl Roth
K_2SO_4	200	Merck
$CaSO_4$ x $2H_2O$	130	Carl Roth
Na_2SO_4	100	Merck
$MgSO_4$ x 7 H_2O	60	Carl Roth
KH_2PO_4	30	Carl Roth
$C_{10}H_{12}FeN_2O_8$	7.8	Carl Roth

Supplemental Table 5 Composition of Long Ashton solution for plant irrigation

All compounds were mixed in 100 L distilled H_2O. The recipe was adapted from Hewitt (1952). Suppliers: Merck, Darmstadt, Germany; Carl Roth, Darmstadt, Germany.

Compound	Finale concentration [g mL^{-1}]	Supplier
KNO_3	0.0202	Carl Roth
$Ca(NO_3)_3$ x 4 H_2O	0.1063	Carl Roth
$MgSo_4$ x 7 H_2O	0.0740	Merck
KH_2PO_4	0.0816	Carl Roth
K_2HPO_4	0.0072	Merck
H_3BO_3	$6.180x10^{-4}$	Carl Roth
$MNSO_4$ x H_2O	$3.380x10^{-4}$	Merck
Na_2MoO_4 x 2 H_2O	$1.692x10^{-3}$	Merck
$CoSo_4$ x 7 H_2O	$1.120x10^{-5}$	Merck
$ZnSO_4$ x 7 H_2O	$5.760x10^{-5}$	Merck
$CuSO_4$	$3.200x10^{-5}$	Merck
$C_{10}H_{12}FeN_2O_8$	$3.671x10^{-5}$	Carl Roth

Supplemental Table 6 RNAseq reads after computational processing

S1-S3 = technical replicates, t0-t7 time points, SW = sandwich, W = weck jar, C = control, Lb = *L. bicolor* treatment; The computational data processing and differential transcription analysis were carried out by Dr. Johannes Ballauff (Department of Forest Botany and Tree Physiology, University of Göttingen, Germany)

ID	RIN	reads input	reads after quality filtering		reads unique mapped		reads multiple mapped		reads annotated	
S1-t0-SW	8.7	22,844,405	22,826,719	[99.92 %]	18,964,977	[83.02 %]	1,236,180	[5.41 %]	17,828,406	[78.04 %]
S1-t0-W	8.6	21,761,753	21,738,240	[99.89 %]	18,128,371	[83.30 %]	1,172,682	[5.39 %]	17,099,470	[78.58 %]
S1-t1-C	8.2	25,555,988	25,533,148	[99.91 %]	21,370,329	[83.62 %]	1,296,886	[5.07 %]	20,184,008	[78.98 %]
S1-t1-Lb	8.8	27,696,881	27,663,508	[99.88 %]	23,132,438	[83.52 %]	1,397,827	[5.05 %]	21,832,125	[78.83 %]
S1-t2-C	8.8	28,165,460	28,145,458	[99.93 %]	23,589,267	[83.75 %]	1,423,782	[5.06 %]	22,336,556	[79.30 %]
S1-t2-Lb	9.4	27,673,002	27,652,832	[99.93 %]	23,180,703	[83.77 %]	1,441,363	[5.21 %]	21,913,487	[79.19 %]
S1-t4-C	8.4	26,716,373	26,688,359	[99.90 %]	22,068,230	[82.60 %]	1,492,863	[5.59 %]	20,670,429	[77.37 %]
S1-t4-Lb	8.3	26,560,418	26,532,209	[99.89 %]	22,122,903	[83.29 %]	1,352,024	[5.09 %]	20,790,706	[78.28 %]
S1-t7-C	9.0	29,591,908	29,560,920	[99.90 %]	24,747,867	[83.63 %]	1,486,367	[5.02 %]	23,325,691	[78.82 %]
S1-t7-Lb	8.4	30,232,588	30,187,610	[99.85 %]	25,138,228	[83.15 %]	1,534,936	[5.08 %]	23,660,539	[78.26 %]
S2-t0-SW	9.3	33,847,758	33,817,723	[99.91 %]	28,495,796	[84.19 %]	1,609,544	[4.76 %]	26,881,619	[79.42 %]
S2-t0-W	8.6	17,545,304	17,539,669	[99.97 %]	14,810,921	[84.42 %]	888,540	[5.06 %]	14,032,769	[79.98 %]
S2-t1-C	7.5	32,741,951	32,709,401	[99.90 %]	27,085,352	[82.72 %]	1,796,885	[5.49 %]	25,364,369	[77.47 %]
S2-t1-Lb	8.5	23,425,850	23,373,413	[99.78 %]	19,570,578	[83.54 %]	1,185,452	[5.06 %]	18,496,231	[78.96 %]
S2-t2-C	8.1	30,045,965	30,019,533	[99.91 %]	25,222,049	[83.94 %]	1,492,894	[4.97 %]	23,782,798	[79.15 %]
S2-t2-Lb	8.5	28,702,386	28,679,002	[99.92 %]	24,091,760	[83.94 %]	1,425,341	[4.97 %]	22,724,222	[79.17 %]
S2-t4-C	8.4	24,923,741	24,896,990	[99.89 %]	20,888,774	[83.81 %]	1,233,321	[4.95 %]	19,647,545	[78.83 %]
S2-t4-Lb	8.3	28,126,749	28,074,669	[99.81 %]	23,485,487	[83.50 %]	1,432,766	[5.09 %]	22,107,305	[78.60 %]
S2-t7-C	8.3	42,054,689	42,000,050	[99.87 %]	35,216,615	[83.74 %]	2,092,205	[4.97 %]	33,155,615	[78.84 %]
S2-t7-Lb	8.5	27,329,815	27,278,255	[99.81 %]	22,739,255	[83.20 %]	1,364,854	[4.99 %]	21,319,336	[78.01 %]

Supplemental Table 6 continued

ID	RIN	reads input	reads after quality filtering		reads unique mapped		reads multiple mapped		reads annotated	
S3-t0-SW	8.6	35,898,723	35,870,288	[99.92 %]	29,753,052	[82.88 %]	2,082,271	[5.80 %]	27,975,306	[77.93 %]
S3-t0-W	8.1	23,573,587	23,555,295	[99.92 %]	19,678,952	[83.48 %]	1,213,721	[5.15 %]	18,479,812	[78.39 %]
S3-t1-C	8.2	29,443,639	29,408,602	[99.88 %]	24,342,728	[82.68 %]	1,655,059	[5.62 %]	22,864,054	[77.65 %]
S3-t1-Lb	8.5	26,832,411	26,767,702	[99.76 %]	22,043,157	[82.15 %]	1,579,775	[5.89 %]	20,660,436	[77.00 %]
S3-t2-C	8.4	32,798,040	32,777,180	[99.94 %]	27,348,045	[83.38 %]	1,764,298	[5.38 %]	25,764,735	[78.56 %]
S3-t2-Lb	8.6	29,056,012	29,022,845	[99.89 %]	24,108,492	[82.97 %]	1,613,767	[5.55 %]	22,671,708	[78.03 %]
S3-t4-C	8.1	30,139,581	30,054,379	[99.72 %]	24,536,986	[81.41 %]	1,884,470	[6.25 %]	22,851,167	[75.82 %]
S3-t4-Lb	8.3	29,175,022	29,136,458	[99.87 %]	24,328,932	[83.39 %]	1,512,391	[5.18 %]	22,885,474	[78.44 %]
S3-t7-C	7.8	29,784,806	29,754,492	[99.90 %]	24,895,999	[83.59 %]	1,509,067	[5.07 %]	23,381,798	[78.50 %]
S3-t7-Lb	8.8	30,167,519	30,137,060	[99.90 %]	25,158,175	[83.39 %]	1,592,782	[5.28 %]	23,716,267	[78.62 %]

Supplemental Table 7 Primer used in this study

Target-specific primers were designed using PerlPrimer (Marshall, 2004) and synthesized by Microsynth (Microsynth, Wolfurt, Austria)

Primer Name	Primer sequence	Primer efficiency	Potri.id	Comment
Populus* × *canescens				
A_Ref2_F	ATCGTTCCAAGTCAAGTATGTG	1.01	Potri.015G001600	reference gene (Strijkstra, 2021)
A_Ref2_R	TCAAGGGAGCAACTTTACAG			
C_Ref1_F	GCAATGTGAGGAGTTTAGGG	0.95	Potri.012G141400	reference gene (Strijkstra, 2021)
C_Ref1_R	TATTAAATGTCTGTGCTGTAGTGTG			
PtKTIup1_RT_F	GTGTCCAACTACAAGCTCCT	0.98	Potri.019G088200	most induced KTI Kaling et al. (2018) & overlap seven days sterile and twelve weeks outdoors
PtKTIup1_RT_R	TCAAAGCCAGGTATCTAATCCC			
PtMLP423_RT_F	ACCATCTCATTCCTAAGGCTG	0.99	Potri.010G000600	overlap seven days sterile and twelve weeks outdoors
PtMLP423_RT_R	TACTTGTATCCAGTACCTTCACC			
PtAOS1_RT_F	CCATCTGAACCAACCAAACTC	1.02	Potri.002G130700	
PtAOS1_RT_R	TTTGAAATACTCGTCTCTGCCT			
PtERF1_RT_F	TTCCAGAGCAATTCACTTCCT	0.98	Potri.005G223200	
PtERF1_RT_R	CACTTCCTCTTCCTTAATTCCAC			
PtPR1_RT_F	ATAATAATCCCTCTATCCCTTGCC	0.90	Potri.T131500	
PtPR1_RT_R	GACAATATTTCCAACACCTACCTG			
Botrytis cinerea				
Bc3F	GCTGTAATTTCAATGTGCAGAATCC			Suarez et al. (2005) and Diguta et al. (2010), intergenic spacer
Bc3R	GGAGCAACAATTAATCGCATTTC			

Supplemental Table 8 Genes with changed transcript abundances in leaves after seven days of direct contact between *L. bicolor* and *P.* × *canescens* roots (this thesis) and seven days of exposure of *P.* × *canescens* to *L. bicolo*r (*Lb*) VOCs (Jakobi, 2021)

Potri.id	Ara.id	*Arabidopsis* gene symbol	*Arabidopsis* gene description	Log2FC *Lb* VOCs	Log2Fc direct contact
Potri.003G085700	AT4G17670		senescence-associated family protein (DUF581)	1.53	1.99
Potri.005G122200	AT1G75250	RL6	RAD-LIKE 6	1.56	1.69
Potri.001G288600	AT2G14610	PR1	PATHOGENESIS-RELATED GENE 1	1.67	-1.56
Potri.001G311300	AT1G17840	ABCG11	WHITE-BROWN COMPLEX HOMOLOG PROTEIN 11	1.69	1.07
Potri.008G116500	AT1G75290		sequence is similar to an isoflavone reductase	1.87	1.99
Potri.010G129800	AT1G75290		sequence is similar to an isoflavone reductase	2.02	2.08
Potri.003G176700	AT5G13930	TT4	CHALCONE SYNTHASE, TRANSPARENT TESTA 4	2.14	1.98
Potri.001G051600	AT5G13930	TT4	CHALCONE SYNTHASE, TRANSPARENT TESTA 4	2.14	2.49
Potri.008G194100	AT1G69880	TH8	THIOREDOXIN H-TYPE 8	2.22	3.20
Potri.003G144300	AT2G47460	MYB12	MYB DOMAIN PROTEIN 12	2.25	1.70
Potri.003G176900	AT5G13930	TT4	CHALCONE SYNTHASE, TRANSPARENT TESTA 4	2.32	2.52
Potri.003G176800	AT5G13930	TT4	CHALCONE SYNTHASE, TRANSPARENT TESTA 4	2.34	2.37
Potri.001G051500	AT5G13930	TT4	CHALCONE SYNTHASE, TRANSPARENT TESTA 4	2.35	3.04
Potri.017G138800	AT5G17220	TT19	GLUTATHIONE S-TRANSFERASE PHI 12, TRANSPARENT TESTA 19	2.40	2.01
Potri.007G021300	AT3G11480	BSMT1	S-adenosyl-L-methionine-dependent methyltransferase	2.40	1.41
Potri.005G223200	AT3G23240	ERF1	ETHYLENE RESPONSE FACTOR 1	2.52	1.80
Potri.T055700	AT4G13440		Calcium-binding EF-hand family protein	2.64	2.82
Potri.019G028800	AT4G13440		Calcium-binding EF-hand family protein	2.82	2.79
Potri.011G126400	AT4G27360		Dynein light chain type 1 family protein	3.25	1.49
Potri.014G019200	AT5G48810	CB5-D	CYTOCHROME B5 ISOFORM D	4.34	2.94

7.3. Material used in this study

The suppliers are mentioned in the text or tables. Chemicals were supplied by Carl Roth (Darmstadt, Germany), Sigma-Aldrich (Taufkirchen, Germany), Merck (Darmstadt, Germany), or Duchefa Biochemie (Haarlem, Netherlands). Plastic ware was supplied by Sarstedt (Nümbrecht, Germany), Greiner (Kremsmünster, Austria), or Starlab (Hamburg, Germany).

7.4. Devices used in this study

Device	Model	Supplier	Location
Autoclave	HST 6x6x6	Zirbus technology	Bad Grund, Germany
Centrifuge	5427R	Eppendorf	Hamburg, Germany
Centrifuge	J2-HS	Beckman Coulter	Brea, USA
Cultivation chamber	AR 75-L	Percival	Perry, USA
Cultivation chamber lamps	Alto 32 Watt	Philips	Amsterdam, Netherlands
Cultivation chamber lamps	LG4507.4	Megaman	Langenselbold, Germany
Fragment Analyzer		Advanced Analytical Technologies	Heidelberg, Germany
Lamps culture room	Lumilux L15W/84	Osram	Munich, Germany
LED greenhouse	16314L34	Schuch	Worms, Germany
Microscope	Axio Observer Z1	Carl Zeiss	Oberkochen, Germany
Optical sensor	DUALEX	Metos	Weiz, Austria
Photometer	BioPhotometer 6131	Eppendorf	Hamburg, Germany
Portable photosynthesis system	LI-6800	LI-COR Biosciences	Bad Homburg, Germany
qRT-PCR cycler	qTower3G	Analytik Jena	Jena, Germany
Sequencer	HiSeq4000	Illumina	San Diego, USA
Shaker	G10 gyratory shaker	New Brunswick Scientific	Edison, USA
Spectrophotometer	NanoDrop One	Thermo Fisher Scientific	Waltham, USA
Stereomicroscope	M205FA	Leica Microsystems	Wetzlar, Germany
Sterile bench	Hersasafe 2030o	Thermo Fisher Scientific	Waltham, USA
Sterilizer	STERI 350	Simon Keller	Burgdorf, Switzerland

Devices used in this study continued

Device	Model	Supplier	Location
Swing Mill	MM400	Retsch	Haan, Germany
Thermocycler	Labcycler Gradient	Sensoquest	Göttingen, Germany
Ultra-pure water	Arium Pro	Sartorius	Göttingen, Germany
Vibratome	VT1200	Leica	Wetzlar, Germany
Vortex	Reax top	Heidolph	Schwabach, Germany
Water Bath		PolyScience	Philadelphia, USA

7.5. Kits used in this study

Kit	Supplier	Location
innuMIX qPCR DSGreen Standard	Analytik Jena	Jena, Germany
innuPREP Plant DNA Kit	Analytik Jena	Jena, Germany
innuPREP Plant RNA Kit	Analytik Jena	Jena, Germany
RevertAid First Strand cDNA Synthesis Kit	Thermo Fisher Scientific	Waltham, USA
TruSeq RNA Library Preparation Kit v2, Set A	Illumina	San Diego, USA

7.6. Local Responses and Systemic Induced Resistance Mediated by Ectomycorrhizal Fungi

Steven Dreischhoff, Ishani S. Das, Mareike Jakobi, Karl Kasper and Andrea Polle

Author contributions:

AP conceived the study, supervised writing, and revised the manuscript. SD led the writing. ID, KK, and MJ contributed sections to the manuscript. All authors read and approved the final submission.

This article was published in *Frontiers in Plant Science* on 14th December 2020 https://doi.org/10.3389/fpls.2020.590063

frontiers in Plant Science

REVIEW
published: 14 December 2020
doi: 10.3389/fpls.2020.590063

Local Responses and Systemic Induced Resistance Mediated by Ectomycorrhizal Fungi

*Steven Dreischhoff, Ishani S. Das, Mareike Jakobi, Karl Kasper and Andrea Polle**

Forest Botany and Tree Physiology, University of Göttingen, Göttingen, Germany

Ectomycorrhizal fungi (EMF) grow as saprotrophs in soil and interact with plants, forming mutualistic associations with roots of many economically and ecologically important forest tree genera. EMF ensheath the root tips and produce an extensive extramatrical mycelium for nutrient uptake from the soil. In contrast to other mycorrhizal fungal symbioses, EMF do not invade plant cells but form an interface for nutrient exchange adjacent to the cortex cells. The interaction of roots and EMF affects host stress resistance but uncovering the underlying molecular mechanisms is an emerging topic. Here, we focused on local and systemic effects of EMF modulating defenses against insects or pathogens in aboveground tissues in comparison with arbuscular mycorrhizal induced systemic resistance. Molecular studies indicate a role of chitin in defense activation by EMF in local tissues and an immune response that is induced by yet unknown signals in aboveground tissues. Volatile organic compounds may be involved in long-distance communication between below- and aboveground tissues, in addition to metabolite signals in the xylem or phloem. In leaves of EMF-colonized plants, jasmonate signaling is involved in transcriptional re-wiring, leading to metabolic shifts in the secondary and nitrogen-based defense metabolism but cross talk with salicylate-related signaling is likely. Ectomycorrhizal-induced plant immunity shares commonalities with systemic acquired resistance and induced systemic resistance. We highlight novel developments and provide a guide to future research directions in EMF-induced resistance.

Keywords: ectomycorrhiza, systemic resistance, mycorrhiza, plant defense, phytohormone, chitin, herbivores

OPEN ACCESS

Edited by:
Paulo José Pereira Lima Teixeira, University of São Paulo, Brazil

Reviewed by:
Philipp Franken, Friedrich Schiller University Jena, Germany
Mika Tapio Tarkka, Helmholtz Centre for Environmental Research (UFZ), Germany

****Correspondence:***
Andrea Polle
apolle@gwdg.de

Specialty section:
This article was submitted to Plant Symbiotic Interactions, a section of the journal Frontiers in Plant Science

Received: *31 July 2020*
Accepted: *10 November 2020*
Published: *14 December 2020*

Citation:
Dreischhoff S, Das IS, Jakobi M, Kasper K and Polle A (2020) Local Responses and Systemic Induced Resistance Mediated by Ectomycorrhizal Fungi. Front. Plant Sci. 11:590063. doi: 10.3389/fpls.2020.590063

INTRODUCTION

Plants live in close relationship with microbes, which colonize their hosts as symbiotrophic, saprotrophic or pathogenic organisms (Bonfante and Anca, 2009; Vandenkoornhuyse et al., 2015). An important example is the beneficial interaction between certain soil fungi and plant roots, leading to the formation of a new organ, the mycorrhiza (from Greek μύκης mι kçs, "fungus," and ßζα rhiza, "root"). The mycorrhizal symbiosis is well characterized by a bidirectional exchange of nutrients (Smith and Read, 2008). The fungus receives photosynthesis-derived carbohydrates from the plant and supplies essential, often rarely available nutrients like nitrogen or phosphorus from the soil to the plant (van der Heijden et al., 2015; Nehls and Plassard, 2018).

Mycorrhizal symbiosis enhances the performance of plants (Smith and Read, 2008) and, thus, most likely drastically facilitated the evolution of land plants (Wang et al., 2010). Approximately 85 % (˜340,000 species) of all plant species are colonized by mycorrhizal fungi (˜50,000 species) (van der Heijden et al., 2015; Brundrett and Tedersoo, 2018; Genre et al., 2020). The most ancient and widely spread symbiosis is formed by arbuscular mycorrhizal fungi (AMF) (Bonfante and Anca, 2009; Martin et al., 2018). In forests of the temperate and boreal zone, ectomycorrhizal symbioses with the roots of tree species are predominant (Brundrett, 2009). Ectomycorrhizal fungi (EMF) have evolved independently multiple times from saprotrophic clades, making EMF no homogenous group (Martin et al., 2016; Genre et al., 2020). EMF and AMF are the most well studied groups among mycorrhiza-forming fungi, however, exhibiting different lifestyles. While AMF form hyphopodia to invade the plant and grow inside cortical root cells, EMF cover the root tip with a hyphal mantle and grow between the root epidermis and outer layers of cortical cells, forming the Hartig net (Bonfante and Anca, 2009). Both AMF and EMF generate extraradical hyphae as the main structures for nutrient uptake from soil.

There is now growing awareness that mycorrhizas do not only improve plant nutrition but also enhance plant resistance against abiotic and biotic cues. Resistance is the ability of a plant to restrict the growth and development or the damage caused by a specific pest or pathogen. Resistance can be achieved by activation of defense mechanisms or is the result of tolerance, i.e., the ability to endure the stress (Larcher, 1995). The term "mycorrhiza-induced resistance" (MIR) has been used to describe this phenomenon for the interaction of a mycorrhizal fungus with a host plant (Cameron et al., 2013; Mauch-Mani et al., 2017). MIR shares similarities with both systemic acquired resistance (SAR), induced after pathogen attack, while induced systemic resistance (ISR) is conferred by beneficial soil microbes. In this review, we focus on ectomycorrhiza-induced systemic resistance, which is a rapidly expanding research area. We define systemic effects as those effects that occur in distal tissues (here leaves) that are not in direct contact with the mycorrhizal fungus, while local responses occur in tissues (here roots) in contact with the EMF. We discuss local responses to EMF colonization, leading to long-distance signaling, systemic transcriptional rewiring and metabolic changes induced by EMF. We address the role of phytohormones in MIR and discuss commonalities with SAR and ISR. Since MIR by EMF is an emerging field, we also include examples for MIR induced by AMF highlighting similarities in defense activation.

A GLIMPSE ON SYSTEMIC RESISTANCE IN PLANTS—SAR AND ISR

The two major types of systemic resistance intensely studied in plant microbial interactions are SAR (Spoel and Dong, 2012) and ISR (Pieterse et al., 2014). SAR and ISR are based on distinct phytohormonal signals. SAR describes defenses against (hemi-)biotrophic pathogens activated after local challenge by a pathogen in systemic, uninfected tissues. The SAR signaling cascade is triggered by microbe-associated molecular patterns (MAMPs) leading to MAMP-triggered immunity or triggered by pathogen effectors leading to effector-triggered immunity (Jones and Dangl, 2006). Subsequently, the defense in systemic uninfected tissues is induced in an SA dependent manner and acts against a broad range of pathogens (Vlot et al., 2009; Spoel and Dong, 2012). Various compounds have been proposed as potential signals for SAR activation. For instance, methyl salicylate is a phloem-mobile compound that can be transported to systemic plant parts, where it is hydrolyzed to the bio-active SA to induce resistance (Park et al., 2007). For defense induction and in addition for attracting predators of herbivores, methyl SA might also act as a volatile signal (Shulaev et al., 1997; Koo et al., 2007; Ament et al., 2010; Rowen et al., 2017). Recently, the non-proteinogenic amino acid pipecolic acid (Pip) and its derivative N-hydroxypipecolic acid have been identified as essential for SAR signaling (Návarová et al., 2012; Chen et al., 2018; Hartmann et al., 2018; Wang et al., 2018). The mobile signals activate MAPK (MITOGEN-ACTIVATED PROTEIN KINASE) cascades (Conrath et al., 2015) and induce the expression of pathogenesis-related (PR) proteins, especially PR1 (PATHOGENESIS-RELATED 1) involving antagonistic key regulators NPR1 and NPR3/4 [NON-EXPRESSER OF PR GENES (Ding et al., 2018)]. Other compounds invoked as mobile SAR signals are azaleic acid (a C_9 lipid peroxidation product), lipid transfer proteins, and the diterpene dihydroabietinal (Vlot et al., 2017). Ultimately, an enhanced defense is achieved either through direct defenses (e.g., callose deposition) or trough priming, whereby the plant exhibits stronger defenses toward a secondary infection (Conrath et al., 2006; Jung et al., 2009, 2012; Pieterse et al., 2014; Mauch-Mani et al., 2017).

In contrast to SAR induced by pathogens, ISR is conferred by beneficial microbes. They interact with roots and make the whole plant more resistant or tolerant against stressors. The picture for ISR is less specific than for SAR because different microbial species might recruit different compounds for ISR signaling (Haney et al., 2018). In general, jasmonic acid (JA) and its derivatives, in particular JA-Isoleucine (JA-Ile) are the key phytohormones and their signaling pathways are modulated by either ethylene (defense against necrotrophic pathogens) or abscisic acid (against herbivores) (Pieterse et al., 2012). JAZ (JASMONATE-ZIM-DOMAIN PROTEIN), which stabilize the JA receptor COI1 (CORONATINE INSENSITIVE 1), and MYB (MYB DOMAIN PROTEIN) transcription factors are essential in ISR. Similar to SAR, more than one component might act as a long-distance signal (see section "Long-Distance Signaling in Systemic Resistance—Tapping Around in the Dark"). At the cellular level, the pathways for systemic defenses, ISR and SAR often appear to be regulated antagonistically. When SA signaling is upregulated, JA signaling is suppressed, implying trade-off for the resistance against necrotrophic pathogens when the defense against biotrophic pathogens is upregulated and vice versa (Pieterse et al., 2012).

SHEDDING LIGHT ON ECTOMYCORRHIZAL INDUCED DEFENSES

Defense Signaling in Local Root Tissue Interacting With EMF Unveils Commonalty With Pathogen-Triggered Responses

In the process of establishing an active symbiosis, host plant and EMF exchange an array of molecules with different properties, e.g., flavonoids, auxin, and secreted proteins, etc. (Felten et al., 2009; Garcia et al., 2015). Genome, transcriptome, and secretome analyses of EMF from distant phyla (basidiomycota: *Laccaria bicolor,* ascomycota: *Tuber melanosporu* and *Cenococcum geophilum* (Vincent et al., 2012; Doré et al., 2015; Kohler et al., 2015; Pellegrin et al., 2015; de Freitas Pereira et al., 2018) uncovered a huge battery of small secreted proteins, among which a subset was strongly up-regulated during mycorrhizal colonization of the host. Three mycorrhizal-induced small proteins, MiSSP7, 7.6, and 8 (named after their atomic mass in kDa) of *L. bicolor* were closer investigated and found to be essential for symbiosis establishment (Plett et al., 2011; Pellegrin et al., 2019; Kang et al., 2020).

In *Populus* × *canescens, Lb*MiSSP7 interacts locally with JAZ6 to stabilize this protein (Plett et al., 2014). JAZ6 is a key repressor of the F-box protein COI1, which is the receptor for JA-Ile, the active form of JA, in the SCF(COI1) complex (Thines et al., 2007). When COI1 binds JA-Ile, JAZ6 is degraded via the proteasome and the transcription of JA responsive genes is activated (Howe et al., 2018). Thus, by stabilizing *Populus* JAZ6 the JA signaling pathways is locally suppressed. Application of JA acts negatively on the establishment of symbiotic structures (Plett et al., 2014). Because of the JA-SA antagonism (see section "A Glimpse on Systemic Resistance in Plants—SAR and ISR"), this regulation is surprising as it may be intuitively expected to facilitate defenses against biotrophic fungi (including EMF). Plett et al. (2011) demonstrated that MiSSP7 also induces the transcription of auxin-responsive genes in root tissues.

Circumstantial evidence suggests that *Lb*MiSSP7.6 may also interfere with local plant immunity. *Lb*MiSSP7.6 interacts with two *Populus* Trihelix transcription factors (*Pt*Trihelix1 and *Pt*Trihelix2) in the nucleus of plant cells. The closest *Arabidopsis thaliana* homolog of *Pt*Trihelix2 is *At*ASR3 (ARABIDOPSIS SH4-RELATED3) (Kang et al., 2020), which is a phosphorylation substrate of MAPK4 and thus, may negatively regulate immunity. Furthermore, pattern-triggered immunity is negatively regulated through phosphorylation of *At*ASR3 by MAPK4 (Li et al., 2015).

Additional support for the modulation of immune responses by small secreted proteins comes from studies on the AMF-host interactions (*Glomus intraradices* with *Medicago truncatula*) (Kloppholz et al., 2011). The AMF fungal protein *Gi*SP7 (secreted protein 7) interacts with *Mt*ERF19 (ETHYLENE-RESPONSIVE FACTOR) transcription factor in the plant nucleus and interferes with *Mt*ERF19-related and, thus, ethylene-modulated defense (Kloppholz et al., 2011). Moreover, *Mt*ERF19 is induced by pathogens and is involved in activating defense against biotrophic pathogens (Kloppholz et al., 2011). Taken together, these examples show that mycorrhizal fungi interact with parts of the plants defense local machinery involving small secreted protein.

Not only small secreted protein could be responsible for the initiation of defense induction, but also a number of other metabolites. It is known for AMF that chitin oligomers and lipochitooligosaccharides are part of Myc factors, which are used for communication with their host (Maillet et al., 2011; Sun et al., 2015). These compounds are also produced by the EMF *L. bicolor* (Cope et al., 2019). In poplar, lipochitooligosaccharides from *L. bicolor* activate the common symbiosis pathway including calcium-spiking (Cope et al., 2019), which plays a role in activating defense responses to microbes (Yuan et al., 2017). Lipochitooligosaccharides were also found to modulate host immunity (Limpens et al., 2015). Furthermore, chitin and chitin-related components (e.g., chitosan) are known elicitors (MAMPs) for plant defense (Boller and Felix, 2009). Chitosan formulations have been applied as a biological control agents to leaves and roots to boost plant defenses (El Hadrami et al., 2010; Pusztahelyi, 2018) but their mode of action is unclear.

Chitin is a cell wall component of fungi but not of plants. Novel results assign a crucial role to chitin in fungal perception and defense stimulation (Zhang et al., 2015; Vishwanathan et al., 2020). When Arabidopsis roots were treated with chitin enhanced protection against leaf herbivory was observed similar to that found in response to *L. bicolor* inoculation of Arabidopsis roots (Vishwanathan et al., 2020). This finding shows that—at least part of—MIR by EMF does not require formation of a functional mycorrhiza because Arabidopsis is a non-host to mycorrhizal fungi. This result further shows that chitin, an abundant compound in many potentially hazardous organisms (fungi, insects), is sufficient for the defense induction. The plant chitin receptor CHITIN ELICITOR RECEPTOR KINASE 1 (CERK1) (Miya et al., 2007) is well known for its central role in mediating plant immunity (Gong et al., 2020). In Arabidopsis knock-out mutants *cerk1-2* MIR induced by EMF was abolished (Vishwanathan et al., 2020; **Figure 1**), demonstrating the critical role of chitin in the non-host interaction of *Arabidopsis* with *L. bicolor*. Other components such as LYK4 and LYK5 forming a complex with CEKR1 necessary for defense induction (Xue et al., 2019), may also be involved but this assumption has yet to be experimentally tested. Upon chitin or *L. bicolor* exposure, the MAP kinase signaling cascade (MAPK 3, 4, and 6) was activated in Arabidopsis (Vishwanathan et al., 2020). MAPKs belong like calcium influx and oxidative burst to the microbial triggered immunity responses (Boller and Felix, 2009), suggesting that *L. bicolor* activates a general microbial defense pathway via chitin perception. In rice, CERK1 has also a function in defense signaling and AMF symbiosis (Zhang et al., 2015).

Chitin is released from fungal cell walls by plant chitinases as part of defenses against fungal pathogens (Sharma et al., 2011). It was first reported for the interaction of *Amanita muscaria* with *Picea abies* that EMF also induce chitinases in host roots (Sauter and Hager, 1989). Similarly Albrecht et al. (1994a,b) showed that chitinases are induced upon contact of the EMF *Pisolithus tinctorius* with *Eucalyptus globulus* and

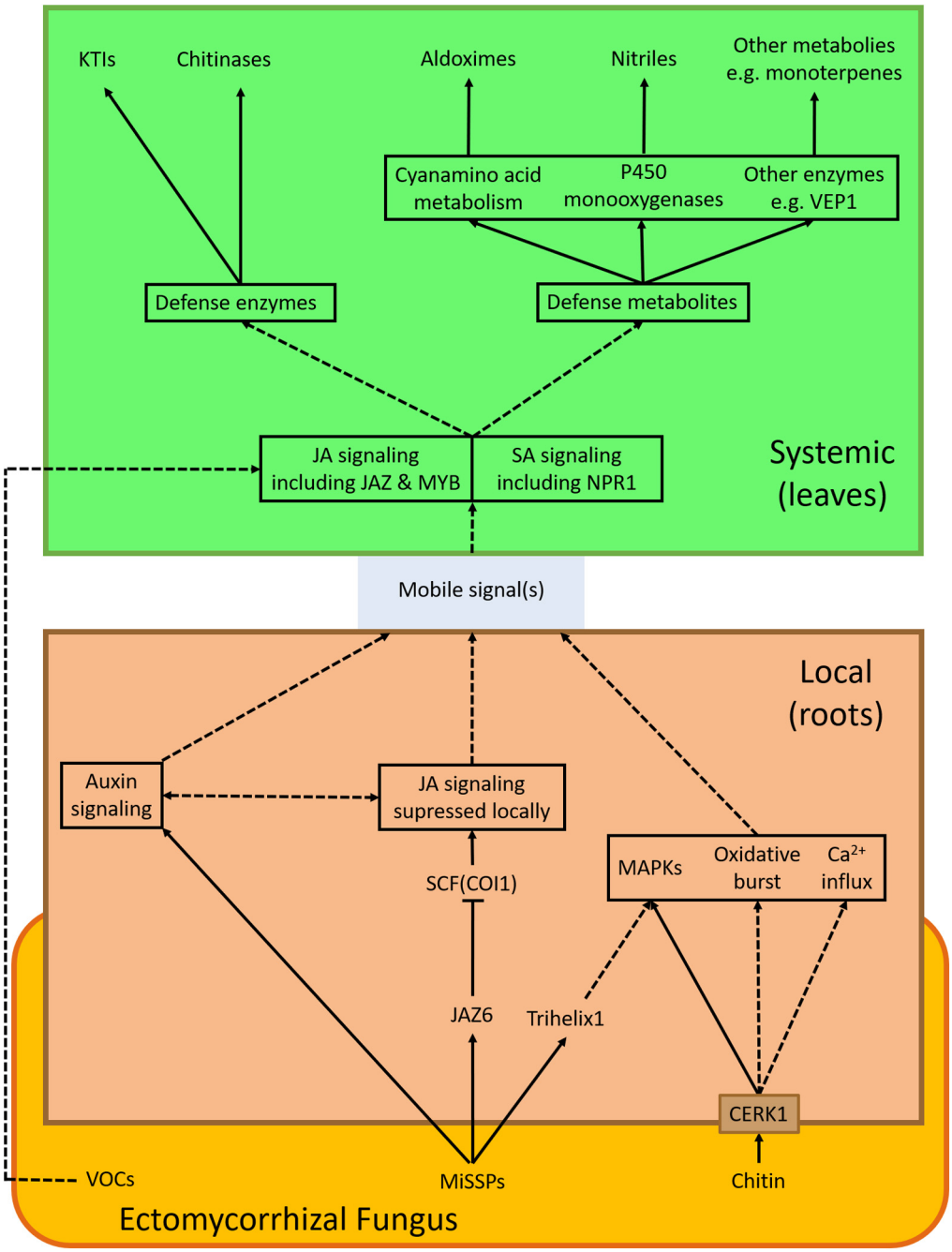

FIGURE 1 | EMF-induced signaling cascade(s). The scheme summarizes signaling components discussed in this review displaying processes induced by an ectomycorrhizal fungus (red) in the root (brown) and in leaves (green). Arrows show interactions/connections (full lines: direct evidence, dashed lines: speculative). VOCs—Volatile organic compounds; JAZ6—JASMONATE-ZIM-DOMAIN PROTEIN 6; CERK1—CHITIN ELICITOR RECEPTOR KINASE 1; SCF(COI1)—CORONATINE INSENSITIVE 1—Skp, Cullin, F-box containing complex; MAPKs—mitogen-activated protein kinases; JA—jasmonic acid; MYB—MYB DOMAIN PROTEIN; KTIs—Kunitz trypsin inhibitors; VEP1—VEIN PATTERNING 1.

that the strength of this defense response correlated with the extent of colonization by the fungus. Many previous studies showed transient transcriptional activation of chitinases in concert with other defenses (e.g., metallothionein-like proteins and glutathione-*S*-transferases) when EMF interacted with host roots (Franken and Gnädinger, 1994; Johansson et al., 2004; Duplessis et al., 2005; Frettinger et al., 2007; Heller et al., 2008).

A number of studies indicate that host colonization by EMF activates local host defenses only transiently. For example, the transcription of defense genes was locally upregulated in

birch roots during the formation of the ectomycorrhizal mantle and the Hartig net by *Paxillus involutus* (Le Quéré et al., 2005). In later developmental stages when the mycorrhiza was mature, plant defense genes were repressed (Le Quéré et al., 2005). In oak colonized by the EMF *Piloderma croceum*, genes of the phenylpropanoid metabolism were down-regulated (Tarkka et al., 2013). A recent study shows that the transcriptional responses in oak vary substantially depending on the ectomycorrhizal fungal species that is colonizing the root, but a common response induced by the tested EMF species was the reduction of defense gene transcript levels, when the roots had been colonized (Bouffaud et al., 2020). It is therefore possible that initially fungal MAMPs induce defenses, which are subsequently suppressed by mechanisms similar to those employed pathogenic fungi (Barsoum et al., 2019).

Altogether, these studies highlight that EMF locally trigger (a subset of) plant defenses against fungal pathogens, at least during the initial stages of colonization. Chitin signaling is required to elicit systemic responses in distant tissues. Intriguing questions for future research are whether MIR is part of the universal non-host response of plants to microbes or whether MIR in a functional mycorrhiza as the result of compatible EMF-host interactions has additional facets.

Long-Distance Signaling in Systemic Resistance—Tapping Around in the Dark

Mobile inter-organ signaling is required to achieve MIR in systemic tissues. The most direct and fastest connection between mycorrhizal roots and the shoot is the xylem. In addition to its function in water and mineral nutrition transport, the composition of the xylem sap is characterized by a plethora of compounds such as phytohormones, proteins, peptides, and amino acids, etc. (Shabala et al., 2016). In response to nodulation by rhizobia or symbiosis with AMF, specific small peptides (CLE) have been found (Okamoto et al., 2013; Le Marquer et al., 2019), which are part of the plant autoregulation of symbiotic interactions (Wang et al., 2018). Given the similarities of the genetic make-up of root symbiotic interactions for EMF, AMF, and rhizobia (Cope et al., 2019), it is tempting to speculate that CLE peptides may also signal the root mycorrhizal status in EMF plants. However, to date neither peptides nor phytohormones or other molecules have been identified in xylem sap that were functionally linked with MIR in EMF plants.

MIR influences the performance of phytophagous insects (Pozo and Azcón-Aguilar, 2007). Therefore, it is conceivable that JA(-derivatives), which are known to mount defenses against wounding and insect feeding (Zhang and Hu, 2017), play a role in long-distance signaling of MIR. JA-derived molecules such methyl-JA can be transported in both the xylem and the phloem (Thorpe et al., 2007). Mutants of tomato, which are unable to mount systemic defenses, revealed that the systemic wound response requires local JA biosynthesis and the ability to perceive a JA signal systemically (Schilmiller and Howe, 2005).

Vascular transport of mobile signals has most intensely been studied for SAR. The phloem was identified as the major signaling route (Shah and Zeier, 2013). Upon interaction with biotrophic pathogens or virulence factors, compounds such as the methyl ester of salicylic acid (Dempsey and Klessig, 2012), JA (Truman et al., 2007), and pipecolic acid (Shah and Zeier, 2013) accumulate in the vasculature and were able to induce SAR independently of other compounds. Azelaic acid (Jung et al., 2009), a glycerol-3-phosphate-derived molecule (Chanda et al., 2011) and the abietane diterpenoid dehydroabietinal (Chaturvedi et al., 2012) are bound to the lipid transport protein DIR1 (DEFECTIVE IN RESISTANCE1) for transport through the vasculature, leading to SAR induction (Isaacs et al., 2016). Most of the potential SAR signaling molecules accumulate in petiole exudates (Maldonado et al., 2002; Thorpe et al., 2007; Truman et al., 2007; Jung et al., 2009; Chanda et al., 2011; Sato et al., 2011; Chaturvedi et al., 2012; Champigny et al., 2013; Isaacs et al., 2016). Feeding petiole exudates of SAR-induced wildtype Arabidopsis to transgenic lines, unable to express the signaling compound glycerol-3-phosphate or *DIR1*, recovered SAR in the mutants (Chanda et al., 2011; Isaacs et al., 2016). In poplar, SA or methyl-SA can induce resistance in systemic tissues (Li et al., 2018). These phytohormones are also required for the activation flavan-3-ols synthesis as defense against rust fungi (Ullah et al., 2019). Whether SA or its derivatives also play a role in the transmission of EMF-induced signals in trees is still unknown.

In addition to the classical pathways through xylem and phloem for the directed transport of molecules, volatile organic compounds (VOCs) are undirected aerial signals, serving inter-kingdom communication between plants and fungi (Werner et al., 2016; Schulz-Bohm et al., 2017). EMF emit a rich spectrum of VOCs, dominated by mono- and sequiterpenes (Müller et al., 2013). Among these VOCs, β-caryophyllene mounts plant defenses against bacterial pathogens (Huang et al., 2012; Hammerbacher et al., 2019). Furthermore, EMF influence the VOC emission pattern of mycorrhizal poplar, leading for example to slightly suppressed ocimene levels (Kaling et al., 2018). The perception of VOCs and stimulation of defenses can be amplified, activating SAR from plant to plant (Wenig et al., 2019). Since direct evidence for genes responsive to VOCs and EMF is missing, we screened the literature for genes regulated in response to VOCs (Godard et al., 2008; Riedlmeier et al., 2017; Lee et al., 2019) overlapping with those responsive to EMF (Luo et al., 2009; Kaling et al., 2018; **Table 1**). Notably, many of these genes are involved in JA signaling and play roles in wounding or pathogen defense (*JAZ1, JAZ7, JAZ8, WRKY40,* β*-1,3-ENDO-GLUCANASE, SIS, CYP94B1, and GSTU1*; **Table 1**). These observations suggest that long-distance signaling by VOCs should be taken into account in future studies of systemic defense activation.

Mycorrhiza Induced Resistance in Systemic Tissues—Signals and Defense Activation

Phytohormones orchestrate the expression of defense-related genes in systemic tissues. In response to biotrophic pathogens,

TABLE 1 | Transcriptional regulation of Arabidopsis genes by volatile organic compounds (VOCs) and their poplar orthologs responsive to ectomycorrhiza symbiosis.

Gene name	Gene function	AGI	Regulation	Host	Treatment	Experimental set-up	Sample tissue	References
GSTU1	Glutathione S-transferase TAU 1, responsive to ME-JA	AT2G29490	Up	*P. x canescens*	*L. bicolor*	Pot, in root contact	Leaves	Kaling et al., 2018
			Up	*A. thaliana*	Monoterpene isolated from plants	Pot, exposed to Ocimene	Rosette leaves, stems, cauline leaves	Godard et al., 2008
GSTU4	Glutathione S-transferase tau 4, involved in defense from necrotrphic pathogens	AT2G29460	Up	*P. x canescens*	*P. involutus*	Pot, in root contact	Roots	Luo et al., 2009
			Up	*A. thaliana*	Monoterpene isolated from plants	Pot, exposed to Ocimene	Rosette leaves, stems, cauline leaves	Godard et al., 2008
JAZ1	JAZ1, involved in jasmonate signaling, defense, wounding. JAZ1 transcript levels rise in response to a jasmonate stimulus.	AT1G19180	Down	*P. x canescens*	*L. bicolor*	Pot, in root contact	Leaves	Kaling et al., 2018
			Up	*A. thaliana*	Monoterpene isolated from plants	Pot, exposed to Ocimene	Rosette leaves, stems, cauline leaves	Godard et al., 2008
JAZ7	Jasmonate-zim-domain protein 7; wounding response	AT2G34600	Up	*A. thaliana*	Monoterpene isolated from plants	Pot, exposed to Ocimene	Rosette leaves, stems, cauline leaves	Godard et al., 2008
			Down	*A. thaliana*	1-decene isolated from Trichoderma	Plants in petri dish, 1-decene added	shoots	Lee et al., 2019
JAZ8	Jasmonate-zim-domain protein 8; wounding response	AT1G30135	Down	*P. x canescens*	*L. bicolor*	Pot, in root contact	Leaves	Kaling et al., 2018
			Down	*A. thaliana*	1-decene isolated from Trichoderma	Plants in petri dish, 1-decene added	Shoots	Lee et al., 2019
WRKY40	Probable WRKY transcription factor 40; Pathogen-induced transcription factor, response to chitin, SA, Me-JA	AT1G80840	Up	*P. x canescens*	*P. involutus*	pot, in root contact	Roots	Luo et al., 2009
			Up	*A. thaliana*	Monoterpene isolated from plants	Pot, exposed to Ocimene	Rosette leaves, stems, cauline leaves	Godard et al., 2008
			Down	*A. thaliana*	1-decene isolated from Trichoderma	Plants in petri dish, 1-decene added	Shoots	Lee et al., 2019
			Up	*A. thaliana*	Monoterpene isolated from plants	Pot, exposed to Pinene	Leaves	Riedlmeier et al., 2017

(Continued)

TABLE 1 | Continued

Gene name	Gene function	AGI	Regulation	Host	Treatment	Experimental set-up	Sample tissue	References
SPX1	SPX domain-containing protein 1; response to phosphate starvation, response to *Pseudomonas syringae*	AT5G20150	up or down (depending on poplar homolog)	*P. x canescens*	*P. involutus*	Pot, in root contact	Roots	Luo et al., 2009
				A. thaliana	Rhizobacteria	Bi-compartmented petri dishes, no contact	Seedlings	Wenke et al., 2012
PAP1	Purple acid phosphatase, response phosphate (Pi) and phosphite (Phi), response to non-host bacteria.	AT1G13750	Down	*P. x canescens*	*P. involutus*	Pot, in root contact	Roots	Luo et al., 2009
			Up	*A. thaliana*	Monoterpene isolated from plants	Pot, exposed to Pinene	Leaves	Riedlmeier et al., 2017
BBE8	FAD-binding Berberine family protein, response avirulent *Pseudomonas synrigae*, response to non-host bacteria	AT1G30700	Up	*P. x canescens*	*P. involutus*	Pot, in root contact	Roots	Luo et al., 2009
			Up	*A. thaliana*	Monoterpene isolated from plants	Pot, exposed to Pinene	Leaves	Riedlmeier et al., 2017
-	Putative β-1,3-endoglucanase, response to nematode, response to fungus	AT4G16260	Up	*P. x canescens*	*L. bicolor*	Pot, in root contact	Leaves	Kaling et al., 2018
			Up	*A. thaliana*	Monoterpene isolated from plants	Pot, exposed to Pinene	Leaves	Riedlmeier et al., 2017
PRX47	Peroxidase superfamily protein,response to oxidative stress	AT4G33420	Down	*P. x canescens*	*L. bicolor*	Pot, in root contact	Leaves	Kaling et al., 2018
			Up	*A. thaliana*	Monoterpene isolated from plants	Pot, exposed to Pinene	Leaves	Riedlmeier et al., 2017
-	Tetratricopeptide repeat (TPR)-like superfamily protein	AT4G37380	Down	*P. x canescens*	*P. involutus*	Pot, in root contact	Roots	Luo et al., 2009
			Down	*A. thaliana*	Monoterpene isolated from plants	Pot, exposed to Pinene	Leaves	Riedlmeier et al., 2017

(Continued)

TABLE 1 | Continued

Gene name	Gene function	AGI	Regulation	Host	Treatment	Experimental set-up	Sample tissue	References
SIS	Salt Induced Serine rich, response to salt, response to virulent *Pseudomonas syringae*	AT5G02020	Up	*P. x canescens*	*P. involutus*	Pot, in root contact	Roots	Luo et al., 2009
			Up	*A. thaliana*	Monoterpene isolated from plants	Pot, exposed to Pinene	Leaves	Riedlmeier et al., 2017
KAT5	3-keto-acyl-CoA thiolase 2 precursor, involved in flavonoid biosynthesis	AT5G48880	Up	*P. x canescens*	*L. bicolor*	Pot, in root contact	Leaves	Kaling et al., 2018
			Down	*A. thaliana*	Monoterpene isolated from plants	Pot, exposed to Pinene	Leaves	Riedlmeier et al., 2017
CCT101	Member of ASML2 family of CCT domain proteins, high expression in eds16 mutants (isochorimate synthase for SA synthesis)	AT5G53420	Down	*P. x canescens*	*L. bicolor*	Pot, in root contact	Leaves	Kaling et al., 2018
			Down	*A. thaliana*	Monoterpene isolated from plants	Pot, exposed to Pinene	Leaves	Riedlmeier et al., 2017
CYP94B1	cytochrome P450, family 94, subfamily B, polypeptide 1, JA metabolic process, wounding	AT5G63450	Down	*P. x canescens*	*L. bicolor*	Pot, in root contact	Leaves	Kaling et al., 2018
			Down	*A. thaliana*	Monoterpene isolated from plants	Pot, exposed to Pinene	Leaves	Riedlmeier et al., 2017

The table summarizes differentially expressed genes overlapping between VOC and EMF response. AGI shows Arabidopsis Gene Identity for the best poplar match. Treatment indicates the EMF used for plant inoculation or the VOC to which plants were exposed to. Experimental set-up indicates non-sterile conditions when plants were grown in pots or sterile growth systems. The gene functions were taken from the TAIR data base (https://www.arabidopsis.org/) and response were also searched via the eFP browser implemented in TAIR.

accumulation of SA is accompanied by the induction of *PR* (Pathogenesis-related) gene expression (Dixon et al., 1994; Hammond-Kosack and Jones, 1997; Brodersen et al., 2005; Radojičić et al., 2018). The most prominent representative of the PR proteins is PR1, which is characteristic for the SA defense pathway (Nimchuk et al., 2003; Durrant and Dong, 2004; Glazebrook, 2005). AMF can activate SA defenses in their host plants (Barea and Jeffries, 1995; García-Garrido and Ocampo, 2002). AMF-colonized crops exhibit enhanced resistance against *Phytophthora infestans* (potato, Gallou et al., 2011), *Magnaporthe oryzae* (rice, Campos-Soriano et al., 2012), and *Alternaria solani* (tomato, Song et al., 2015). The defense induction was attributed to MIR by AMF (**Table 2**) and has similarities with SAR (see section "A Glimpse on Systemic Resistance in Plants—SAR and ISR").

Likewise, the EMF-induced systemic resistance also involves components of SAR signaling. The fitness of caterpillars feeding on SAR signaling mutants of Arabidopsis (*npr1, npr3/4*) was reduced, similar to the effects imposed by *L. bicolor* inoculation (Vishwanathan et al., 2020). In poplar leaves, transcriptional regulation of *NPR1* was detected in EMF-colonized compared to non-colonized plants (Kaling et al., 2018). Pfabel et al. (2012) observed enhanced levels of SA in poplars colonized by the EMF *Hebeloma mesophaeum* as well as in poplars challenged with rust fungi *Melampsora larici-populina.* Therefore, it is likely that similarly to AMF, EMF systemically activate components of the SAR pathway (**Figure 1**).

In AMF, the induction of down-stream defenses against pathogens is often less pronounced than by SAR and therefore, the alerted stage induced by mycorrhizal colonization has been considered as "priming" (Cameron et al., 2013). As defined by Pozo and Azcón-Aguilar (2007), the phenomenon of priming is the pre-conditioning of the plant host for a more efficient activation of plant defenses upon pathogen attack (Jung et al., 2012). "Priming" by AMF involves, for instance, transcriptional regulation of *PR1* and *NPR1*, hallmarks of the SA pathway (Cameron et al., 2013). However, AMF also prime the JA pathway in the host plant as an "alert" signal against necrotrophic pathogens and leaf-chewing insects (Glazebrook, 2005; Pozo and Azcón-Aguilar, 2007; Jung et al., 2012). These responses include transcriptional regulation of *MYBs* (many of these transcription factors are induced by JA), *LOX* (*LIPOXYGENASE*), *OPR* (*12−OXOPHYTODIENOATE REDUCTASE*), *COI* (*CORONATINE−INSENSITIVE*), *AOC* (*ALLENE OXIDE CYCLASE*), and *AOS* (*ALLENE OXIDE SYNTHASE*) etc. (**Table 2**). While most studies tested alleviation of damage by necrotrophic pathogens (**Table 2**), increased resistance against herbivores such as cabbage looper (*Trichoplusia ni*) and cotton bollworm (*Helicoverpa armigera*) was also reported for AMF crops (Song et al., 2013; Schoenherr et al., 2019).

Ecological studies often show beneficial effects of EMF-colonization on the resistance of tree species from different habitats and different phylogenetic origin, e.g., *Larix sibirica, Betula pubescens,* and *Eucalyptus urophylla* against herbivores (*Otiorhyncus* spp., *Anomala cupripes*, and *Strepsicrates* spp. (Halldórsson et al., 2000; Gange et al., 2005; Shen et al., 2015). For example, on the leaves of birch, the birch aphid *Calaphis flava* produces significantly less nymphs when the trees are colonized with EMF (*Paxillus involutus* or *Leccinum versipelle*) compared with non-mycorrhizal trees (Nerg et al., 2008). However, beneficial effects of EMF on the host are not always observed. Larval growth of the autumnal moth *Epirrita autumnata* was not attenuated on EMF-colonized birch trees (Nerg et al., 2008) and EMF colonization of pine roots had no effect on the oviposition of generalist herbivore *Lygus rugulipennis* (Manninen et al., 1998). These studies suggest that the resistance induced by EMF is context-dependent. This idea is also supported by recent transcriptome analyses showing that host defense gene expression of leaves can be diminished when the tree roots are colonized by EMF and depends on the specific host—EMF combination (Maboreke et al., 2016; Bacht et al., 2019; Bouffaud et al., 2020).

Genetic studies exploring the systemic consequences of EMF-plant interaction are scarce. Arabidopsis knock-out mutants of *coi1-16*, which cannot activate the JA pathway, are more susceptible to cabbage looper feeding than the wildtype, indicating that the protective effect of *L. bicolor* is lost when the JA signaling is compromised (Vishwanathan et al., 2020). In poplar, *L. bicolor* induced a transcriptional network characterized by six major gene ontology (GO) terms: "regulation of phytohormones," "immune response," "response to wounding," "flavonoid metabolism," "secondary metabolism," and "response to toxic substance" (**Figure 2**). "Regulation of phytohormones" and "immune response" comprise mainly transcription factors such as *JAZ1* (orthologs of *JAR1* and *JAR8*) and *MYBs* (orthologs of *MYB4, MYB5, MYB14,* and *MYB108*) which are key the regulators of the JA responses (Goossens et al., 2016). Altogether, these studies imply that regulation of MIR by EMF involves both JA and SA signaling pathways (**Figure 1**).

Induction of JA and SA-related gene expression also occurs in beneficial fungi, which do not form mycorrhizal structures such as *Serpendita indica* (formerly known as *Piriformospora indica,* Sebacinales, Basidiomycota), and *Trichoderma* sp. (Basidiomycota) (**Table 2**). *Serpendita indica* activates *PR1* as well as PDF1.2 (defensin) expression in its host (Stein et al., 2008; Molitor et al., 2011). *Trichoderma harzianum* induces JA- and SA-dependent defenses against *Botrytis cineria* by stimulating defense proteins such as PROTEINASE INHIBITOR II and MULTICYSTATIN (Martinez-Medina et al., 2013). *Trichoderma* sp., which is available as commercial inoculum, has often been reported to be a potent biocontrol agent against pathogens (Sharon et al., 2011; Kumar and Ashraf, 2017). For example, in cucumber *Trichoderma harzianum* caused an increased expression of defense genes [*PR*4, *LOX* (lipoxygenase), *GOL* (galactinol synthase)] against the damping-off disease caused by the pathogen *Phytophthora melonis* (Sabbagh et al., 2017). Similar responses were also observed for the AMF *Glomus mosseae*, suggesting that both are effective in diminishing diseases (Sabbagh et al., 2017). Under field conditions, it is also possible that the induction SA and JA-dependent defenses is the consequence of an interaction of AMF (inducing SA defenses) and beneficial rhizobacteria (inducing JA defense) (Cameron et al., 2013). Similar interactions are feasible for

TABLE 2 | Systemic defense activation by mycorrhizal plants.

Gene name	Gene function	Proposed defense pathway	Mycorrhiza Type	Mycorrhiza species	Effects of mycorrhiza	Plant host	Resistance against	Disease/Effect	References
PMR4	Callose synthase	JA pathway	AMF	*Rhizoglomus irregularis*	Fungal biomass- *B. cinerea* reduced to 66%	Tomato- *Solanum lycopersicum*	Fungus- *Botrytis cinerea*	Gray mold	Sanmartín et al., 2020
ATL31	Carbon/Nitrogen insensitive 1(Arabidopsis Toxicos en Levadura 31)								
SYP121	Vesicular trafficking protein								
VCH3	Chitinase	Chitinase induced defense pathway	AMF	*Glomus versiforme*	Significant reduction in *M. incognita* infection	Grapevine- *Vitis amurensis*	Nematode- *Meloidogyne incognita*	Root knot	Li et al., 2006
CHI	Chitinase 1b	JA and SA pathway	AMF	*Glomus intraradices*	*X. index* count in soil and galls reduced significantly (after 35 days)	Grapevine- *Vitis berlandieri* × *Vitis riparia*	Nematode- *Xiphinema index*	Root gall	Hao et al., 2012
PR10	Pathogenesis-related 10								
GST	Glutathione S-transferase								
STS	Stilbene synthase 1								
ESPS	5-enolpyruvyl shikimate-3-phosphate synthase								
PR1-a	Pathogenesis-related 1	SA pathway	AMF	*Glomus mosseae*	74—84% decrease in necroses andintraradical pathogen hyphae of *P. phytophthora*	Tomato- *Solanum lycopersicum*	Pathogen- *Phytophthora parasitica*	Fruit rot	Cordier et al., 1998
OsNPR1	Non-expressor of PR1	JA and SA pathway	AMF	*Glomus intraradices*	Significant reduction in spore count of *M. oryzae*	Rice- *Oryza sativa L.*	Fungus- *Magnaporthe oryzae*	Rice blast	Campos-Soriano et al., 2012
OsAP2	APETALA2								
OsEREBP	Ethylene-responsive element-binding protein								
OsJAmyb	JA-regulated myb transcription factor								
PR	Pathogenesis-related								

(Continued)

TABLE 2 | Continued

Gene name	Gene function	Proposed defense pathway	Mycorrhiza Type	Mycorrhiza species	Effects of mycorrhiza	Plant host	Resistance against	Disease/Effect	References
PR2a	Pathogenesis-related 2a	DIMBOA-phytoalexin based defense and JA pathway	AMF	*Glomus mosseae*	Disease index of *R. solani* reduced by 50%	Corn- *Zea mays*	Fungus- *Rhizoctonia solani*	Sheath blight	Song et al., 2011
PAL	Phenylalanine ammonia-lyase								
AOS	Allene oxide synthase								
BX9	DIMBOA (2,4-dihydroxy-7-methoxy-2 H-1,4-benzoxazin-3(4 H)-one) biosynthesis pathway gene								
PR1, PR2	Pathogenesis-related 1, pathogenesis-related 2	SA pathway	AMF	*Glomus* sp.	Leaf infection index decreased significantly.	Potato- *Solanum tuberosum*	Pathogen- *Phytophthora infestans*	Late blight	Gallou et al., 2011
POX381	Peroxidase	SA pathway	AMF	*Funneliformis mosseae*	*B. graminis* infection on leaves reduced to 78%.	Wheat- *Triticum* sp.	Fungus- *Blumeria graminis f.* sp. *Tritici*	Powdery mildew	Mustafa et al., 2017
PAL	Phenylalanine ammonia lyase								
CHI1	Chitinase 1								
NPR1	Non-expressor of pathogenesis-related proteins 1								
PAL	Phenylalanine ammonia lyase	JA pathway	AMF	*Glomus Macrocarpum; Glomus Fasciculatum*	*F. oxysporum* disease severity reduced to ∼ 75%	Tomato- *Solanum lycopersicum*	Fungus- *Fusarium Oxysporum f.* sp. *Lycopersici*	Fusarium wilt	Kapoor, 2008
LOX	Lipoxygenase	JA pathway	AMF	*Glomus fasciculatum*	Significant decrease in the severity of fusarium wilt disease.	Tomato- *Solanum lycopersicum*	Fungus- *Fusarium Oxysporum f.* sp. *Lycopersici*	Fusarium wilt	Nair et al., 2015

(Continued)

TABLE 2 | Continued

Gene name	Gene function	Proposed defense pathway	Mycorrhiza Type	Mycorrhiza species	Effects of mycorrhiza	Plant host	Resistance against	Disease/Effect	References
LOX	Lipoxygenase	JA pathway	AMF	*Glomus fasciculatum*	Decrease in disease severity of *A. alternata*	Tomato- *Solanum lycopersicum*	Pathogen-*Alternaria alternata*	Fruit rot	Nair et al., 2015
OPR3	12-oxophytodienoate reductase 3								
COI1	Coronatine-insensitive1								
PR1, PR2, PR3	Pathogenesis related1, Pathogenesis related 2, Pathogenesis related 3	JA and SA pathway	AMF	*Funneliformis mosseae*	Disease index of *A. solani* reduced by 54.3%	Tomato- *Solanum lycopersicum*	Pathogen- *Alternaria solani*	Early blight	Song et al., 2015
LOX	Lipoxygenase								
AOC	Allene oxide cyclase								
PAL	Phenylalanine ammonia-lyase								
LOXD	Lipoxygenase D	JA pathway	AMF	*Glomus mosseae*	62.3% less weight gain of *H. arimegera* larvae	Solanum lycopersicum Mill.	Insect- *Helicoverpa arimigera*	Herbivory	Song et al., 2013
AOC	Allene oxide cyclase								
PI-I and PI-II	Serine protease inhibitors I and II								
AOS1	Allene oxide synthase 1	JA pathway, phenylpropanoid pathway and protease inhibitor activity	AMF	*Rhizophagus irregularis*	Larvae weigh ∼40 mg which is significantly lower than the control (after 8 days).	Potato- *Solanum tuberosum*	Insect- *Trichoplusia ni*	Herbivory	Schoenherr et al., 2019
OPR3	12-oxo-phytodienoate reductase 3								
PI-I	Protease inhibitor type								
PAL	Phenylalanine ammonia lyase								

(Continued)

TABLE 2 | Continued

Gene name	Gene function	Proposed defense pathway	Mycorrhiza Type	Mycorrhiza species	Effects of mycorrhiza	Plant host	Resistance against	Disease/Effect	References
JAZ(JAR1, JAR8)	Jasmonate zim domain 1	JA pathway	EMF	*Laccaria bicolor*	Significant less oviposition by beetles on mycorrhizal host plant.	Poplar- *Populus* × *canescens*	Insect- *Chrysomela populi*	Herbivory	Kaling et al., 2018
MYB (MYB4, MYB5, MYB14 and MYB108)	Transcription factors of JA								
NAS3	Nicotianamine synthase								
KPI	Kunitz protease inhibitors								
CHI	Chitinases								
CERK1	Chitin receptor	Both JA and SA pathway	EMF	*Laccaria bicolor*	27% reduction in larval weight on *L. bicolor* colonized host plant.	Arabidopsis	Insect- *Trichoplusia ni*	Herbivory	Vishwanathan et al., 2020
PR1, PR2 and PR5	Pathogenesis related 1, Pathogenesis related 2, Pathogenesis related 5	SA pathway	Endophyte	*Piriformospora indica*	33—59% reduction in colony numbers of *B. graminis*	Barley- *Hordeum vulgare*	Fungus- *Blumeria graminis f.* sp. *Hordei*	Powdery mildew	Molitor et al., 2011
Hsp70, Hsp17.9	Heat shock proteins70; Heat shock proteins17.9								
BCI-7	Barley chemically induced 7								
PR1, PR5	Pathogenesis-related 1, Pathogenesis-related 5	JA and SA pathway	Endophyte	*Piriformospora indica*	∼ 50% reduction in the number of conidia of *G. orontii* formed per mycelium.	Arabidopsis	Fungus- *Golovinomyces orontii*	Powdery mildew	Stein et al., 2008
ERF1	Ethylene response factor 1								
PDF1.2	Plant defensin 1.2								
VSP	Vegetative storage protein								

Symbiotic relationships between mycorrhiza and plants were reviewed with regard to the defense induction by mycorrhiza. Genes were grouped upon their function as well as their effect on the disease of pathogens on their hosts.

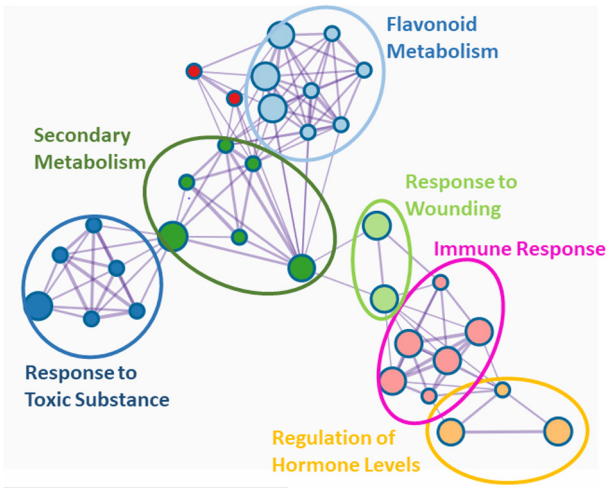

FIGURE 2 | Network of GO terms in systemic leaves after ectomycorrhizal colonization of poplar. Data of differentially expressed genes (DEGs) between mycorrhizal and non-mycorrhizal trees were taken from the Supplemental Table S1 in Kaling et al. (2018). It should be noted that many DEGS were down regulated. The best matches of Arabidopsis orthologs of the poplar genes were uploaded and analyzed in Metascape (Zhou et al., 2019). Significant GO terms ($P_{adjusted} < 0.05$) are shown.

EMF and mycorrhizal helper bacteria, which might be able to boost plant tolerance by growth stimulation (Labbé et al., 2014; Zhao et al., 2014).

Mycorrhiza Induced Resistance in Systemic Tissues—Preparing the Weapons

In practical terms, the production of defense enzymes and defense metabolites including VOCs are important for enhanced resistance. Enzymes such as peroxidases (PRX), polyphenol oxidases, and laccases and their substrates (phenolic compounds) are important to strengthen the cell wall, thereby, erecting barriers against the spreading of pathogens (Carroll and Hoffman, 1980; Darvill and Albersheim, 1984; Baldwin, 1988). Other enzymes (defensins, chitinases, etc.) have antibiotic activities by attenuating pathogens' growth (Freeman and Beattie, 2008; War et al., 2012). In poplar colonized by *L. bicolor* the transcript levels of putative chitinases (Kaling et al., 2018) and in *Eucalyptus* colonized by *Pisolithus tinctorius* the activity of chitinases were increased in systemic leaves (Albrecht et al., 1994c; **Figure 1**). Chitinases hydrolyze glycosidic bonds of chitin, a constituent of the insect exoskeletons and thereby, affect the fitness of herbivores or pathogenic fungi.

An important class of proteins acting as a biocidal compounds against insect-herbivores are the protease inhibitors (PIs) (Conconi et al., 1996; Lawrence and Koundal, 2002; Kim et al., 2009; Dunse et al., 2010). Proteases are vital gut enzymes of insects. PIs disturb the activity of proteases, thus, reducing the overall fitness of herbivorous insects (Zhu-Salzman and Zeng, 2015). PIs have also antimicrobial activities inhibiting the physiological development of pathogens (Jashni et al., 2015). EMF colonization of poplar results in upregulated transcription of Kunitz Trypsin Inhibitors (KTI, a class of PIs) and is accompanied by negative consequences for oviposition (Kaling et al., 2018). AMF colonization of crop plants (potato, tomato) affects *PI* expression, leads to reduced diet quality for larvae of *Trichoplusia ni* and *Helicoverpa armigera,* and reduced growth of the caterpillars (Song et al., 2013; Schoenherr et al., 2019). Therefore, we speculate that PIs are part of the systemically induced defense, irrespective of the mycorrhizal type.

Enzymes commonly induced for biotic defense and involved in MIR are the LOXs (lipoxygenases) (Feussner and Wasternack, 2002; Kawano, 2003; La Camera et al., 2004; Shah, 2005; Baysal and Demirdöven, 2007). LOXs catalyze the hydroperoxidation of polyunsaturated fatty acids (Rosahl, 1996). The resulting hydroperoxides are used as substrates by AOS activating JA-based defenses or by hydroperoxide lyase stimulating "volatile phytoalexins" production (Bate and Rothstein, 1998; Wasternack, 2007; Bruinsma et al., 2009; Lyons et al., 2013; Zhou et al., 2014). In AMF colonized tomato plants upregulation of LOX is associated with defense responses against fungal pathogens (*Alternaria solani*, *Alternaria alternata*, *Fusarium oxysporum*) and cotton bollworm (Song et al., 2013, 2015; Nair et al., 2015).

EMF colonization of roots does not only trigger defense proteins but also results in changes of the leaf metabolome (Pfabel et al., 2012; Cameron et al., 2013; Adolfsson et al., 2017; Hill et al., 2018; Kaling et al., 2018). The compounds mainly involved in enhancing plant tolerance or resistance can be chemically categorized as terpenes, phenolic compounds, nitrogenous, and sulfurous compounds (Mazid et al., 2011; Pedone-Bonfim et al., 2015; Wink, 2018). The terpenes and terpenoids comprise a large class of plant metabolites. Many of these compounds are VOCs, which increase drastically in response to herbivory ("Herbivore-Induced Plant Volatiles", Pieterse et al., 2014). VOCs act as repellents for herbivores or as attractants to other arthropods that prey upon or parasitize herbivores (Loreto and Schnitzler, 2010). These ecologically important VOCs are produced by the plant down-stream the JA signaling pathway (Ament et al., 2004; van Schie et al., 2007). Since a role of VOCs for plant-insect interactions has often been reviewed (Holopainen and Gershenzon, 2010; Bouwmeester et al., 2019), we illustrate this area just by few selected examples: β-ocimene (monoterpene) and β-caryophyllene (sesquiterpene) emissions are enhanced by AMF-colonized bean plants and recruit natural predators of spider mites (Schausberger et al., 2012). In tomato, AMF colonization enhanced terpene levels and defenses against larvae of the beet armyworm (Shrivastava et al., 2015).

Phenolic compounds are part of the plant defense arsenal and often higher in EMF than in non-mycorrhizal plants (Gange and West, 1994; Baum et al., 2009; Fontana et al., 2009; Schweiger et al., 2014). While phenol-based compounds enhance antibiosis, e.g., against rust (Pfabel et al., 2012), they are not effective against adapted herbivores such as lepidopteran species feeding on Salicaceae (Lindroth and St. Clair, 2013; Boeckler et al., 2014). For example, poplar leaf beetle (*Chrysomela populii*) prefers phenolic-rich leaves (Behnke et al., 2010). Therefore, transcriptional down-regulation of enzymes required for production of secondary compounds (e.g., tannins,

flavonoids, phenolic glycosides, proanthocyanidin dimers, and trimers) in EMF-colonized poplar and upregulation of aldoxime production suggests that MIR triggers a metabolic shift from carbon-based to N-based defense (Kaling et al., 2018). Aldoximes and other nitrile-derived compounds are very effective herbivore repellents (Irmisch et al., 2013, 2014; McCormick et al., 2014). The changes induced in systemic tissues by EMF are often subtle or unfold only after biotic attack. Therefore, it will be important to enhance research with a wider range of model systems such as poplar, oak, and conifers, etc., that are amenable to functional studies by transgenic approaches and can be handled under controlled conditions.

CONCLUSION

The field of EMF-induced systemic resistance is still scattered but putting the puzzle pieces together, a picture is starting to emerge. EMF in contact with local tissue (roots) activate systemic induced resistance via chitin receptors in Arabidopsis. Since Arabidopsis is a non-host for any mycorrhizal interaction, it will be important to show whether chitin also plays a fundamental role in triggering MIR in EMF-host interactions. EMF-host interactions often positively influence resistance against biotrophic pathogens and herbivory in leaves. The nature of long-distance signaling from roots to leaves remains elusive. Besides vascular routes, aerial transmission via VOCs cannot be excluded (Ditengou et al., 2015). In addition to other effects, systemic leaves show suppressed expression of JAZ transcription factors, whereby transcription of defense proteins and enzymes for the production of defense metabolites is set on. Collectively, studies on AMF or EMF inoculated plants point to activation of JA-related pathways. Still, the recruitment of SA-related defense cannot be dismissed because an involvement of NPR1 and NPR3/4 (positive and negative regulators of SA) has been shown for EMF-induced systemic resistance. The defense responses are versatile. Most of our current knowledge on EMF-activated defenses stems from poplar. Since poplars can be colonized by both EMF and AMF (Khasa et al., 2002; Liu et al., 2015), an increased understanding of MIR requires comparative studies of AMF- and EMF-induced systemic resistance in this host species as well as additional investigations with tree species that can only be colonized by EMF. Since different tree species exhibit a vast range of secondary compounds, there is much work ahead to better understand pathways, which stimulate tree-specific defenses. This is an important task for the future. Since climate change is affecting plant-pest interactions for the worse (Linnakoski et al., 2019), more insights into resistance mechanisms are urgently needed to guide tree selection and breeding for stable future forests.

AUTHOR CONTRIBUTIONS

AP conceived the study, supervised writing, and revised the manuscript. SD led the writing. ID, KK, and MJ contributed sections to the manuscript. All authors read and approved the final submission.

FUNDING

The work in AP's laboratory is funded by German Science Foundation (DFG). SD, ID, and KK were supported in the framework of the International Research Training Group "PRoTECT" (IRTG 2172, M1 and M2.2) and MJ by project Poplar Communication (PO362/20-2).

ACKNOWLEDGMENTS

We are grateful to our laboratory technicians for permanent excellent support.

REFERENCES

Adolfsson, L., Nziengui, H., Abreu, I. N., Šimura, J., Beebo, A., Herdean, A., et al. (2017). Enhanced secondary- and hormone metabolism in leaves of arbuscular mycorrhizal *Medicago truncatula*. *Plant Physiol.* 175, 392–411. doi: 10.1104/pp.16.01509

Albrecht, C., Asselin, A., Piché, Y., and Lapeyrie, F. (1994a). Chitinase activities are induced in Eucalyptus globulus roots by ectomycorrhizal or pathogenic fungi, during early colonization. *Physiol. Plant.* 91, 104–110. doi: 10.1111/j.1399-3054.1994.tb00665.x

Albrecht, C., Burgess, T., Dell, B., and Lapeyrie, F. (1994b). Chitinase and peroxidase activities are induced in eucalyptus roots according to aggressiveness of Australian ectomycorrhizal strains of Pisolithus sp. *New Phytol.* 127, 217–222. doi: 10.1111/j.1469-8137.1994.tb04273.x

Albrecht, C., Laurent, P., and Lapeyrie, F. (1994c). Eucalyptus root and shoot chitinases, induced following root colonization by pathogenic versus ectomycorrhizal fungi, compared on one- and two-dimensional activity gels. *Plant Sci.* 100, 157–164. doi: 10.1016/0168-9452(94)90071-X

Ament, K., Kant, M. R., Sabelis, M. W., Haring, M. A., and Schuurink, R. C. (2004). Jasmonic acid is a key regulator of spider mite-induced volatile terpenoid and methyl salicylate emission in tomato. *Plant Physiol.* 135, 2025–2037. doi: 10.1104/pp.104.048694

Ament, K., Krasikov, V., Allmann, S., Rep, M., Takken, F. L. W., and Schuurink, R. C. (2010). Methyl salicylate production in tomato affects biotic interactions. *Plant J.* 62, 124–134. doi: 10.1111/j.1365-313X.2010.04132.x

Bacht, M., Tarkka, M. T., López, I. F., Bönn, M., Brandl, R., Buscot, F., et al. (2019). Tree response to herbivory is affected by endogenous rhythmic growth and attenuated by cotreatment with a mycorrhizal fungus. *Mol. Plant Microbe Interect* 32, 770–781. doi: 10.1094/MPMI-10-18-0290-R

Baldwin, I. T. (1988). Short-term damage-induced increases in tobacco alkaloids protect plants. *Oecologia* 75, 367–370. doi: 10.1007/BF00376939

Barea, J. M., and Jeffries, P. (1995). "Arbuscular mycorrhizas in sustainable soil-plant systems," in *Mycorrhiza*, eds A. Varma and B. Hock (Berlin: Springer), 521–560. doi: 10.1007/978-3-662-08897-5_23

Barsoum, M., Sabelleck, B., Spanu, P. D., and Panstruga, R. (2019). Rumble in the effector jungle: candidate effector proteins in interactions of plants with powdery mildew and rust fungi. *Crit. Rev. Plant. Sci.* 38, 255–279. doi: 10.1080/07352689.2019.1653514

Bate, N. J., and Rothstein, S. J. (1998). C6-volatiles derived from the lipoxygenase pathway induce a subset of defense-related genes. *Plant J.* 16, 561–569. doi: 10.1046/j.1365-313x.1998.00324.x

Baum, C., Toljander, Y. K., Eckhardt, K.-U., and Weih, M. (2009). The significance of host-fungus combinations in ectomycorrhizal symbioses for the chemical

quality of willow foliage. *Plant Soil* 323, 213–224. doi: 10.1007/s11104-009-9928-x

Baysal, T., and Demirdöven, A. (2007). Lipoxygenase in fruits and vegetables: a review. *Enzyme Microb. Technol.* 40, 491–496. doi: 10.1016/j.enzmictec.2006.11.025

Behnke, K., Kaiser, A., Zimmer, I., Brüggemann, N., Janz, D., Polle, A., et al. (2010). RNAi-mediated suppression of isoprene emission in poplar transiently impacts phenolic metabolism under high temperature and high light intensities: a transcriptomic and metabolomic analysis. *Plant. Mol. Biol.* 74, 61–75. doi: 10.1007/s11103-010-9654-z

Boeckler, G. A., Towns, M., Unsicker, S. B., Mellway, R. D., Yip, L., Hilke, I., et al. (2014). Transgenic upregulation of the condensed tannin pathway in poplar leads to a dramatic shift in leaf palatability for two tree-feeding Lepidoptera. *J. Chem. Ecol.* 40, 150–158. doi: 10.1007/s10886-014-0383-7

Boller, T., and Felix, G. (2009). A renaissance of elicitors: perception of microbe-associated molecular patterns and danger signals by pattern-recognition receptors. *Annu. Rev. Plant Biol.* 60, 379–406. doi: 10.1146/annurev.arplant.57.032905.105346

Bonfante, P., and Anca, I.-A. (2009). Plants, mycorrhizal fungi, and bacteria: a network of interactions. *Annu. Rev. Microbiol.* 63, 363–383. doi: 10.1146/annurev.micro.091208.073504

Bouffaud, M.-L., Herrmann, S., Tarkka, M. T., Bönn, M., Feldhahn, L., and Buscot, F. (2020). Oak displays common local but specific distant gene regulation responses to different mycorrhizal fungi. *BMC Genomics* 21:399. doi: 10.1186/s12864-020-06806-5

Bouwmeester, H., Schuurink, R. C., Bleeker, P. M., and Schiestl, F. (2019). The role of volatiles in plant communication. *Plant J.* 100, 892–907. doi: 10.1111/tpj.14496

Brodersen, P., Malinovsky, F. G., Hématy, K., Newman, M.-A., and Mundy, J. (2005). The role of salicylic acid in the induction of cell death in Arabidopsis acd11. *Plant Physiol.* 138, 1037–1045. doi: 10.1104/pp.105.059303

Bruinsma, M., Posthumus, M. A., Mumm, R., Mueller, M. J., van Loon, J. J. A., and Dicke, M. (2009). Jasmonic acid-induced volatiles of Brassica oleracea attract parasitoids: effects of time and dose, and comparison with induction by herbivores. *J. Exp. Bot.* 60, 2575–2587. doi: 10.1093/jxb/erp101

Brundrett, M. C. (2009). Mycorrhizal associations and other means of nutrition of vascular plants: understanding the global diversity of host plants by resolving conflicting information and developing reliable means of diagnosis. *Plant Soil* 320, 37–77. doi: 10.1007/s11104-008-9877-9

Brundrett, M. C., and Tedersoo, L. (2018). Evolutionary history of mycorrhizal symbioses and global host plant diversity. *New Phytol.* 220, 1108–1115. doi: 10.1111/nph.14976

Cameron, D. D., Neal, A. L., van Wees, S. C. M., and Ton, J. (2013). Mycorrhiza-induced resistance: more than the sum of its parts? *Trends Plant Sci.* 18, 539–545. doi: 10.1016/j.tplants.2013.06.004

Campos-Soriano, L., García-Martínez, J., and Segundo, B. S. (2012). The arbuscular mycorrhizal symbiosis promotes the systemic induction of regulatory defence-related genes in rice leaves and confers resistance to pathogen infection. *Mol. Plant Pathol.* 13, 579–592. doi: 10.1111/j.1364-3703.2011.00773.x

Carroll, C. R., and Hoffman, C. A. (1980). Chemical feeding deterrent mobilized in response to insect herbivory and counteradaptation by Epilachna tredecimnotata. *Science* 209, 414–416. doi: 10.1126/science.209.4454.414

Champigny, M. J., Isaacs, M., Carella, P., Faubert, J., Fobert, P. R., and Cameron, R. K. (2013). Long distance movement of DIR1 and investigation of the role of DIR1-like during systemic acquired resistance in Arabidopsis. *Front. Plant Sci.* 4:230. doi: 10.3389/fpls.2013.00230

Chanda, B., Xia, Y., Mandal, M. K., Yu, K., Sekine, K.-T., Gao, Q., et al. (2011). Glycerol-3-phosphate is a critical mobile inducer of systemic immunity in plants. *Nat. Genet.* 43, 421–427. doi: 10.1038/ng.798

Chaturvedi, R., Venables, B., Petros, R. A., Nalam, V., Li, M., Wang, X., et al. (2012). An abietane diterpenoid is a potent activator of systemic acquired resistance. *Plant J.* 71, 161–172. doi: 10.1111/j.1365-313X.2012.04981.x

Chen, Y.-C., Holmes, E. C., Rajniak, J., Kim, J.-G., Tang, S., Fischer, C. R., et al. (2018). N -hydroxy-pipecolic acid is a mobile metabolite that induces systemic disease resistance in Arabidopsis. *Proc. Natl. Acad. Sci. U.S.A.* 115, E4920–E4929. doi: 10.1073/pnas.1805291115

Conconi, A., Smerdon, M. J., Howe, G. A., and Ryan, C. A. (1996). The octadecanoid signalling pathway in plants mediates a response to ultraviolet radiation. *Nature* 383, 826–829. doi: 10.1038/383826a0

Conrath, U., Beckers, G. J. M., Flors, V., García-Agustín, P., Jakab, G., Mauch, F., et al. (2006). Priming: getting ready for battle. *Mol. Plant Microbe Interact.* 19, 1062–1071. doi: 10.1094/mpmi-19-1062

Conrath, U., Beckers, G. J. M., Langenbach, C. J. G., and Jaskiewicz, M. R. (2015). Priming for enhanced defense. *Annu. Rev. Phytopathol.* 53, 97–119. doi: 10.1146/annurev-phyto-080614-120132

Cope, K. R., Bascaules, A., Irving, T. B., Venkateshwaran, M., Maeda, J., Garcia, K., et al. (2019). The ectomycorrhizal fungus Laccaria bicolor produces lipochitooligosaccharides and uses the common symbiosis Pathway to colonize Populus roots. *Plant Cell* 31, 2386–2410. doi: 10.1105/tpc.18.00676

Cordier, C., Pozo, M. J., Barea, J. M., Gianinazzi, S., and Gianinazzi-Pearson, V. (1998). Cell defense responses associated with localized and systemic resistance to Phytophthora parasitica induced in tomato by an arbuscular mycorrhizal fungus. *Mol. Plant Microbe Interact.* 11, 1017–1028. doi: 10.1094/MPMI.1998.11.10.1017

Darvill, A. G., and Albersheim, P. (1984). Phytoalexins and their elicitors-a defense against microbial infection in plants. *Annu. Rev. Plant Physiol.* 35, 243–275. doi: 10.1146/annurev.pp.35.060184.001331

de Freitas Pereira, M., Veneault-Fourrey, C., Vion, P., Guinet, F., Morin, E., Barry, K. W., et al. (2018). secretome analysis from the ectomycorrhizal ascomycete Cenococcum geophilum. *Front. Microbiol.* 9:141. doi: 10.3389/fmicb.2018.00141

Dempsey, D. A., and Klessig, D. F. (2012). SOS – too many signals for systemic acquired resistance? *Trends Plant Sci.* 17, 538–545. doi: 10.1016/j.tplants.2012.05.011

Ding, Y., Sun, T., Ao, K., Peng, Y., Zhang, Y., Li, X., et al. (2018). Opposite roles of salicylic acid receptors NPR1 and NPR3/NPR4 in transcriptional regulation of plant Immunity. *Cell* 173, 1454–1467. doi: 10.1016/j.cell.2018.03.044

Ditengou, F. A., Müller, A., Rosenkranz, M., Felten, J., Lasok, H., Doorn, M. M. V., et al. (2015). Volatile signalling by sesquiterpenes from ectomycorrhizal fungi reprogrammes root architecture. *Nat. Commun.* 6:6279. doi: 10.1038/ncomms7279

Dixon, R. A., Harrison, M. J., and Lamb, C. J. (1994). Early events in the activation of plant defense responses. *Annu. Rev. Phytopathol.* 32, 479–501. doi: 10.1146/annurev.py.32.090194.002403

Doré, J., Perraud, M., Dieryckx, C., Kohler, A., Morin, E., Henrissat, B., et al. (2015). Comparative genomics, proteomics and transcriptomics give new insight into the exoproteome of the basidiomycete Hebeloma cylindrosporum and its involvement in ectomycorrhizal symbiosis. *New Phytol.* 208, 1169–1187. doi: 10.1111/nph.13546

Dunse, K. M., Stevens, J. A., Lay, F. T., Gaspar, Y. M., Heath, R. L., and Anderson, M. A. (2010). Coexpression of potato type I and II proteinase inhibitors gives cotton plants protection against insect damage in the field. *Proc. Natl. Acad. Sci. U.S.A.* 107, 15011–15015. doi: 10.1073/pnas.1009241107

Duplessis, S., Courty, P.-E., Tagu, D., and Martin, F. (2005). Transcript patterns associated with ectomycorrhiza development in *Eucalyptus globulus* and *Pisolithus microcarpus*. *New Phytol.* 165, 599–611. doi: 10.1111/j.1469-8137.2004.01248.x

Durrant, W. E., and Dong, X. (2004). Systemic acquired resistance. *Annu. Rev. Phytopathol.* 42, 185–209. doi: 10.1146/annurev.phyto.42.040803.140421

El Hadrami, A., Adam, L. R., El Hadrami, I., and Daayf, F. (2010). Chitosan in plant protection. *Mar. Drugs* 8, 968–987. doi: 10.3390/md8040968

Felten, J., Kohler, A., Morin, E., Bhalerao, R. P., Palme, K., Martin, F., et al. (2009). The ectomycorrhizal fungus Laccaria bicolor stimulates lateral root formation in poplar and Arabidopsis through Auxin transport and signaling. *Plant Physiol.* 151, 1991–2005. doi: 10.1104/pp.109.147231

Feussner, I., and Wasternack, C. (2002). The lipoxygenase pathway. *Annu. Rev. Plant Biol.* 53, 275–297. doi: 10.1146/annurev.arplant.53.100301.135248

Fontana, A., Reichelt, M., Hempel, S., Gershenzon, J., and Unsicker, S. B. (2009). The effects of arbuscular mycorrhizal fungi on direct and indirect defense metabolites of Plantago lanceolata L. *J. Chem. Ecol.* 35, 833–843. doi: 10.1007/s10886-009-9654-0

Franken, P., and Gnädinger, F. (1994). Analysis of parsley arbuscular endomycorrhiza: infection development and mRNA levels of defense-related genes. *Mol. Plant Microbe Interact.* 7, 612–620. doi: 10.1094/mpmi-7-0612

Freeman, B., and Beattie, G. (2008). An overview of plant defenses against pathogens and herbivores. *Plant Health Instruct.* 149, 1–12. doi: 10.1094/PHI-I-2008-0226-01

Frettinger, P., Derory, J., Herrmann, S., Plomion, C., Lapeyrie, F., Oelmüller, R., et al. (2007). Transcriptional changes in two types of pre-mycorrhizal roots and in ectomycorrhizas of oak microcuttings inoculated with Piloderma croceum. *Planta* 225, 331–340. doi: 10.1007/s00425-006-0355-4

Gallou, A., Lucero Mosquera, H. P., Cranenbrouck, S., Suárez, J. P., and Declerck, S. (2011). Mycorrhiza induced resistance in potato plantlets challenged by Phytophthora infestans. *Physiol. Mol. Plant Pathol.* 76, 20–26. doi: 10.1016/j.pmpp.2011.06.005

Gange, A. C., Gane, D. R. J., Chen, Y., and Gong, M. (2005). Dual colonization of Eucalyptus urophylla S.T. Blake by arbuscular and ectomycorrhizal fungi affects levels of insect herbivore attack. *Agric. For. Entomol.* 7, 253–263. doi: 10.1111/j.1461-9555.2005.00268.x

Gange, A. C., and West, H. M. (1994). Interactions between arbuscular mycorrhizal fungi and foliar-feeding insects in *Plantago lanceolata* L. *New Phytol.* 128, 79–87. doi: 10.1111/j.1469-8137.1994.tb03989.x

Garcia, K., Delaux, P.-M., Cope, K. R., and Ané, J.-M. (2015). Molecular signals required for the establishment and maintenance of ectomycorrhizal symbioses. *New Phytol.* 208, 79–87. doi: 10.1111/nph.13423

García-Garrido, J. M., and Ocampo, J. A. (2002). Regulation of the plant defence response in arbuscular mycorrhizal symbiosis. *J. Exp. Bot.* 53, 1377–1386. doi: 10.1093/jexbot/53.373.1377

Genre, A., Lanfranco, L., Perotto, S., and Bonfante, P. (2020). Unique and common traits in mycorrhizal symbioses. *Nat. Rev. Microbiol.* 18, 649–660. doi: 10.1038/s41579-020-0402-3

Glazebrook, J. (2005). Contrasting mechanisms of defense against biotrophic and necrotrophic pathogens. *Annu. Rev. Phytopathol.* 43, 205–227. doi: 10.1146/annurev.phyto.43.040204.135923

Godard, K.-A., White, R., and Bohlmann, J. (2008). Monoterpene-induced molecular responses in *Arabidopsis thaliana*. *Phytochemistry* 69, 1838–1849. doi: 10.1016/j.phytochem.2008.02.011

Gong, B.-Q., Wang, F.-Z., and Li, J.-F. (2020). Hide-and-seek: chitin-triggered plant immunity and fungal counterstrategies. *Trends Plant Sci.* 25, 805–816. doi: 10.1016/j.tplants.2020.03.006

Goossens, J., Fernández-Calvo, P., Schweizer, F., and Goossens, A. (2016). Jasmonates: signal transduction components and their roles in environmental stress responses. *Plant Mol. Biol.* 91, 673–689. doi: 10.1007/s11103-016-0480-9

Halldórsson, G., Sverrisson, H., Eyjólfsdóttir, G. G., and Oddsdóttir, E. S. (2000). Ectomycorrhizae reduce damage to russian larch by Otiorhyncus larvae. *Scand. J. For. Res.* 15, 354–358. doi: 10.1080/028275800447986

Hammerbacher, A., Coutinho, T. A., and Gershenzon, J. (2019). Roles of plant volatiles in defence against microbial pathogens and microbial exploitation of volatiles. *Plant Cell Environ.* 42, 2827–2843. doi: 10.1111/pce.13602

Hammond-Kosack, K. E., and Jones, J. D. G. (1997). Plant disease resistance genes. *Physiol. Mol. Biol. Plants* 48, 575–607. doi: 10.1146/annurev.arplant.48.1.575

Haney, C. H., Wiesmann, C. L., Shapiro, L. R., Melnyk, R. A., O'Sullivan, L. R., Khorasani, S., et al. (2018). Rhizosphere-associated *Pseudomonas* induce systemic resistance to herbivores at the cost of susceptibility to bacterial pathogens. *Mol. Ecol.* 27, 1833–1847. doi: 10.1111/mec.14400

Hao, Z., Fayolle, L., van Tuinen, D., Chatagnier, O., Li, X., Gianinazzi, S., et al. (2012). Local and systemic mycorrhiza-induced protection against the ectoparasitic nematode Xiphinema index involves priming of defence gene responses in grapevine. *J. Exp. Bot.* 63, 3657–3672. doi: 10.1093/jxb/ers046

Hartmann, M., Zeier, T., Bernsdorff, F., Reichel-Deland, V., Kim, D., Hohmann, M., et al. (2018). Flavin monooxygenase-generated N-hydroxypipecolic acid is a critical element of plant systemic immunity. *Cell* 173, 456.e16–469.e16. doi: 10.1016/j.cell.2018.02.049

Heller, G., Adomas, A., Li, G., Osborne, J., van Zyl, L., Sederoff, R., et al. (2008). Transcriptional analysis of *Pinus sylvestris* roots challenged with the ectomycorrhizal fungus Laccaria bicolor. *BMC Plant Biol.* 8:19. doi: 10.1186/1471-2229-8-19

Hill, E. M., Robinson, L. A., Abdul-Sada, A., Vanbergen, A. J., Hodge, A., and Hartley, S. E. (2018). Arbuscular mycorrhizal fungi and plant chemical defence: effects of colonisation on aboveground and belowground metabolomes. *J. Chem. Ecol.* 44, 198–208. doi: 10.1007/s10886-017-0921-1

Holopainen, J. K., and Gershenzon, J. (2010). Multiple stress factors and the emission of plant VOCs. *Trends Plant Sci.* 15, 176–184. doi: 10.1016/j.tplants.2010.01.006

Howe, G. A., Major, I. T., and Koo, A. J. (2018). Modularity in jasmonate signaling for multistress resilience. *Annu. Rev. Plant Biol.* 69, 387–415. doi: 10.1146/annurev-arplant-042817-040047

Huang, M., Sanchez-Moreiras, A. M., Abel, C., Sohrabi, R., Lee, S., Gershenzon, J., et al. (2012). The major volatile organic compound emitted from *Arabidopsis thaliana* flowers, the sesquiterpene (E)-β-caryophyllene, is a defense against a bacterial pathogen. *New Phytol.* 193, 997–1008. doi: 10.1111/j.1469-8137.2011.04001.x

Irmisch, S., McCormick, A. C., Boeckler, G. A., Schmidt, A., Reichelt, M., Schneider, B., et al. (2013). Two herbivore-induced cytochrome P450 Enzymes CYP79D6 and CYP79D7 catalyze the formation of volatile aldoximes involved in poplar defense. *Plant Cell* 25, 4737–4754. doi: 10.1105/tpc.113.118265

Irmisch, S., McCormick, A. C., Günther, J., Schmidt, A., Boeckler, G. A., Gershenzon, J., et al. (2014). Herbivore-induced poplar cytochrome P450 enzymes of the CYP71 family convert aldoximes to nitriles which repel a generalist caterpillar. *Plant J.* 80, 1095–1107. doi: 10.1111/tpj.12711

Isaacs, M., Carella, P., Faubert, J., Champigny, M. J., Rose, J. K. C., and Cameron, R. K. (2016). Orthology analysis and in vivo complementation studies to elucidate the role of DIR1 during systemic acquired resistance in *Arabidopsis thaliana* and *Cucumis sativus*. *Front. Plant Sci.* 7:627. doi: 10.3389/fpls.2016.00566

Jashni, M. K., Mehrabi, R., Collemare, J., Mesarich, C. H., and de Wit, P. J. G. M. (2015). The battle in the apoplast: further insights into the roles of proteases and their inhibitors in plant–pathogen interactions. *Front. Plant Sci.* 6:584. doi: 10.3389/fpls.2015.00584

Johansson, T., Le Quéré, A., Ahren, D., Söderström, B., Erlandsson, R., Lundeberg, J., et al. (2004). Transcriptional responses of *Paxillus involutus* and *Betula pendula* during formation of ectomycorrhizal root tissue. *Mol. Plant Microbe Interact.* 17, 202–215. doi: 10.1094/MPMI.2004.17.2.202

Jones, J. D. G., and Dangl, J. L. (2006). The plant immune system. *Nature* 444, 323–329. doi: 10.1038/nature05286

Jung, H. W., Tschaplinski, T. J., Wang, L., Glazebrook, J., and Greenberg, J. T. (2009). Priming in systemic plant immunity. *Science* 324, 89–91. doi: 10.1126/science.1170025

Jung, S. C., Martinez-Medina, A., Lopez-Raez, J. A., and Pozo, M. J. (2012). Mycorrhiza-induced resistance and priming of plant defenses. *J. Chem. Ecol.* 38, 651–664. doi: 10.1007/s10886-012-0134-6

Kaling, M., Schmidt, A., Moritz, F., Rosenkranz, M., Witting, M., Kasper, K., et al. (2018). Mycorrhiza-triggered transcriptomic and metabolomic networks impinge on herbivore fitness. *Plant Physiol.* 176, 2639–2656. doi: 10.1104/pp.17.01810

Kang, H., Chen, X., Kemppainen, M., Pardo, A. G., Veneault-Fourrey, C., Kohler, A., et al. (2020). The small secreted effector protein MiSSP7.6 *of Laccaria bicolor* is required for the establishment of ectomycorrhizal symbiosis. *Environ. Microbiol.* 1462-2920, 14959. doi: 10.1111/1462-2920.14959

Kapoor, R. (2008). Induced resistance in mycorrhizal tomato is correlated to concentration of jasmonic acid. *Online J. Biol. Sci.* 8, 49–56. doi: 10.3844/ojbsci.2008.49.56

Kawano, T. (2003). Roles of the reactive oxygen species-generating peroxidase reactions in plant defense and growth induction. *Plant Cell Rep.* 21, 829–837. doi: 10.1007/s00299-003-0591-z

Khasa, P. D., Chakravarty, P., Robertson, A., Thomas, B. R., and Dancik, B. P. (2002). The mycorrhizal status of selected poplar clones introduced in Alberta. *Biomass Bioenergy* 22, 99–104. doi: 10.1016/S0961-9534(01)00072-1

Kim, J.-Y., Park, S.-C., Hwang, I., Cheong, H., Nah, J.-W., Hahm, K.-S., et al. (2009). Protease inhibitors from plants with antimicrobial activity. *Int. J. Mol. Sci.* 10, 2860–2872. doi: 10.3390/ijms10062860

Kloppholz, S., Kuhn, H., and Requena, N. (2011). A secreted fungal effector of Glomus intraradices promotes symbiotic biotrophy. *Curr. Biol.* 21, 1204–1209. doi: 10.1016/j.cub.2011.06.044

Kohler, A., Kuo, A., Nagy, L. G., Morin, E., Barry, K. W., Buscot, F., et al. (2015). Convergent losses of decay mechanisms and rapid turnover of symbiosis genes in mycorrhizal mutualists. *Nat. Genet.* 47, 410–415. doi: 10.1038/ng.3223

Koo, Y. J., Kim, M. A., Kim, E. H., Song, J. T., Jung, C., Moon, J.-K., et al. (2007). Overexpression of salicylic acid carboxyl methyltransferase reduces salicylic

acid-mediated pathogen resistance in *Arabidopsis thaliana*. *Plant. Mol. Biol.* 64, 1–15. doi: 10.1007/s11103-006-9123-x

Kumar, M., and Ashraf, S. (2017). "Role of Trichoderma spp. as a Biocontrol Agent of Fungal Plant Pathogens," in *Probiotics and Plant Health*, eds V. Kumar, M. Kumar, S. Sharma, and R. Prasad (Singapore: Springer), 497–506. doi: 10.1007/978-981-10-3473-2_23

La Camera, S., Gouzerh, G., Dhondt, S., Hoffmann, L., Fritig, B., Legrand, M., et al. (2004). Metabolic reprogramming in plant innate immunity: the contributions of phenylpropanoid and oxylipin pathways. *Immunol. Rev.* 198, 267–284. doi: 10.1111/j.0105-2896.2004.0129.x

Labbé, J. L., Weston, D. J., Dunkirk, N., Pelletier, D. A., and Tuskan, G. A. (2014). Newly identified helper bacteria stimulate ectomycorrhizal formation in Populus. *Front. Plant Sci.* 5:579. doi: 10.3389/fpls.2014.00579

Larcher, W. (1995). *Physiological Plant Ecology: Ecophysiology and Stress Physiology of Functional Groups*. Berlin: Springer, 514.

Lawrence, P. K., and Koundal, K. R. (2002). Plant protease inhibitors in control of phytophagous insects. *Electron. J. Biotechnol.* 5, 93–109.

Le Marquer, M., Bécard, G., and Frei dit Frey, N. (2019). Arbuscular mycorrhizal fungi possess a CLAVATA3/embryo surrounding region-related gene that positively regulates symbiosis. *New Phytol.* 222, 1030–1042. doi: 10.1111/nph.15643

Le Quéré, A., Wright, D. P., Söderström, B., Tunlid, A., and Johansson, T. (2005). Global patterns of gene regulation associated with the development of ectomycorrhiza between birch (*Betula pendula* Roth.) and *Paxillus involutus* (Batsch) Fr. *Mol. Plant Microbe Interact.* 18, 659–673. doi: 10.1094/MPMI-18-0659

Lee, S., Behringer, G., Hung, R., and Bennett, J. (2019). Effects of fungal volatile organic compounds on Arabidopsis thaliana growth and gene expression. *Fungal Ecol.* 37, 1–9. doi: 10.1016/j.funeco.2018.08.004

Li, B., Jiang, S., Yu, X., Cheng, C., Chen, S., Cheng, Y., et al. (2015). Phosphorylation of trihelix transcriptional repressor ASR3 by MAP KINASE4 negatively regulates Arabidopsis immunity. *Plant Cell* 27, 839–856. doi: 10.1105/tpc.114.134809

Li, H.-Y., Yang, G.-D., Shu, H.-R., Yang, Y.-T., Ye, B.-X., Nishida, I., et al. (2006). Colonization by the arbuscular mycorrhizal fungus Glomus versiforme induces a defense response against the root-knot nematode Meloidogyne incognita in the grapevine (*Vitis amurensis* Rupr.), which includes transcriptional activation of the class III chitinase gene VCH3. *Plant Cell Physiol.* 47, 154–163. doi: 10.1093/pcp/pci231

Li, Y., Zhang, W., Dong, H., Liu, Z., Ma, J., and Zhang, X. (2018). Salicylic acid in Populus tomentosa is a remote signalling molecule induced by *Botryosphaeria dothidea* infection. *Sci. Rep.* 8:14059. doi: 10.1038/s41598-018-32204-9

Limpens, E., van Zeijl, A., and Geurts, R. (2015). Lipochitooligosaccharides modulate plant host immunity to enable endosymbioses. *Annu. Rev. Phytopathol.* 53, 311–334. doi: 10.1146/annurev-phyto-080614-120149

Lindroth, R. L., and St. Clair, S. B. (2013). Adaptations of quaking aspen (*Populus tremuloides* Michx.) for defense against herbivores. *Forest. Ecol. Manag* 299, 14–21. doi: 10.1016/j.foreco.2012.11.018

Linnakoski, R., Kasanen, R., Dounavi, A., and Forbes, K. M. (2019). Editorial: forest health under climate change: effects on tree resilience, and pest and pathogen dynamics. *Front. Plant Sci.* 10:1157. doi: 10.3389/fpls.2019.01157

Liu, T., Sheng, M., Wang, C. Y., Chen, H., Li, Z., and Tang, M. (2015). Impact of arbuscular mycorrhizal fungi on the growth, water status, and photosynthesis of hybrid poplar under drought stress and recovery. *Photosynthetica* 53, 250–258. doi: 10.1007/s11099-015-0100-y

Loreto, F., and Schnitzler, J.-P. (2010). Abiotic stresses and induced BVOCs. *Trends Plant Sci.* 15, 154–166. doi: 10.1016/j.tplants.2009.12.006

Luo, Z.-B., Janz, D., Jiang, X., Goebel, C., Wildhagen, H., Tan, Y., et al. (2009). Upgrading toot physiology for stress tolerance by ectomycorrhizas: insights from metabolite and transcriptional profiling into reprogramming for stress anticipation. *Plant Physiol.* 151, 1902–1917. doi: 10.1104/pp.109.143735

Lyons, R., Manners, J. M., and Kazan, K. (2013). Jasmonate biosynthesis and signaling in monocots: a comparative overview. *Plant Cell Rep.* 32, 815–827. doi: 10.1007/s00299-013-1400-y

Maboreke, H. R., Feldhahn, L., Bönn, M., Tarkka, M. T., Buscot, F., Herrmann, S., et al. (2016). Transcriptome analysis in oak uncovers a strong impact of endogenous rhythmic growth on the interaction with plant-parasitic nematodes. *BMC Genomics* 17:627. doi: 10.1186/s12864-016-2992-8

Maillet, F., Poinsot, V., André, O., Puech-Pagès, V., Haouy, A., Gueunier, M., et al. (2011). Fungal lipochitooligosaccharide symbiotic signals in arbuscular mycorrhiza. *Nature* 469, 58–63. doi: 10.1038/nature09622

Maldonado, A. M., Doerner, P., Dixon, R. A., Lamb, C. J., and Cameron, R. K. (2002). A putative lipid transfer protein involved in systemic resistance signalling in Arabidopsis. *Nature* 419, 399–403. doi: 10.1038/nature00962

Manninen, A.-M., Holopainen, T., and Holopainen, J. K. (1998). Susceptibility of ectomycorrhizal and non-mycorrhizal Scots pine (*Pinus sylvestris*) seedlings to a generalist insect herbivore, *Lygus rugulipennis*, at two nitrogen availability levels. *New Phytol.* 140, 55–63. doi: 10.1046/j.1469-8137.1998.00246.x

Martin, F., Kohler, A., Murat, C., Veneault-Fourrey, C., and Hibbett, D. S. (2016). Unearthing the roots of ectomycorrhizal symbioses. *Nat. Rev. Microbiol.* 14, 760–773. doi: 10.1038/nrmicro.2016.149

Martin, F. M., Harrison, M. J., Lennon, S., Lindahl, B., Öpik, M., Polle, A., et al. (2018). Cross-scale integration of mycorrhizal function. *New Phytol.* 220, 941–946. doi: 10.1111/nph.15493

Martinez-Medina, A., Fernandez, I., Sánchez-Guzmán, M. J., Jung, S. C., Pascual, J. A., and Pozo, M. J. (2013). Deciphering the hormonal signalling network behind the systemic resistance induced by Trichoderma harzianum in tomato. *Front. Plant Sci.* 4:206. doi: 10.3389/fpls.2013.00206

Mauch-Mani, B., Baccelli, I., Luna, E., and Flors, V. (2017). Defense priming: an adaptive part of induced resistance. *Annu. Rev. Plant Biol.* 68, 485–512. doi: 10.1146/annurev-arplant-042916-041132

Mazid, M., Khan, T., and Mohammad, F. (2011). Role of secondary metabolites in defense mechanisms of plants. *Biol. Med.* 3, 232–249.

McCormick, A. C., Irmisch, S., Reinecke, A., Boeckler, G. A., Veit, D., Reichelt, M., et al. (2014). Herbivore-induced volatile emission in black poplar: regulation and role in attracting herbivore enemies. *Plant Cell Environ.* 37, 1909–1923. doi: 10.1111/pce.12287

Miya, A., Albert, P., Shinya, T., Desaki, Y., Ichimura, K., Shirasu, K., et al. (2007). CERK1, a LysM receptor kinase, is essential for chitin elicitor signaling in Arabidopsis. *Proc. Natl. Acad. Sci. U.S.A.* 104, 19613–19618. doi: 10.1073/pnas.0705147104

Molitor, A., Zajic, D., Voll, L. M., Pons-Kühnemann, J., Samans, B., Kogel, K.-H., et al. (2011). Barley leaf transcriptome and metabolite analysis reveals new aspects of compatibility and *Piriformospora indica*–mediated systemic induced resistance to powdery mildew. *Mol. Plant Microbe Interact.* 24, 1427–1439. doi: 10.1094/MPMI-06-11-0177

Müller, A., Faubert, P., Hagen, M., zu Castell, W., Polle, A., Schnitzler, J.-P., et al. (2013). Volatile profiles of fungi – Chemotyping of species and ecological functions. *Fungal Genet. Biol.* 54, 25–33. doi: 10.1016/j.fgb.2013.02.005

Mustafa, G., Khong, N. G., Tisserant, B., Randoux, B., Fontaine, J., Magnin-Robert, M., et al. (2017). Defence mechanisms associated with mycorrhiza-induced resistance in wheat against powdery mildew. *Funct. Plant Biol.* 44, 443–454. doi: 10.1071/FP16206

Nair, A., Kolet, S. P., Thulasiram, H. V., and Bhargava, S. (2015). Role of methyl jasmonate in the expression of mycorrhizal induced resistance against Fusarium oxysporum in tomato plants. *Physiol. Mol. Plant. Path.* 92, 139–145. doi: 10.1016/j.pmpp.2015.10.002

Návarová, H., Bernsdorff, F., Döring, A.-C., and Zeier, J. (2012). Pipecolic acid, an endogenous mediator of defense amplification and priming, is a critical regulator of inducible plant immunity. *Plant Cell* 24, 5123–5141. doi: 10.1105/tpc.112.103564

Nehls, U., and Plassard, C. (2018). Nitrogen and phosphate metabolism in ectomycorrhizas. *New Phytol.* 220, 1047–1058. doi: 10.1111/nph.15257

Nerg, A.-M., Kasurinen, A., Holopainen, T., Julkunen-Tiitto, R., Neuvonen, S., and Holopainen, J. K. (2008). The significance of ectomycorrhizas in chemical quality of silver birch foliage and above-ground insect herbivore performance. *J. Chem. Ecol.* 34, 1322–1330. doi: 10.1007/s10886-008-9542-z

Nimchuk, Z., Eulgem, T., Holt, I. I. I. B. F., and Dangl, J. L. (2003). Recognition and response in the plant immune system. *Annu. Rev. Genet.* 37, 579–609. doi: 10.1146/annurev.genet.37.110801.142628

Okamoto, S., Shinohara, H., Mori, T., Matsubayashi, Y., and Kawaguchi, M. (2013). Root-derived CLE glycopeptides control nodulation by direct binding to HAR1 receptor kinase. *Nat. Commun.* 4, 1–7.

Park, S.-W., Kaimoyo, E., Kumar, D., Mosher, S., and Klessig, D. F. (2007). Methyl salicylate is a critical mobile signal for plant systemic acquired resistance. *Science* 318, 113–116. doi: 10.1126/science.1147113

Pedone-Bonfim, M. V. L., da Silva, F. S. B., and Maia, L. C. (2015). Production of secondary metabolites by mycorrhizal plants with medicinal or nutritional potential. *Acta Physiol. Plant.* 37, 27.

Pellegrin, C., Daguerre, Y., Ruytinx, J., Guinet, F., Kemppainen, M., Frey, N. F. D., et al. (2019). Laccaria bicolor MiSSP8 is a small-secreted protein decisive for the establishment of the ectomycorrhizal symbiosis. *Environ. Microbiol.* 21, 3765–3779. doi: 10.1111/1462-2920.14727

Pellegrin, C., Morin, E., Martin, F. M., and Veneault-Fourrey, C. (2015). Comparative analysis of secretomes from ectomycorrhizal fungi with an emphasis on small-secreted proteins. *Front. Microbiol.* 6:1278. doi: 10.3389/fmicb.2015.01278

Pfabel, C., Eckhardt, K.-U., Baum, C., Struck, C., Frey, P., and Weih, M. (2012). Impact of ectomycorrhizal colonization and rust infection on the secondary metabolism of poplar (Populus trichocarpa × deltoides). *Tree Physiol.* 32, 1357–1364. doi: 10.1093/treephys/tps093

Pieterse, C. M., Zamioudis, C., Berendsen, R. L., Weller, D. M., Van Wees, S. C., and Bakker, P. A. (2014). Induced systemic resistance by beneficial microbes. *Annu. Rev. Phytopathol.* 52, 347–375.

Pieterse, C. M. J., Van der Does, D., Zamioudis, C., Leon-Reyes, A., and Van Wees, S. C. M. (2012). Hormonal modulation of plant immunity. *Annu. Rev. Cell Dev. Biol.* 28, 489–521. doi: 10.1146/annurev-cellbio-092910-154055

Plett, J. M., Daguerre, Y., Wittulsky, S., Vayssières, A., Deveau, A., Melton, S. J., et al. (2014). Effector MiSSP7 of the mutualistic fungus Laccaria bicolor stabilizes the Populus JAZ6 protein and represses jasmonic acid (JA) responsive genes. *Proc. Natl. Acad. Sci. U.S.A.* 111, 8299–8304. doi: 10.1073/pnas.1322671111

Plett, J. M., Kemppainen, M., Kale, S. D., Kohler, A., Legué, V., Brun, A., et al. (2011). A secreted effector protein of Laccaria bicolor is required for symbiosis development. *Curr. Biol.* 21, 1197–1203. doi: 10.1016/j.cub.2011.05.033

Pozo, M. J., and Azcón-Aguilar, C. (2007). Unraveling mycorrhiza-induced resistance. *Curr. Opin. Plant Biol.* 10, 393–398. doi: 10.1016/j.pbi.2007.05.004

Pusztahelyi, T. (2018). Chitin and chitin-related compounds in plant–fungal interactions. *Mycology* 9, 189–201. doi: 10.1080/21501203.2018.1473299

Radojičić, A., Li, X., and Zhang, Y. (2018). Salicylic acid: a double-edged sword for programed cell death in plants. *Front. Plant Sci.* 9:1133. doi: 10.3389/fpls.2018.01133

Riedlmeier, M., Ghirardo, A., Wenig, M., Knappe, C., Koch, K., Georgii, E., et al. (2017). Monoterpenes support systemic acquired resistance within and between plants. *Plant Cell* 29, 1440–1459. doi: 10.1105/tpc.16.00898

Rosahl, S. (1996). Lipoxygenases in plants -their role in development and stress response. *Z. Naturforsch. C* 51, 123–138. doi: 10.1515/znc-1996-3-401

Rowen, E., Gutensohn, M., Dudareva, N., and Kaplan, I. (2017). Carnivore attractant or plant elicitor? multifunctional roles of methyl salicylate lures in tomato defense. *J. Chem. Ecol.* 43, 573–585. doi: 10.1007/s10886-017-0856-6

Sabbagh, S. K., Roudini, M., and Panjehkeh, N. (2017). Systemic resistance induced by Trichoderma harzianum and Glomus mossea on cucumber damping-off disease caused by Phytophthora melonis. *Arch. Phytopathol. Pflanzenschutz* 50, 375–388. doi: 10.1080/03235408.2017.1317953

Sanmartín, N., Pastor, V., Pastor-Fernández, J., Flors, V., Pozo, M. J., and Sánchez-Bel, P. (2020). Role and mechanisms of callose priming in mycorrhiza-induced resistance. *J. Exp. Bot.* 71, 2769–2781. doi: 10.1093/jxb/eraa030

Sato, C., Aikawa, K., Sugiyama, S., Nabeta, K., Masuta, C., and Matsuura, H. (2011). Distal transport of exogenously applied jasmonoyl–isoleucine with wounding stress. *Plant Cell Physiol.* 52, 509–517. doi: 10.1093/pcp/pcr011

Sauter, M., and Hager, A. (1989). The mycorrhizal fungus *Amanita muscaria* induces chitinase activity in roots and in suspension-cultured cells of its host *Picea abies*. *Planta* 179, 61–66. doi: 10.1007/BF00395771

Schausberger, P., Peneder, S., Jürschik, S., and Hoffmann, D. (2012). Mycorrhiza changes plant volatiles to attract spider mite enemies. *Funct. Ecol.* 26, 441–449. doi: 10.1111/j.1365-2435.2011.01947.x

Schilmiller, A. L., and Howe, G. A. (2005). Systemic signaling in the wound response. *Curr. Opin. Plant Biol.* 8, 369–377. doi: 10.1016/j.pbi.2005.05.008

Schoenherr, A. P., Rizzo, E., Jackson, N., Manosalva, P., and Gomez, S. K. (2019). Mycorrhiza-induced resistance in potato involves priming of defense responses against cabbage looper (Noctuidae: Lepidoptera). *Environ. Entomol.* 48, 370–381. doi: 10.1093/ee/nvy195

Schulz-Bohm, K., Martín-Sánchez, L., and Garbeva, P. (2017). Microbial volatiles: small molecules with an important role in intra- and inter-kingdom interactions. *Front. Microbiol.* 8:2484. doi: 10.3389/fmicb.2017.02484

Schweiger, R., Baier, M. C., Persicke, M., and Müller, C. (2014). High specificity in plant leaf metabolic responses to arbuscular mycorrhiza. *Nat. Commun.* 5:3886. doi: 10.1038/ncomms4886

Shabala, S., White, R. G., Djordjevic, M. A., Ruan, Y.-L., and Mathesius, U. (2016). Root-to-shoot signalling: integration of diverse molecules, pathways and functions. *Funct. Plant Biol.* 43, 87. doi: 10.1071/FP15252

Shah, J. (2005). Lipids, lipases, and lipid-modifying enzymes in plant disease resistance. *Annu. Rev. Phytopathol.* 43, 229–260. doi: 10.1146/annurev.phyto.43.040204.135951

Shah, J., and Zeier, J. (2013). Long-distance communication and signal amplification in systemic acquired resistance. *Front. Plant Sci.* 4:30. doi: 10.3389/fpls.2013.00030

Sharma, N., Sharma, K., Gaur, R., and Gupta, V. (2011). Role of chitinase in plant defense. *Asian J. Biochem.* 6, 29–37. doi: 10.3923/ajb.2011.29.37

Sharon, E., Chet, I., and Spiegel, Y. (2011). "Trichoderma as a Biological Control Agent," in *Biological Control of Plant-Parasitic Nematodes: Building Coherence between Microbial Ecology and Molecular Mechanisms Progress in Biological Control*, eds K. Davies and Y. Spiegel (Dordrecht: Springer), 183–201. doi: 10.1007/978-1-4020-9648-8_8

Shen, Z., Sun, J., Yao, J., Wang, S., Ding, M., Zhang, H., et al. (2015). High rates of virus-induced gene silencing by tobacco rattle virus in Populus. *Tree Physiol.* 35, 1016–1029.

Shrivastava, G., Ownley, B. H., Augé, R. M., Toler, H., Dee, M., Vu, A., et al. (2015). Colonization by arbuscular mycorrhizal and endophytic fungi enhanced terpene production in tomato plants and their defense against a herbivorous insect. *Symbiosis* 65, 65–74. doi: 10.1007/s13199-015-0319-1

Shulaev, V., Silverman, P., and Raskin, I. (1997). Airborne signalling by methyl salicylate in plant pathogen resistance. *Nature* 385, 718–721. doi: 10.1038/385718a0

Smith, S. E., and Read, D. J. (2008). *Mycorrhizal symbiosis*. San Diego, CA: Academic Press, 800.

Song, Y., Chen, D., Lu, K., Sun, Z., and Zeng, R. (2015). Enhanced tomato disease resistance primed by arbuscular mycorrhizal fungus. *Front. Plant Sci.* 6:786. doi: 10.3389/fpls.2015.00786

Song, Y. Y., Cao, M., Xie, L. J., Liang, X. T., Zeng, R. S., Su, Y. J., et al. (2011). Induction of DIMBOA accumulation and systemic defense responses as a mechanism of enhanced resistance of mycorrhizal corn (*Zea mays* L.) to sheath blight. *Mycorrhiza* 21, 721–731. doi: 10.1007/s00572-011-0380-4

Song, Y. Y., Ye, M., Li, C. Y., Wang, R. L., Wei, X. C., Luo, S. M., et al. (2013). Priming of anti-herbivore defense in tomato by arbuscular mycorrhizal fungus and involvement of the jasmonate pathway. *J. Chem. Ecol.* 39, 1036–1044. doi: 10.1007/s10886-013-0312-1

Spoel, S. H., and Dong, X. (2012). How do plants achieve immunity? Defence without specialized immune cells. *Nat. Rev. Immunol.* 12, 89–100. doi: 10.1038/nri3141

Stein, E., Molitor, A., Kogel, K.-H., and Waller, F. (2008). Systemic resistance in Arabidopsis conferred by the mycorrhizal fungus Piriformospora indica requires jasmonic acid signaling and the cytoplasmic function of NPR1. *Plant Cell Physiol.* 49, 1747–1751. doi: 10.1093/pcp/pcn147

Sun, J., Miller, J. B., Granqvist, E., Wiley-Kalil, A., Gobbato, E., Maillet, F., et al. (2015). Activation of symbiosis signaling by arbuscular mycorrhizal fungi in legumes and rice. *Plant Cell* 27, 823–838. doi: 10.1105/tpc.114.131326

Tarkka, M. T., Herrmann, S., Wubet, T., Feldhahn, L., Recht, S., Kurth, F., et al. (2013). OakContigDF159.1, a reference library for studying differential gene expression in *Quercus robur* during controlled biotic interactions: use for quantitative transcriptomic profiling of oak roots in ectomycorrhizal symbiosis. *New Phytol.* 199, 529–540. doi: 10.1111/nph.12317

Thines, B., Katsir, L., Melotto, M., Niu, Y., Mandaokar, A., Liu, G., et al. (2007). JAZ repressor proteins are targets of the SCF(COI1) complex during jasmonate signalling. *Nature* 448, 661–665. doi: 10.1038/nature05960

Thorpe, M. R., Ferrieri, A. P., Herth, M. M., and Ferrieri, R. A. (2007). 11C-imaging: methyl jasmonate moves in both phloem and xylem, promotes transport of jasmonate, and of photoassimilate even after proton transport is decoupled. *Planta* 226, 541–551. doi: 10.1007/s00425-007-0503-5

Truman, W., Bennett, M. H., Kubigsteltig, I., Turnbull, C., and Grant, M. (2007). Arabidopsis systemic immunity uses conserved defense signaling pathways and is mediated by jasmonates. *Proc. Natl. Acad. Sci. U.S.A.* 104, 1075–1080. doi: 10.1073/pnas.0605423104

Ullah, C., Tsai, C., Unsicker, S. B., Xue, L., Reichelt, M., Gershenzon, J., et al. (2019). Salicylic acid activates poplar defense against the biotrophic rust fungus Melampsora larici-populina via increased biosynthesis of catechin and proanthocyanidins. *New Phytol.* 221, 960–975. doi: 10.1111/nph.15396

van der Heijden, M. G. A., Martin, F. M., Selosse, M.-A., and Sanders, I. R. (2015). Mycorrhizal ecology and evolution: the past, the present, and the future. *New Phytol.* 205, 1406–1423. doi: 10.1111/nph.13288

van Schie, C. C., Haring, M. A., and Schuurink, R. C. (2007). Tomato linalool synthase is induced in trichomes by jasmonic acid. *Plant Mol. Biol.* 64, 251–263. doi: 10.1007/s11103-007-9149-8

Vandenkoornhuyse, P., Quaiser, A., Duhamel, M., Van, A. L., and Dufresne, A. (2015). The importance of the microbiome of the plant holobiont. *New Phytol.* 206, 1196–1206. doi: 10.1111/nph.13312

Vincent, D., Kohler, A., Claverol, S., Solier, E., Joets, J., Gibon, J., et al. (2012). Secretome of the free-living mycelium from the ectomycorrhizal basidiomycete Laccaria bicolor. *J. Proteome Res.* 11, 157–171. doi: 10.1021/pr200895f

Vishwanathan, K., Zienkiewicz, K., Liu, Y., Janz, D., Feussner, I., Polle, A., et al. (2020). Ectomycorrhizal fungi induce systemic resistance against insects on a nonmycorrhizal plant in a CERK1-dependent manner. *New Phytol.* 228, 728–740. doi: 10.1111/nph.16715

Vlot, A. C., Dempsey, D. A., and Klessig, D. F. (2009). Salicylic acid, a multifaceted hormone to combat disease. *Annu. Rev. Phytopathol.* 47, 177–206. doi: 10.1146/annurev.phyto.050908.135202

Vlot, A. C., Pabst, E., and Riedlmeier, M. (2017). *"Systemic signalling in plant defence." in eLS*. Chichester: John Wiley& Sons, Ltd, doi: 10.1002/9780470015902.a0001322.pub3

Wang, B., Yeun, L. H., Xue, J.-Y., Liu, Y., Ané, J.-M., and Qiu, Y.-L. (2010). Presence of three mycorrhizal genes in the common ancestor of land plants suggests a key role of mycorrhizas in the colonization of land by plants. *New Phytol.* 186, 514–525. doi: 10.1111/j.1469-8137.2009.03137.x

Wang, C., Liu, R., Lim, G.-H., Lorenzo, L. D., Yu, K., Zhang, K., et al. (2018). Pipecolic acid confers systemic immunity by regulating free radicals. *Sci. Adv.* 4:eaar4509. doi: 10.1126/sciadv.aar4509

War, A. R., Paulraj, M. G., Ahmad, T., Buhroo, A. A., Hussain, B., Ignacimuthu, S., et al. (2012). Mechanisms of plant defense against insect herbivores. *Plant Signal. Behav.* 7, 1306–1320. doi: 10.4161/psb.21663

Wasternack, C. (2007). Jasmonates: an update on biosynthesis, signal transduction and action in plant stress response, growth and development. *Ann. Bot.* 100, 681–697. doi: 10.1093/aob/mcm079

Wenig, M., Ghirardo, A., Sales, J. H., Pabst, E. S., Breitenbach, H. H., Antritter, F., et al. (2019). Systemic acquired resistance networks amplify airborne defense cues. *Nat. Commun.* 10, 3813. doi: 10.1038/s41467-019-11798-2

Wenke, K., Wanke, D., Kilian, J., Berendzen, K., Harter, K., and Piechulla, B. (2012). Volatiles of two growth-inhibiting rhizobacteria commonly engage AtWRKY18 function. *Plant J.* 70, 445–459. doi: 10.1111/j.1365-313X.2011.04891.x

Werner, S., Polle, A., and Brinkmann, N. (2016). Belowground communication: impacts of volatile organic compounds (VOCs) from soil fungi on other soil-inhabiting organisms. *Appl. Microbiol. Biotechnol.* 100, 8651–8665. doi: 10.1007/s00253-016-7792-1

Wink, M. (2018). Plant secondary metabolites modulate insect behavior-steps toward addiction? *Front. Physiol.* 9:364. doi: 10.3389/fphys.2018.00364

Xue, D.-X., Li, C.-L., Xie, Z.-P., and Staehelin, C. (2019). LYK4 is a component of a tripartite chitin receptor complex in Arabidopsis thaliana. *J. Exp. Bot.* 70, 5507–5516. doi: 10.1093/jxb/erz313

Yuan, P., Jauregui, E., Du, L., Tanaka, K., and Poovaiah, B. (2017). Calcium signatures and signaling events orchestrate plant–microbe interactions. *Curr. Opin. Plant Biol.* 38, 173–183. doi: 10.1016/j.pbi.2017.06.003

Zhang, H., and Hu, Y. (2017). Long-distance transport of prosystemin messenger RNA in Tomato. *Front. Plant Sci.* 8:1894. doi: 10.3389/fpls.2017.01894

Zhang, X., Dong, W., Sun, J., Feng, F., Deng, Y., He, Z., et al. (2015). The receptor kinase CERK1 has dual functions in symbiosis and immunity signalling. *Plant J.* 81, 258–267. doi: 10.1111/tpj.12723

Zhao, L., Wu, X.-Q., Ye, J.-R., Li, H., and Li, G.-E. (2014). Isolation and characterization of a mycorrhiza helper bacterium from rhizosphere soils of poplar stands. *Biol. Fertil. Soils* 50, 593–601. doi: 10.1007/s00374-013-0880-9

Zhou, G., Ren, N., Qi, J., Lu, J., Xiang, C., Ju, H., et al. (2014). The 9-lipoxygenase Osr9-LOX1 interacts with the 13-lipoxygenase-mediated pathway to regulate resistance to chewing and piercing-sucking herbivores in rice. *Physiol. Plant.* 152, 59–69. doi: 10.1111/ppl.12148

Zhou, Y., Zhou, B., Pache, L., Chang, M., Khodabakhshi, A. H., Tanaseichuk, O., et al. (2019). Metascape provides a biologist-oriented resource for the analysis of systems-level datasets. *Nat. Commun.* 10, 1523. doi: 10.1038/s41467-019-09234-6

Zhu-Salzman, K., and Zeng, R. (2015). Insect response to plant defensive protease inhibitors. *Annu. Rev. Entomol* 60, 233–252. doi: 10.1146/annurev-ento-010814-6

Conflict of Interest: The authors declare that the research was conducted in the absence of any commercial or financial relationships that could be construed as a potential conflict of interest.

VI. Acknowledgments

First, I thank Prof. Dr. Andrea Polle for allowing me to pursue a Ph.D. in her department and become a member of the IRTG 2172: PRoTECT. I am grateful for her continuous support, trust, and valuable advice. I also thank the second referee and member of my thesis advisory committee, Prof. Dr. Guus Bakkeren, for hosting me in his lab in Canada and for his valuable input during discussions. Many thanks to all examination board members: Prof. Dr. Gerhard Braus, Prof. Dr. Ivo Feußner, Prof. Dr. Kai Heimel, and Prof. Dr. Marcel Wiermer.

Thank you to Prof. Dr. Volker Lipka, PD Dr. Thomas Teichmann, and Dr. Masha Muhr (Department of Plant Cell Biology, University of Göttingen) for providing the *cerk1* KO poplar plants for my research. I am very grateful to Andrea Vasquez for helping me with the ROS burst and MAP kinase assay.

I thank Prof. Dr. Michael Rostás and Noor Agha Nawakht (Agricultural Entomology, Department for Crop Sciences, University of Göttingen) for providing *Helicoverpa armigera* larvae.

I would like to thank the German Science Foundation (DFG) for funding the International Research Training Group 2172: PRoTECT: Plant Response to Eliminate Critical Threats (project number 273134146) and thus funding my project (M2.2)

This thesis was made possible with the help of many people. I want to thank all my Forest Botany and Tree Physiology colleagues at the University of Göttingen for creating an excellent work environment. I want to thank some people in particular: Merle for helping with various problems regarding micropropagation and for her overall support, Cathrin for continuous help and advice in the greenhouse, Thomas for his constant support regarding questions about molecular work, Monika for her general support, Bernd for this technical support and Rike for her help regarding all questions with microscopy. In addition, I thank Johannes for his help processing the RNAseq data and for his advice in statistics. Special thanks to Nina for keeping the department together on the administrative side.

Furthermore, I want to thank all the past and present members of the "mensa crew": Christian, Dennis, Jacob, Johannes, Karl, Mareike, Marvin, and Victoria. You made all lunch breaks very enjoyable with very professional and unprofessional discussions. Thank you,

Ishani, for being an awesome office mate and for many great conversations. I could not have handled the work without the two HiWis who worked with me. Thank you so much, Malvine and Felix.

All members of the IRTG made this Ph.D. very special. Despite the extra workload at times, it was always great fun with all of you. Thank you very much for all our time together and for sticking with me as a student representative, even though I sometimes demanded a lot. Special thanks to Alisa for being the deputy student representative and helping me immensely. Many thanks also to the people who coordinated the IRTG and thus made my life a lot easier: Anja, Judith, and Steffi.

Last but not least, I want to thank all my friends for keeping me sane during this very challenging time. Thank you very much, Isabel, for all the time we spent together, all the runs (and especially the half marathon(s)) we did, and all the great food we had together. Thank you, Lennart, for sharing rooms with me at the first retreat and becoming a close friend afterward. I am very grateful that friends from Aachen stayed with me the whole time despite not seeing each other so much anymore. I am thankful to Kathrin for having started my academic lab experiences with you and even more grateful that you became a very dear friend throughout all these years. Thank you, Christian, Christopher, Henning, Jochen, Jonas, and Vale, that the "Jünger" are still close together and for every JüSaKo.

Thank you, Annika, for everything.

Finally, I thank my family, especially my parents, who always let me pursue my dreams and supported me immensely.

VIII. Publications

Journal article

Dreischhoff, S., Das I. S., Häffner, F., Wolf, A. M., Polle A., and Kasper K. (2023) "A fast and easy *Botrytis cinerea* infection assay for various poplar species" *Plant Methods 19, 32*

Dreischhoff, S., Das, I. S., Jakobi, M., Kasper, K., and Polle, A. (2020) "Local responses and systemic induced resistance mediated by ectomycorrhizal fungi." *Frontiers in Plant Science 11, 590063*

Poster

Dreischhoff, S., Das, I. S., Häffner, F., Wolf A. M., Polle, A., and Kasper, K. "A novel poplar infection assay with molecular detection of *Botrytis cinerea" GGNB Science Day 2022 (October 18th, 2022)*

Dreischhoff, S., Das, I. S., Häffner, F., Wolf, A. M., Polle, A., and Kasper, K. "A fast and easy *Botrytis cinerea* infection assay for various poplar species" *International Conference of the German Society for Plan Sciences "Botanik-Tagung" 2022 (August 28th – September 1st, 2022)*

Das, I. S., Dreischhoff, S., and Polle A. “Functional characterization of protease inhibitors involved in induced systemic defenses in poplar” *International Conference of the German Society for Plan Sciences "Botanik-Tagung" 2022 (August 28th – September 1st, 2022)*

Dreischhoff, S., Ballauff, J., Teichmann, T., Lipka, V., and Polle, A. “*Laccaria bicolor* alters systemic defenses in poplar.” *IS-MPMI: eSymposia series Plant-microbe interactions in the environment (December 1st & 2nd, 2021)*